TECHNISCHE UNIVERSITÄT MÜNCHEN

Fakultät für Chemie

Interaction of Latex Polymers with Cement-Based Building Materials

Stefan Matthias Baueregger

Vollständiger Abdruck der von der Fakultät für Chemie der Technischen Universität München zur Erlangung des akademischen Grades eines

Doktors der Naturwissenschaften (Dr. rer. nat.)

genehmigten Dissertation.

Vorsitzender:	Univ.-Prof. Dr. Michael Schuster
Prüfer der Dissertation:	1. Univ.-Prof. Dr. Johann Peter Plank 2. Univ.-Prof. Dr. Dr. h.c. Bernhard Rieger 3. apl. Prof. Dr. Hans-Ulrich Hummel, Friedrich-Alexander-Universität Erlangen-Nürnberg

Die Dissertation wurde am 14.10.2014 bei der Technischen Universität München eingereicht und durch die Fakultät für Chemie am 10.11.2014 angenommen.

ACKNOWLEDGEMENT

The research work presented in this thesis was performed in the time period from August 2011 to September 2014 at the Chair for Construction Chemistry, Technische Universität München. Hereby, I would like to thank all those who have contributed to the success of my PhD project.

First, I would like to express my deep gratitude to my academic teacher and supervisor **Prof. Dr. Johann Peter Plank** for providing this challenging and interesting research subject, his interest and contribution to the success of my PhD project, the continuous support of my work, but also for enabling me to visit and present at international conferences. His wide knowledge and broad experience in the exciting field of construction chemistry mediated the fascination for this research field and made my work exciting at any time.

My heartfelt thanks also go to **Dr. Marga Perello** from Dow Chemical Company for this nice collaboration, the rich and lively scientific discussions during our meetings and enabling me to work in such a creative manner. I also want to thank **Dr. Robert Baumann**, **Dr. Jürgen Dombrowski**, **Dr. Mark Westmeyer** and **Dr. Hartmut Kühn** from Dow Chemical Company for their interest and participation in our meetings. Finally, I thank **Dow Chemical Company** for sponsoring this PhD project.

Dr. Oksana Storcheva and **Dr. Roland Sieber**, I thank you for your help and support in all scientific questions and especially for performing the solid-state NMR measurements.

Special thanks also go to the non-scientific staff of the Chair. **Anke Kloiber** and **Tim Dannemann,** I thank you for your help in all administrative and organizational tasks. **Dagmar Lettrich** and **Richard Beiderbeck**, I want to thank you very much for your competent assistance and support concerning the accomplishment of chemical analysis and experiments.

My current and former colleagues deserve great thanks for their collegiality, the excellent working atmosphere at the chair and all the support during my PhD. Special thanks are dedicated to my lab colleagues **Markus Meier** and **Dr. Tobias Kornprobst** for the pleasant working atmosphere, as well as the many scientific discussions and non-scientific conversations, but also to **Thomas Pavlitschek** for introducing me and sharing his experience in the field of latex polymers and environmental scanning electron microscopy. Furthermore I want to thank all other PhD colleagues: **Alex Lange**, **Julia Pickelmann**, **Johanna de Reese**, **Timon Echt**, **Thomas Hurnaus**, **Manuel Ilg**, **Vipasri Kanchanason**, **Somruedee Klaithong**, **Lei Lei**, **Huiqun Li**, **Maike Müller**, **Markus Schönlein**, **Dr. Nan Zou**, **Dr. Salami Taye**, **Dr. Constantin Tiemeyer**, **Michael Glanzer-Heinrich**, **Dr. Daniel Bülichen**, **Dr. Elina Dubina**, **Dr. Geok Bee Serina Ng**, **Dr. Ahmad Habbaba** and **Dr. Hang Bian**.

Special thanks go to **Dr. Teresa Piqué** and my Master student and successor **Michael Kaul**. I wish you all the best and success in continuing the research in the fascinating field of latex polymers. Furthermore, I thank my interns **Stephanie Weicker** and **Patrick Schreiber** for their interest in my research subject and their enthusiasm in the lab.

Last but not least, I would like to sincerely thank my family, especially my parents **Heike** and **Ferdinand Baueregger**, for making this education possible, their continuous motivation and tireless support at any time.

Stefan, October 2014

LIST OF PAPERS

The following scientific manuscripts were published as a result of this research project. The thesis includes the papers #1-6.

Peer reviewed SCI(E) journal papers:

1) **Role of PVOH and kaolin on colloidal stability of liquid and powder EVA and SB latexes in cement pore solution**
   S. Baueregger, M. Perello, J. Plank
   Colloids and Surfaces A: Physicochemical and Engineering Aspects, 434 (2013), 145-153.

2) **Influence of anti-caking agent kaolin on film formation of ethylene-vinylacetate and carboxylated styrene-butadiene latex polymers**
   S. Baueregger, M. Perello, J. Plank
   Cement and Concrete Research, 58 (2014), 112-120.

3) **On the role of colloidal crystal-like domains in the film forming process of a carboxylated styrene-butadiene latex copolymer**
   S. Baueregger, M. Perello, J. Plank
   Progress in Organic Coatings, 77 (2014), 685-690.

Manuscripts submitted to peer reviewed SCI(E) journals:

4) **Influence of Carboxylated Styrene-Butadiene Latex Copolymer on Portland Cement Hydration**
   S. Baueregger, M. Perello, J. Plank
   Cement and Concrete Composites
   (submitted on September 3, 2014, under review).

5) **Impact of Carboxylated Styrene-Butadiene Copolymer on the Hydration Kinetics of OPC and OPC/CAC/AH: The Effect of Ca^{2+} Sequestration from Pore Solution**
S. Baueregger, M. Perello, J. Plank
Cement and Concrete Research
(submitted on September 12, 2014, under review).

Refereed conference paper:

6) **Use of a Nano Clay for Early Strength Enhancement of Portland Cement**
S. Baueregger, L. Lei, M. Perello, J. Plank
Proceedings of the 5th International Symposium on Nanotechnology in Construction (NICOM 5), Chicago (2015)
(submitted on August 14, 2014, accepted).

Conference papers:

7) **A kinetic and mechanistic investigation on the film formation of a carboxylated styrene-butadiene latex**
S. Baueregger, M. Perello, J. Plank
GDCh Monographie 46, Berlin (2013), 57-60.

8) **Einfluss von Latexpolymeren auf die Hydratation von Portlandzement sowie des ternären Bindemittelsystems OPC / CAC / Anhydrit**
S. Baueregger, M. Perello, J. Plank
GDCh Monographie 47, Kassel (2014), 248-251.

9) **Optimization of Admixtures for Calcium Sulfate Based Building Products**
S. Baueregger, J. Plank
Alit Inform (2014), in print.

LIST OF ABBREVIATIONS

Cement chemistry notation:

Mineral name	Oxidic composition	Cement notation*
Tricalcium sulicate	$3\ CaO \cdot SiO_2$	C_3S
Dicalcium silicate	$2\ CaO \cdot SiO_2$	C_2S
Tricalcium aluminate	$3\ CaO \cdot Al_2O_3$	C_3A
Tetracalcium aluminate ferrite	$4\ CaO \cdot Al_2O_3 \cdot Fe_2O_3$	C_4AF
Ettringite	$3\ CaO \cdot Al_2O_3 \cdot 3\ CaSO_4 \cdot 32\ H_2O$	$C_3A\bar{S}_3H_{32}$
Monosulfate	$3\ CaO \cdot Al_2O_3 \cdot CaSO_4 \cdot 12\ H_2O$	$C_3A\bar{S}H_{12}$

*C = CaO; A = Al_2O_3; S = SiO_2, F = Fe_2O_3, H = H_2O, $\bar{S}$ = SO_3

General abbreviations:

Abbreviations	
AAS	Atomic absorption spectroscopy
ACA	Anti-caking agent
AFM	Atomic force microscopy
CAC	Calcium aluminate cement
C-A-H	Calcium aluminate hydrate
ccc	Critical coagulation concentration
CEM I	Portland cement
cmc	Critical micelle concentration
C-S-H	Calcium silicate hydrate
DLS	Dynamic light scattering
DLVO	*Derjaguin*, *Landau*, *Verwey*, *Overbeek*
EDL	Electrochemical double layer
EDX	Energy dispersive X-ray spectroscopy
EIFS	External insulation & finishing system
ESEM	Environmental scanning electron microscopy

EVA	Ethylene-vinylacetate
FRET	Fluorescence resonance energy transfer
HAC	High aluminate cement
HEMC	Hydroxy ethyl methyl cellulose
HDI	Hexamethylene diisocyanate
HLB	Hydrophilic-lipophilic-balance
HPMC	Hydroxy propyl methyl cellulose
IC	Ion chromatography
IPDI	Isophorone diisocyanate
IHP	Inner *Helmholtz* plane
IR	Infrared
LDH	Layered double hydroxide
MDI	Methylene diphenyl diisocyanate
MFFT	Minimum film forming temperature
OHP	Outer *Helmholtz* plane
OPC	Ordinary Portland cement
o/w	Oil-in-water
PDADMAC	Poly(diallyl dimethyl ammonium chloride)
Pe	*Peclet* number
PU	Poly(urethane)
PVOH	Poly(vinylalcohol)
p/c	Polymer-to-cement ratio
RDP	Re-dispersible powder
SANS	Small-angle neutron scattering
SB	Styrene-Butadiene
SCPS	Synthetic cement pore solution
T_g	Glass transition temperature
TDI	Toluene diisocyanate
VeoVa	Vinylester of versatic acid
w/c	Water-to-cement ratio
XRD	X-ray diffraction

TABLE OF CONTENTS

1 INTRODUCTION

Modern drymix mortar formulations for building applications represent complex multi-component systems consisting of inorganic binders, organic binders, aggregates or fillers and chemical admixtures [1]. The broad portfolio of chemical admixtures such as dispersants, water retention agents, retarders, accelerators or defoamers allows to control the workability (rheology), setting behavior and material properties of the mortar [2]. Typical drymix mortar applications include self-leveling underlayments, tile adhesives and grouts, waterproofing membranes, plasters, repair mortars or adhesive and basecoat mortars for exterior insulation & finishing systems (EIFS).

Drymix mortars are prepared by controlled mixing and homogenization of the powdery components by means of automatic dosing devices [3]. This way, customized formulations for special applications can be produced with constant product quality and high productivity [4]. On the job site, the drymix mortars only need to be mixed together with water whereby dosage errors are avoided and a high level of application reliability is guaranteed [5].

The composition of the inorganic binder allows controlling the strength development as well as the shrinkage behavior of the mortar. More often ternary binder systems consisting of Portland cement, calcium aluminate cement and calcium sulfate (anhydrite or hemihydrate) are applied [6]. Calcium aluminate cement leads to an acceleration of the hydration of Portland cement and therefore is used mainly in rapid hardening systems such as self-leveling underlayments or repair mortars [7, 8]. These rapid hardening systems contribute to a fast progress in the construction and thus minimize the costs of construction projects. By combining calcium aluminate cement with calcium sulfates the reactivity of CAC can be controlled depending on the type or solubility of the calcium sulfate salt [9, 10]. Additionally, these systems show low shrinkage [11-13] which is particularly favorable in the application of thin layers (thin bed mortars) in order to prevent crack formation.

Inorganic binders are characterized by low cohesion and adhesion of the fresh mortar onto substrates and low flexural strength in the hardened state. Therefore, products composed of only inorganic binders do not meet the quality standards required for many high performance drymix mortar products. For improvement of these properties, re-dispersible latex powders are added as organic co-binders [14-17]. The resulting composite material combines the positive properties of both inorganic and organic binders. Re-dispersible latex powders improve the adhesion, cohesion and flexural strength due to the formation of a homogeneous and flexible polymer film within the brittle cementitious matrix and on the interface between mortar and substrate [18, 19].

The dosage of the organic binder varies greatly depending on the application. Tile adhesives are formulated with up to 5 % by weight of cement of re-dispersible latex powder, whereas waterproofing membranes contain very high dosages of 20-50 % of polymeric binder. Due to the high dosages of organic binders in drymix mortar formulations, a strong influence on cement hydration can be expected. Additionally, the question on the interaction between organic and inorganic binder arises.

Owing to their complex composition dry mortars are still in the focus of current industrial and academic research despite many years of application. Dry mortar products are mainly developed empirically in the industry based on application-related experiments and experience. Therefore, scientific literature on these complex formulations hardly exists because the elucidation of the underlying fundamental mechanisms plays a minor role in the development of products.

Against this background, the interaction between inorganic and organic binder was investigated within the scope of this fundamental research work. The interaction involves both the influence of the inorganic binder on the key properties of the latex polymers, as well as the effect of the polymers on cement hydration. For these scientific studies model systems consisting of only inorganic binder and latex polymer were chosen.

2 AIMS AND SCOPE

In this study the interaction of non-ionic ethylene-vinylacetate (EVA) and anionic styrene-butadiene (SB) latex copolymers with inorganic binders was investigated. Experiments were performed with both EVA and SB aqueous latex dispersions and corresponding re-dispersible latex powders. The EVA and SB powder samples were prepared by spray drying of the aqueous mother liquors under the addition of the spraying aids poly(vinylalcohol) (protective colloid) and kaolin (anti-caking agent).

Essential quality characteristics of latex polymers for construction applications are their colloidal stability and film-forming ability in cement pore solution. In the literature numerous publications dealing with the stability of colloidal systems and the underlying stabilization mechanisms exist. However, the colloidal stability of latex particles in cement pore solution and especially the influence of the spraying aids PVOH and kaolin on the electrokinetic properties of re-dispersed latex powders have not been described yet. For a fundamental understanding of the performance and working mechanism of latex polymers in cement-based binder systems these properties need to be understood.

Furthermore, the influence of the spraying aids PVOH and kaolin on the film formation of re-dispersed latex powders so far has not been published in the scientific literature. Several papers reported on the film formation of latex dispersions in the presence of electrolytes. For example, it has been shown that latex film formation in saline systems such as cement pore solution can be greatly delayed, compared to the salt-free aqueous medium. As main reasons for this effect adsorption of oppositely charged ions onto latex particle surfaces and the formation of salt crusts surrounding the latex particles were presented. Both phenomena were shown to hinder the coalescence of latex particles and thus delay film formation [20, 21].

For this reason, in the first step of this research the colloidal and chemical properties of EVA and SB latex dispersions and re-dispersible powder samples were determined. Subsequently, the colloidal stability and film formation of liquid latex dispersions and

their re-dispersed powders in aqueous medium and synthetic cement pore solution were compared. Here, the impact of the spraying aids PVOH and/or kaolin on the colloidal stability and film formation was of particular interest. The colloidal stability of latex dispersions was analyzed by photometric turbidity measurements. Environmental scanning electron microscopy (ESEM) was applied for the investigation of latex film formation.

In the next step, the influence of the EVA and SB latex copolymers on the hydration of inorganic binders was examined. In previous works the effect of synthetic latex polymers on the material properties of cement-based systems has been studied extensively [22-24]. However, little literature which systematically describes the impact of latex dispersions and their re-dispersible powders on cement hydration exists [25, 26]. Only *R. Wang* et al. examined the influence of styrene-butadiene (SB) latex and powder on Portland cement hydration [12, 27]. In these papers, however, no information on the composition of the SB copolymer, the chemistry of the spraying aids and the colloidal properties of the latex particles was provided. Physical interactions between latex particles and mineral binders are controlled by the electrokinetic surface properties of the latex particles. Hence, for complete understanding of the latex-cement-interaction, the impact of latex polymers on cement hydration needs to be linked to the colloidal properties of the latex particles.

Furthermore, no literature on the influence of latex polymers on the hydration of the ternary binder system OPC/CAC/anhydrite exists. In modern drymix mortar applications such as repair mortars, self-leveling underlayments or waterproofing membranes, latex powders are often combined with ternary inorganic binders. Owing to these various applications, a thorough investigation of this interaction is highly interesting.

In view of the above, the interaction of non-ionic ethylene-vinylacetate (EVA) and anionic styrene-butadiene (SB) copolymers with Portland cement and the ternary binder system OPC/CAC/anhydrite was studied. In addition, the influence of the individual spraying aids PVOH or kaolin was determined. Experimentally, the

reactivity of the hydrating binders was monitored via isothermal heat flow calorimetry. The formation of hydrate phases within the first 48 h of cement hydration was tracked via in-situ XRD measurements. Adsorption of latex particles onto cement was determined by electroacoustic zeta potential. Analysis of cement pore solutions were carried out by ion chromatography (IC) and atomic absorption spectroscopy (AAS).

3 THEORETICAL BACKGROUND AND STATE OF THE ART

3.1 Polymer dispersions

Polymer or latex dispersions are defined as stable colloidal dispersions consisting of polymer particles with a diameter ranging from 10 to 1000 nm in a continuous aqueous phase which is usually referred to as serum phase. It contains water-soluble compounds such as co-monomers, oligomers, surfactants or salts [28].

The term latex was derived from the milky fluid produced from plants which represents a polymer dispersion. Natural latex is mainly obtained from the rubber tree *Hevea brasiliensis* and is composed of cis-1,4-poly(isoprene)-based polymer particles holding a diameter of 100 to 1500 nm and a glass transition temperature (T_g) of around – 85 °C (**Figure 1**). The aqueous serum phase of natural latex contains proteins, resins, fatty acids, salts or polysaccharides.

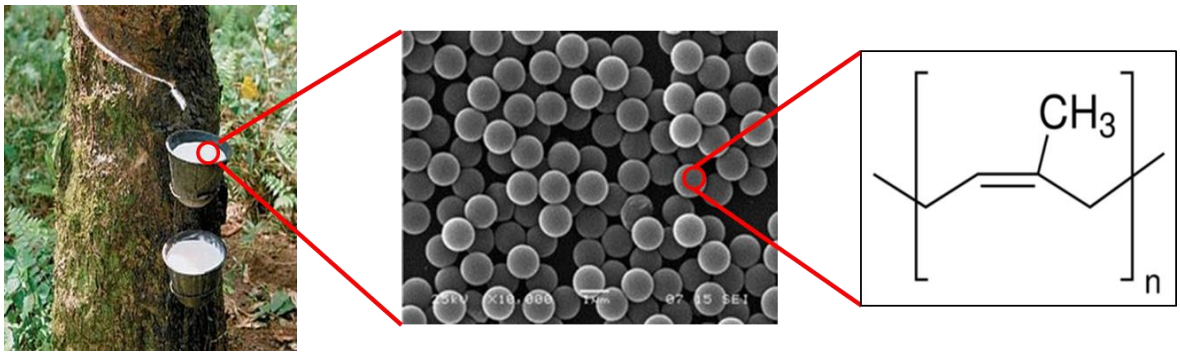

Figure 1. Segregation of natural latex from the rubber tree. The colloidal polymer particles are mainly composed of cis-1,4-poly(isoprene) [29].

Synthetic polymer dispersions are divided into primary and secondary dispersions. Primary polymer dispersions are obtained directly from heterophase polymerization, while secondary dispersions are prepared by dispersing previously synthesized polymers into a continuous phase. In the following, the chemistry, synthesis and properties of synthetic polymer dispersions are discussed.

3.1.1 Chemistry of polymer dispersions

Most of the synthetic polymer dispersions are prepared in heterogeneous phase from olefins via free radical copolymerization. Typical products are styrene-butadiene copolymers, vinylacetate homo- and copolymers or acrylate-based copolymers. But there also exist some more specific dispersions such as ethylene, styrene, vinylester, vinylchloride, vinylidene chloride/fluoride or chloroprene dispersions [28]. Generally, a large variety of copolymers with tailor-made material properties can be synthesized due to the wide choice of different monomers as shown in **Figure 2**.

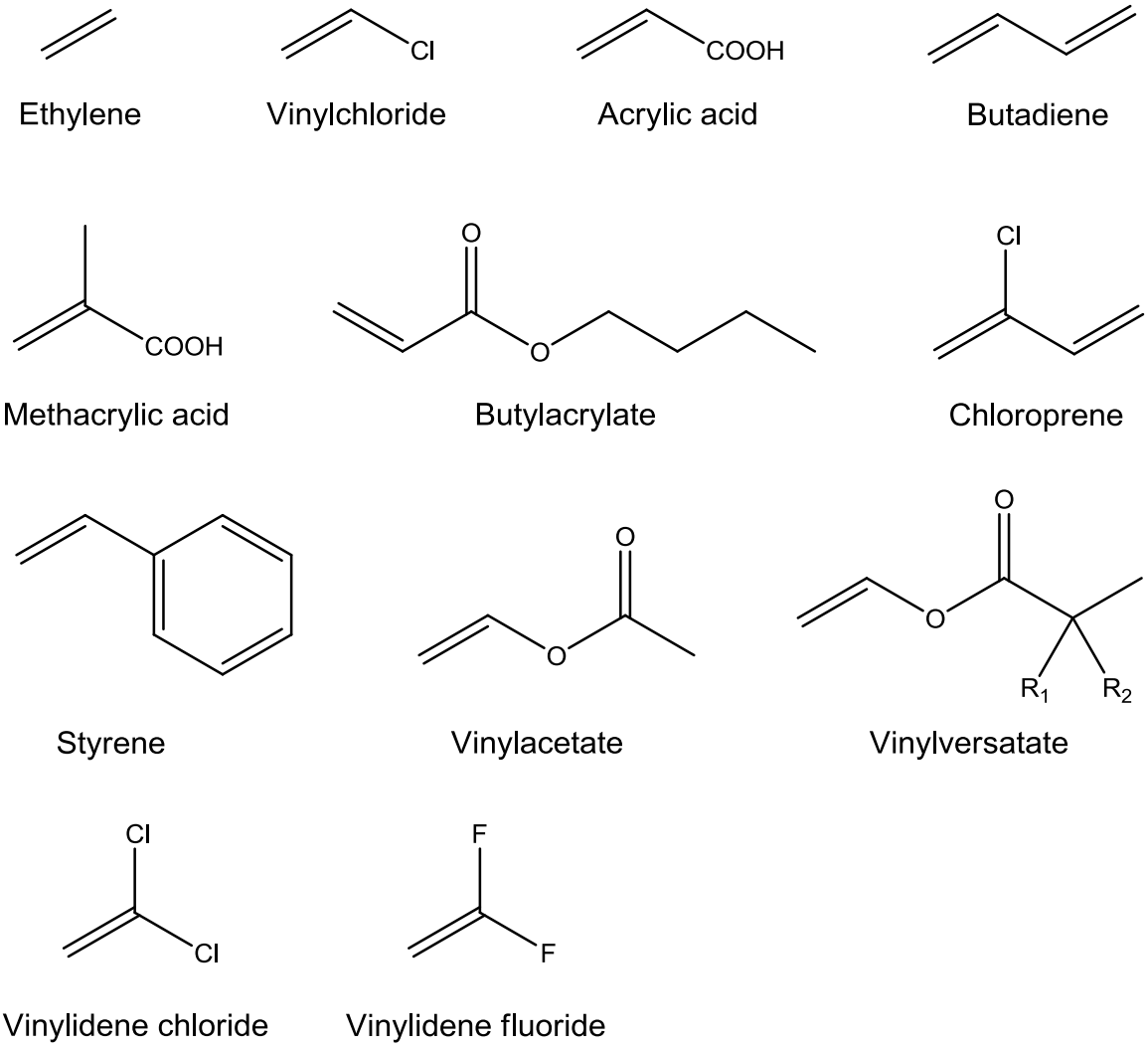

Figure 2. Typical monomers used for the preparation of latex dispersions via emulsion polymerization.

The colloidal properties of the polymer particles such as surface charge can be controlled by chemical incorporation of ionic co-monomers or emulsifiers. For example, latex particles can be internally stabilized by the incorporation of itaconic acid, but also the chemistry of the emulsifier (ionic or non-ionic) allows adjusting the surface properties of the latex particles.

Water-based polyurethane (PU) dispersions gained increasing importance due to their outstanding material properties such as adhesion to several substrates, resistance to chemicals, solvents and water, abrasion resistance or flexibility. Generally, polyurethane dispersions are formed in a step-growth polymerization by reaction of diisocyanates with polyols. In the first step, a PU prepolymer chain is formed from diisocyanates and polyols, which is then further extended by using diamines. Four main diisocyanate compounds (**Figure 3**) are used for industrial PU dispersions: methylene diphenyl diisocyanate (MDI), toluene diisocyanate (TDI), hexamethylene diisocyanate (HDI) and isophorone diisocyanate (IDPI). Polyols can be differentiated into polyether polyols which are usually prepared from epoxides, and polyester polyols which are synthesized via polycondensation reaction of multifunctional carboxylic acids and alcohols [30].

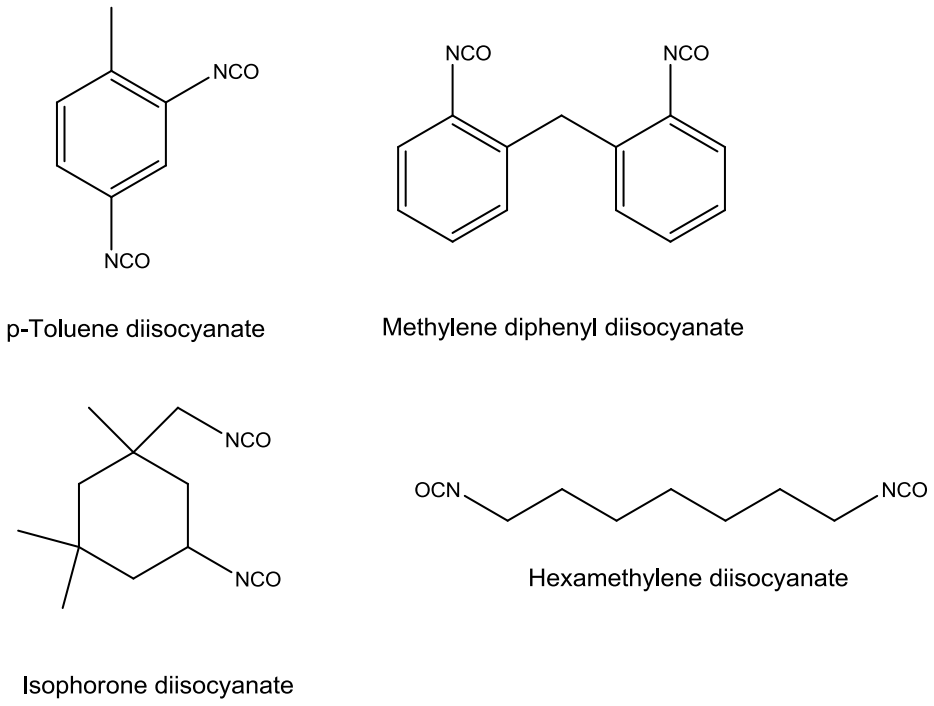

Figure 3. Chemical structures of diisocyanates used for PU prepolymer synthesis.

For coating applications where color or transparency are important product features, PU dispersions are mainly prepared from aliphatic diisocyanates because aromatic compounds tend to darken upon light exposure.

PU dispersions can be synthesized via several methods (e.g. prepolymer mixing, acetone, hot melt or ketamine/ketazine process) which all include the formation of a medium molecular weight PU prepolymer as first step by reacting di- or polyols with a molar excess of di- or polyisocyanates. The prepolymer mixing process and the acetone process are the most important ones applied in the industry. In the prepolymer mixing process prepolymers are emulsified via high shear-force in an aqueous phase. The hydrophobic prepolymers are internally or externally stabilized via emulsifiers. Internal stabilization is achieved by using reactive non-ionic polyethers or OH-terminated poly(vinylpyrrolidones), or ionic compounds containing carboxylate, sulfonate or amine functional groups. High molecular weight poly(vinylpyrrolidones) or alkylphenol-terminated ethylene oxide polyethers are used for external stabilization of the prepolymer emulsion. The major drawback of this process is the formation of foam created upon reaction of isocyanates with water. As is shown in **Figure 4**, the addition of water to isocyanates leads to the formation of metastable carbamic acid which decomposes into an amine under elimination of carbon dioxide.

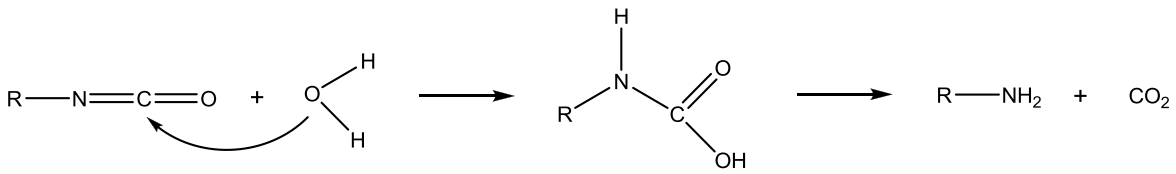

Figure 4. Hydrolysis of isocyanates in the presence of water. CO_2 release from the decomposition of the intermediate carbamic acid induces foaming.

The acetone process is characterized by three main steps. First, the prepolymer is reacted together with diamines in a water-free organic solvent (acetone) forming high-molecular weight PU polymers, which in the second step are dispersed in the aqueous phase. Upon subsequent removal of the organic solvent acetone via distillation, the secondary PU dispersion is obtained.

3.1.2 Synthesis of polymer dispersions via emulsion polymerization

Polymer dispersions based on unsaturated monomers can be prepared via emulsion, miniemulsion, dispersion or suspension polymerization processes. The final products are mainly characterized by their particle size distributions (e.g. d_p(emulsion) = 0.01 – 1 µm; d_p(dispersion) = 1 – 15 µm; d_p(suspension) > 15 µm). The most important process in general, but also for copolymers used in construction applications is the emulsion polymerization which is presented in detail below. Major advantages of heterophase polymerizations compared to polymerization in solution are higher reaction rates, molecular weights and conversions, but also more efficient heat removal, mixing and lower viscosities [31].

Emulsion polymerizations are carried out by polymerizing an oil-in-water emulsion stabilized by surfactants and using an initiator. The reaction system is characterized by the emulsified monomer droplets dispersed in the continuous aqueous phase and monomer-swollen micelles which are formed when the concentration of surfactant in the aqueous phase is above its critical micelle concentration (cmc). Only a small fraction of the monomer is dissolved in the micelles or aqueous phase whereas most of the monomer is present in the monomer droplets which represent a monomer reservoir. The polymerization is initiated by the addition of an initiator, whereby radicals are generated in the aqueous phase. Subsequent particle nucleation and growth was described in the literature by several models [32, 33].

The particle size distribution (monodisperse, bimodal or polydisperse) of the final latex can be explained by the nucleation and growth mechanism during polymerization. Three particle nucleation mechanisms (micellar, homogeneous and monomer droplet nucleation) have been discussed in the literature [34]. According to the micelle nucleation model proposed by *Harkins* [35], *Smith* and *Ewart* [36] and *Gardon* [37], free radicals are captured by micelles due to their enormous oil/water-interfacial area whereby submicron latex particles are generated. *Fitch* and *Tsai* [38], *Priest* [39] and *Roe* [40] suggested a homogeneous nucleation in the aqueous continuous phase. *Hansen* and *Ugelstad* [41] and *Durbin* et al. [42] brought up the

monomer droplet nucleation mechanism which is less accepted among scientists. Monomer droplets cannot compete with micelles in capturing free radicals due to their relatively small surface area.

For particle growth three mechanisms (homogeneous, micellar and coagulative) have been discussed in the literature [31]. In case of homogeneous growth, primary particles are formed in aqueous phase by homogeneous nucleation and grow further under adsorption of surfactant molecules in the continuous phase. The micellar mechanism describes the formation of polymerization nuclei in aqueous phase, which then diffuse into micelles and initiate polymerization there. Upon continued polymerization, micelles grow and pass into surfactant stabilized particles. *Napper* et al. [43] proposed that final latex particles are formed by heterocoagulation. First, primary particles are generated which are stable against homocoagulation (coagulation with particles of similar size), but not against heterocoagulation with larger particles. As a consequence, all newly formed primary particles are immediately captured by large particles which then grow further to the final latex particles.

Based on these mechanisms it can be concluded that in the synthesis of monodisperse latices only one generation of growing particles may be formed which then grow simultaneously to the final latex particles. Thus, the easiest method for preparation of monodisperse latices is a two-step process via heterocoagulation. First, seed latex particles are synthesized and then mixed together with the other components in the second polymerization process whereby the seed particles capture all newly generated primary particles upon heterocoagulation. Here, it is important that enough seed particles are present for capturing all formed primary particles. When the number of seed particles is insufficient to consume all of the formed primary particles, a second population of latex particles is generated and a bimodal particle size distribution is obtained. The final particle size of the latex can be controlled by the size of the seed particles, but also by the monomer concentration.

Furthermore, the particle size can be controlled by the concentration of surfactant in the continuous phase which determines the amount of micelles formed in the emulsion. High surfactant concentrations lead to the formation of a high quantity of primary particles which then grow less at constant monomer concentration and form smaller final latex particles. Furthermore, the chemistry of the surfactant determines the size and geometry of the micelles formed, and thus influences size and morphology of the latex particles.

In industrial scale, the polymerization rate is often limited by the cooling rate. Initially, the reaction mixture is heated up to 75 to 90 °C under stirring and nitrogen atmosphere whereby initiator molecules start to decompose and free radicals are generated. This way, an exothermic polymerization reaction is initiated by free radicals and the mixture needs to be kept at constant temperature. *Frauendorfer* and *Hergeth* [44] and *Hergeth* and *Krell* [45] described the monitoring and control of such polymerization reactions. Typically, reaction calorimetry is applied for analyzing the exothermic polymerization reactions, whereas detailed information about the conversion of monomers can be provided by spectroscopic methods such as near-infrared or *Raman* spectroscopy.

Suitable initiators are redox systems which allow sufficient formation of radicals at polymerization temperature. Typical redox couples are based on peroxides (e.g. H_2O_2) and ferric ions (Fe^{2+}) which even work at lower temperatures compared to thermal initiators such as potassium peroxodisulfate.

Surfactants for emulsion polymerizations need to stabilize o/w emulsions. They are characterized by their HLB-value which should be between 8 and 18. Above the critical micelle concentration (cmc) in the aqueous continuous phase emulsifier molecules self-assemble in highly ordered associates which are referred to as micelles. The ionic character (non-ionic, anionic or cationic) of the surfactant allows controlling the surface properties of the latex particles. They can be differentiated into ionic and non-ionic surfactants which allow controlling the surface properties of the latex particles. As ionic surfactants alkyl sulfonates or sulfates, fatty acids and

quaternary fatty amines are used. Non-ionic surfactants are usually polyaddition products of ethylene oxide and fatty acids, fatty alcohols or alkyl phenols. Surface active polymers such as poly(vinylalcohol) or hydroxy ethylcellulose can also be used for stabilization of o/w emulsions during emulsion polymerization. The emulsions may be stabilized not only by surfactants or surface active polymers, but also via solid nanoparticles which adsorb at the o/w interface, and thus create a physical barrier for coalescence of the oil droplets [46, 47]. Such systems were first described by *Pickering* [48] and are therefore known as *Pickering* emulsions.

Emulsion polymerization is usually carried out in the presence of surfactants which stabilize the emulsion. However, emulsifiers can lead to disadvantages in the application (e.g. slow film formation, weak adhesion or poor water resistance) [49]. In order to avoid these drawbacks, emulsifier-free emulsion polymerizations were developed [50-52]. Here, the monomer is emulsified in the aqueous phase by stirring and the latex particles are stabilized by ionic functional groups stemming from initiator molecules or co-monomers. Furthermore, polymeric compounds referred to as alkali-soluble resins can be used for stabilization [53-55], whereby core-shell latices are fabricated. Such systems are highly interesting for construction applications. Core-shell particles composed of a high T_g shell surrounding a low T_g core are expected to be easily spray-dried, because the high T_g shell will protect the latex from coalescence. Even spray drying in the absence of protective colloids might be possible by using such systems. When added to cement, the alkali-soluble resin will dissolve from the latex particle surface due to the alkaline pH of the cement pore solution and the low T_g core can then form a film.

The EVA and SB copolymers used in this study were synthesized via emulsion polymerization [56]. EVA is synthesized from liquid vinylacetate monomer and gaseous ethylene. Therefore, this reaction is performed under pressure of around 80 bar in order to increase the ethylene concentration in the emulsion. Poly(vinylalcohol) is used as surface active compound stabilizing the emulsion whereby a polydisperse particle size distribution is obtained. The SB polymer was

prepared via seed polymerization from the monomers styrene and butadiene and is thus polymerized under nitrogen atmosphere, but not under pressure.

3.1.3 Drying of latex dispersions – fabrication of latex powders

Dr. *Max Ivanovits*, research chemist at Wacker AG, was the first who developed a process for drying latex dispersions based on poly(vinlyacetate) in 1952 [57]. The main challenge was the fabrication of a latex powder with re-dispersible character, meaning that it decomposes into its precursor latex upon addition of water. With the invention of re-dispersible latex powder the drymix mortar volume increased sharply by ~ 600 % [1].

For construction applications, latex polymers are synthesized with glass transition temperatures below application temperature. In the drying process, hot conditions are required for complete water removal from the dispersions, but at the same time these conditions facilitate latex particle coalescence. Thus, before drying water-soluble colloidal stabilizers are mixed together with the latex dispersion. This mixture is atomized together with an anti-caking agent into a hot air flow whereby water evaporates and a fine powder is obtained. The individual latex particles are coated with a layer of the colloidal stabilizer and thus separated from each other. This way, latex particle are prevented from film formation during the drying process or storage. The addition of an anti-caking agent prevents moisture-induced lump formation and guarantees flowability of the powder. When dispersed in water, the colloidal stabilizer dissolves in the aqueous phase and the latex particles form a dispersion similar to their initial mother liquor. **Figure 5** illustrates the fabrication of latex powders and subsequent re-dispersion in water.

The chemistry of the colloidal stabilizers is based on water soluble polymers. Mainly poly(vinylalcohol) is used for the fabrication of re-dispersible powders, but generally any water soluble polymer (even concrete superplasticizers such as e.g. polycarboxylates) is conceivable as far as it is compatible with the latex polymer and its final application. In this study it was found that the internally stabilized styrene-butadiene latex can also be spray dried in the absence of a colloidal stabilizer. This concept is based on the formation of water-soluble oligomers in the serum phase during polymerization which then act as colloidal stabilizer in the drying process.

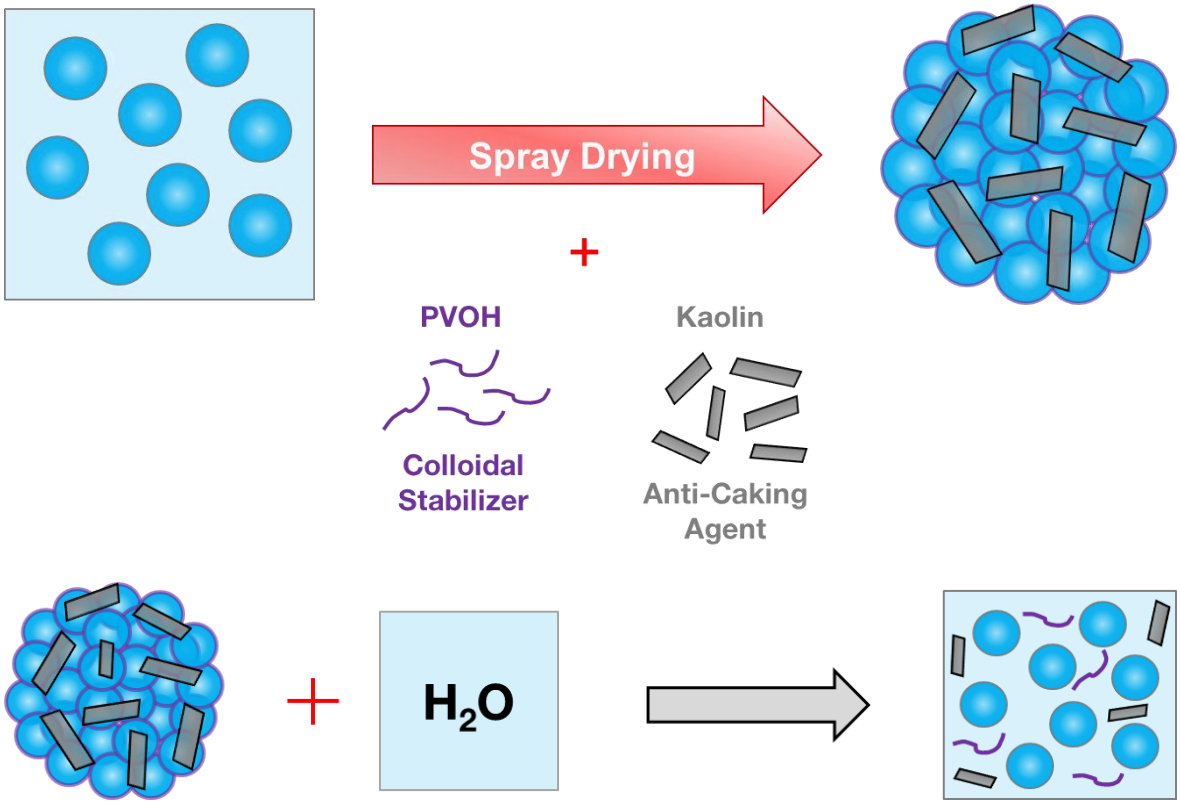

Figure 5. Schematic illustration of the fabrication of re-dispersible latex powders from aqueous latex dispersions under the addition of a colloidal stabilizer and an anti-caking agent, and subsequent disintegration into a latex dispersion upon re-dispersion in water.

The technology of the drying process considerably impacts the quality and performance of the re-dispersible powder because it influences the final powder particle size and morphology [58, 59]. Two techniques exist for atomizing latex dispersions into a hot air flow, either via a nozzle or a rotating disc [60, 61]. Key parameter of the spray drying process is the extremely fine distribution of the dispersion in the air flow, because the amount of heat transferred is directly proportional to the surface area of the droplets. For example, when a droplet with a radius of 1 mm is separated into smaller ones holding radii of 1 µm, the surface area is increased by a factor of 10^6, while at the same time the amount of solvent to be evaporated remains constant. This demonstrates that small droplet sizes contribute significantly to an effective solvent evaporation [62].

By using a rotating disc as spraying device, smaller droplet sizes can be achieved due to the high speed of the rotating disc. This allows drying at more moderate temperatures compared to atomizer-based spray driers and is therefore less harmful for the latex polymer. The droplet size generated by rotating discs can be expressed by **Equation 1** and mainly depends on the speed of the rotating disc n which is typically between 10,000 and 20,000 rounds per minute. Moreover, surface tension σ and density ρ_{fluid} of the dispersion, as well as the radius r of the rotating disc determine the average droplet size.

$$d_p = 98.5 \cdot \sqrt{\frac{\sigma}{r \cdot \rho_{fluid}}} \cdot \frac{1}{n} \qquad \textbf{Equation 1}$$

Powder particles produced by spray drying normally represent intact hollow spheres. Generally, the geometry of the powder particles (intact hollow spheres, spongy or inflated spheres) depends on the temperature of the air flow, especially whether it is above or below the boiling point of the solvent or continuous phase [63]. *Charlesworthy* and *Marshall* [64] described the formation of hollow powder particle spheres as follows: due to the high temperature of the gas surrounding the latex droplets, the solvent first evaporates from the droplet surface. This way, new solvent is delivered from the inner section of the droplet to the surface, whereby a mass transport in radial direction from the center to the surface of the droplet occurs. Thus, dispersed latex particles accumulate at the surface whereas in the inner part of the former droplet a hollow space remains. **Figure 6** shows the morphology of the carboxylated styrene-butadiene latex powder used in this study.

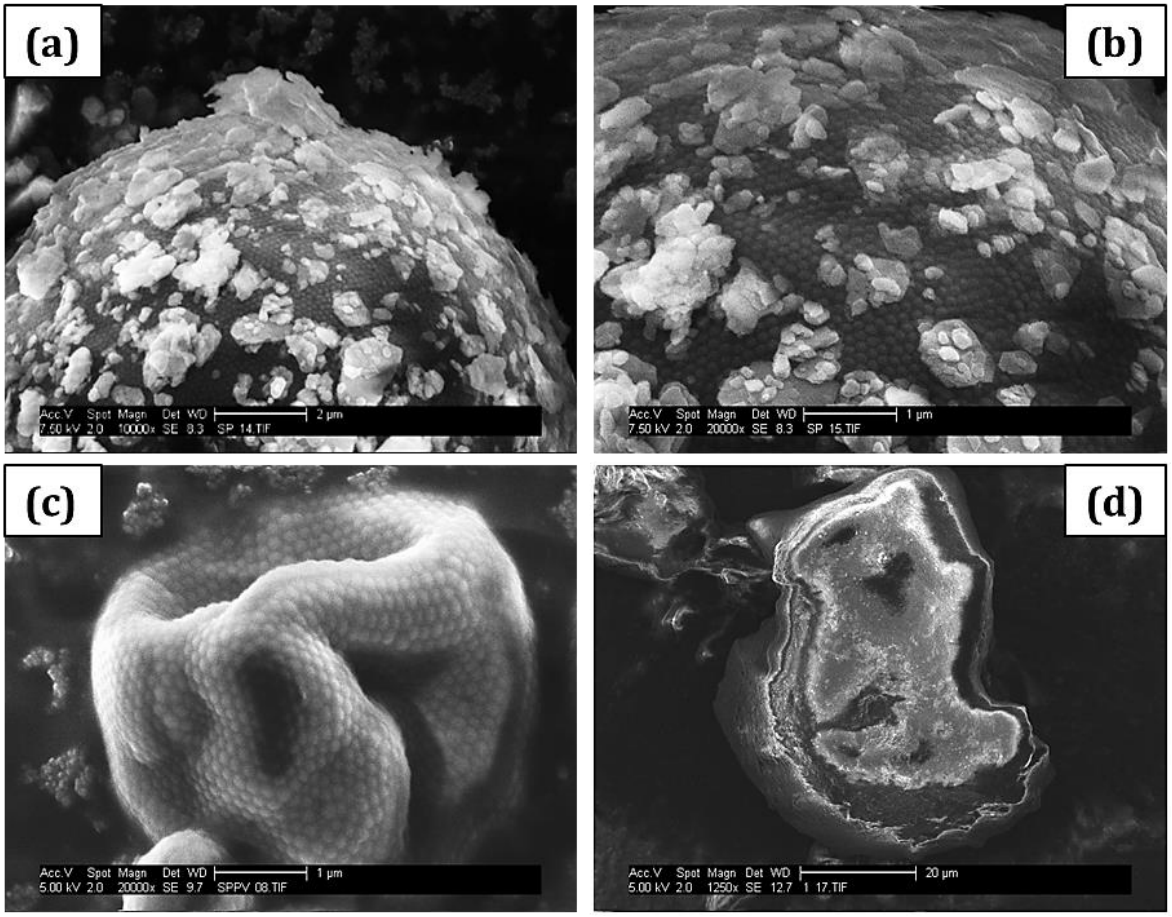

Figure 6. SEM images of styrene-butadiene latex powder particles showing (a, b) that the surface of SB powder particles is partially covered with platelets of the anti-caking agent kaolin and that the powder particles are composed of a dense packing of individual latex particles; (c) powder particles with spongy or reptile morphology or (d) hollow sphere in the inner part of the particle can be obtained.

3.1.4 Colloidal stability

Latex dispersions represent colloidal systems which are characterized by their key properties viscosity and colloidal stability. Both, viscosity and colloidal stability depend on attractive and repulsive interparticle forces occurring between colloids. Generally, latex dispersions are not thermodynamically stable, but they exhibit kinetic stability as long as colloidal particles are kept at distance by interparticle repulsive forces. Coagulation is always preferred because of the resulting reduction in the thermodynamic free energy. The minimization of the free energy can be expressed by the product of the polymer/water interfacial tension multiplied with the change in the interfacial area. Kinetic stability is achieved by electrostatic repulsive forces which maintain a barrier against collision between the particles and thus prevent subsequent coagulation. Four mechanisms called electrostatic, steric, electrosteric and depletion stabilization which are all based on interparticle repulsive forces are known for the stabilization of dispersions. A simplified model for interparticle forces is presented by the *DLVO* theory which describes electrostatic forces between colloidal particles in a dispersion medium. Furthermore, the ion cloud or electrochemical double layer (EDL) surrounding colloids in suspension needs to be considered for complete understanding of the stabilization of polymer dispersions [65].

Colloids dispersed in an aqueous phase always develop a surface charge which is generated by protonation or deprotonation of functional groups, adsorption of ionic polymers, incongruent dissolution of ions from the particle surface or defects stemming from incomplete coordination of surface atoms. *Helmholtz* [66] first described the formation of an electrochemical double layer on the interface between solid materials and electrolytes. This concept was developed further by *Gouy*, *Chapman*, *Stern* [67] and *Grahame* [68] and describes the charge compensation of colloidal particles by counter ions as well as the charge distribution around colloids. *Bockris* [69] extended this model by taking water dipoles into account. **Figure 7** illustrates the composition of the electrochemical double layer according to *Bockris*.

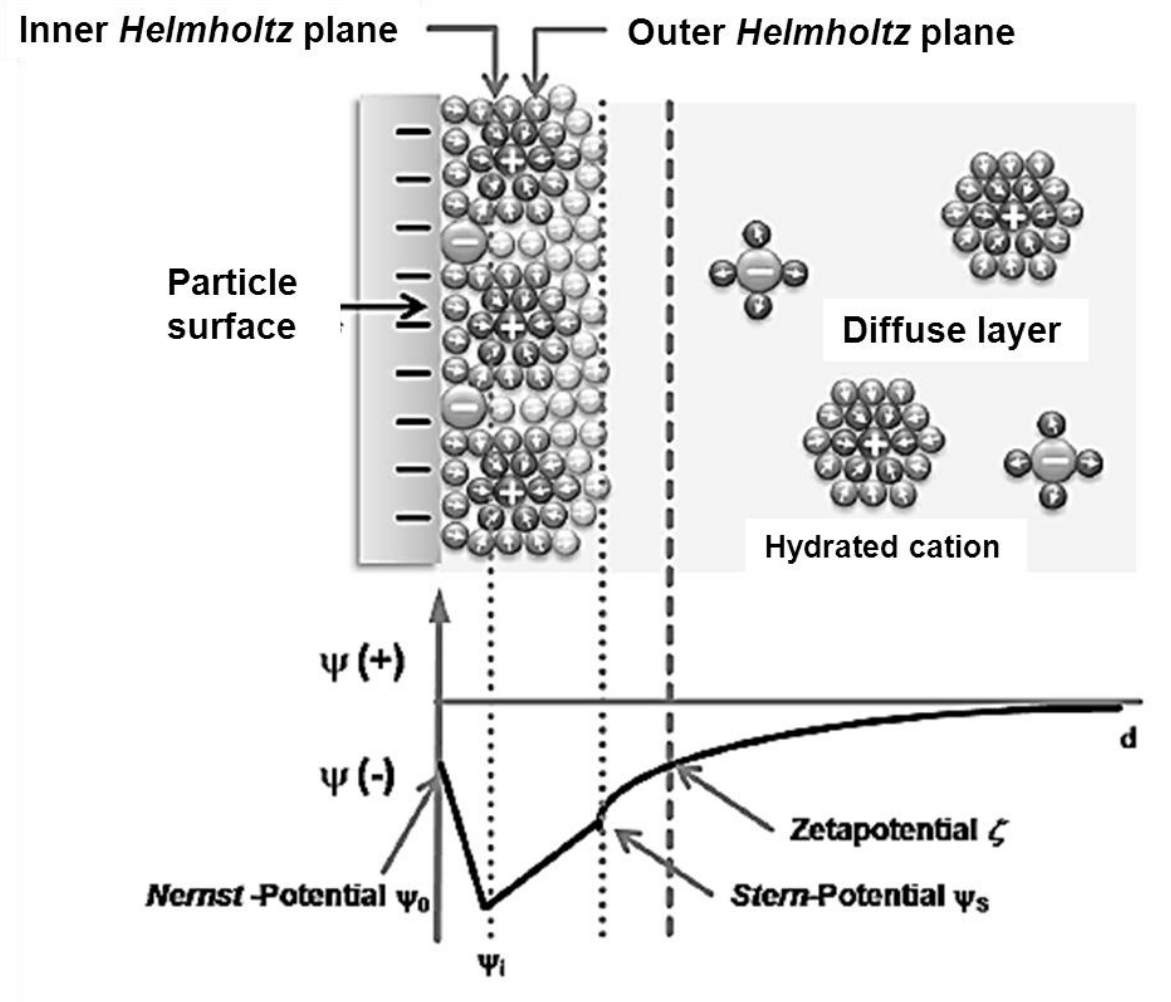

Figure 7. Build-up of the electrochemical double layer (EDL) according to *Bockris* [69].

The surface potential ψ_0 of charged particles is called *Nernst* potential. When dispersed in an electrolyte solution, the surface of charged particles is always surrounded by a layer of non-hydrated anions known as inner *Helmholtz* plane (IHP). In the IHP with the potential ψ_I anions are surrounded by highly oriented water dipoles. The reason for the adsorption of anions also onto negatively charged particles is the dimension of the hydration sphere of anions which is much smaller compared to that of cations. Thus, the strong attractive *Van der Waals* forces override the electrostatic repulsion due to the small distance from the particle surface.

Next, hydrated cations and weakly oriented water dipoles are electrostatically bound onto the IHP and represent the outer *Helmholtz* plane (OHP) holding the potential ψ_S. Inner and outer *Helmholtz* plane together form the so-called *Stern* plane, or layer. The hydration sphere of cations in the OHP has a large steric demand and requires more space compared to the adsorbed non-hydrated anions in the IHP. Thus, the negative charge of the IHP is not completely compensated by cations from the OHP. Complete charge compensation is achieved by the presence of counterions in the diffuse layer (*Gouy-Chapman* layer) where charge is screened completely following an exponential decay within the characteristic length called *Debye* length ($1/\kappa$). The main difference between the *Stern* and diffuse layer is their space requirement and the mobility of the ions. Strong electrostatic interactions between oppositely charged ions within the *Stern* layer lead to the rigid character of this layer which is bound to the particle surface and is composed of immobilized ions. In contrast, ions present in the diffuse layer are weakly sorbed and mobile. The combination of *Stern* and diffuse layer is called electrochemical double layer (EDL) [70, 71].

The thickness of the ion cloud of the diffuse layer can be described with the *Debye* length ($1/\kappa$) which derives from the *Debye-Hückel* theory (**Equation 2**) and depends on the ionic strength of the electrolyte I, the vacuum permittivity ε_0, the dielectric constant ε_r, the *Boltzmann* constant k_B, the temperature T, the *Avogadro* number N_A and the elementary charge e.

$$1/\kappa = \left(\frac{\varepsilon_r \cdot \epsilon_0 \cdot k_B \cdot T}{2 \cdot N_A \cdot e^2 \cdot I}\right)^{1/2} \qquad \textbf{Equation 2}$$

The mobile character of ions and the weak adhesion of the diffuse layer onto the rigid *Stern* layer allow measuring the zeta potential. Zeta potential can be measured via the electrophoretic, electroacoustic or electroosmotic method [72-76]. By applying an electric field on a suspension, movement of particles is induced by electrostatic attraction between the charged particles and the oppositely charged electrode, whereas the dispersion medium remains stationary. Upon particle movement, counter ions present in the diffuse layer are sheared off at the shear plane near the

Stern layer and the resulting potential is determined as zeta potential. The absolute value of the zeta potential significantly depends on the ionic strength of the suspension. With increasing electrolyte concentration an increasing decay of the potential in the diffuse layer is observed which results in different zeta potential values. The potential curve in the diffuse layer depends on the electrolyte concentration and the valency of counter ions. The higher the concentration and valency of counter ions, the lower is the spatial extent of the diffuse layer.

Derjaguin, *Landau*, *Verwey* and *Overbeek* described the total interaction potential between spherical particles in the absence of adsorbed or non-adsorbed macromolecules as the sum of *Van der Waals* attraction and electrochemical double layer repulsion. The attractive and repulsive forces considered in the *DLVO* theory depend on the interparticle distance d. In case of particle collision *Born* repulsive forces occur additionally, but their contribution to the total interaction potential $V_{total}(d)$ is negligible and therefore not considered further. The total interaction potential between two spheres can be described by **Equation 3**, whereby $V_{attractive}(d)$ represents the *Van der Waals* attraction and $V_{repulsive}(d)$ the electrochemical double layer repulsion [77].

$$V_{total}(d) = V_{attractive}(d) + V_{repulsive}(d) \qquad \textbf{Equation 3}$$

Van der Waals attraction occurs at short interparticle distance and originates from interactions due to induced or permanent polarities created in molecules by the electric field of neighboring molecules or due to temporary dipoles caused by a shift of electron density relative to the nuclei. These *Van der Waals* forces can be divided into three categories known as *Keesom* interactions (permanent dipole / permanent dipole interactions), *Debye* interactions (permanent dipole / induced dipole interactions), and *London* interactions (induced dipole / induced dipole interactions). **Equation 4** shows the result of the *Derjaguin* approximation for the *Van der Waals* attraction between two spheres of radii R_1 and R_2 at low interparticle distance, whereby A^H represents the *Hamaker* constant [77].

$$V_{attractive}(d) = -\frac{A_H}{6d} \cdot \left(\frac{R_1 \cdot R_2}{R_1 + R_2}\right) \quad \textbf{Equation 4}$$

For monodisperse colloidal suspensions ($R_1 = R_2 = R$) **Equation 4** can be expressed as follows:

$$V_{attractive}(d) = -\frac{A_H \cdot R}{12d} \qquad \textbf{Equation 5}$$

In comparison, for two spheres of completely different size ($R_1 >> R_2$) **Equation 4** can be modified as follows:

$$V_{attractive}(d) = -\frac{A_H \cdot R}{6d} \qquad \textbf{Equation 6}$$

These results demonstrate that suspensions with monodisperse particle size distribution possess higher colloidal stability compared to polydisperse systems due to the lower *Van der Waals* attractive forces between the colloidal particles.

Depending on their charge, electrostatic forces between the electrochemical double layers of colloidal particles can be attractive or repulsive. Here, it is important to notice that interactions do not occur between the particle surfaces, instead interactions between the electrochemical double layers surrounding the colloidal particles in dispersion need to be considered. **Equation 7** describes the electrostatic repulsion between two spheres which depends on the interparticle distance d, the particle radius a, the permittivity ε, the permittivity of vacuum ε_0, the charge of ions ϑ, the *Faraday* (F) and universal gas constant (R), the temperature T and γ which is represented by the following term: $(e^{z/2} - 1)/(e^{z/2} + 1)$ with $z = \nu F\psi 0/RT$.

$$V_{repulsive}(d) = \frac{a \cdot 32 \cdot \varepsilon \cdot \varepsilon_0}{\vartheta} \cdot \left(\frac{R \cdot T}{F}\right)^2 \cdot \gamma^2 \cdot e^{-\kappa d} \quad \textbf{Equation 7}$$

The electrostatic repulsion strongly depends on the *Debye* length 1/κ and thus on the thickness of the diffuse ion cloud. Here, it becomes obvious that high ionic strength caused by high electrolyte concentrations or multivalent ions lead to significant reduction of repulsive electrostatic interparticle forces.

This relation can also be described with the *Schultz-Hardy* rule which states that the critical coagulation concentration (ccc) varies with the inverse sixth power of the counter ion charge. When salt is added, the electrochemical double layer repulsion is screened whereby *Van der Waals* attraction dominates and induces coagulation [78]. The overall interaction potential considering *Van der Waals* attraction and electrostatic repulsion is illustrated in **Figure 8**.

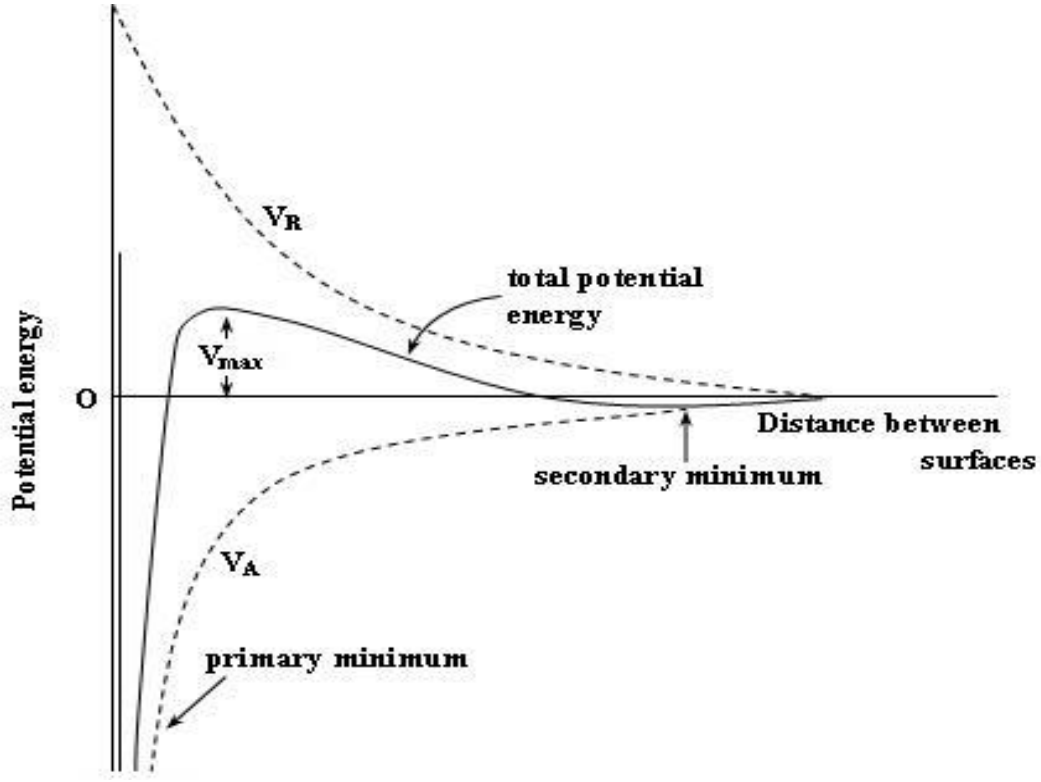

Figure 8. Total interaction potential derived from Van der Waals attractive forces and electrostatic repulsive forces [77].

Steric repulsive forces owed to the presence of adsorbed or non-adsorbed macromolecules are not considered in the *DLVO* theory. However, the steric repulsion which arises from adsorbed polymers on the surface of colloidal particles is even

more effective than the electrostatic double layer repulsion. Polymers adsorbed onto colloids cause steric hindrance between particles and thus prevent them from approaching or contacting each other. The thickness of the adsorbed polymer layer, the so-called adsorbed layer thickness δ, plays an important role for the stabilization, as was described first by *Ottewill* and *Walker* [79, 80] (**Equation 8**). Additionally, the steric repulsive force depends on the concentration of the adsorbate (polymer) in the adsorbed layer C_V, the molecular volume of the solvent molecules ϑ, the density of the adsorbate f_2, the entropy (ψ_1) and enthalpy (κ) parameter, the radius of the adsorbate R and the distance d between two adsorbate particles.

$$V_{steric}(d) = \frac{4 \cdot \pi \cdot k_B \cdot T \cdot C_V^2}{3 \cdot \vartheta^2 \cdot f_2^2} \cdot (\psi_1 - \kappa) \cdot (\delta - d)^2 \cdot (3R + 2\delta + d/2)$$

Equation 8

Non-adsorbed polymers cause the so-called depletion stabilization when present in high concentrations in the dispersion medium. When particles approach each other closer than the radius of gyration R_g of the polymers present, polymer molecules are depleted from the interparticle region. As a consequence, a concentration gradient of polymer between the interparticle region and the dispersion medium is established leading to an osmotic pressure. The osmotic pressure prevents the depletion of polymer molecules from the interparticle region and thus prevents reduction of entropy. This way, dispersions can be stabilized by the presence of high concentrations of water-soluble macromolecules [81].

3.1.5 Latex film formation

In applications such as paints, coatings or mortars, polymer dispersions always undergo a drying step. Due to water loss by evaporation, chemical reaction or a porous substrate a homogeneous polymer film is formed. The quality of the dry latex film which is characterized by its homogeneity or elasticity for example is responsible for the final product properties whereas the properties of the dispersion such as colloidal stability or viscosity only affect the workability of the latex [82].

Generally, the term latex film formation describes the process starting from an aqueous polymer dispersion which is transferred into a homogeneous polymer film. For the evaluation of the film quality and of factors influencing this process, a fundamental understanding of the film forming mechanism is necessary. In literature, early works published by *Bradford* et al. [83, 84] or *Brown* et al. [85] between 1950 and 1960 deal with the film forming process. Modern analysis techniques such as environmental (ESEM) or cryo scanning electron microscopy [86-91], atomic force microscopy (AFM) [92-97], small-angle neutron scattering (SANS) [98-106], ellipsometry [88, 89, 107, 108] or fluorescence resonance energy transfer (FRET) [109-114] have significantly contributed to the development of a fundamental understanding of the film forming process. Particularly non-destructive techniques allowing an in-situ observation of the drying latex (e.g. ESEM) without inducing film formation during measurement had a major contribution.

Based on the actual state of the art, the mechanism of polymer film formation can be described by four characteristic stages occurring along the temporal path upon drying, particle deformation and coalescence (**Figure 9**). Starting from an aqueous latex dispersion (stage I) the concentration of latex polymer increases continuously upon water removal until the latex particles arrange in a dense packing (stage II). Interparticle spaces are still filled with water at this stage. The packing density of latex particles is determined by their average particle size and its distribution.

After water removal from the interparticle spaces, particle deformation (phase III) occurs at temperatures above the minimum film forming temperature (MFFT) whereby interparticle spaces disappear upon the formation of a hexagonal honeycomb structure. The thermodynamic driving force for particle deformation is the reduction of the free surface energy by minimization of the polymer/air interface. At this stage, the individual latex particles can still be clearly distinguished from each other whereby emulsifier molecules located on the surface of the latex particles form a hydrophilic boundary layer and thus separate the individual particles. Additionally, water-soluble oligomers, co-monomers or salts contained in the serum phase accumulate in this boundary layer.

Coalescence of the latex particles occurs when the ambient temperature exceeds the glass transition temperature of the polymer. Here, interfaces between the latex particles break up and polymer chains of the individual particles diffuse into each other (interdiffusion) resulting in a coherent and transparent polymer film (stage IV). Depending on the drying conditions, hydrophilic constituents such as emulsifier molecules are either entrapped in the polymer film or sequestered on the surface.

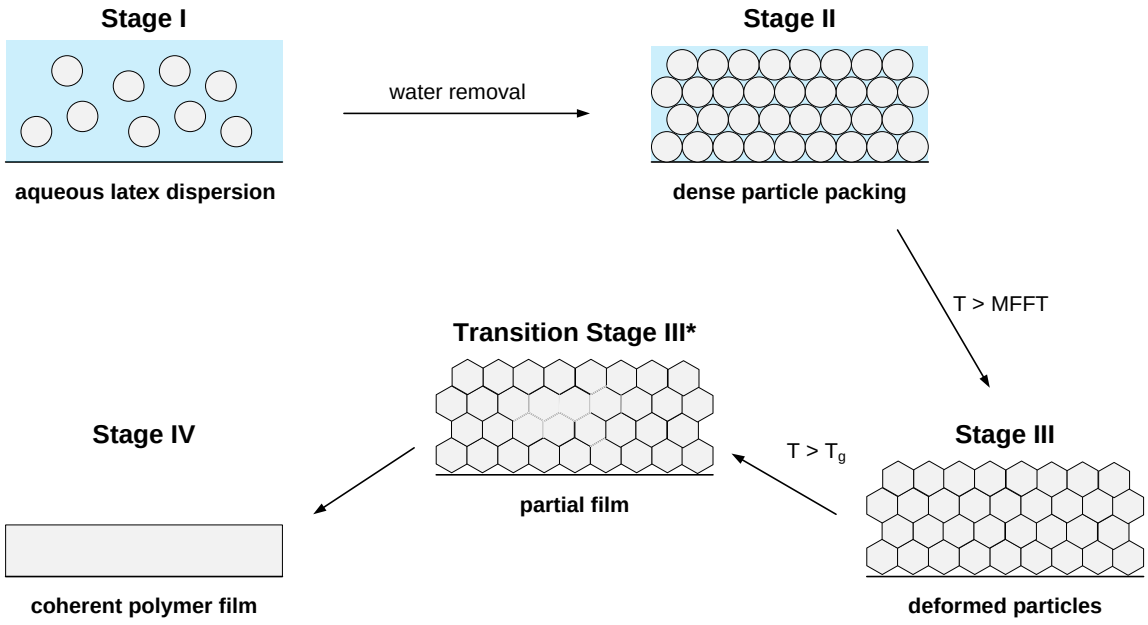

Figure 9. Schematic illustration of the four-stage model for the mechanism of latex film formation.

In the literature several works described the influence of emulsifiers, co-monomers or salts on the film forming process [18]. It was shown that the presence of electrolytes in the serum phase impacts particle coalescence. For the film formation of latices which are applied in cement-based construction materials, especially the influence of salts is of great interest since cement pore solutions represent highly saline media. In the study here, the focus was on the effect of the spraying aids PVOH and kaolin contained in re-dispersible latex powders.

For example, *Keddie* et al. [115] investigated the drying of latex dispersions in the presence of salts and observed that film formation is not only influenced by the concentration and valency of the ions in the salt, but also by their particular chemistry. *Erkselius* et al. [21] studied the film formation of latex dispersions with varying concentrations of sodium dodecylsulfate and sodium persulfate by using a sorption balance. The authors observed a significantly decreased drying rate with increasing volume fraction of polymer.

Plank et al. [20, 116] monitored the time-dependent film formation of a carboxylated styrene-butylacrylate copolymer in water and synthetic cement pore solution via environmental scanning electron microscopy. The study revealed that in cement pore solution film formation is significantly retarded compared to the aqueous system. This effect is due to the presence of calcium ions. Cations adsorb onto the anionic latex particle surfaces, thus forming a dense layer surrounding the particles which hinders subsequent interdiffusion of polymer chains.

Similar investigations were performed by *Plank* et al. [117] for a liquid ethylene-vinylacetate latex dispersion which was stabilized with PVOH. Opposite to the anionic styrene-acrylate latex, film formation in synthetic cement pore solution occurred faster than in water. This effect was ascribed to the presence of the colloidal stabilizer PVOH on the surface of the latex particles. In water, PVOH forms a shell around the latex particles which presents a diffusion barrier for the macromolecules and thus hinders particle coalescence. In cement pore solution PVOH becomes insoluble and precipitates, thus this polymeric barrier between the latex particles is removed,

which leads to a faster film formation. Exactly the same result was observed for the non-ionic EVA copolymer in this study.

Recent research works [118-123] evidenced that at the stage of dense particle packing latex particles can arrange in ordered domains similar to colloidal crystals. Furthermore, the effect of self-assembling of colloidal particles was also observed for colloidal silica particles, for example [121, 124-129]. As was reported by several authors, such arrangement of latex particles in highly ordered domains only occurs when the rate of water evaporation is slow enough. Additionally, in this study it was found that for film forming latices which arrange in such highly ordered domains (colloidal crystals) at the stage of dense particle packing, particle interdiffusion first begins in these domains before it spreads across the entire film. This effect was ascribed to the higher packing density within these colloidal crystals compared to the surrounding particle packing. Furthermore, such crystallization of latex particles was only observed for monodisperse latices.

The individual steps of drying, particle deformation and coalescence are rather complex and therefore in the following are discussed further from a scientific point of view.

a) Drying / water evaporation

Water evaporation (drying) from an aqueous latex dispersion follows a complex mechanism and influences the mechanical properties of the resulting polymer film. *Winnik* et al. [130, 131] distinguished between three different drying modes (homogeneous, vertical or lateral drying) which occur simultaneously during latex film formation. Homogeneous drying is characterized by a uniformly distributed water concentration in the drying film.

Vertical drying describes the transport of water in vertical direction to the film surface, meaning that water evaporates from the top of the latex film towards the substrate. As a consequence, the top of the film dries faster compared to the regions near the substrate which leads to the formation of a polymer skin near the interface

region to the air (**Figure 10**). *Vanderhoff et al.* [132] published the first paper where vertical drying was observed. He studied the drying of latex dispersions gravimetrically and developed a three-stage model of the drying process which was complemented by the findings of other authors. For example, *Sheetz* [133] described that the film surface contains much less water than the interior region due to the accumulation of latex particles on the surface of the drying latex film. *Croll* et al. [134] confirmed these results and additionally observed a layer of coalesced film above the wet latex. *Eckersley* and *Rudin* [135] demonstrated that this skin is porous enough that water transport through this polymer layer is still possible. *Okubo* et al. [136] showed that a skin is only formed on the film surface when the latex flocculates in the interface region. When the latex is stabilized and flocculation is prevented skin formation does not occur. *Routh* and *Russel* [137] showed that a skin is expected to form when the convection induced by the negative capillary pressure transports more latex particles from the bulk to the region near the surface than are transported back to the bulk via diffusion.

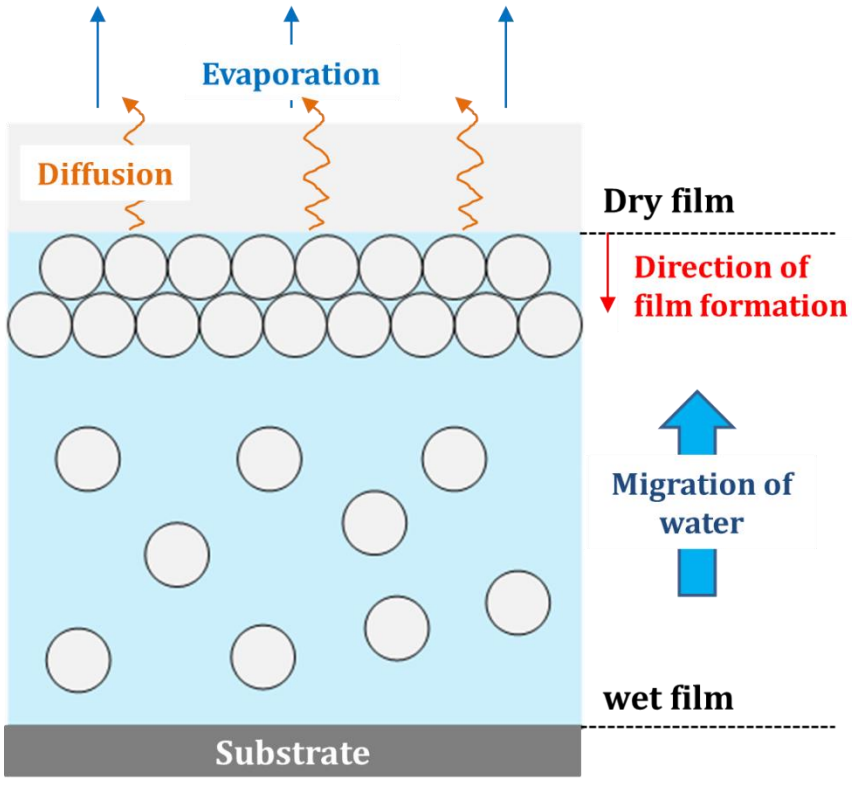

Figure 10. Schematic illustration of the vertical drying of a latex film which causes the formation of a skin on the surface of the drying film.

Based on these works the following model of vertical drying is commonly accepted: first, water evaporates quickly at a constant rate similar to that of pure water or latex serum in vertical direction. Second, the evaporation rate is diminished at the water/air interface due to the accumulation of latex particles in the region near the water/air interface. Thus, the total water/air interface is reduced and evaporation slows down. In the third step, water can only escape by diffusion through a layer of a dry polymer film. As a consequence, the evaporation rate is further decreased and controlled by diffusion and thus depends on the thickness of the dry film.

Lateral drying leads to a coalescence front which starts from the edges and is moving to the center of the film (**Figure 11**). *Hwa* [138] first observed lateral non-uniformity in the drying rates of an acrylic latex. He described the existence of three characteristic regions in the plane of the drying latex film (horizontal direction). The center of the drying film was found to be wet and turbid, whereas the peripheral region showed optical transparency. These two regions were separated by a partly cloudy region. Similar observations were made by *Sheetz* [133] and *Croll* [134], but also other authors confirmed these results [139-147].

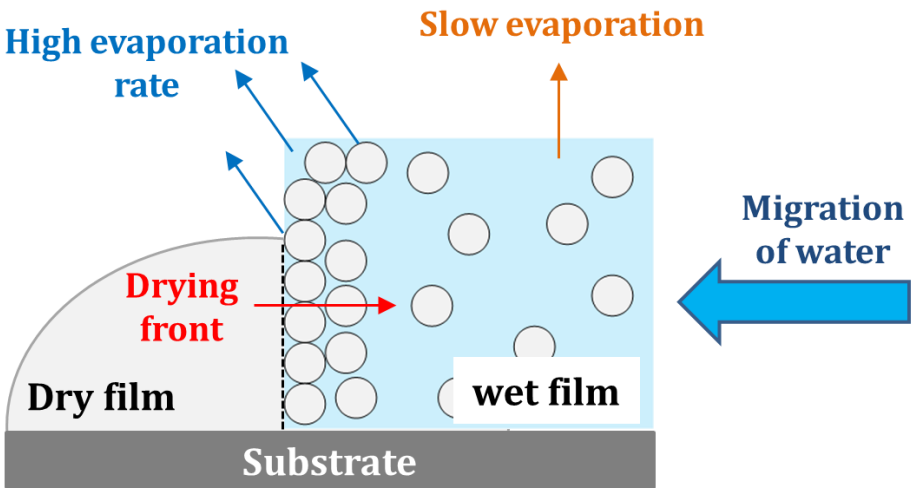

Figure 11. Schematic illustration of lateral drying of a latex film.

Nowadays it is known that due to the contact angle of water the thickness of the drying latex near the edges is lower compared to the center of the film. Thus, film regions near the edges dry faster whereby water is depleted in this peripheral region

first which leads to a gradient in the concentration of water in horizontal direction. In order to compensate this concentration gradient, water migrates from the center of the film to the peripheral region where a large air/water interface causes fast water evaporation. Due to this lateral water migration within the drying latex the evaporation rate in vertical direction is slowed down. The result is a drying front moving from the edge to the center of the film. Upon lateral drying, water soluble compounds contained in the serum phase are preferred to concentrate in the center of drying latex films.

Routh and *Russel* [137, 146] developed a model which describes the mode drying will proceed, either as drying front in horizontal direction or as a compaction front in vertical direction. Depending on the *Peclet* number (Pe) which defines the ratio of the rate of water evaporation and particle diffusion one can differentiate between vertical and horizontal drying. When diffusion controls the transport of matter ($Pe << 1$), particles are uniformly distributed in vertical direction of the drying latex film and thus lateral drying occurs as a moving front in horizontal direction. When the evaporation rate overrides the diffusion ($Pe >> 1$), particles are not uniformly distributed in the vertical direction and a skin composed of latex particles is formed at the surface of the drying latex which further grows with time.

The differences between vertical and lateral drying need to be considered especially in applications such as paints or coatings where the latex is applied on a large area onto the substrate. Cement-based mortars, where a minor amount of latex is mixed together with other solids, represent a completely different system where these different drying modes mostly can be ignored. In this study, the film forming process was investigated via ESEM. Therefore, latex films with a thickness of around 10 µm were spread on an ESEM sample holder with a diameter of 7 mm. Here, it was found that the rate determining steps for the film formation are the particle deformation and interdiffusion, whereas the drying modes can be ignored as well due to the very small film area.

b) Particle deformation

For film forming latices it was found that particles undergo deformation during the film forming process, whereas non film forming latices show less or no deformation in comparison. Upon particle deformation, interparticle voids are eliminated and the overall surface free energy is minimized. As driving forces for particle deformation, tensions occurring at the water/air, polymer/water or polymer/air interfaces, as well as osmotic or adhesive forces (interfacial tensions) are considered in the literature.

Brown [148], *Lin* and *Meier* [149, 150] and *Tirumkudulu* and *Russel* [142] suggested that the capillary forces on the air/water interface play an important role for particle deformation and called this effect 'capillary deformation'. *Dobler* [151] as well as *Eckersley* and *Rudin* [152] confirmed these results but reported that capillary forces only initiate the deformation of particles, whereas polymer/water or polymer/air interfacial tensions cause subsequent deformation.

Dillon et al. [83] and other authors [153, 154] considered the polymer/air interface of dried latices. They claimed that the latex first dries completely before particle deformation occurs. According to *Frenkel's* theory the deformation caused by the polymer/air interfacial tension was called 'dry sintering', an expression which was derived from metallurgy.

Other authors [133, 151, 155] suggested that the interfacial tension between polymer and water induces particle deformation ('wet sintering'). According to their theory, at first capillary forces press particles into close contact. When the repulsion between their electrochemical double layers is overcome, the polymer/water interfacial tension causes deformation of the latex particles.

Sheetz [133] described an osmotic force which causes particle deformation ('*Sheetz* deformation'). According to his theory, vertical drying causes the accumulation of latex particles on the surface of the drying film. This layer of latex particles acts as a membrane which is permeable for water on top of the wet latex and thus allows further evaporation of water. When water diffuses through this permeable membrane

to the film surface a compressive force vertical to the polymer layer is generated which causes particle deformation.

c) Particle coalescence

The minimum film forming temperature (MFFT) is determined on the so called *Kofler* bench. A temperature gradient is applied on a metal plate and a thin film of the latex dispersion is spread on it. At a specific temperature, the minimum film forming temperature (MFFT), optical clarity of the film is observed. Above the MFFT latex particles of the dense particle packing start to deform. Upon particle deformation, interparticle voids are much reduced whereby light is no longer scattered by heterogeneities in the refractive index. Here, it is important to note that a transparent film does not necessarily represent a coherent and homogeneous film where interdiffusion of the latex particles is complete. This observation was also confirmed in this study. By using environmental electron microscopy it was found that transparent films often are composed of a dense packing of deformed particles.

The application of modern analysis techniques such as small angle neutron scattering (SANS) or fluorescence resonance energy transfer (FRET) could evidence that particle interdiffusion occurs during film formation. *Hahn* et al. [156] came up with an evidence on a deuterated acrylate-based latex polymer by using SANS. *Johannsmann* et al. [110] and *Winnik* et al. [109] revealed the occurrence of particle coalescence via FRET. The concentration profile of a chromophoric donor-acceptor-pair between two isolated particles and a homogeneous film can be distinguished. Additionally, this study showed that interdiffusion is required in order to achieve the final mechanical properties of the film. Only if the molecules entangle over a distance in the order of the radius of gyration of the polymer, the maximum mechanical strength can be achieved for a polymer film.

In this study here, the progress in the film forming process was monitored using environmental scanning electron microscopy. In several publications it was demonstrated that ESEM is a suitable method for evaluation of the film formation [86, 89, 157-159].

3.1.6 Application of latex polymers in cement-based construction materials

Hydrated cement mortars represent hard and brittle materials characterized by their poor adhesion onto substrates whereby many difficulties arise for the application in thin layers. Latex polymers can be used as sole organic binders (e.g. in paints or coatings), but also as co-binders in cement-based construction applications. Typical applications for latex polymers in cement-based systems are tile adhesives or grouts, adhesive or basecoat mortars for EIFS, repair mortars, self-leveling underlayments, plasters or waterproofing membranes. The addition of latex polymers improves the adhesion of the fresh and hardened mortar onto substrates, as well as its flexural strength. Furthermore, the density and thus the durability, as well as the abrasion resistance of mortars can be improved by latex addition. As illustrated in **Figure 12**, the polymer-to-cement ratio represents the key for the improvement of these material properties.

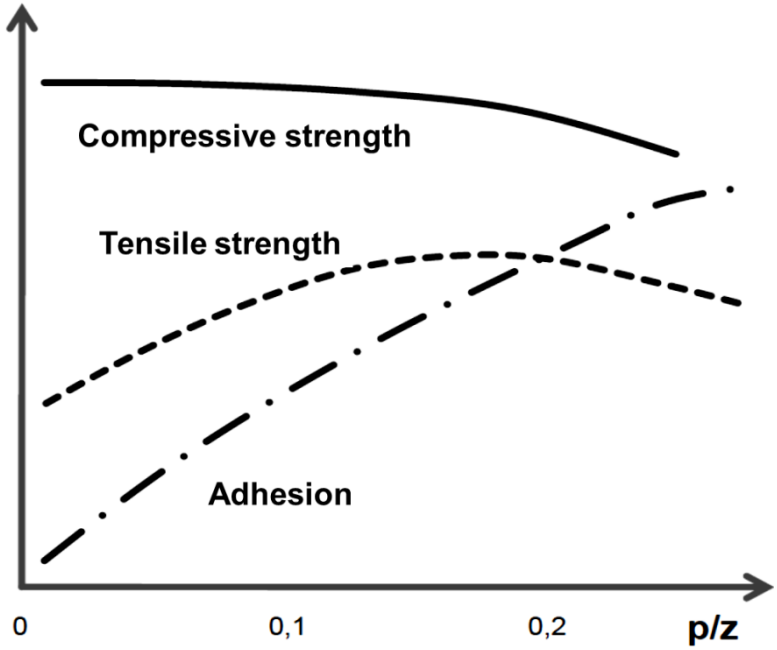

Figure 12. Dependence of compressive, tensile and adhesion strength of mortars from the polymer to cement ratio [160].

Fundamental properties of latex dispersions or re-dispersible powders used in construction are colloidal stability and film forming ability under application conditions. For example, polymers used in cement-based systems are required to

exhibit colloidal stability and film forming ability in highly saline cement pore solution. Furthermore, the glass transition temperatures of latex polymers are adjusted to temperatures below the application temperature by combining monomers with high and low T_g. Polymers for construction applications are based on the following chemistries:

- poly(vinylacetate)
- ethylene-vinylacetate copolymers
- styrene-acrylate copolymers
- styrene-butadiene copolymers
- vinylacetate-vinylversatate copolymers
- ethylene-vinylacetate-vinylversatate terpolymers
- vinylacetate-vinylversatate-acrylate terpolymers

Copolymers based on vinylesters or acrylates are not stable against hydrolysis. Especially in the alkaline cement pore solution, the ester groups of such monomer units undergo saponification. Hence, these polymers possess low alkali resistance. For example, ethylene-vinylacetate copolymers are well known to hydrolyze in alkaline medium, following the reaction shown in **Figure 13**.

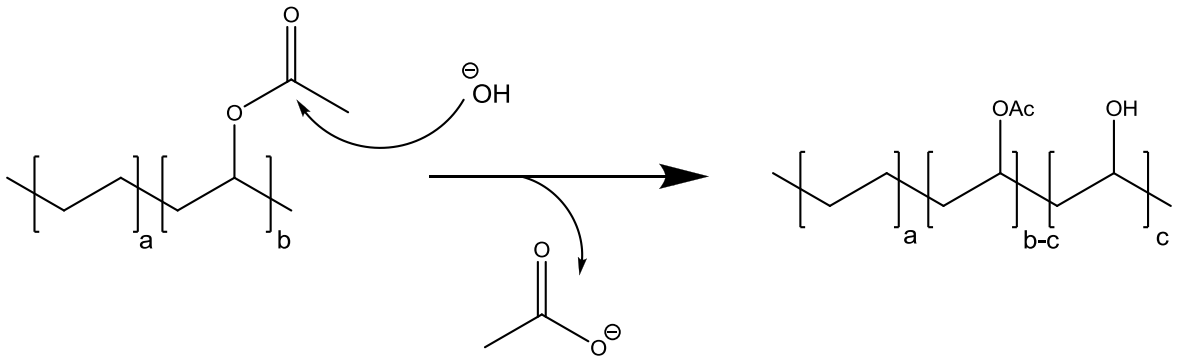

Figure 13. Hydrolysis of the ester group in vinylacetate of EVA latex polymers under elimination of acetate.

For improving alkali resistance of vinyl or acrylate-based polymers, more unconventional monomers such as vinylesters of versatic acid (VeoVa) have been

incorporated. Typically, the vinylester of neodecanoic acid, a saturated monocarboxylic acid with a highly branched structure containing ten carbon atoms (structure see **Figure 14**) is used in construction applications. The incorporation of this highly branched aliphatic structure of neodecanoic acid into a copolymer sterically protects the ester bonds of VeoVa, but also of adjacent monomer units against hydrolysis resulting in enhanced alkali or chemical resistance. Additionally, the hydrophobicity of such copolymers is improved by incorporation of VeoVa monomer, whereby resistance to water or other polar liquids, as well as leveling and adhesion are improved. This way, VAE-VeoVa polymers are highly recommended for self-leveling flooring compounds [161]. Self-leveling flooring compounds are formulated with 2 – 8 % copolymer such as ethylene-vinylacetate, styrene-acrylate or vinylacetate-vinylversatate copolymers.

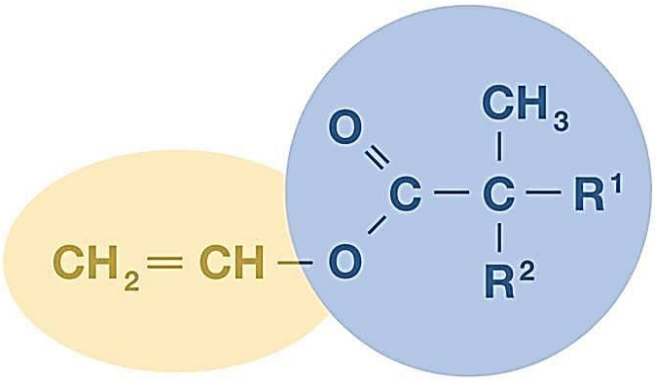

Figure 14. Chemical structure of the vinylester of versatic acid. The total amount of carbon atoms in versatic acid is 10. The alkyl groups R^1 and R^2 contain 7 carbon atoms in total [161].

Generally, non-ionic copolymers (e.g. EVA) show good performance in gypsum-based systems such as crack fillers, due to their better compatibility with calcium ions as compared to anionic latex polymers. Also, in gypsum-based mineral binders hydrolysis of ester-based copolymers such as EVA is less pronounced due to the lower pH value of the binder paste.

Tile adhesives are the most common application for latex polymers in cement-based construction materials. Here, a large variety of different latex polymers (e.g. styrene-

acrylate, vinylacetate-ethylene, vinylacetate-vinylversatate, vinylacetate-vinylversatate-ethylene or styrene-butadiene) is used for mortar-modification. The quality of the tile adhesive much depends on the polymer dosage which is typically between 2 and 5 %. Recent results published by *Zurbriggen* [162] showed that failures in tile adhesives are often not caused by the poor performance of the latex polymers, but instead by processing defaults. Especially the time period between spreading of the mortar and tiling (open time) was found to be the main source of failure. When the mortar is spread on the substrate an extremely high surface area is exposed to the surrounding air. This way, the uppermost layer of the adhesive mortar undergoes carbonation whereby a salt crust with a thickness of several micrometers is formed. Furthermore, water-soluble polymers such as the colloidal stabilizer PVOH migrate to the interface. These two effects prevent subsequent film formation of the latex polymer on the transition zone to the ceramic tile.

Waterproofing membranes (sealing slurries) need to be impermeable for water and thus require high water and alkali resistance, but also high elasticity for crack-bridging, meaning that cracks formed in the substrate (e.g. masonry) may not induce crack-formation in the waterproofing membrane. In order to achieve these properties extremely high polymer-to-cement ratios (0.3 – 0.8) are required in the application. Especially highly hydrophobic polymers such as styrene-butadiene, styrene-acrylate or ethylene-vinylacetate prevent migration of water and therefore show unique performance in mineral sealing slurries. Typically, such sealing slurries are used in bathrooms, swimming pools, underground parking lots, basement walls or foundations to effectively protect floors and walls from moisture.

Polymeric binders also represent highly important ingredients for adhesive and basecoat mortars for external insulation & finishing systems (EIFS). They guarantee adhesion of the mortar to all substrates (e.g. connection exterior wall / insulation panel or insulation panel / plaster) and provide high elasticity which is required to prevent crack formation caused by different thermal expansion coefficients of the materials used. **Figure 15** shows the composition of a typical external insulation & finishing system.

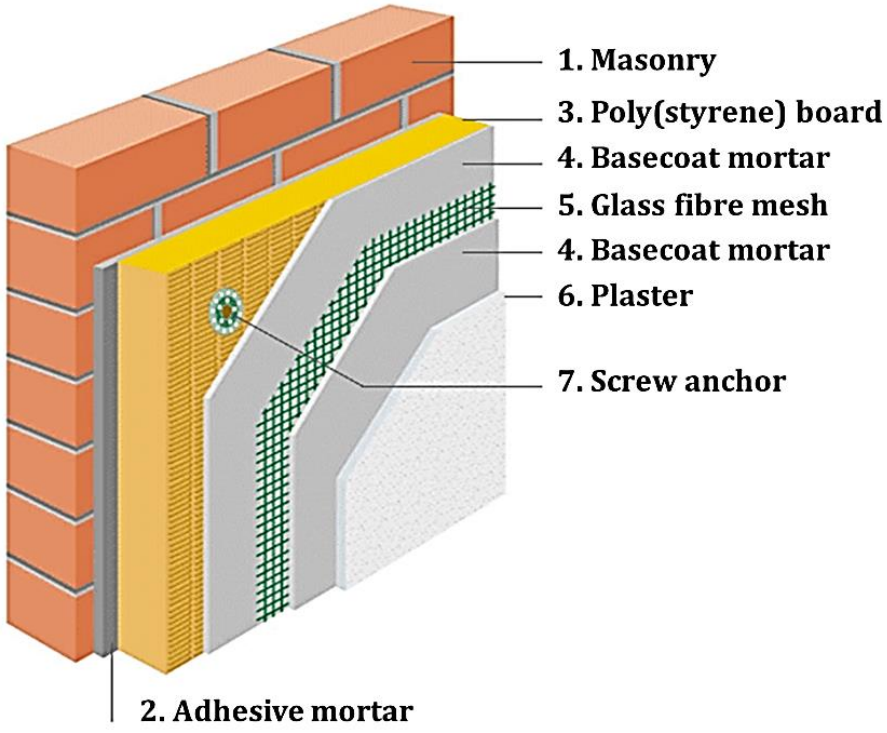

Figure 15. Composition of an external insulation & finishing system (EIFS) [163].

Here, the poly(styrene) insulation board is connected to the exterior wall via an adhesive mortar containing polymeric binder. Then, a glass fibre reinforced basecoat mortar is applied on top of the insulation panel before the plaster and finally the paint are spread on it. The organic poly(styrene) panels exhibit a different thermal expansion coefficient compared to the surrounding mineral masonry and plaster, thus leading to crack formation at temperature changes. The basecoat mortar provides high elasticity and therefore prevents crack formation in the mortar, but also in the connected materials. In the development of such polymer-modified basecoat mortars application tests such as heat resistance provide important information about the performance of the product. Typically, ethylene-vinylacetate-vinylchloride terpolymers are applied in mortars for EIFS due to their low inflammability which is another important quality criterion with respect to safety. This property is mainly provided by the vinylchloride monomer. Less often styrene-acrylate or vinylacetate-vinylversatate copolymers are used.

3.2 Inorganic binders

Dry mortars are usually composed of a mixture of mineral and polymer binders. Ordinary Portland cement represents the main mineral binder in dry mortar products, but it is often combined with calcium aluminate cement or calcium sulfates in order to control setting and shrinkage of the mortar. Such binary or ternary mineral binder systems show different reactivity compared to their individual components and therefore are discussed further in this chapter.

3.2.1 Portland cement

One of the most important product requirements for Portland cements used in dry mortar applications is their constant product quality, meaning that Portland cements originating from different production charges exhibit nearly the same clinker composition. This issue is challenging due to the varying chemical composition of the raw materials. The main reason for this demand is the sensitivity of chemical admixtures contained in dry mortars to clinker phases or side products.

Ordinary Portland cement is produced by calcination of calcium oxide (CaO), silicon oxide (SiO_2), aluminum oxide (Al_2O_3) and ferric oxide (Fe_2O_3) typically stemming from limestone, chalk or marl combined with shale, clay, slate, blast furnace slag, silica sand or iron ore. These raw materials are gradually heated to a temperature of around 1,450 °C in a rotary kiln whereby the clinker phases alite (C_3S), belite (C_2S), tricalcium aluminate (C_3A) and tetracalcium aluminate ferrite (C_4AF) are formed in a partial smelting. During the burning process, the metastable clinker phases are doped with metal ions which prevent the conversion to their thermodynamically stable compounds, but also increase their hydraulic activity. In order to prevent conversion of metastable alite into less reactive belite, and of hydraulically very reactive β-belite into non-reactive γ-belite, the partial melt is immediately quenched after calcination. Finally, the ceramic clinker is grinded in ball mills and mixed with a calcium sulfate source (e.g. gypsum) as set-regulator whereby the clinker powder is obtained. The

mass content of cement clinker in ordinary Portland cement (CEM I) is at least 90 % [164-166].

Cement hydration is referred to as the reaction of cement clinker with water under formation of water-containing compounds called cement hydrate phases which cause setting and strength development of cement pastes. In the hydration of the silicate phases C_3S and C_2S, calcium silicate hydrates (C-S-H) with varying composition are formed depending on the water-to-cement ratio. For example, at a w/c ratio of 0.45 the C-S-H phase $C_3S_2H_3$ is formed. Generally, the composition of the C-S-H phases can vary between jennite ($C_9S_6H_{11}$) and tobermorite ($C_5S_6H_9$). The reaction pathway for the hydration of the silicates is shown in **Figure 16**.

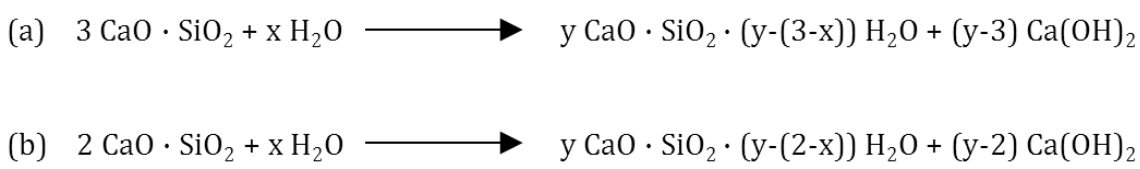

Figure 16. Hydration reactions of (a) C_3S and (b) C_2S under formation of C-S-H phases and portlandite ($Ca(OH)_2$).

The solubility of alite in water is higher compared to that of belite, leading to much faster hydration of alite. Portlandite ($Ca(OH)_2$) is formed as side product in the hydration of the silicates and thus contributes to the alkaline pH of at least 12.5 of cement pastes. The dense matrix of interlocked nano-sized and needle-like C-S-H phases is primarily responsible for the strength development of cement.

The hydration of tricalcium aluminate (C_3A) strongly depends on the concentration of sulfate in cement pore solution. In the absence or at low concentrations of sulfate, calcium aluminate hydrate phases (C-A-H) which represent hydrocalumite-type layered double hydroxides (LDH) are formed immediately after mixing with water, due to the high solubility of C_3A. These thin and foil-like C-A-H crystals bridge the pore space in the cement paste and thus induce sudden setting. This reaction proceeds via C_2AH_8 and $C_4AH_{13\text{-}19}$ as intermediates under formation of cubic katoite (C_3AH_6) as the thermodynamically stable hydration product.

At sulfate concentrations in cement pore solution above 2.35 mg/L, ettringite ($C_3A\bar{S}_3H_{32}$) is formed in a topochemical reaction from C_3A and through homogeneous nucleation in solution, whereby a prolonged workability of the cement paste is assured. When the sulfate concentration drops to lower concentrations, ettringite is transformed into monosulfate ($C_3A\bar{S}H_{12}$). **Figure 17** describes the hydration reaction of tricalcium aluminate.

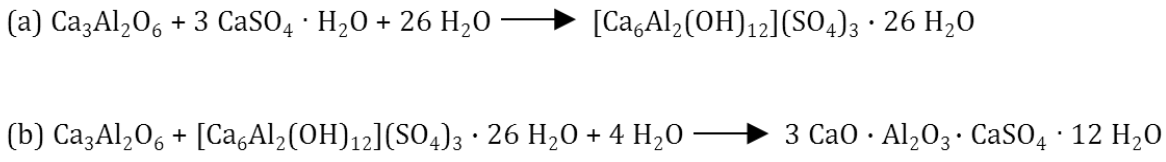

Figure 17. Hydration reaction of C_3A. (a) Formation of ettringite from C_3A and gypsum and (b) conversion of ettringite into monosulfate.

The hydration reaction of tetracalcium aluminate ferrite (C_4AF), and especially the role of iron during the hydration are not completely understood even until today. Generally, two theories describing the hydration reaction of the ferrite phase are discussed in the literature. *Taylor* [166] describes the hydration reaction of C_4AF in the presence of sulfate similar to that of C_3A. First, iron ettringite is formed which then converts into iron monosulfate and iron hydroxide. According to *Stark* [167], aluminate is leached from the ferrite phase into pore solution and further reacts together with sulfate and calcium hydroxide under formation of ettringite. The ettringite formed via this pathway is free of iron and also converts into monosulfate at lower sulfate concentrations. As a result, aluminate is leached more and more from the ferrite phase which accumulates iron.

For the interaction of cement with organic admixtures, its colloidal properties in aqueous suspension need to be considered. Generally, cement grains develop a heterogeneous surface charge, meaning that some areas exhibit positive charge, while others are negatively charged (mosaic charge structure). This effect can be ascribed to the different surface charges of the silicate (negative) and aluminate (positive) phases. Furthermore, hydrate phases such as ettringite (positively charged) represent adsorption sites for organic compounds.

3.2.2 Calcium aluminate cement

Calcium aluminate phases contained in calcium aluminate cement react with water under formation of calcium aluminate hydrates. Due to the high content of aluminates in CAC this binder shows special characteristics such as rapid setting or strength development, high sulfate resistance and excellent thermal and chemical resistance.

The production of calcium aluminate clinker can be achieved by either sintering or fusion of the raw materials and subsequent grinding of the clinker. Typical raw materials for CAC are bauxite and limestone. The main clinker phase in CAC is monocalcium aluminate (CA) which is highly reactive when getting in contact with water. Less reactive constituents of CAC include CA_2 and $C_{12}A_7$ (mayenite) [168]. By using raw materials with low SiO_2 contents the amount of silicate clinker (C_2S or C_2AS) formed in the mixture is negligible. According to *Smirnov* et al. [169], these cement powders which are almost white can be described via the binary system CaO/Al_2O_3. Depending on the aluminum content of CAC which can vary between 38 and 82 wt.% it can be divided into different quality grades. The content of iron oxide (0 – 25 wt.%) determines the color of the cement.

Crystals of monoclinic monocalcium aluminate (CA) show pseudo-hexagonal prismatic morphology. The crystal structure of CA was described by *Hörkner* and *Müller-Buschbaum* [170]. The fundamental building blocks are AlO_4-tetrahedra which are linked to six-membered rings via their edges. Several of such six-membered rings form a two-dimensional stack of infinite layers whereby in the interlayer space calcium ions are incorporated between the AlO_4 tetrahedra for charge compensation.

Ramachandran and *Feldman* [171] and *Sorrentino* et al. [172] reported that the kind of calcium aluminate hydrate formed during the hydration reaction depends on the temperature. The thermodynamically stable products of CA are C_3AH_6 (katoite) and AH_3 (gibbsite).

The application of CAC for primary structures is not permitted in Germany since 1962 because at room temperature the hydrate phases CAH_{10} and C_2AH_8 represent metastable compounds which convert into thermodynamically stable katoite and aluminum hydroxide. This process comes with a significant strength retrogression.

3.2.3 Binary and ternary binder systems

Several drymix mortar applications such as tile adhesives, repair mortars or self-leveling underlayments require fast setting and adequate final strength. Therefore, mixtures of Portland cement, calcium aluminate cement and calcium sulfate combining the rapid setting of CAC with the high final strength of OPC are applied. Calcium sulfates mainly control the hydration reaction depending on their solubility. Mixtures of two mineral binders such as OPC and CAC are referred to as binary binder systems, whereas mixtures of three binder components such as OPC, CAC and anhydrite are called ternary binder systems [173].

Mixtures of Portland cement and calcium aluminate cement represent typical binary binder systems. Several works published in the literature describe the setting and strength development of such binary OPC/CAC mixtures. *Cottin* [174] examined the initial and final setting of mixtures of Portland cement and ferrous calcium aluminate cement at room temperature. As is shown in **Figure 18**, the hydration of both cements is accelerated at any mixing ratio. Dosages between 40 and 80 wt.% of Portland cement lead to maximum acceleration of this binary binder mixture.

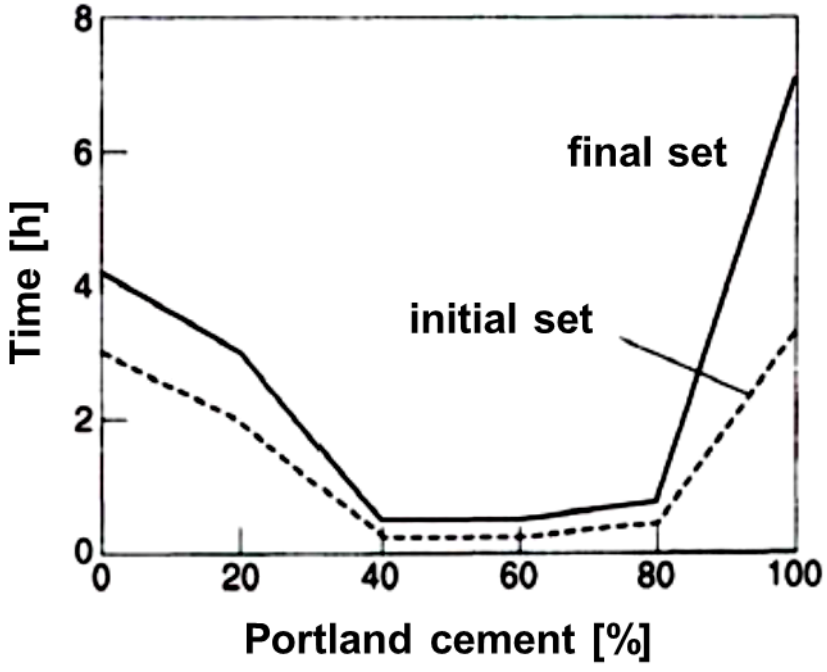

Figure 18. Initial and final setting times of OPC/CAC mixtures [172].

However, the setting time not only depends on the mixing ratio of OPC and CAC, but also on the water-to-cement ratio and the temperature. In rapid hardening systems, especially the amount and type of calcium sulfate present in the mixture, as well as the content of monocalcium aluminate (CA) in CAC are important parameters.

Scrivener and *Campas* [173] reported that even small additions of calcium aluminate cement holding high monocalcium aluminate content strongly accelerate the setting of OPC. *Gu* et al. [175] showed that in OPC/CAC binary cement pastes, ettringite can be formed in the first few minutes of the hydration, mainly through the reactions of monocalcium aluminate with gypsum, calcium oxide and water or from tricalcium aluminate, gypsum and water. In such systems, OPC normally provides the sulfate, whereas CAC is the primary source of aluminates. The amount of ettringite formed depends on the ratio of aluminate and sulfate, and ideally should be around 1.43. This result explains why any mixture of OPC and CAC leads to an accelerated setting and an increased early compressive strength due to ettringite formation.

Bensted [176] claimed that the products CAH_{10} and C_2AH_8 formed from CA and C_3A hydration contribute to the early strength of OPC/CAC binary systems, but this conclusion was rejected by other authors [174]. Furthermore it has been shown that the silicate reaction is delayed in OPC/CAC mixtures, leading to a slow strength development. C_3A seems to remain unreacted until the conversion of early hydration products is completed. Similar results were found for ternary binder mixtures composed of OPC, CAC and anhydrite.

Zhang et al. [177] reported that ettringite formed from sulfate depleted cement pastes possessing an excess of aluminates converts into monosulfate. According to *Amathieu* et al. [7], ettringite is not formed topochemically on C_3A grains in OPC/CAC mixtures, and thus passivation of clinker grains is prevented. When the content of CA is high enough to capture the sulfate completely, no sulfate ions for the reaction with C_3A are present anymore. This way, passivation is prevented and an uncontrolled reaction of C_3A with water leads to rapid setting of OPC/CAC mixtures.

Bayoux et al. [8] studied the impact of the solubility of the calcium sulfate in CAC/calcium sulfate mixtures on the hydration reaction and morphology of ettringite. They distinguished between two reaction pathways, depending on whether the sulfate salt dissolves faster or slower compared to monocalcium aluminate (CA). By using sulfate salts such as hemihydrate with better solubility compared to CA, short and more compact ettringite crystals are formed, whereas by using a slowly dissolving sulfate such as anhydrite, ettringite crystallizes as long and thin needles.

Drymix mortars are often formulated with ternary binder systems composed of Portland cement, calcium aluminate cement and calcium sulfate. The reactivity of such systems is controlled by the ratio of the individual binders, and especially by the solubility of the calcium sulfate salt. The role of calcium sulfate is to provide sulfate ions in cement pore solution which then react with the aluminates under ettringite formation, as discussed above. Hence, this reaction is greatly influenced by the solubility of the calcium sulfate, which varies between hemihydrate, gypsum or anhydrite. At room temperature, anhydrite exhibits a low water solubility of 2.7 g/L which is only slightly higher than that of gypsum (2.0 g/L), whereas hemihydrate is much more soluble in water (6 – 8 g/L). As was found in this study, by using highly soluble sulfate salts such as potassium sulfate or sodium sulfate, the early ettringite formation can be accelerated even more.

The hydration reaction of such ternary binders used in application systems is normally further controlled by the addition of lithium carbonate as accelerator for CAC and K/Na-tartrate as retarder for OPC. By adding accelerating and retarding agents, sufficiently long workability periods and high early strengths are achieved at the same time [178].

Currell et al. [179] published a paper dealing with the influence of different alkali metal salts on the setting of high aluminate cement. From the measurement of setting time and temperature rise of the cement slurries they showed that both cations and anions have an effect on HAC hydration and that anions, except hydroxide, cause a retardation of the setting. *Matusinović* and *Čurlin* [180] studied the influence of small

quantities of alkali metal salts on the setting behavior of high aluminate cement. They found that compared to other metal ions lithium has the greatest effect on the setting time.

Rodger and *Double* [181] investigated the effect of accelerators, and in particular of lithium salts, as well as of citric acid on the setting time of high alumina cement by means of calorimetry, analysis of cement pore solution and X-ray diffraction. They concluded that a nucleation barrier for the precipitation of CAH_{10} and C_2AH_8 exists and that lithium salts initiate the precipitation of a lithium aluminate hydrate which then acts as a heterogeneous nucleation compound.

These results were extended by *Goetz-Neunhoeffer* [182] who developed a model for the working mechanism of Li_2CO_3 and tartaric acid in CAC/hemihydrate mixtures. Li_2CO_3 selectively accelerates the hydration of CA by increasing its dissolution rate and forming a lithium aluminum layered double hydroxide (LDH) compound. **Figure 19** illustrates the typical lamellar structure of such layered double hydroxide compounds.

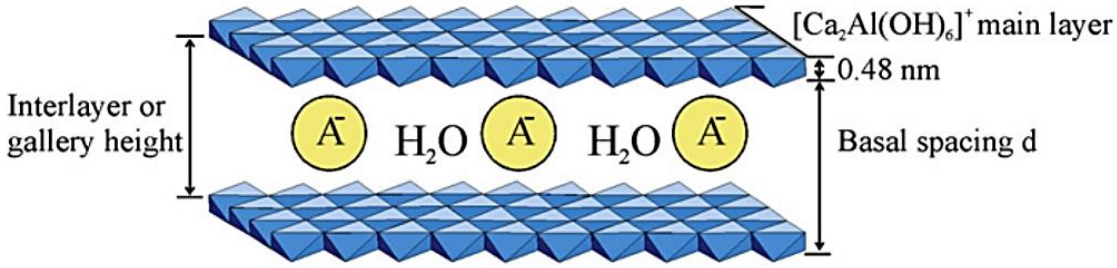

Figure 19. Schematic illustration of the calcium aluminate layered double hydroxide (LDH) structure [183].

In the absence of Li^+ ions a non-crystalline layer of aluminum hydroxo hydrate $[Al(OH)_x(H_2O)_y]$ is formed due to the low solubility of Al^{3+} under those slightly alkaline conditions. This aluminum hydroxo hydrate wraps the CA phases, thus acting as a diffusion barrier and preventing its further dissolution. In the presence of Li_2CO_3, Al^{3+} is converted into a lithium aluminum hydroxide hydrate LDH compound (LA_2H_{10}) which presents a precursor for ettringite formation. This way Li^+ ions act as a catalyst

for the ettringite crystallization. The retarding effect of *Seignette* salt which is specific for Portland cement can be ascribed to the complexation of Ca^{2+} ions from cement pore solution and the formation of a calcium tartrate precipitate which covers the surfaces of the clinker and thus limits the access of water via diffusion.

Another important issue for drymix mortars is their shrinkage behavior which is especially critical in the application of thin bed mortars. In order to prevent crack formation upon drying, typically mineral binders forming large quantities of ettringite are applied [13, 184-186]. Ettringite incorporates 48.9 wt.-% of water into its crystal structure, and thus consumes large amounts of water which explains the fast setting of the mortars due to chemical desiccation. The massive uptake of water and the growth of ettringite needles in the pore space lead to expansion and this way shrinkage is compensated. The pillared structure of ettringite and the needle-like morphology of its crystals are illustrated in **Figure 20**.

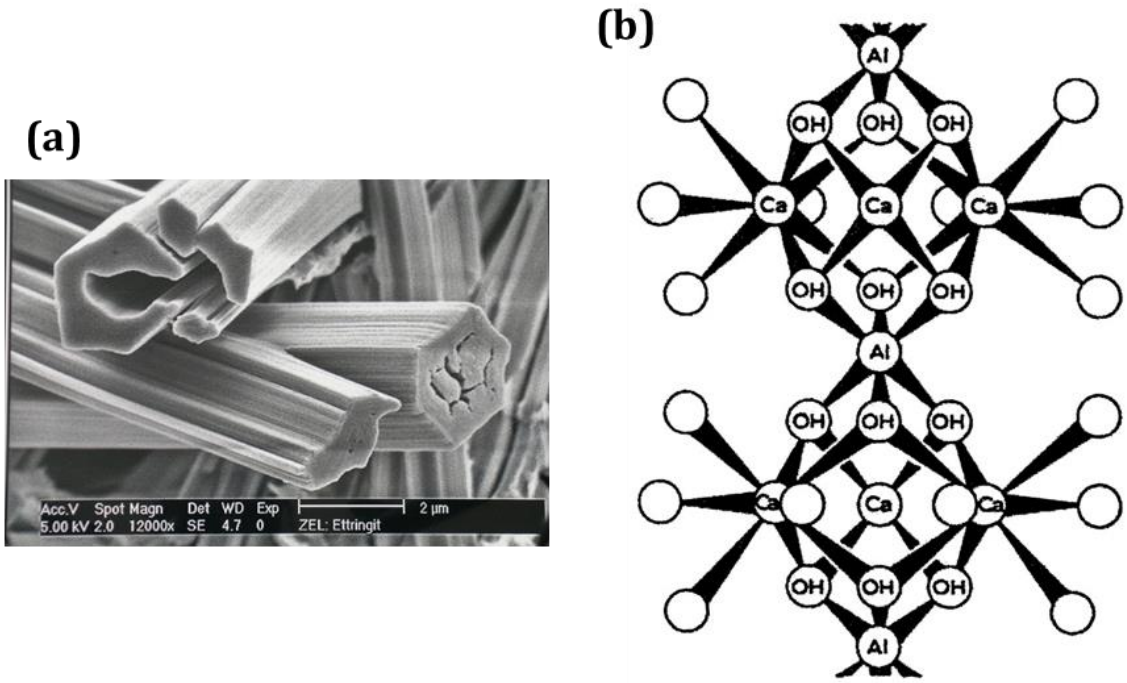

Figure 20. Schematic illustration of (a) the needle-like morphology of ettringite [187] and (b) its pillared crystal structure [188].

3.3 Interaction of latex polymers with mineral surfaces

The material properties of polymer-modified and cement-based construction materials can be derived from the microstructure of the hardened cementitious matrix which represents a porous solid built up from cement hydrate phases, polymers, aggregates and fillers. Important factors determining the microstructure are the nature and morphology of the cement hydrate phases, the distribution of hydrate phases and polymer as well as the resulting pore size distribution. This way, the influence of latex polymers on the hydration reaction of cement which determines all these parameters is of great interest in order to understand the final material properties. Numerous articles about the macroscopic properties of polymer-modified mortars exist, however there is a lack of fundamental research work on the interaction between the colloidal latex particles and inorganic cement grains in suspension during cement hydration.

3.3.1 Microstructure of polymer-modified mortar matrix

Literature dealing with latex-cement interaction is mainly based on descriptions of the microstructural development of polymer-modified mortars. However, due to the large variety of different latex dispersions, mineral binders and aggregates as well as the complex mechanism of hydration, it is challenging to develop a generally valid description for the microstructural formation. *Ohama* et al. [15, 189] developed a generally accepted model for the formation of the polymer-cement co-matrix. As is shown in **Figure 21**, the mechanism describing the formation of the microstructure of polymer-modified cementitious systems includes four main steps.

Immediately after mixing, polymer particles are homogeneously distributed in the cement paste. As a consequence of cement hydration calcium hydroxide is released into the pore solution and calcium silicate hydrate phases (C-S-H) start to form. Simultaneously, latex particles are deposited on the surfaces of the clinker grains or early hydration products and with proceeding cement hydration accumulate in the capillary pores, whereby a dense layer of latex particles covers both the hydrating

binder as well as the aggregates. Subsequent water loss initiates coalescence of the latex particles resulting in the formation of a network of polymer film. This way, a co-matrix of interpenetrating polymer film and mineral phases is formed.

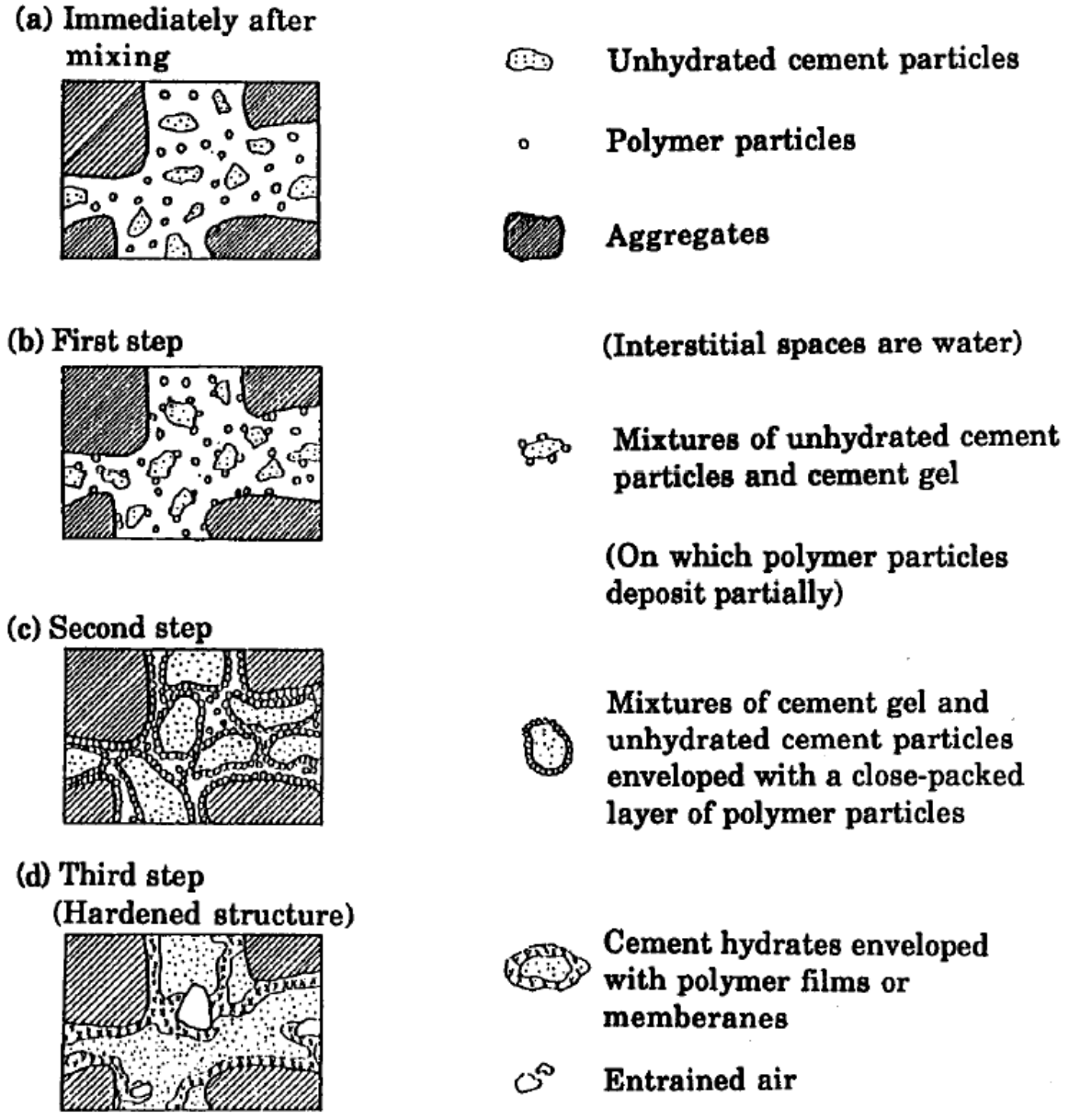

Figure 21. Formation of the polymer-cement co-matrix [15].

Jennings et al. [190] confirmed these results by monitoring the evolution of the microstructure of cement pastes containing styrene-acrylate copolymer. By means of environmental scanning electron microscopy (ESEM) the authors showed that a certain proportion of latex particles adsorbs onto cement immediately after mixing

and forms a film whereby the hydration reaction is slowed down. Film formation of the residual latex dispersed in the cement pore solution starts when water is sufficiently removed by hydration or evaporation.

In the literature some works discuss the distribution of latex particles in cementitious mortars. As mentioned above, *Ohama* described a homogeneous distribution of latex particles in the fresh and hardened mortar matrix. This observation was further confirmed by *Jenni* et al. [14] who investigated the distribution of latex particles, cellulose ether and poly(vinylalcohol) in cementitious mortars by using a multi-method approach. The authors revealed that the water soluble polymers CE and PVOH migrate to the mortar surface due to the migration of water within the pore system, whereas latex particles remain homogeneously dispersed in the pore solution.

De Gasparo et al. [191] published somehow contradictory results about the distribution of organic additives (latex, PCE, CE, casein and PVOH) in self-leveling flooring compounds. Their conclusions were obtained from laser-scanning microscopy measurements. To achieve selective visualization of the additives, they were tagged with a fluorescent dye. Similar to *Jenni* et al. the authors revealed an accumulation of organic additives in regions near the surface of the mortar resulting from migration of water in the pore system. However, the authors observed a gradient distribution of latex polymer as well which contradicts the results from previous authors. *Tian* et al. [192] investigated the microstructure of poly(acrylate) latex-modified cementitious materials in the time period beginning from mixing to hardening. By using scanning electron microscopy (SEM) and energy-dispersive X-ray spectroscopy (EDX) the authors revealed that latex particles are localized at specific sites within the mortar.

These results suggest that latex particles can be homogeneously dispersed, but also localized on specific sites within the cementitious microstructure, depending on their chemistry or colloidal properties. Furthermore, it is also important to consider the

colloidal stability of the latex. When the latex is destabilized and flocculates in the cement pore solution it will not be randomly distributed.

Generally, it is accepted that latex particles form polymer films within the cementitious matrix which intertwine with cement hydrates and bridge the pore space. As a consequence, the density and flexibility of the hardened matrix is improved. For example, *Tabassi* et al. [193] investigated the porosity and pore size distribution of mortars modified with styrene-butadiene, vinylacetate-ethylene and poly(acrylic ester) polymers. The authors reported that with increasing polymer dosage the porosity of the mortar is significantly reduced. Similar results were obtained in this research project from mercury intrusion porosimetry measurements of cement samples cured for 28 d containing 5, 10 or 20 % bwoc of styrene-butadiene or ethylene-vinylacetate copolymer.

Similar effects were reported by *Shi* et al. [178] who evaluated the chloride permeability and microstructure of Portland cement mortar modified by styrene–butadiene latex. The authors observed less chloride penetration for the latex-modified sample and ascribed this effect to a denser microstructure. By using field-emission scanning electron microscopy such improvements in the pore structure and the formation of a latex-cement co-matrix were confirmed.

Furthermore, the microstructure strongly depends on the polymer content of the cement paste. In this study it was found that at higher latex dosages a continuous matrix of polymer films is formed whereby cement hydrate phases are embedded. *Muthadhi* and *Kothandaraman* [194] published correlating results in a paper which presents the effect of heat exposure on the strength properties of styrene-butadiene-modified concrete (dosages: 5, 10 and 20 %) cured for 7 or 28 d respectively. Their results demonstrate that specimens containing 20 % of polymer lose their strength after heat exposure at 400 °C, whereas samples containing lower polymer dosages maintain their stability. At such high temperatures the organic polymer is burned away whereby only the mineral matrix remains.

Water soluble polymers such as poly(vinylalcohol) which is commonly used as colloidal stabilizer in the fabrication of latex powders can introduce significant amounts of air into cement pastes due to their surface activity. The hydrophobic backbone of PVOH is oriented to the 'hydrophobic' air, whereas its hydroxyl groups interact with the aqueous phase and thus stabilize the water/air interface. As was reported by *Jenni* et al. [14] and also found in this research project, PVOH accumulates on the water/air interface of air bubbles, as is shown in **Figure 22**. This way, latex powders always need to be combined with defoamers which prevent air entrainment.

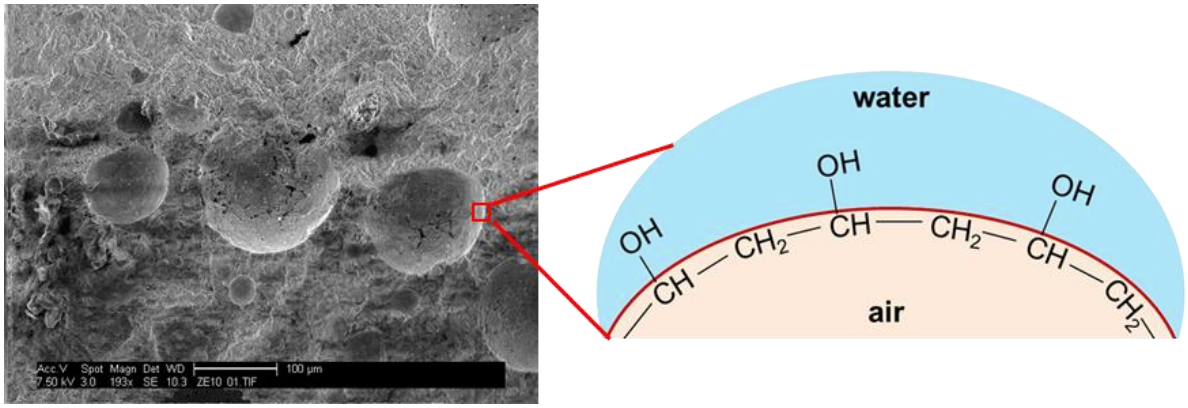

Figure 22. Accumulation of PVOH at the water/air interface of air pores contained in mortars.

3.3.2 Effect of latex polymers on the properties of fresh mortar

Several works published in the scientific literature describe the properties of fresh polymer-modified mortar. They present that latex polymers can positively affect the workability of cement-based mortar, reduce its water demand or lead to improved water retention [195-197]. For evaluation of these properties it is important to consider the stabilization system of the latex dispersion as well as the composition of the serum phase. Water-soluble oligomers present in the serum phase can act as dispersants when they possess similar molecular structure compared to superplasticizer molecules.

Betioli et al. [24] studied the influence of EVA copolymer on the rheological behavior of cement pastes. It was shown that the shear thinning behavior of the neat cement paste changes to shear thickening as a result of EVA addition. However, this effect was only observed in the first minutes after mixing, whereas after 60 min a plasticizing effect of the sample modified with EVA copolymer was observed which was ascribed to a ball-bearing effect.

Pei et al. [198] assessed the effect of two styrene–butylacrylate copolymer latices with different stabilization systems on the workability of fresh polymer-modified mortar. It was concluded that a polymeric emulsifier shows much better performance regarding the workability compared to a low molecular weight emulsifier.

These results suggest that for applications which require excellent flowability of the mortar such as self-leveling underlayments, the dispersions could be synthesized with remaining water-soluble oligomers in the serum phase acting as plasticizing agents. Another possibility would be a synthesis in the presence of an alkali-soluble resin as surfactant which further acts as dispersant when applied in the mortar. Such systems could simplify some of the complex drymix mortar formulations and prevent incompatibilities between different chemical admixtures.

3.3.3 Interactions on the interface adhesive mortar/mineral substrate

The improved adhesion represents a key property of latex modified-mortars and was investigated by several authors [199-201]. As presented in **Figure 23**, the adhesion of latex-modified mortars onto mineral substrates such as ceramic tiles is mainly ascribed to the formation of polymer films between the interfaces of the mortar matrix and the substrate.

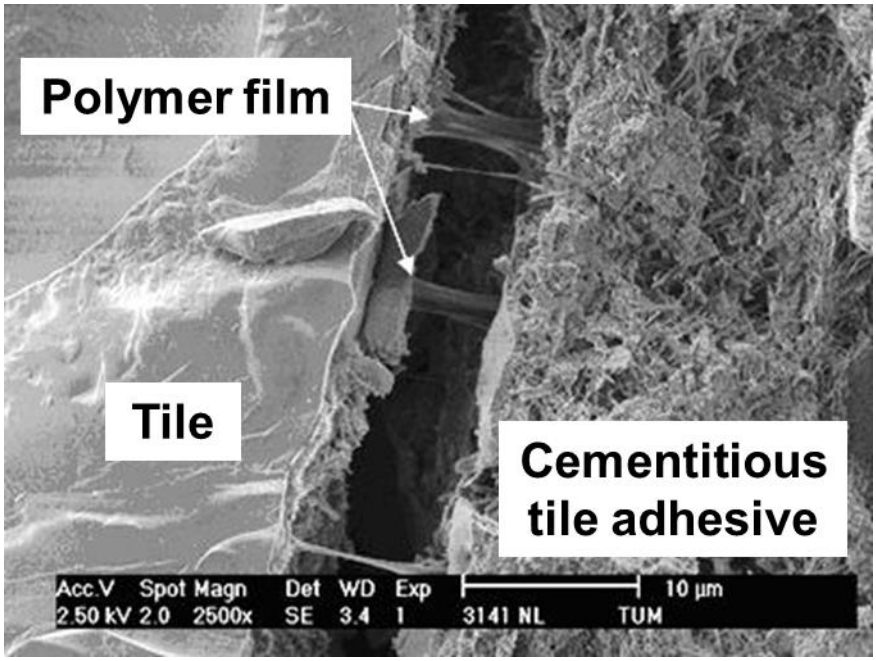

Figure 23. SEM image of the interface between a cementitious mortar matrix and a ceramic tile. Both materials are linked via polymer films which provide the adhesion [202].

Rottstegge et al. [199] investigated the interfacial interactions between latex-modified Portland cement and polymer fibers by means of scanning electron microscopy and solid-state NMR spectroscopy. Their results demonstrate that the addition of re-dispersible latex powder to the cement paste increases adhesion between the cementitious matrix and the polymer fibers significantly by the formation of a homogeneous polymer film bridging the interfaces.

Brien and *Mahboub* [203] examined the influence of latex polymers exhibiting different glass transition temperatures on the adhesion characteristics of a rapid hardening mortar consisting of a blend of calcium sulfoaluminate cement and Portland cement. In their investigation the following latex powders were used for mortar modification: poly(methacrylic acid) with T_g = -10 °C, styrene-butadiene-copolymer with T_g = 15 °C and two ethylene-vinylacetate copolymers, one with T_g = -7 °C and the other with T_g = 20 °C. Pull-off test results revealed that latex polymers possessing lower glass transition temperature show better adhesion performance.

Similar results were published by *Kaufmann* et al. [204]. Using zeta potential and atomic force microscopy measurements they studied the interaction between mineral substrates and latex particles based on varying chemistries and stabilization systems. In order to mimic the ionic conditions of a cement pore solution, measurements were performed in Ca^{2+} containing aqueous solutions. From the AFM results the authors derived a so-called flat index which represents the ratio of height to diameter of the latex particles deposited on the different mineral substrates (ceramic tiles and mica). The flat indices indicate the affinity of the polymer to the mineral substrate. It was shown that especially the glass transition temperatures as well as the nature of the protective colloid impact the polymer-mineral-interactions.

3.3.4 Latex-cement interparticle interactions (adsorption)

Several authors mentioned the occurrence of adsorption of latex particles onto cement or hydrate phases, but did not provide further evidence in their articles. *Van Damme* et al. [205] published one of the first experimental works dealing with this question. In his work the adsorption of non-ionic alkyl-phenol-poly(ethylene oxide) surfactants and of methyl methacrylate-butylacrylate latex particles on several individual clinker or hydrate phases contained in Portland cement was investigated by determining the depletion of the latex concentration in the pore solution resulting from adsorption. It was found that the non-ionic surfactant molecules do not adsorb onto mineral surfaces, whereas the anionic acrylic latex particles adsorb onto hydrating tricalcium silicate phases, thus forming a monolayer on their surface. This effect was ascribed to attractive electrostatic interactions between the positively charged mineral surfaces and the negatively charged latex particles. Furthermore, it was demonstrated that adsorption of the latex onto silicate phases is negatively influenced by the presence of sulfate ions due to competitive adsorption, and that the acrylic latex particles interact only little with gypsum or portlandite.

Generally, when measuring the adsorption of latex particles via the depletion method it is important to consider the colloidal stability of these latex particles. This method only provides reliable results when the latex particles exhibit colloidal stability in the saline aqueous environment, otherwise they will partly start to sediment and pretend an adsorption.

However, the results published by *Van Damme* et al. provided no direct evidence for adsorption of ionic latex particles on Portland cement. *Plank* and *Gretz* [206] were the first who evidenced the adsorption of anionic and cationic latex copolymers onto hydrating Portland cement by means of electroacoustic zeta potential measurements and adsorption isotherms. The latex polymers used in this study were self-synthesized and based on styrene-butylacrylate chemistry, whereby the anionic charge was generated via incorporation of methacrylic acid into the copolymer, and the cationic charge was provided by a cationic surfactant. For all latex polymers,

Langmuir type adsorption isotherms were obtained. By means of electron microscopy it was confirmed that charged latex particles adsorb selectively onto specific surface sites of hydrating cement possessing opposite charge, whereby domains of organic latex polymers are formed on the mineral surfaces, as is illustrated in **Figure 24**.

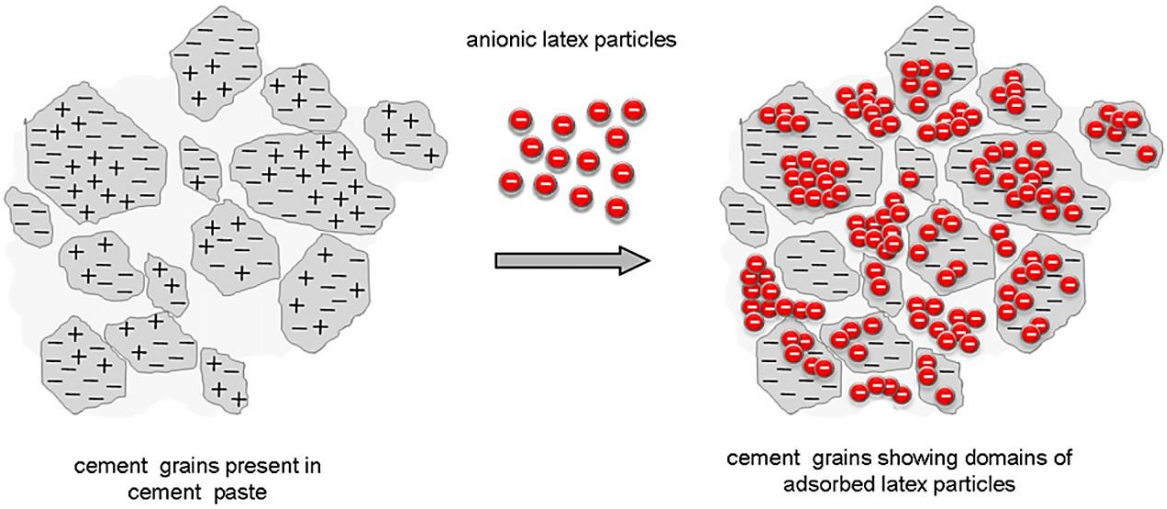

Figure 24. Schematic illustration of the adsorption of anionic latex particles on the surface of hydrating cement [206].

These results were further confirmed by *Zhong* et al. [207] who investigated the adsorption of different anionic latex polymers (e.g. styrene-acrylate or poly(acrylic) latices) using similar methods. Additionally, these authors reported that the presence of superplasticizer or cellulose ether molecules can decrease the adsorbed amount of latex particles due to competitive adsorption.

In this research project it was found that the adsorbed amount of latex particles depends on their specific anionic charge density. Electroacoustic zeta potential measurements revealed different adsorbed amounts for liquid and powder carboxylated styrene-butadiene latex onto Portland cement owing to the lower anionic charge density of re-dispersed powder particles. In contrast, non-ionic ethylene-vinylacetate latex particles show no adsorption onto mineral surfaces due to a lack of attractive electrostatic forces between the uncharged polymer and the mineral surfaces.

3.3.5 Influence of latex polymers on cement hydration

The influence of latex polymers on the hydration kinetics of cement greatly affects the workability, but also of the final material properties of cement-based building materials. As was discussed in the chapters above, interactions between latex particles and cement or hydrate phases may occur depending on the surface charge of the colloidal particles. As a consequence, it can be expected that the hydration reaction of cement is strongly influenced by those colloidal interactions. For water-soluble polymers such as superplasticizers many articles demonstrated that strong interactions with cement lead to a significant impact on the hydration reaction [2, 208].

The interaction of ethylene-vinylacetate copolymers with cement is of great interest due to their widespread application in mortars. Therefore, several works dealing with this subject were published in the literature.

Betioli et al. [23] investigated the hydrolysis of liquid and powder ethylene-vinylacetate latex in Portland cement pastes during the first hours of hydration via thermogravimetric analysis. It was shown that the EVA copolymer undergoes hydrolysis in the alkaline cement pore solution whereby the released acetate chelates calcium ions from the pore solution under formation of calcium acetate. As a consequence, the concentration of portlandite is reduced. *Pöllmann* and *Sieksmeier* [209] confirmed the saponification of ethylene-vinylacetate in cement pore solution as well.

Comparable results were published by *Silva* et al. [210] who examined the interaction between EVA copolymer and cement by means of thermogravimetric analysis, *Fourier*-transform infrared spectroscopy and scanning electron microscopy. Additionally, the authors mentioned that ettringite crystals are well formed in the presence of EVA and that many *Hadley* grains were observed in the hardened cementitious matrix. Furthermore, *Silva* and *Monteiro* [211] published a work about the effect of EVA copolymer on the hydration of tricalcium aluminate (C_3A) and

tricalcium silicate (C_3S) investigated via soft X-ray transmission microscopy. From the results it was concluded that the EVA particles accumulate around hydrating C_3A and C_3S grains and thus inhibit the formation of ettringite crystals at the early stage of hydration.

Spiess et al. [26] measured the influence of poly(vinylacetate)-based latex polymers stabilized by poly(vinylalcohol) on cement hydration using solid state NMR spectroscopy and scanning electron microscopy. Opposite to *Silva* or *Betioli*, the authors showed that the vinylacetate-based latex dispersion was relatively stable against hydrolysis in cement pore solution and that the silicate reaction is only minor affected in the presence of the latex. Furthermore, the latex particles were found to be adsorbed onto mineral surfaces, however no direct prove was given. Here, it is important to differentiate whether adsorption of the latex particles occurred as a result of electrostatic attraction, or whether the latex particles simply attach to the mineral substrate upon drying.

Su et al. [212] showed that styrene-acrylate or vinylpropionate-vinylidene chloride latex dispersions retard the setting and hydration of cement. *Larbi* and *Bijen* [213] reported on the interaction of latex polymers based on similar chemistry with ions released during Portland cement hydration. It was found that the latex polymers primarily interact with calcium, but also with sulfate and hydroxide ions. This effect was ascribed to the hydrolysis of the acrylate ester latex polymers in the alkaline cement pore solution whereby carboxylate groups are formed which then can chelate calcium ions.

Wang et al. [11, 12, 27, 214, 215] investigated the effect of styrene-butadiene rubber (SBR) latex and powder on the cement hydrate phases ettringite and portlandite within the first 72 h of hydration by X-ray diffraction. Furthermore, C-S-H formation was studied via environmental scanning electron microscopy. The authors showed that both liquid and powder SBR latex promote ettringite formation, whereas C-S-H and portlandite crystallization is reduced at the same time. These effects are more pronounced for the SB powder sample. As was shown from XRD measurements,

liquid and powder SB latex accelerate the reaction of calcium aluminates with gypsum, and thus promote and increase the quantity and stability of ettringite, whereas the formation of C_4AH_{13} is inhibited. Furthermore, it was reported that after a curing time of 3 d the structure of the SB-modified cement paste appeared to be similar compared to the neat cement paste.

Latex powders contain colloidal stabilizers which are expected to dissolve upon water immersion, thus their interaction with hydrating cement is of much interest as well. The most common protective colloid for spray drying latex powders is poly(vinylalcohol), but also other water-soluble polymers (e.g. superplasticizers such as MFS or PCE) are used. *Jansen* et al. [216-218] examined the impact of poly(vinylalcohol) and poly(diallyl dimethyl ammonium chloride) (PDADMAC) on the formation of cement hydrate phases using quantitative X-ray diffraction and heat calorimetry. It was found that poly(vinylalcohol) retards the dissolution of the aluminate phases and of the sulfate carrier and leads to an increased ettringite formation only after 16 h of hydration. For the cationic PDADMAC the chemistry of the anionic counter ion determines its behavior. In the presence of OH^- as counter ion, the solubility of calcium sulfate is increased and thus C_3S hydration is accelerated. Oppositely, by using SO_4^{2-} as counter ion, precipitation of secondary gypsum occurs whereby the Ca^{2+} concentration in cement pore solution is reduced and hydration is retarded.

These results clearly indicate that the water-soluble spraying aids impact cement hydration and therefore need to be considered when studying the effect of re-dispersible latex powders. In this research work the influence of poly(vinylalcohol) on cement hydration was studied as well. The results revealed that the pH value of the cement pore solution is decreased in the presence of PVOH due the consumption of hydroxide ions in the hydrolysis of the vinylacetate monomer unit. This way, the solubility of the silicate phases is significantly increased and large quantities of portlandite precipitate.

Although many literature dealing with the influence of latex polymers on cement hydration exists, no article systematically presents the different colloid chemical properties of liquid latices and their re-dispersible powders with respect to their interaction with cement and their influence on cement hydration. Especially the colloid chemical properties of latex particles such as surface charge or particle size are decisive for the understanding of their interaction with mineral phases or ions contained in cement pore solution. The chemical nature of the polymer is less relevant since mainly electrokinetic surface properties are responsible for physical interactions. The major drawback of many publications on this subject is that the colloid chemical properties of the latex particles or the stabilization system of re-dispersible powders are not disclosed or even considered. As mentioned above, several works on the influence of latex polymers on OPC hydration exist in the scientific literature. However, no work dealing with the influence of latex polymers on the hydration of the ternary binder system OPC/CAC/anhydrite has been published yet. Owed to the widespread use of such TBS in drymix mortar formulations it is highly relevant to study the interaction between the mineral and polymer binders. This study aims to close these gaps of knowledge.

4 MATERIALS AND METHODS

This chapter presents a general overview of the experimental procedures (see **Figure 25**) followed during this research and the materials used. Furthermore, all methods which are not sufficiently described in the publications attached are presented here in detail.

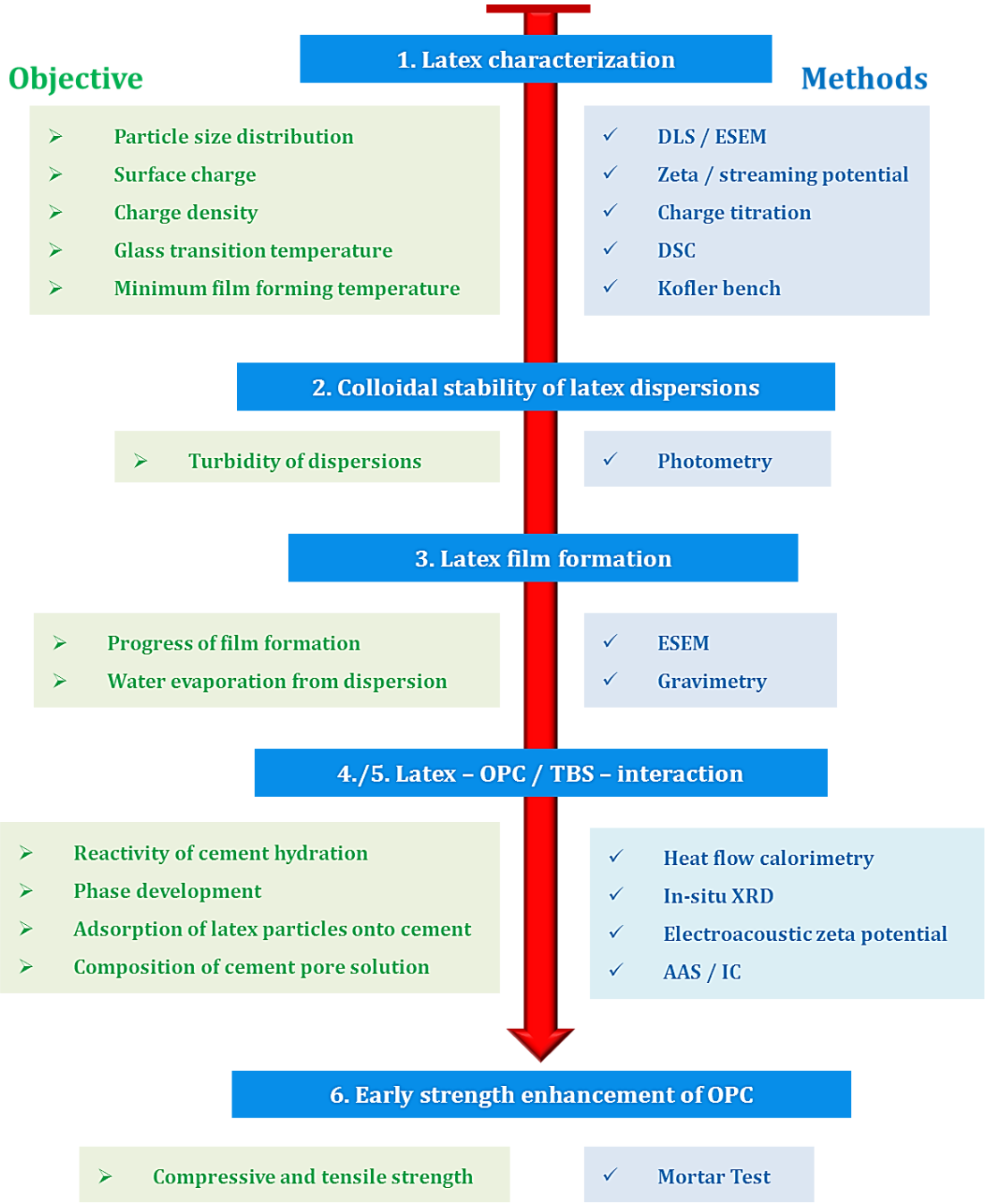

Figure 25. Experimental pathway taken in this research project.

4.1 Latex polymers

The ethylene-vinylacetate (EVA) and carboxylated styrene-butadiene (SB) latex samples used in this study were applied as liquid dispersions as well as re-dispersible powders. The latex powders were obtained by spray drying of the liquid dispersions under the addition of poly(vinylalcohol) as colloidal stabilizer and kaolin as anti-caking agent. **Figure 26** presents the chemical structures of the EVA and SB copolymers.

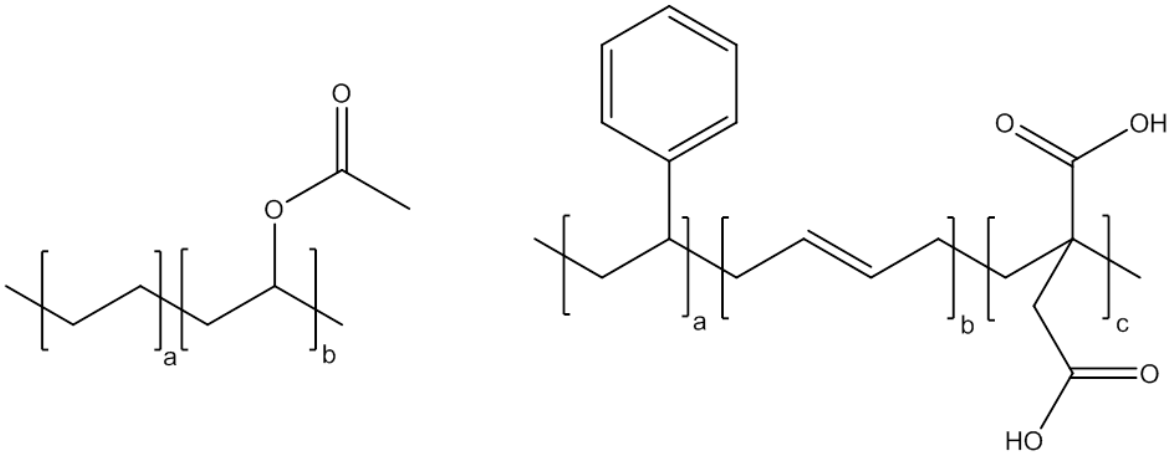

Figure 26. Chemical structures of ethylene-vinylacetate (a:b = 1:3) and of carboxylated styrene-butadiene (a:b = 18:55) copolymer.

The EVA dispersion was synthesized in the presence of PVOH as colloidal stabilizer (concentration: 5 wt.% of the total polymer), whereas the SB dispersion was stabilized via incorporation of itaconic acid into the copolymer. As illustrated in **Figure 27**, both EVA and SB latex powder samples are composed of 78 wt.% latex polymer, 12 wt.% anti-caking agent kaolin and 10 wt.% colloidal stabilizer poly(vinylalcohol).

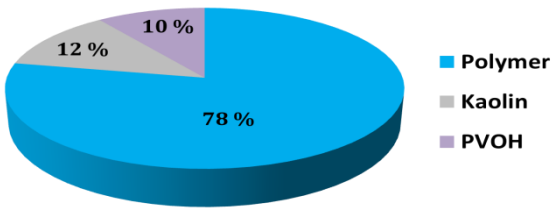

Figure 27. Composition of the re-dispersible latex powder samples used in this study.

The molecular weight of the partially hydrolyzed PVOH is 36,000 g/mol, its degree of hydrolysis is 88 %. The EVA copolymer particles exhibit a broad size distribution in the range between 300 – 1750 nm, whereby the SB copolymer exhibits a mono-disperse particle size distribution ~ 220 nm.

4.2 Characterization of latex dispersions and powders

4.2.1 Solid content of liquid latex

The solid content of the aqueous latex dispersions was determined on a MA-30 infrared drying balance (Sartorius, Hamburg, Germany). Prior to measurement, 2 g of the aqueous polymer dispersion were evenly distributed on a filter paper in an aluminum tray which was placed on the balance. Then the sample was heated up to a temperature of 115 °C within a time frame of 10 min. The solid content was directly calculated by the instrument from the weight of residual solid.

4.2.2 Quantification of kaolin in re-dispersible powders

The amount of kaolin contained in the re-dispersible latex powders was determined from the ash content. 10 g of the latex powder were weighed into porcelain crucibles and stored in an oven for one hour at 1000 °C. Under these conditions, the polymer is completely burned to carbon dioxide and kaolin is dehydrated. Thus, the residual ash exclusively originates from the kaolin contained in the powder. From the mass difference before and after the combustion and under consideration of the water content of kaolin its amount was calculated.

4.2.3 Glass transition temperature (T_g) of the latex polymers

Glass transition temperatures (T_g) of the latex samples were measured via differential scanning calorimetry (DSC) using a DSC 200 F3 Maia instrument (Netzsch, Selb, Germany). The liquid latex dispersions were freeze-dried on an ALPHA 1-4 LD plus instrument (Martin Christ Freeze Dryers GmbH, Osterode, Germany) prior to measurement of the T_g. Therefore, 10 mL of the aqueous latex dispersion were transferred into a 100 mL round-bottomed glass flask which then was stored for several minutes in liquid nitrogen until the dispersion was completely frozen. Next, the glass flasks were connected with the freeze dryer until the water had sublimated completely. Drying conditions were set to an ice condenser temperature of - 55 °C

and a vacuum of 0.03 mbar. For measurement of the T_g, 10 – 20 mg of the solid latex were weighed into an aluminum crucible which then was placed into the DSC instrument. Finally, the temperature program (see **Figure 28**) was set via the computer software before measurement was started. The T_g was calculated from the second heating curve at a heating rate of 5 K/min.

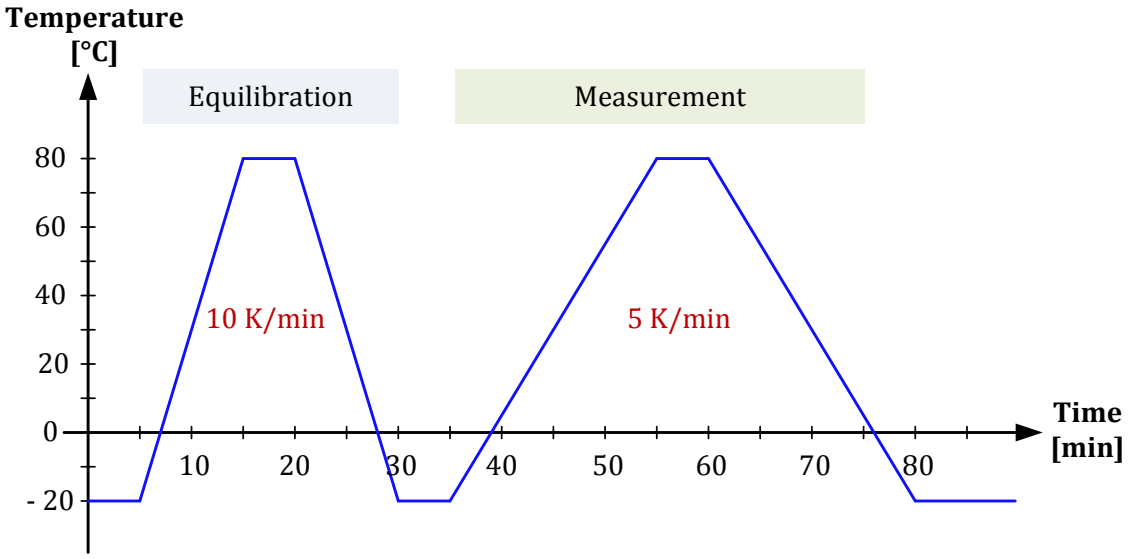

Figure 28. Temperature program for the measurement of the glass transition temperature of the latex polymers.

4.2.4 Minimum film forming temperature (MFFT) of latex polymers

The minimum film forming temperatures (MFFT) of the latex polymers were determined on a MFT Thermostair Kofler bench (Coesfeld Materialtest, Dortmund, Germany). Before each measurement, the metal plate of the instrument was covered with an aluminum foil. Next, 2.5 mL of the latex dispersion (solid content ~ 50 wt.%) were evenly spread out over the entire length of the *Kofler* bench with a layer thickness of around 300 µm. The temperature gradient applied on the metal plate was adjusted to ± 10 °C of the expected MFFT. For the drying process an air flow with a speed of 1 m/s was passed over the wet latex film until it was completely dry. As is shown in **Figure 29**, the region where the latex film starts to appear transparent represents the minimum film forming temperature.

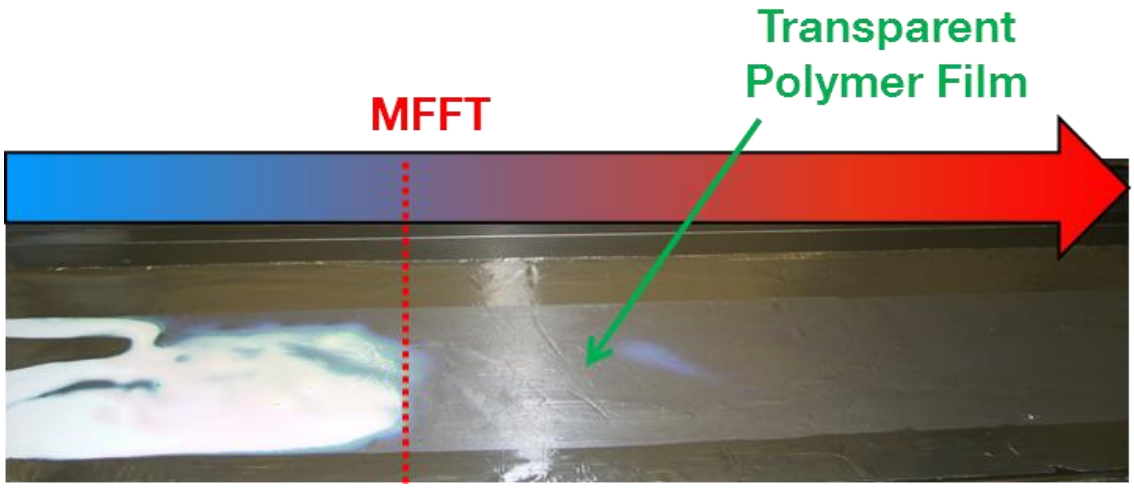

Figure 29. Photograph showing the appearance of the polymer film at the final stage of the MFFT measurement.

5 RESULTS AND DISCUSSION

This chapter includes a summary of each publication attached to this thesis and briefly states the novelty of the work. Furthermore, additional results which are not yet published in the scientific literature are presented.

5.1 Influence of spraying aids PVOH and kaolin on colloidal stability of latex copolymers (paper #1)

In the scientific literature, no work exists which describes the influence of the spray drying on the colloidal properties of latex powder particles under the addition of colloidal stabilizers and anti-caking agents. Among scientists it is accepted that in a powder particle the individual latex particles are embedded into a matrix of the colloidal stabilizer which completely dissolves after re-dispersion in water. In this study, the influence of the spraying aids PVOH and kaolin on the electrokinetic surface properties of EVA and SB latex copolymers, as well as their colloidal stability in synthetic cement pore solution was investigated.

The experiments evidenced that the colloidal properties of individual latex particles can be influenced by the addition of PVOH and kaolin during spray drying. For EVA and SB copolymers it was demonstrated that during spray drying a layer of PVOH is formed on the latex particle surface which does not dissolve completely upon re-dispersion in water. As a consequence, the colloidal stability of anionic styrene-butadiene latex powder particles in cement pore solution is significantly increased compared to its liquid latex. This effect was ascribed to the PVOH coating which covers the carboxylate groups located on the SB latex particle surface, thus preventing their interaction with calcium ions and subsequent coagulation. **Figure 30** illustrates the formation of such PVOH coating on the surface of the latex particles during the spray drying. The EVA latex particles are coated with PVOH as well during spray drying, however, due to their non-ionic character the colloidal stability is less affected.

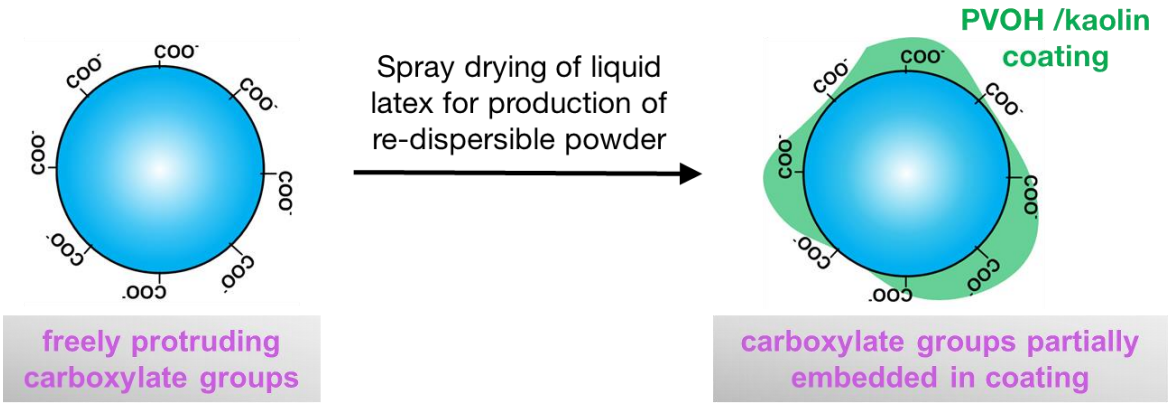

Figure 30. Formation of a PVOH coating on the surface of carboxylated SB latex particles during spray drying.

These results established a basis for the understanding of the film formation of liquid and powder latices, and especially for their interaction with cement which is mainly driven by the colloidal properties of the latex particles.

5.2 Influence of PVOH and kaolin on film formation of latex copolymers (paper #2)

Several papers described that the presence of salts, co-monomers or emulsifiers in the serum phase of latex dispersions can retard the polymer film formation. Upon drying, these compounds accumulate on the latex particle surfaces and thus act as a barrier for interparticle diffusion. Nonetheless, no work describing the impact of spraying aids on the film formation has been published in the scientific literature. In this work, the influence of the spraying aids PVOH and kaolin on the film formation of EVA/SB liquid and powder latex dispersed in water and synthetic cement pore solution was studied.

Time-dependent ESEM monitoring showed that the film formation of latex reconstituted from the powder sample occurs faster in both water and SCPS, compared to its liquid precursor. From spray dried styrene-butadiene model powders containing only PVOH or kaolin it was found that the anti-caking agent kaolin is responsible for an acceleration of the film formation, whereas PVOH retards the latter. **Figure 31** compares the progress over time of the film formation of aqueous latices prepared from the SB latex model powders (SB+kaolin and SB+PVOH) after a drying time of 2 h. The SB+PVOH sample still exhibits individual particles which are densely packed whereas the latex prepared from SB+kaolin already shows a homogeneous polymer film.

As was discussed in paper #1, the PVOH coating formed on the latex particle surface during spray drying acts as a barrier between the latex particles and thus retards their interpenetration (coalescence). The accelerating effect of kaolin in re-dispersible powders overrides the retarding effect of PVOH on the film formation by enhancing particle interpenetration. Exactly the same behavior was found for the non-ionic ethylene-vinylacetate copolymer.

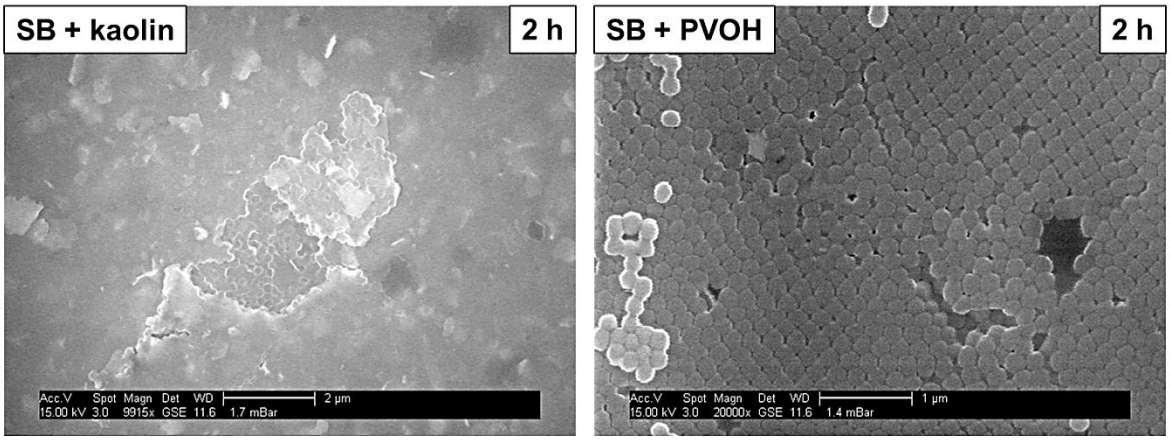

Figure 31. ESEM micrographs of re-dispersed powders which were prepared via spray drying of SB + kaolin and SB + PVOH after 2 h of storage on an ESEM sample holder.

These experiments further revealed that PVOH and kaolin do not only present auxiliaries for the spray drying of latex dispersions. Instead, the spraying aids significantly impact the key properties of latices such as colloidal stability and the rate of film formation. In the following it is presented that compared to their liquid mother liquors EVA or SB latex powders show different impact on the hydration kinetics of Portland cement and a ternary binder system.

Furthermore, it was shown for the first time that carboxylated styrene-butadiene latex powder can be spray dried even without adding spraying aids while the re-dispersible character of the powder is still maintained. These results suggest that water-soluble oligomers formed during the emulsion polymerization act as colloidal stabilizer and thus prevent film formation during the drying process.

5.3 ESEM investigations on the film forming mechanism of carboxylated styrene-butadiene latex (paper #3)

Some scientists described the arrangement of colloidal particles in crystalline domains upon dehydration of aqueous dispersions. However, no work dealing with the influence of such crystalline domains on the film forming process was published yet. Owing to this lack of knowledge, the role of colloidal crystal-like assemblies in the film forming process of carboxylated styrene-butadiene copolymer was investigated. The film forming process was tracked via time-dependent ESEM monitoring of the three-dimensional (3D) arrangement of latex particles in the drying film.

The experiments revealed that monodisperse SB latex particles can arrange in crystalline domains at the stage of dense particle packing. Subsequent particle coalescence was found to begin within these crystalline domains before it spreads across the entire matrix. This effect was ascribed to the higher packing density within the colloidal crystals, thus leading to an increased contact area between the ordered latex particles and promoting their interpenetration. **Figure 32** illustrates the modified film forming mechanism including the film formation in crystalline domains.

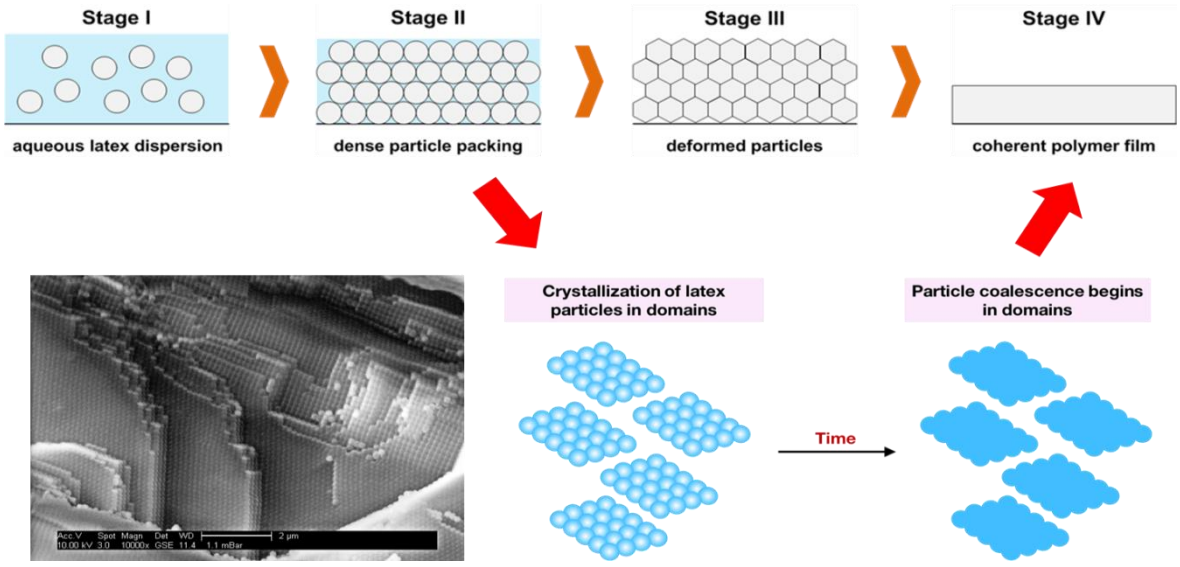

Figure 32. Schematic illustration of latex particle interdiffusion preferentially occurring in crystalline domains formed during the film forming process.

Such arrangement in highly ordered domains was only observed for monodisperse SB latices which are more likely to form a dense packing compared to polydisperse latices such as EVA which were not found to self-assemble in colloidal crystals during the film forming process. Even the presence of irregularly shaped kaolin particles in the SB powder latex disturbs the crystallization of the latex particles.

5.4 Influence of latex polymers on the hydration kinetics of Portland cement

Many articles about the interaction of latex polymers and mineral phases in general were published in the scientific literature. However, no work exists which systematically reflects the different electrokinetic surface properties of liquid latices and their re-dispersible powders with respect to their interaction with Portland cement. The objective of this study was to evaluate the influence of the surface properties of liquid and powder EVA/SB latex, as well as the impact of the spraying aids PVOH and kaolin on the hydration kinetics of Portland cement.

5.4.1 Anionic styrene-butadiene latex and powder (paper #4)

This paper presents a study on the influence of carboxylated styrene-butadiene liquid and powder latex on the hydration of OPC. The hydration characteristics of OPC pastes containing 5, 10 or 20 % bwoc liquid and powder SB latex or the respective amount of spraying aids were analyzed. The results show that anionic SB copolymer generally causes a strong retardation of cement hydration. In-situ XRD measurements and the calorimetric data revealed that the silicate reaction is significantly retarded whereas the aluminate reaction is suppressed almost completely. By means of electroacoustic zeta potential measurements is was confirmed that the mechanism behind the suppressed ettringite formation is based on the adsorption of anionic SB particles onto positively charged surface sites of hydrating cement, as is illustrated in **Figure 33**. The layer of adsorbed SB latex particles hinders the access of ions to the mineral surface and thus negatively impacts crystal growth.

Analysis of the cement pore solution showed that anionic SB particles chelate calcium ions whereby portlandite crystallization is retarded. These effects are less pronounced for the SB powder samples compared to their mother liquor due to their lower anionic charge density. As a consequence of their PVOH coating, the physical interactions between SB powder particles and mineral phases or ions are reduced.

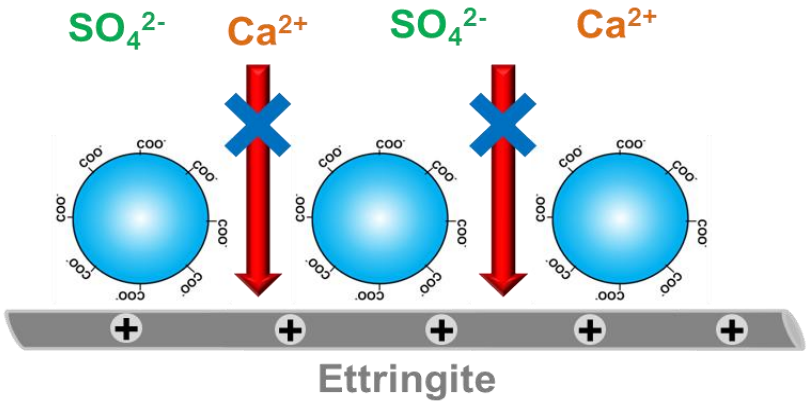

Figure 33. Schematic illustration of the adsorption of anionic latex particles onto positively charged sites of hydrating cement which hinders the access of ions to provide further crystal growth.

From this paper it can be concluded that the colloidal properties of anionic styrene-butadiene latex particles, and in particular their surface properties, determine their interaction with mineral surfaces (clinker or hydrate phases) or ions present in cement pore solution. As a consequence, the different influence of liquid and powder SB latex on cement hydration can be ascribed to their different colloidal properties. This effect is owed to the spraying aids PVOH and kaolin which are present in the SB powder. Upon spray drying, the SB powder particles are coated with a layer of PVOH whereby the anionic surface charge of the SB powder particles is reduced compared to its liquid precursor. This way, carboxyl groups present on the SB powder particle surface are partially embedded into this PVOH coating and therefore show less interaction with cement, hydrate phases or ions.

5.4.2 Non-ionic ethylene-vinylacetate latex and powder

Similar investigations as presented for the carboxylated styrene-butadiene latex were performed for the non-ionic ethylene-vinylacetate copolymer. The results are discussed in this section.

First, hydration of Portland cement in the presence of 5, 10 and 20 % bwoc liquid and powder EVA latex was tracked via isothermal heat flow calorimetry. As presented in **Figure 34** and **Figure 35**, the addition of liquid or powder EVA latex impacts the heat flow curve only minor (slight retardation of the dormant period).

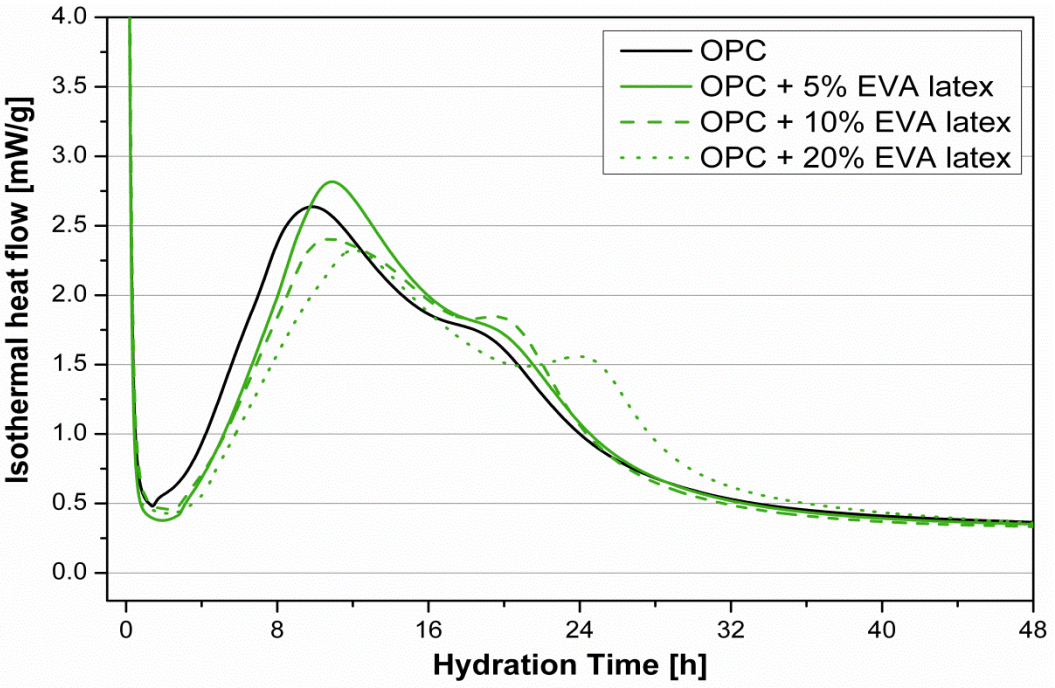

Figure 34. Time-dependent heat flow of OPC pastes recorded in the presence and absence of liquid EVA latex (dosages: 5, 10 and 20 % bwoc.).

Generally, EVA copolymer increases the intensity of the second heat flow maximum with increasing dosage, while the intensity of the main heat flow maximum is decreased. These effects are more pronounced for the EVA powder sample compared to its liquid latex. **Figure 36** displays the heat flow curve of OPC pastes containing the spraying aid PVOH in the dosage as present in the RDP. From the result it becomes obvious that the behavior of the EVA copolymer appears to be similar to that of individual PVOH.

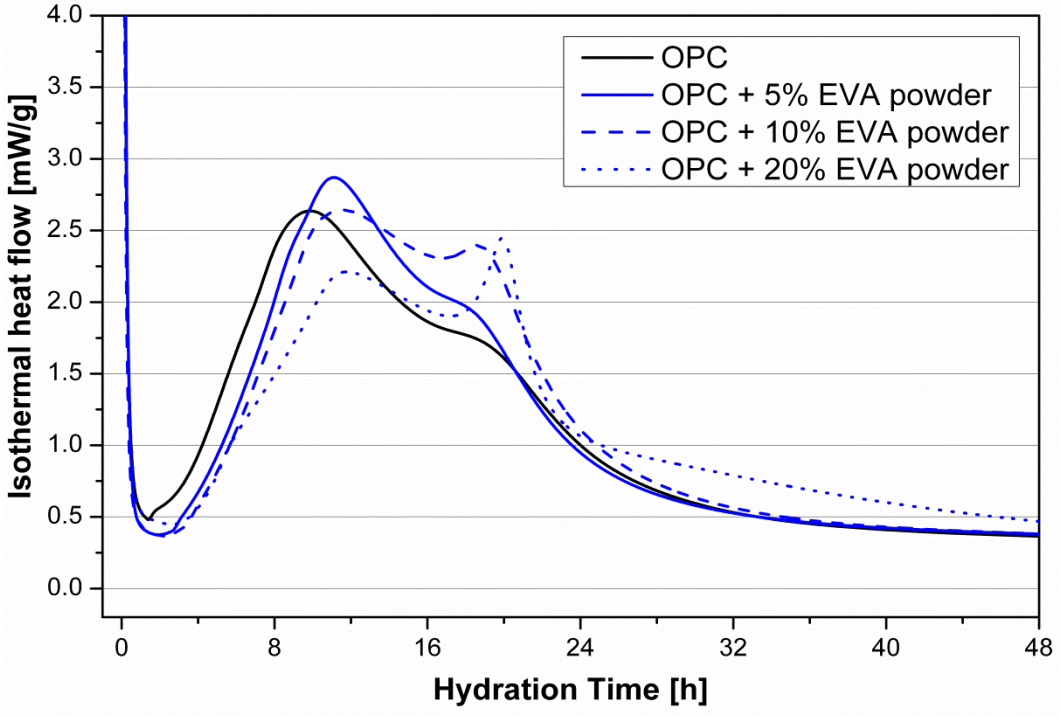

Figure 35. Time-dependent heat flow of OPC pastes recorded in the presence and absence of powder EVA latex (dosages: 5, 10 and 20 % bwoc.).

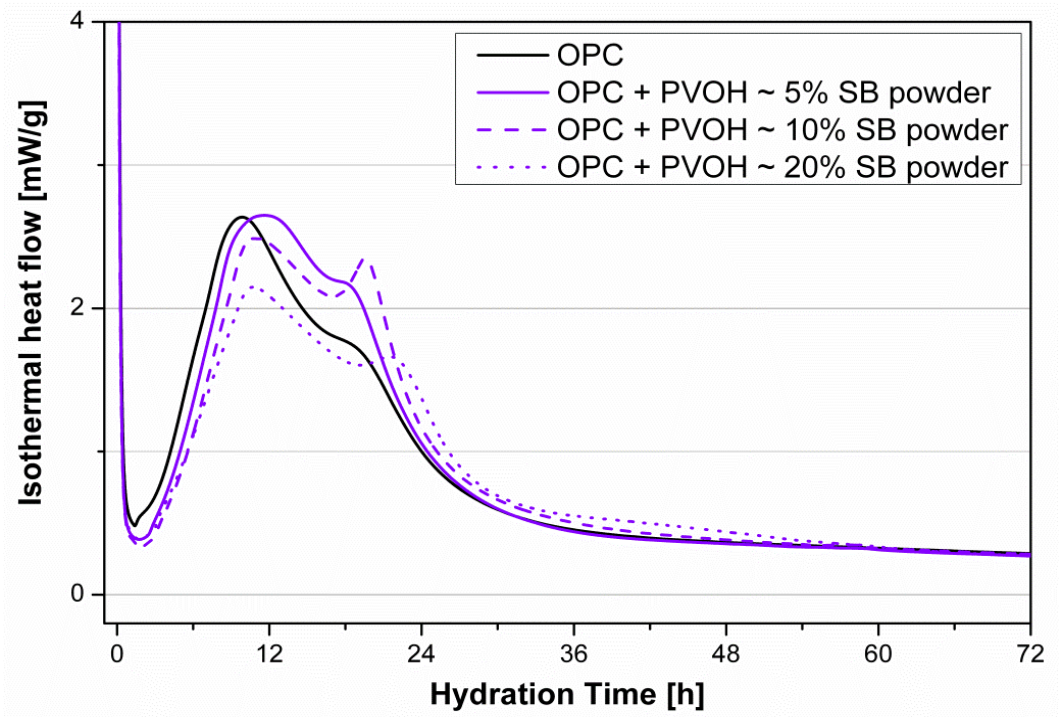

Figure 36. Time-dependent heat flow of OPC pastes recorded in the presence and absence of PVOH (dosage same as contained in 5, 10 and 20 % bwoc addition of powder EVA).

This conclusion was confirmed via in-situ XRD measurements. **Figure 37** summarizes the time-dependent evolution of ettringite within the first 48 h of hydration in the presence and absence of liquid and powder EVA latex and PVOH. The result clearly shows that ettringite formation is only slightly affected by the presence of EVA copolymer. The time-dependent evolution of ettringite is not affected at all in the presence of liquid EVA latex, whereas at higher dosages of EVA powder or PVOH the signal intensity of ettringite is decreased. Again, the EVA powder sample containing PVOH as spraying aid behaves similar compared to the cement modified with PVOH only.

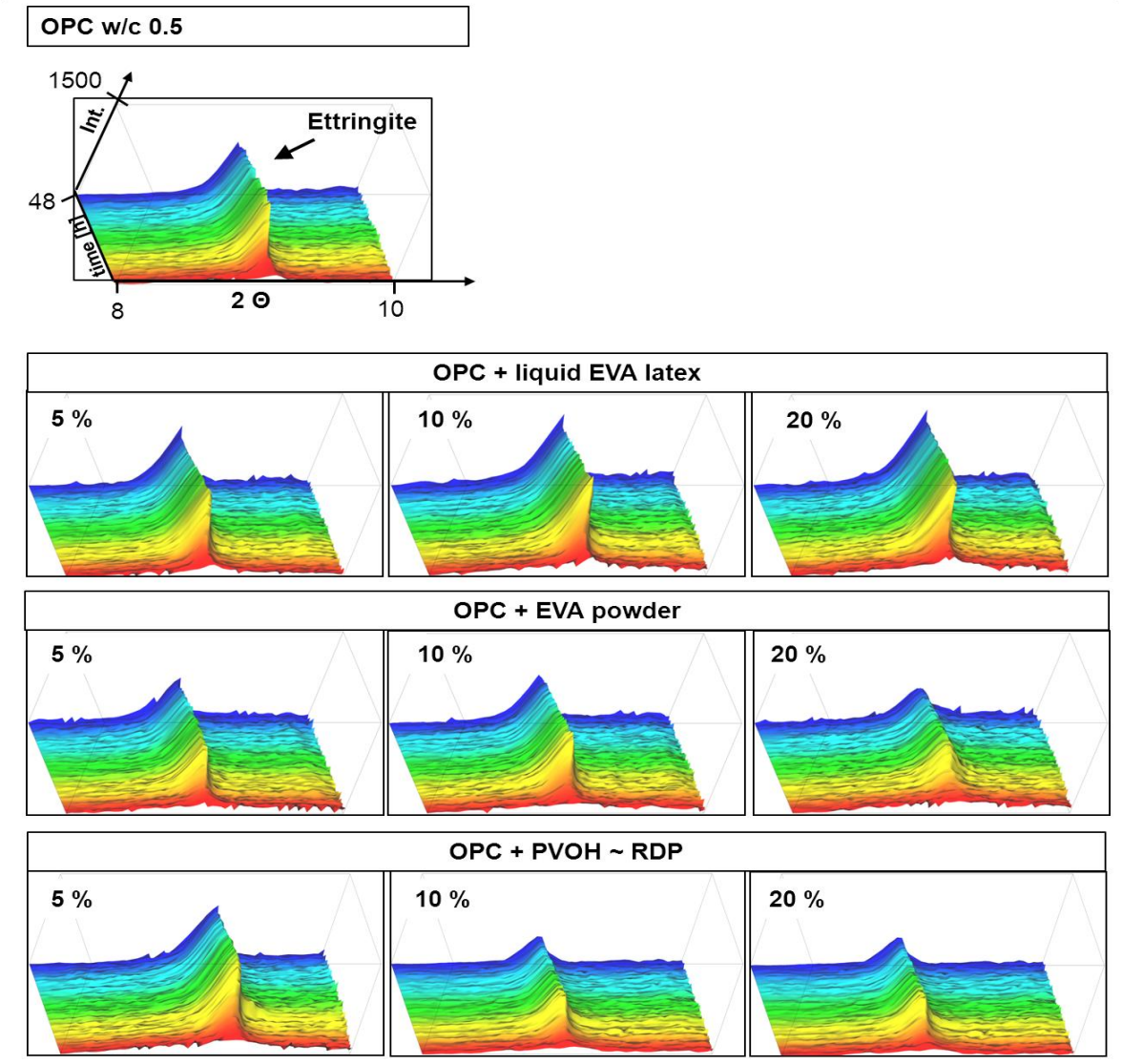

Figure 37. Time-dependent evolution of ettringite during OPC hydration in the absence and presence of liquid or powder EVA latex and PVOH. The scaling of all XRD patterns is similar (2Θ range: 8-10°; time frame: 48 h; intensity: 1500 counts).

Figure 38 provides an overview of the time-dependent evolution of portlandite within the first 48 h of hydration in the presence and absence of liquid or powder EVA latex and PVOH. In the neat cement paste, portlandite crystallization starts 4 h after mixing with water. The starting point of portlandite crystallization in the presence of liquid and powder EVA latex is almost similar to that in the neat cement paste, whereas the signal intensity for portlandite increases with increasing dosage of EVA copolymer. This effect is much more pronounced for the EVA powder sample which again shows a similar trend, compared to the system containing PVOH only.

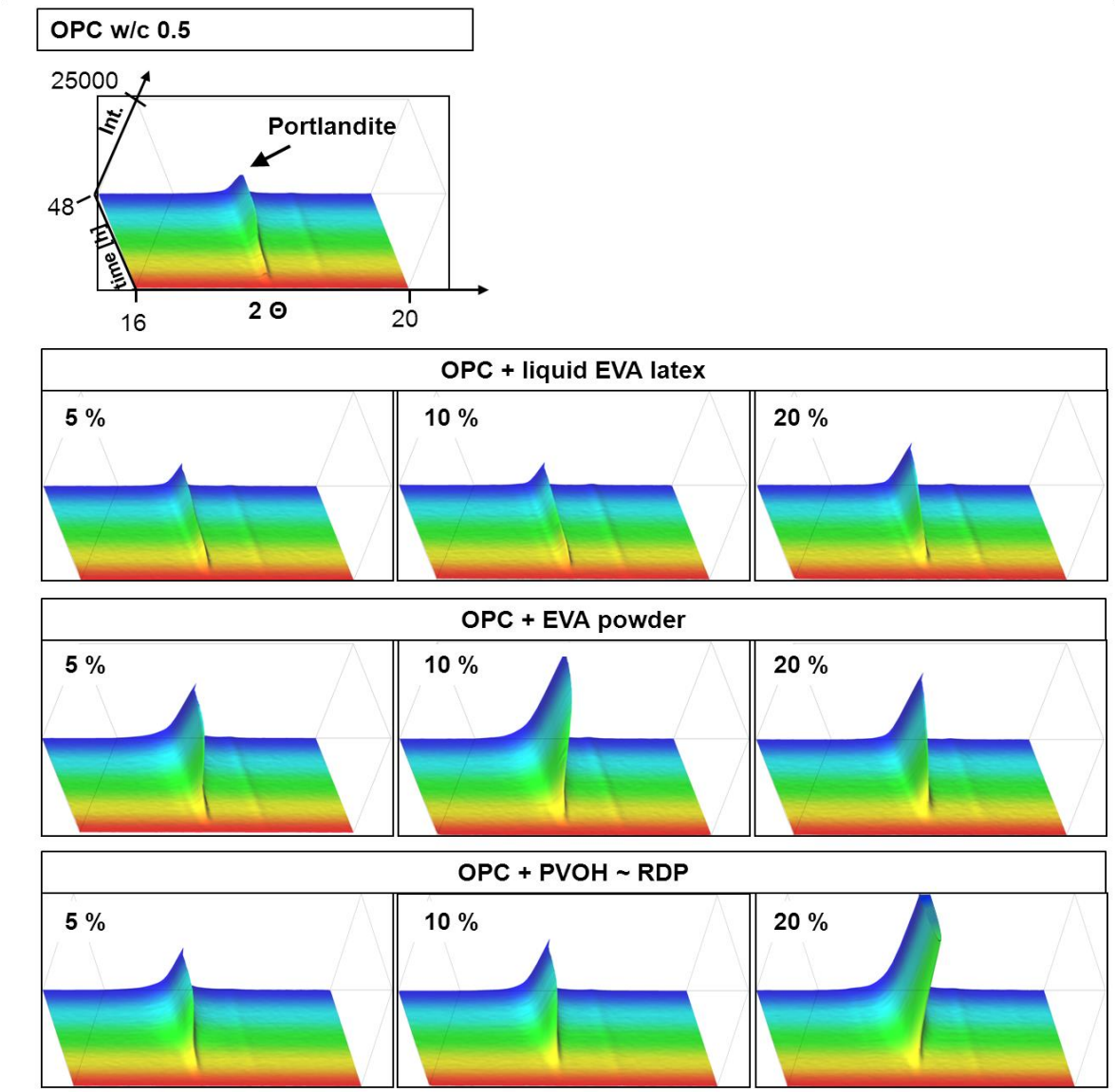

Figure 38. Time-dependent evolution of portlandite during OPC hydration in the absence and presence of liquid or powder EVA latex and PVOH. The scaling of all XRD patterns is similar (2Θ range: 16-20°; time frame: 48 h; intensity: 25000 counts).

As was already explained in paper #5, in the presence of PVOH portlandite crystallization is slightly retarded for the system containing 20 % bwoc PVOH ~ RDP and the signal intensity increases significantly with PVOH dosage. This effect was ascribed to the hydrolysis of PVOH in the cement paste whereby hydroxide ions are consumed and thus the pH of the cement slurry is decreased. Resulting from the lower pH, the solubility of the silicate phases C_2S and C_3S increases and more calcium ions can precipitate as calcium hydroxide. Exactly the same effect occurs in the presence of liquid and powder EVA latex. In liquid EVA latex only a small amount of PVOH is present which was added as colloidal stabilizer during the emulsion polymerization process, thus the pH value of cement slurries is only slightly decreased. However, in the EVA powder samples higher amounts of PVOH are present which cause a similar trend compared to the cement paste modified with PVOH only.

Figure 39 shows the time-dependent pH values of cement slurries modified with 5, 10 or 20 % bwoc liquid or powder EVA latex. Generally, the pH value of cement pastes is decreased with increasing dosage of EVA copolymer. The effect of EVA addition on the pH value of the cement pastes depends on the amount of PVOH contained in the EVA latex sample, thus EVA powder exhibits a much more pronounced effect on the pH value compared to its mother liquor. Furthermore, the pH value of cement slurries containing 10 or 20 % bwoc EVA latex shows a strong time-dependence which can be ascribed to the gradual hydrolysis of PVOH over time.

Figure 40 demonstrates the effect of the decreased pH value of cement slurries in the presence of EVA copolymer or PVOH on the concentration of calcium ions present in cement pore solution. The calcium ion concentration in cement pore solution is significantly increased by the colloidal stabilizer PVOH. Thus, a similar but less pronounced trend was observed for the cement modified with EVA copolymer containing PVOH. Again, this effect is more pronounced for the EVA powder sample which contains a higher amount of PVOH compared to its mother liquor. This result explains the increased formation of portlandite in cement slurries containing PVOH such as EVA powder or individual PVOH.

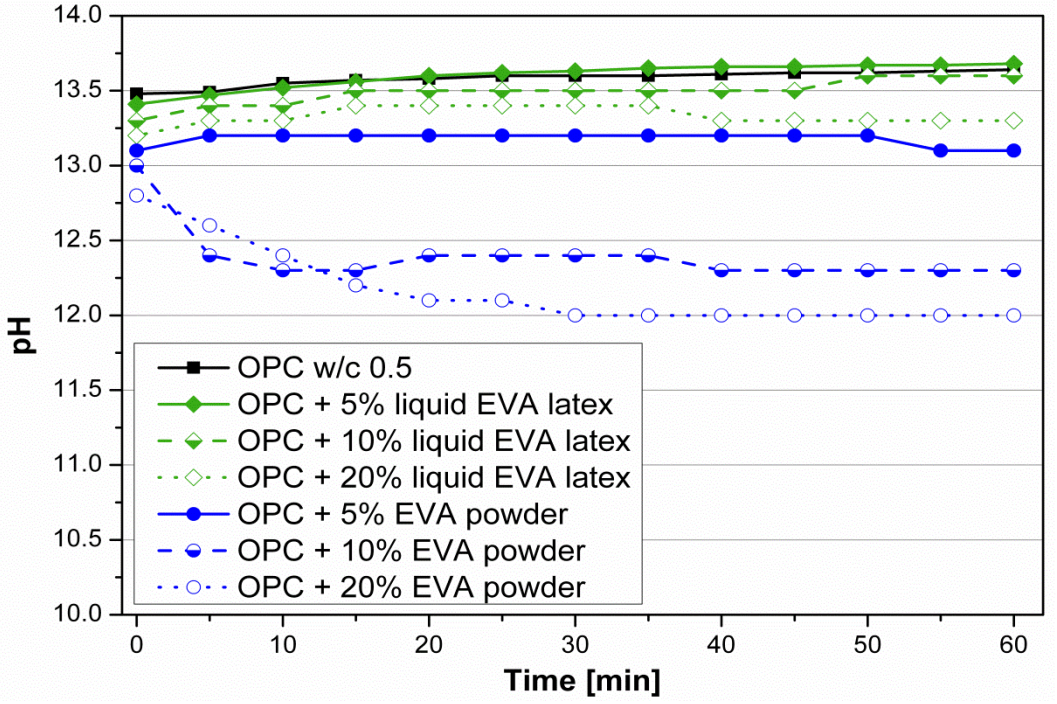

Figure 39. Time-dependent evolution of the pH value of cement slurries in the presence and absence of liquid and powder EVA latex within a time interval of 60 minutes after mixing.

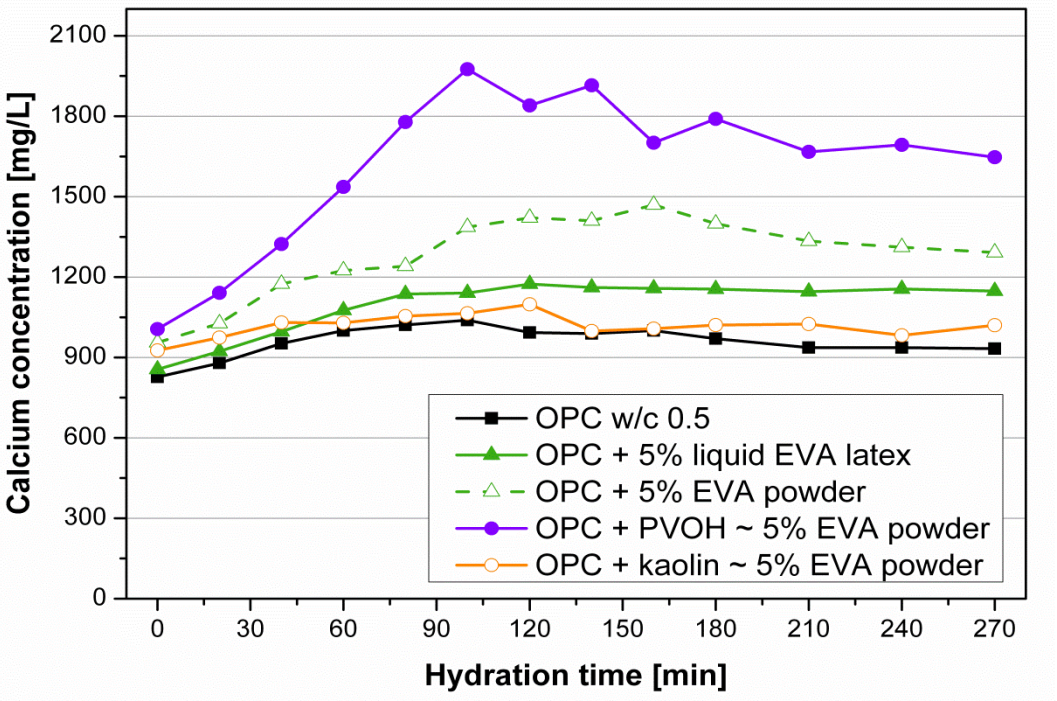

Figure 40. Concentration of calcium ions in the pore solution of OPC hydrating in the presence and absence of liquid and powder EVA latex, PVOH and kaolin, measured during the first 270 min of hydration.

Figure 41 displays the sulfate concentration of the cement pore solution in the presence and absence of 5 % bwoc liquid and powder EVA latex, PVOH and kaolin within the first 270 min after mixing with water. In the presence of liquid and powder EVA latex or PVOH the equilibrium concentration of sulfate is lower compared to that in the neat cement. This effect is most pronounced for the PVOH-modified cement paste, followed by the EVA powder sample which contains a higher amount of PVOH compared to the liquid EVA latex. This result indicates a decreased solubility of the sulfate agent in the presence of EVA and PVOH polymer.

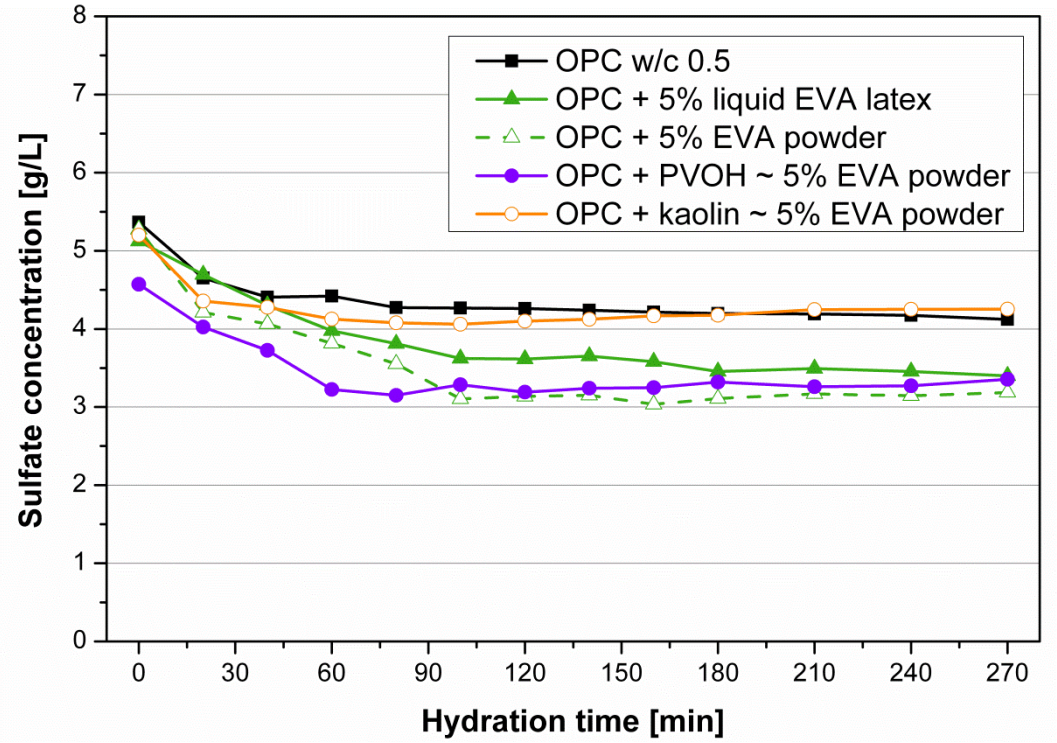

Figure 41. Sulfate concentration in the pore solution during OPC hydration in the presence and absence of EVA latex, EVA powder, PVOH and kaolin, measured during the first 270 min of hydration.

The zeta potential of the neat cement slurry and of slurries containing liquid or powder EVA latex was measured in order to investigate their potential interaction with dispersed cement grains. Cement particles dispersed in water develop a heterogeneous surface charge due to the formation of different hydrate phases and thus provide adsorption sites for oppositely charged polymers or colloids. **Figure 42** shows the evolution of the zeta potential of cement pastes in the presence and

absence of liquid or powder EVA latex at varying dosages (5, 10 and 20 % bwoc) within the first hour after mixing with water. The results clearly show that the value for the zeta potential is not changed in the presence of non-ionic EVA copolymer. Generally, adsorption represents a physical process which is driven by the electrostatic attraction between colloidal particles. Thus, the driving force for the adsorption of non-ionic EVA particles is not high enough to shift the equilibrium in favor of adsorption. From the result it can be concluded that the influence of the EVA copolymer on cement hydration is not characterized by colloidal interactions, instead the influence on the pH value of the cement pore solution seems to be most relevant.

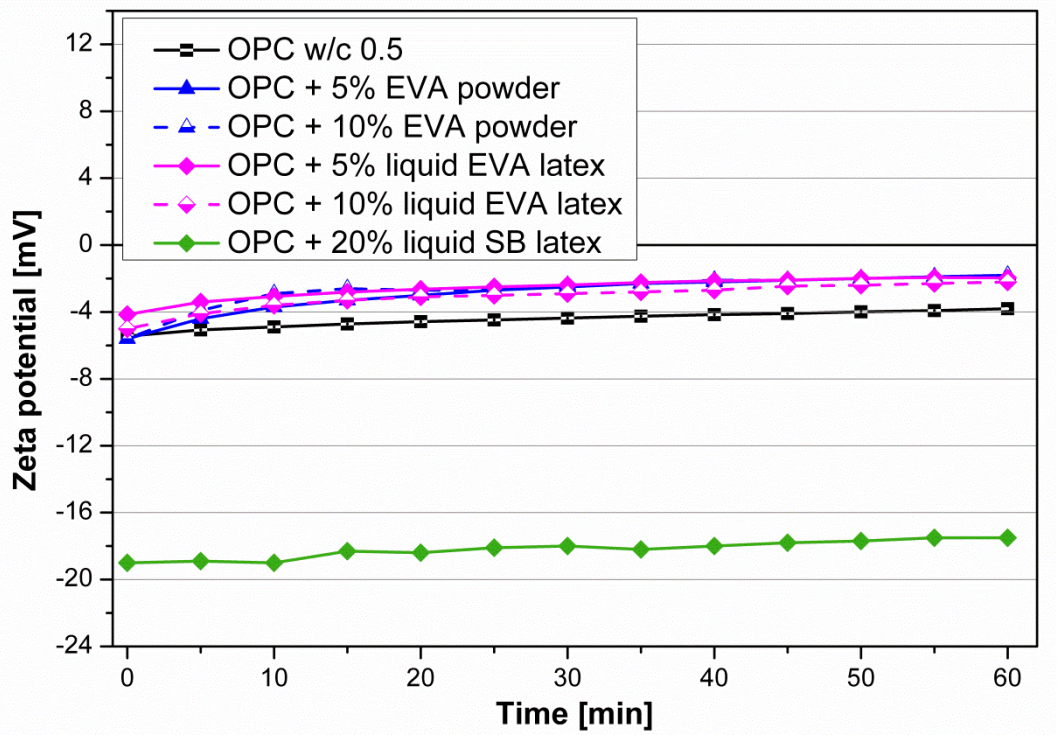

Figure 42. Time-dependent zeta potential of cement pastes (w/c 0.5) in the presence and absence of liquid and powder EVA or SB latex (dosages: 5, 10 and 20 % bwoc).

The experiments on the influence of EVA copolymer on the hydration kinetics of Portland cement demonstrate that the minor effect of EVA can be ascribed to the missing physical interaction with cement or ions from pore solution. As a consequence, the impact of EVA is mainly controlled by the presence of the colloidal stabilizer PVOH which undergoes hydrolysis in the alkaline cement pore solution and thus decreases its pH value, leading to enhanced dissolution of the silicate phases.

This behavior is much more pronounced for the EVA powder due to its higher PVOH content compared to the liquid EVA dispersion. Furthermore, the results reveal that the influence of non-ionic EVA copolymer on cement is characterized by a completely different mechanism compared to the anionic SB, meaning that the impact of non-ionic EVA is controlled by the presence of the spraying aids whereas the effect of anionic SB is controlled by its specific anionic surface charge density and the resulting physical interactions with mineral surfaces or ions.

5.5 Influence of latex polymers on the hydration kinetics of a ternary binder system (paper #5)

Ternary binder systems are commonly used in rapid hardening dry mortar applications and therefore often combined with latex polymers. Nonetheless, no work dealing with the influence of latex polymers on the hydration kinetics of the ternary binder system OPC/CAC/anhydrite has yet been published in the literature. Therefore, this study aimed to investigate the impact of carboxylated styrene-butadiene latex on the hydration of the TBS and to develop a fundamental working mechanism. As was presented in paper #4, anionic styrene-butadiene latex copolymer significantly retards or even suppresses the hydration of Portland cement. However, hydration of the ternary binder system OPC/CAC/anhydrite is accelerated by the addition of increasing amounts of SB latex, as was confirmed via calorimetry and in-situ XRD. **Figure 43** and **Figure 44** show the heat flow curves of OPC and TBS hydration in the presence of liquid SB latex.

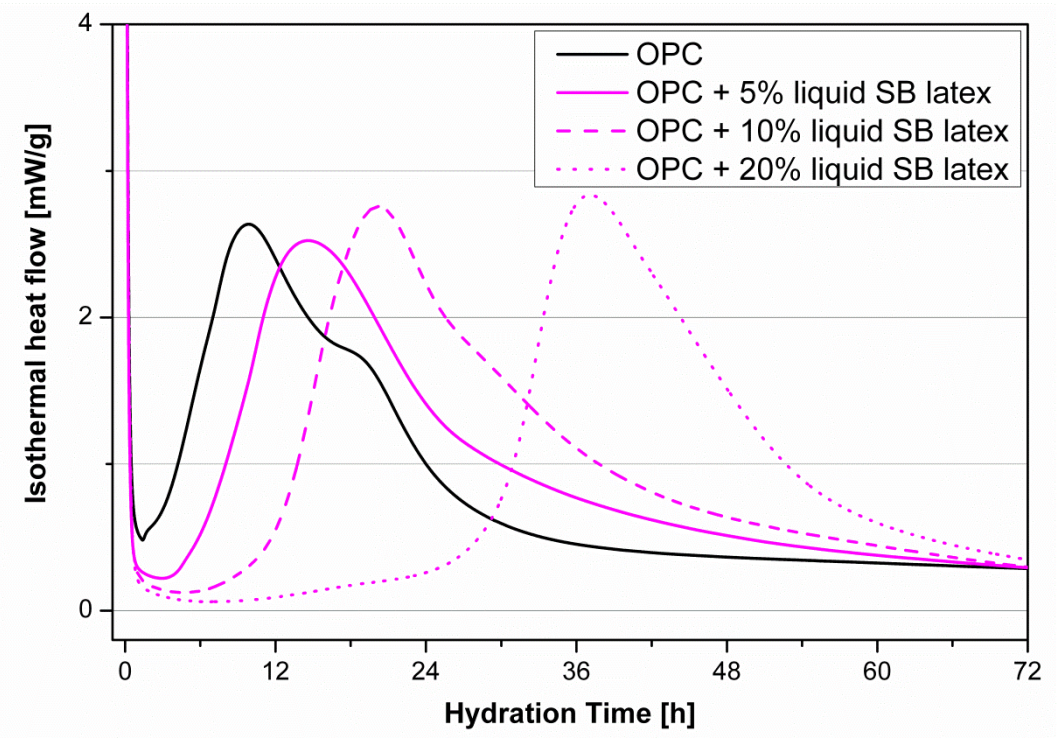

Figure 43. Time-dependent heat flow of OPC pastes recorded in the presence and absence of liquid SB latex (dosages: 5, 10 and 20 % bwoc).

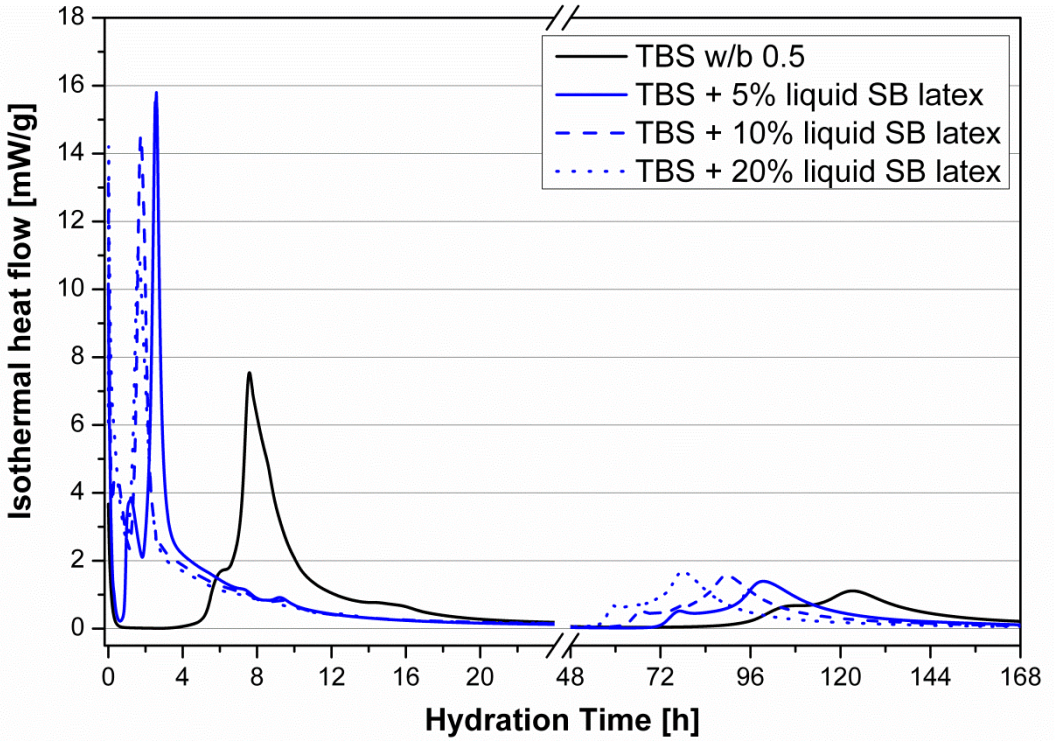

Figure 44. Time-dependent heat flow of TBS pastes recorded in the presence and absence of liquid SB latex (dosages: 5, 10 and 20 % bwob).

The reason behind the accelerating effect of SB latex in the TBS was found to be the sequestration of calcium ions from cement pore solution, whereby the solubility equilibrium of calcium sulfate is shifted in favor of sulfate. Thus, the sulfate concentration in cement pore solution increases significantly and this way ettringite crystallization is promoted.

Additional results on the influence of SB powder on TBS hydration are presented in **Figure 45**. Here, it becomes obvious that the accelerating effect of the SB powder is less pronounced compared to the liquid SB latex. This behavior can be ascribed to the lower anionic charge density of powder SB latex whereby upon chelation via carboxylate groups less calcium ions are depleted from cement pore solution. As a result, the dissolution of anhydrite is less promoted and the effect on ettringite crystallization is minor only.

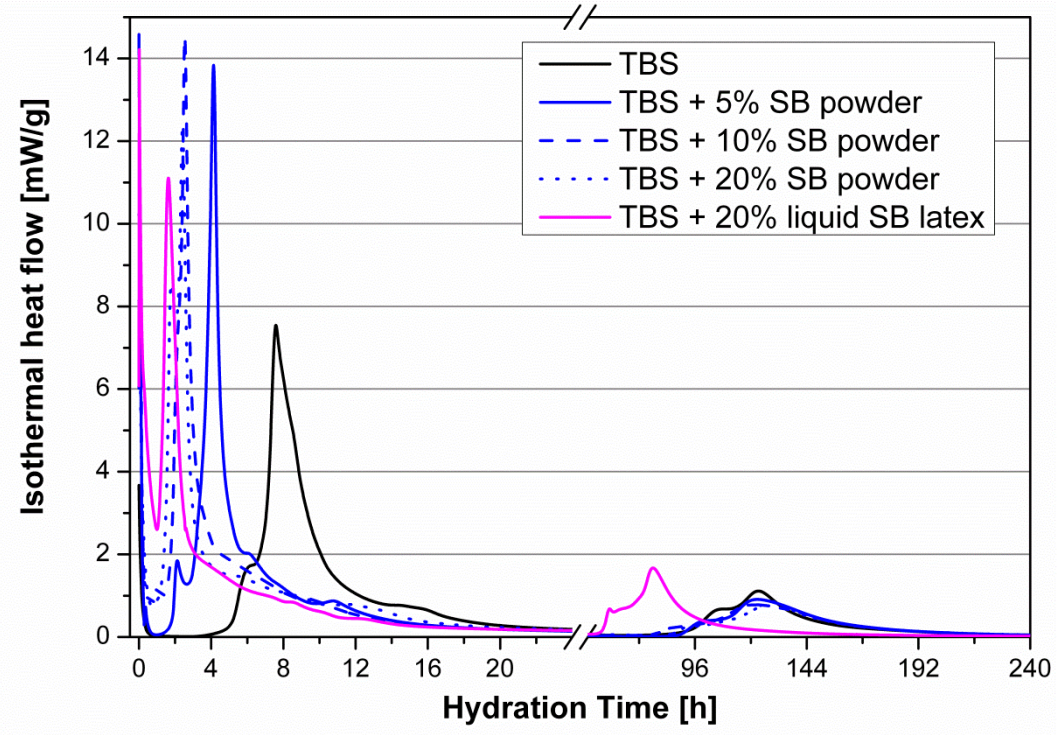

Figure 45. Time-dependent heat flow of TBS pastes recorded in the presence and absence of powder SB latex (dosages: 5, 10 and 20 % bwob).

These experiments revealed that the SB latex copolymer impacts the hydration kinetics of OPC and TBS in a completely different way.

Complementary, the influence of EVA latex and powder on the hydration kinetics of the ternary binder system OPC/CAC/anhydrite was studied. Similar investigations as presented in paper #5 were performed for this purpose. Preliminary results showed that the non-ionic EVA copolymer does not influence the early formation of ettringite in the ternary binder system. However, the late silicate reaction is significantly retarded which is especially detrimental for the strength development of such a system (**Figure 46**). The mechanism underlying this behavior was not analyzed within this thesis. A possible explanation could be the formation of an EVA polymer film which embeds the cement grains and thus prevents water access and subsequent hydration reaction.

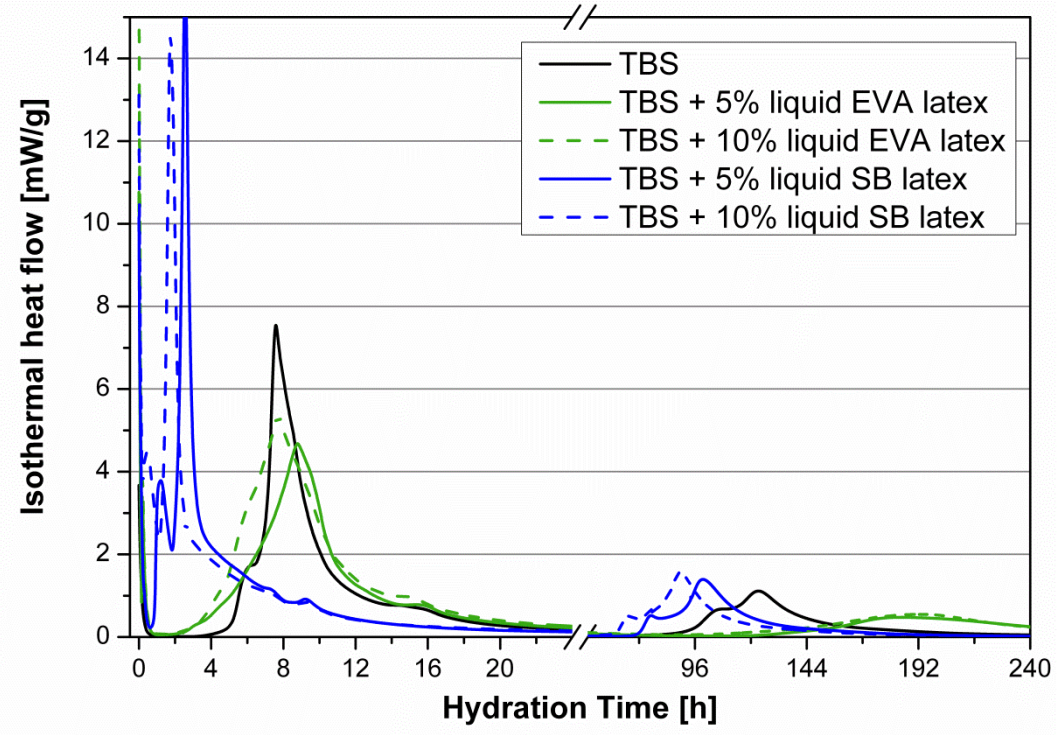

Figure 46. Time-dependent heat flow of TBS pastes recorded in the presence and absence of liquid EVA or SB latex (dosages: 5, 10 and 20 % bwob).

5.6 Effect of nano clay on early strength development of Portland cement (paper #6)

Investigations on the influence of the spraying aids PVOH and kaolin on Portland cement hydration have shown that kaolin increases the overall heat development as was evidenced via heat flow calorimetry. Based on that it was expected that the early strength of OPC may be enhanced by the addition of kaolin as well. Therefore, the 12, 16 and 24 h early strengths of mortar specimens containing additional amounts of kaolin were measured. The results clearly show that the addition of nano-sized kaolin boosts the 16 h early compressive and tensile strengths of Portland cement up to 60 % without negatively impacting the final strength after 28 d. Heat calorimetry and in-situ XRD measurements revealed an increased reactivity of the silicate and aluminate phases which is responsible for strength enhancement in the presence of kaolin. The effectiveness of kaolin addition was found to be more pronounced for slowly hydrating cements.

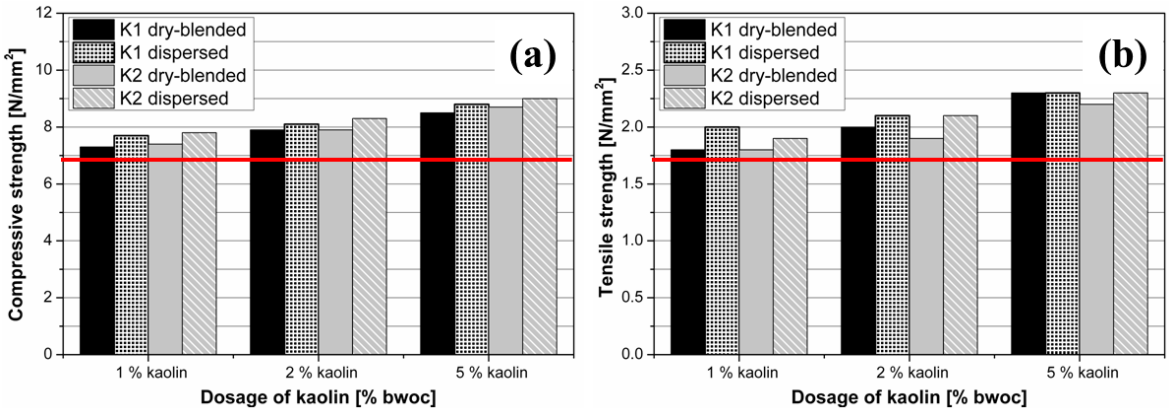

Figure 47. (a) Compressive and (b) tensile strength after 16 h of mortar specimens prepared from CEM I 52.5 N containing 1, 2 or 5 % bwoc of kaolin sample K1 or K2. The red line represents the strength of the reference mortar without kaolin.

In the literature crystalline clays such as kaolin were known to decrease the final strength of concrete, whereas non-crystalline clays react in the pozzolanic reaction and thus increase the final strength. Our results show that also crystalline clays

exhibiting particle sizes in the nanometer range can in fact enhance the early strength of mortar or concrete without negatively impacting the final strength.

6 SUMMARY AND OUTLOOK

This research work aimed to study the interaction of non-ionic ethylene-vinyl-acetate (EVA) and anionic styrene-butadiene (SB) latex copolymers with inorganic binders (Portland cement and the ternary binder system OPC/CAC/anhydrite). For this purpose, investigations were performed with liquid and powder EVA or SB latex samples respectively, in order to evaluate the potential impact of the spraying aids PVOH and kaolin contained in the latex powder samples.

First of all, the colloidal properties of the latex particles were characterized because they determine their potential interactions with mineral surfaces or ions. Especially the influence of the spray drying process under the addition of PVOH as colloidal stabilizer and kaolin as anti-caking agent on the colloidal properties of the re-dispersed latex powder was of great interest. Subsequently, the effect of the spraying aids on the colloidal stability and film formation of the latex samples was studied. In order to predict their performance in cementitious systems, these investigations were carried out in synthetic cement pore solution complementary to the aqueous system. Finally, the impact of the liquid and powder latex samples, as well as the individual spraying aids PVOH and kaolin on the hydration kinetics of ordinary Portland cement and the ternary binder system OPC/CAC/anhydrite was evaluated and correlated with the colloidal properties of the latex particles.

One of the main findings of this work is that the electrokinetic surface properties of latex particles are significantly influenced by the addition of the spraying aids PVOH and kaolin during the spray drying process in the fabrication of the powder. Depending on the ionic character of the latex sample (non-ionic or anionic), the effect of the PVOH coating on the final properties of the latex can differ. Upon spray drying, the SB powder particles are coated with a film of the colloidal stabilizer PVOH whereby carboxylate groups located on the latex particle surface are partially embedded into this coating. As a result, the anionic charge density decreases and less sites for physical interactions are available. A similar effect was evidenced for the ethylene-vinylacetate copolymer, however, due to its non-ionic character the colloidal

properties and thus physical interactions with ions or mineral surfaces are not affected to such an extent. Surprisingly, upon re-dispersion in water the PVOH layer does not dissolve completely from the surface of the latex particles. In the future it would be interesting to spray dry latex dispersions in the presence of other colloidal stabilizers and to study their effect on the colloidal properties of the re-dispersed latex powders.

Styrene-butadiene dispersions prepared from the re-dispersible powder exhibit a much higher colloidal stability in synthetic cement pore solution compared to their mother liquor. This effect can be ascribed to the reduced interactions with calcium ions from cement pore solution. For the EVA no difference in the colloidal stability of dispersions prepared from the liquid or powder latex was observed due to their non-ionic character. Furthermore, not only the colloidal stability, but also the film formation of dispersions is influenced by the spraying aids PVOH and kaolin. For both, EVA and SB copolymers, film formation occurs much faster from re-dispersed latex powders compared to their liquid precursors. Experiments revealed that kaolin acts as accelerator for the film formation and overrides the decelerating effect originating from PVOH contained in the latex powder samples. The mechanism behind this acceleration of film formation by the addition of the anti-caking agent kaolin could not be clarified within this research work and needs further investigation.

Experiments on the film forming mechanism of the SB copolymer have shown that the film forming process involves more than the four well-known stages. Monodisperse SB particles self-assemble in colloidal crystal-like domains at the stage of a dense particle packing. Next, particle interpenetration first begins within these domains and then further spreads across the entire matrix until a homogeneous and coherent polymer film is achieved. This effect only occurs for monodisperse latices whereas polydisperse latices do not show such crystallization upon water removal.

The influence of latex polymers on the hydration of Portland cement and the ternary binder system OPC/CAC/anhydrite strongly depends on the colloidal properties of

the latex particles. Therefore, the re-dispersible powder of carboxylated styrene-butadiene latex exhibits a different influence on cement hydration compared to its liquid precursor.

Generally, anionic SB particles strongly retard or suppress the silicate and aluminate reaction in the hydration of ordinary Portland cement caused by adsorption of the latex particles onto mineral surfaces or chelation of calcium ions from cement pore solution. Contrary to the anionic SB copolymer, the EVA latex used in this study minor affects the hydration kinetics of Portland cement only minor, due to the absence of physical interactions with cement or ions from pore solution. Thus, the effect of EVA is mainly controlled by the presence of the colloidal stabilizer PVOH which undergoes hydrolysis in the alkaline cement pore solution and thus decreases its pH value which leads to a promoted dissolution of the silicate phases. This behavior is much more pronounced for the EVA powder due to its higher PVOH content compared to the liquid EVA dispersion.

The influence of anionic SB latex on the hydration of the ternary binder system OPC/CAC/anhydrite is completely different compared to that of OPC and is characterized by a significant acceleration of the ettringite formation. The anionic SB latex particles foster the dissolution of sulfate from anhydrite and thus accelerate the crystallization of ettringite. The mechanism behind this effect is a shift in the solubility equilibrium for anhydrite triggered by the sequestration of calcium ions from the pore solution by the carboxylate groups present in the latex particles.

Furthermore, in this study it was demonstrated that styrene-butadiene latex can be spray dried in the absence of a colloidal stabilizer. It would be interesting to modify the synthesis of latex dispersions in a way that the colloidal stabilizer is directly generated in the serum phase during the emulsion polymerization process. Especially the substitution of poly(vinylalcohol) as colloidal stabilizer would be a big step forward in the development of re-dispersible latex powders due to its negative effects in the application. Furthermore, a more detailed study on the effect of the serum phase of latex dispersions on cement hydration would be highly interesting.

In the future, further investigations on the influence of latex polymers on the hydration kinetics of ternary binder systems need to be performed. Especially the effect of the latex polymers on the late silicate reaction of the TBS hydration would be of interest. Preliminary results show that film formation of the latex polymers already starts before the silicate reaction proceeds. This effect may depend on at which clinker phases the latex particles are preferentially anchored and thus on their ionic character. Furthermore, the effect of liquid and powder latex samples on the TBS hydration require further investigation in order to assess the mechanism behind the effect of the spraying aids PVOH and kaolin.

In dry mortar formulations latex polymers are usually combined together with cellulose ethers which are applied as water retention agents and for modification of the rheology of the mortar. Preliminary results showed that the strong retarding effect of the anionic styrene-butadiene latex is mitigated in the presence of hydroxy ethyl methyl cellulose (HEMC) or hydroxyl propyl methyl cellulose (HPMC). The mechanism behind this effect was not a focus within this study but would be interesting for investigations in the future.

Finally, it was shown that nano kaolin clay can boost the early 10-24 h compressive and tensile strengths of Portland cement without negatively impacting the final strength after 28 d. Maximum strength enhancement is obtained in slowly reacting Portland cements such as CEM I 32.5 R, 42.5 R or 52.5 N as compared to a CEM I 52.5 R. This effect is ascribed to an increased reactivity of the silicate and aluminate phases which can be explained by a seeding effect, meaning that due to heterogeneous nucleation, the activation energy for the crystallization of cement hydrates is reduced and thus early strength development is promoted. Additionally, aluminum is leached from kaolin into cement pore solution, whereby the crystallization of the aluminate hydrates is initiated. As a consequence, the effect of kaolin is linked to the particle size of the individual clay platelets.

7 ZUSAMMENFASSUNG

In dieser Arbeit wurde die Wechselwirkung von nicht-ionischen Ethylen-Vinylacetat und anionischen Styrol-Butadien Copolymeren mit anorganischen Bindemitteln (Portlandzement und dem ternären Bindemittelsystem OPC/CAC/Anhydrit) untersucht. Zur Beurteilung des Einflusses der Sprühhilfen Poly(vinylalkohol) und Kaolin, welche in den Dispersionspulver-Proben enthalten sind, wurden die Untersuchungen sowohl mit wässrigen Dispersionen als auch deren re-dispergierbaren Pulvern durchgeführt.

Im ersten Schritt wurden die kolloidchemischen Eigenschaften der Latexpartikel bestimmt, da diese die potentiellen Wechselwirkungen mit mineralischen Oberflächen oder Ionen bestimmen. Insbesondere der Einfluss des Sprühtrocknungsprozesses unter Zugabe von Poly(vinylalkohol) als Schutzkolloid und Kaolin als Antibackmittel auf die kolloidchemischen Eigenschaften der re-dispergierten Dispersionspulver-Partikel war von großem Interesse. Anschließend wurde der Einfluss der Sprühhilfen auf die Kolloidstabilität und die Filmbildung der Dispersionen untersucht. Zur Beurteilung und Vorhersage des Verhaltens in zementgebundenen Systemen wurden diese Untersuchungen ergänzend zum wässrigen System in synthetischer Zementporenlösung durchgeführt. Im letzten Schritt wurde der Einfluss der Dispersionen bzw. Dispersionspulver sowie der Sprühhilfen Poly(vinylalkohol) und Kaolin auf die Hydratationskinetik von Portlandzement und des ternären Bindemittelsystems OPC/CAC/Anhydrit untersucht und mit den kolloidchemischen Eigenschaften der Latexpartikel korreliert.

Im Rahmen dieser Forschungsarbeit wurde gezeigt, dass die elektrokinetischen Oberflächeneigenschaften von Latexpartikeln durch die Zugabe der Sprühhilfen PVOH und Kaolin während der Sprühtrocknung verändert werden. In Abhängigkeit des ionischen Charakters der Dispersion (nicht-ionisch oder anionisch) führt dies zu unterschiedlich starken Effekten auf die endgültigen Eigenschaften der Latexpartikel. SB Pulverpartikel werden während der Sprühtrocknung mit einer Schicht des Schutzkolloids PVOH überzogen, wobei Carboxylgruppen, welche sich an der Latex-

partikeloberfläche befinden, teilweise in diese PVOH-Schicht eingebettet werden. Folglich nimmt die anionische Ladungsdichte der Latexpartikel ab und es stehen weniger funktionelle Gruppen für physikalische Wechselwirkungen zur Verfügung. Ein vergleichbarer Effekt wurde für das Ethylen-Vinylacetat Copolymer nachgewiesen. Aufgrund dessen nicht-ionischen Charakters werden jedoch die kolloidchemischen Eigenschaften und damit die physikalischen Wechselwirkungen mit Ionen oder mineralischen Oberflächen bei EVA weniger beeinflusst. Entgegen dem aktuellen Stand der Technik wurde gezeigt, dass sich die PVOH-Schicht nach dem Redispergieren in Wasser nicht vollständig von der Partikeloberfläche ablöst. Zudem konnten Styrol-Butadien Dispersionen ohne die Zugabe von Schutzkolloid erfolgreich sprühgetrocknet werden.

Styrol-Butadien Dispersionen, welche aus dem re-dispergierbaren Pulver hergestellt werden, weisen im Vergleich zur Ausgangsdispersion eine deutlich höhere Stabilität in synthetischer Zementporenlösung auf. Dieser Effekt kann auf die abgeschwächten Wechselwirkungen mit Calciumionen aus der Zementporenlösung zurückgeführt werden. Für das EVA Copolymer wurde aufgrund seines nicht-ionischen Charakters kein Unterschied in der Kolloidstabilität von Dispersionen, welche aus der Ausgangsdispersion oder dem Dispersionspulver hergestellt wurden, beobachtet. Neben der Kolloidstabilität wird auch die Filmbildung von Dispersionen durch die Sprühhilfen PVOH und Kaolin beeinflusst. Sowohl für das EVA als auch das SB Copolymer erfolgt die Filmbildung der re-dispergierten Pulver schneller im Vergleich zu ihren Ausgangsdispersionen. Experimente zeigten, dass Kaolin eine Beschleunigung der Filmbildung bewirkt und die verzögernde Wirkung des PVOH aufhebt. Der zu Grunde liegende Mechanismus der beschleunigten Filmbildung in Gegenwart des Antibackmittels Kaolin konnte in dieser Arbeit nicht aufgeklärt werden und bedarf weiterer Untersuchungen.

Experimente zum Filmbildungsmechanismus des SB Copolymers zeigten, dass der Prozess der Filmbildung mehr als die bekannten vier Stufen durchläuft. Die monodispersen SB Partikel ordnen sich in kristallinen Domänen in Form einer dichten Kugelpackung an. Dadurch beginnt die Koaleszenz der Latexpartikel zunächst

innerhalb dieser Domänen, bevor sich der Film über die gesamte Matrix ausbreitet und einen homogenen kohärenten Polymerfilm bildet. Dieser Effekt tritt nur für monodisperse Dispersionen auf, wohingegen polydisperse Systeme keine Kristallisation der Latexpartikel infolge des Wasserentzugs zeigen.

Der Einfluss der Latexpolymere auf die Hydratation von Portlandzement und des ternären Bindemittelsystems OPC/CAC/Anhydrit hängt stark von den kolloid-chemischen Eigenschaften der Latexpartikel ab. Folglich zeigt das re-dispergierbare Pulver des carboxylierten Styrol-Butadien Copolymers einen anderen Einfluss auf das Reaktionsverhalten im Vergleich zu seiner Ausgangsdispersion.

Anionische SB Partikel führen zu einer starken Verzögerung der Silikat- und Unterdrückung der Aluminatreaktion in der Hydratation von Portlandzement. Grund ist die Adsorption der Latexpartikel auf mineralischen Oberflächen sowie die Komplexierung von Calciumionen aus der Zementporenlösung. Im Gegensatz zum anionischen SB Copolymer beeinflusst das nicht-ionische EVA Copolymer die Hydratationskinetik von Portlandzement kaum aufgrund fehlender physikalischer Wechselwirkungen mit Zementkornoberflächen oder Ionen der Porenlösung. Die Wirkung des EVA Copolymers wird hauptsächlich durch die Anwesenheit des Schutzkolloids PVOH gesteuert, welches in der alkalischen Zementporenlösung hydrolysiert, dadurch deren pH-Wert absinkt und eine verstärkte Auflösung der Silikate eintritt. Dieses Verhalten ist aufgrund des höheren PVOH-Gehalts für das EVA Pulver deutlich stärker ausgeprägt im Vergleich zur EVA Ausgangsdispersion.

Im ternären Bindemittelsystem OPC/CAC/Anhydrit ist der Einfluss des anionischen SB Copolymers auf die Hydratationsreaktion durch eine starke Beschleunigung der frühen Ettringitbildung charakterisiert, folglich liegt ein völlig anderer Einfluss im Vergleich zu reinem Portlandzement vor. Die anionischen SB Partikel begünstigen die Auflösung des Anhydrits und beschleunigen dadurch die Kristallisation von Ettringit. Der Effekt beruht auf der Verschiebung des Löslichkeits-gleichgewichts des Anhydrits aufgrund der Komplexierung von Calciumionen aus der Porenlösung durch die Carboxylatgruppen der Latexpartikel.

Im letzten Teil der Arbeit wurde gezeigt, dass Kaolin mit einer Partikelgröße im Nanometerbereich die 10-24 h Druck- und Biegezugfestigkeit von Portlandzement erhöht, ohne dabei die 28 d Endfestigkeit negativ zu beeinflussen. Die maximale Erhöhung der Frühfestigkeit wird nur mit langsam reagierenden Portlandzementen erreicht (CEM I 32.5 R, 42.5 R oder 52.5 N im Vergleich zu CEM I 52.5 R). Der Effekt der Frühfestigkeitserhöhung durch Zugabe von Kaolin ist auf eine erhöhte Reaktivität der Silikat- und Aluminatphasen zurückzuführen. Kaolinpartikel wirken als Impfkristalle und reduzieren aufgrund von heterogener Keimbildung die Aktivierungsenergie für die Kristallisation der Zementhydratphasen. Zusätzlich werden Aluminiumionen aus den Kaolinpartikeln in die Zementporenlösung ausgelaugt, wodurch die Kristallisation der Calciumaluminathydrate initiiert wird. Gemäß diesen Mechanismen hängt die Wirkung von Kaolin von der Partikelgröße der einzelnen Tonplättchen ab.

8 REFERENCES

[1] R. Bayer, H. Lutz, Dry mortars, Ullmann's encyclopedia of industrial chemistry (2009).

[2] V.S. Ramachandran, Concrete Admixtures Handbook: Properties, Science, and Technology, Noyes Publications (1995).

[3] U. Dilger, Ready-Mixed Mortar Production Plants, ZKG International, 38 (1985) 2-6.

[4] A. Konietzko, The Application of Modern Dry, Factory Mixed, Mortar Products, ZKG International, 48 (1985) 625-659.

[5] M. Guldner, Production and Processing of Dry, Factory-Mixed, Mortars, ZKG International, 52 (1999) 628-631.

[6] C. Evju, S. Hansen, Expansive properties of ettringite in a mixture of calcium aluminate cement, Portland cement and beta-calcium sulfate hemihydrate, Cement and Concrete Research, 31 (2001) 257-261.

[7] L. Amathieu, T. Bier, K.L. Scrivener, Mechanisms of set acceleration of Portland cement trough CAC addition, Proceedings of the International Conference on Calcium Aluminate Cements, (2001) 303-317.

[8] J.P. Bayoux, A. Bonin, S. Marcdargent, M. Verschaeve, Study of the hydration properties of aluminous cement and calcium-sulfate mixes, International symposium on calcium aluminate cements, London (1990), 320-334.

[9] P.W. Brown, L.O. Liberman, G. Frohnsdorff, Kinetics of the early hydration of tricalcium aluminate in solutions containing calcium-sulfate, Journal of the American Ceramic Society, 67 (1984) 793-795.

[10] F.W. Locher, W. Richartz, S. Sprung, Setting of cement and effect of adding calcium-sulfate, ZKG International, 33 (1980) 271-277.

[11] R. Wang, P. Wang, Effect of styrene-butadiene rubber latex/powder on cement hydrates, Journal of the Chinese Ceramic Society, 36 (2008) 912-919.

[12] R. Wang, L.J. Yao, P.M. Wang, Mechanism analysis and effect of styrene-acrylate copolymer powder on cement hydrates, Construction and Building Materials, 41 (2013) 538-544.

[13] J. Bizzozero, C. Gosselin, K.L. Scrivener, Expansion mechanisms in calcium aluminate and sulfoaluminate systems with calcium sulfate, Cement and Concrete Research, 56 (2014) 190-202.

[14] A. Jenni, L. Holzer, R. Zurbriggen, M. Herwegh, Influence of polymers on microstructure and adhesive strength of cementitious tile adhesive mortars, Cement and Concrete Research, 35 (2005) 35-50.

[15] Y. Ohama, Handbook of Polymer-Modified Concrete and Mortars - Properties and Process Technology, Noyes Publications, New Jersey (1995).

[16] Y. Ohama, Principle of latex modification and some typical properties of latex-modified mortars and concretes, ACI Materials Journal, 84 (1987) 511-518.

[17] J.W. Kardon, Polymer-Modified Concrete: Review, Journal of Materials in Civil Engineering, 9 (1997) 85-92.

[18] J.L. Keddie, Film formation of latex, Materials Science and Engineering: R: Reports, 21 (1997) 101-170.

[19] Y. Chevalier, C. Pichot, C. Graillat, M. Joanicot, K. Wong, J. Maquet, P. Lindner, B. Cabane, Film formation with latex particles, Colloid and Polymer Science, 270 (1992) 806-821.

[20] M. Gretz, J. Plank, An ESEM investigation of latex film formation in cement pore solution, Cement and Concrete Research, 41 (2011) 184-190.

[21] S. Erkselius, L. Wadsö, O. Karlsson, Drying rate variations of latex dispersions due to salt induced skin formation, Journal of Colloid and Interface Science, 317 (2007) 83-95.

[22] A. Jenni, R. Zurbriggen, L. Holzer, M. Herwegh, Changes in microstructures and physical properties of polymer-modified mortars during wet storage, Cement and Concrete Research, 36 (2006) 79-90.

[23] A. Jenni, M. Herwegh, R. Zurbriggen, T. Aberle, L. Holzer, Quantitative microstructure analysis of polymer-modified mortars, Journal of Microscopy, 212 (2003) 186-196.

[24] A.M. Betioli, P.J. Gleize, V.M. John, R.G. Pileggi, Effect of EVA on the fresh properties of cement paste, Cement and Concrete Composites, 34 (2012) 255-260.

[25] A.M. Betioli, J. Hoppe, M.A. Cincotto, P.J.P. Gleize, R.G. Pileggi, Chemical interaction between EVA and Portland cement hydration at early-age, Construction and Building Materials, 23 (2009) 3332-3336.

[26] H.W. Spiess, J. Rottstegge, M. Arnold, L. Herschke, G. Glasser, M. Wilhelm, W.D. Hergeth, Solid state NMR and LVSEM studies on the hardening of latex modified tile mortar systems, Cement and Concrete Research, 35 (2005) 2233-2243.

[27] R. Wang, X.G. Li, P.M. Wang, Influence of polymer on cement hydration in SBR-modified cement pastes, Cement and Concrete Research, 36 (2006) 1744-1751.

[28] D. Distler, Wäßrige Polymerdispersionen, Wiley-VCH, Weinheim (1999).

[29] A. Budholiya, China Natural Rubber Industry, Global Analysis, Overview, Research and Development 2014-2018, Market Research Reports.biz (2014).

[30] U. Meier-Westhues, Polyurethane: Lacke, Kleb- und Dichtstoffe, Vincentz, Hannover (2007).

[31] G. Lagaly, O. Schulz, R. Ziemehl, Dispersionen und Emulsionen: Eine Einführung in die Kolloidik feinverteilter Stoffe einschließlich Tonminerale, Steinkopff, Darmstadt (1997).

[32] R.G. Gilbert, Emulsion polymerization, a mechanistic approach, Academic Press, London (1995).

[33] A.M. Van Herk, Chemistry and Technology of Emulsion Polymerization, Wiley, Chichester (2013).

[34] H. Baharvand, A. Rabiee, H. Jamshidi, An experimental study on particle formation in emulsifier-free emulsion polymerization of styrene, Colloid Journal, 75 (2013) 241-246.

[35] W.D. Harkins, A General Theory of the Mechanism of Emulsion Polymerization, Journal of the American Chemical Society, 69 (1947) 1428-1444.

[36] W.V. Smith, R.H. Ewart, Kinetics of Emulsion Polymerization, The Journal of Chemical Physics, 16 (1948) 592-599.

[37] J.L. Gardon, Emulsion polymerization - Recalculation and extension of the Smith-Ewart theory, Journal of Polymer Science Part A: Polymer Chemistry, 6 (1968) 623-641.

[38] R.M. Fitch, C.H. Tsai, Polymer colloids: Particle formation in non-micellar systems, Journal of Polymer Science Part B: Polymer Letters, 8 (1970) 703-710.

[39] W.J. Priest, Particle Growth in the Aqueous Polymerization of Vinyl Acetate, The Journal of Physical Chemistry, 56 (1952) 1077-1082.

[40] C.P. Roe, Surface Chemistry Aspects of Emulsion Polymerization, Industrial & Engineering Chemistry, 60 (1968) 20-33.

[41] F.K. Hansen, J. Ugelstad, Particle nucleation in emulsion polymerization: Nucleation in emulsifier-free systems investigated by seed polymerization, Journal of Polymer Science: Polymer Chemistry Edition, 17 (1979) 3033-3045.

[42] D.P. Durbin, M.S. El-Aasser, G.W. Poehlein, J.W. Vanderhoff, Influence of monomer pre-emulsification on formation of particles from monomer drops in emulsion polymerization, Journal of Applied Polymer Science, 24 (1979) 703-707.

[43] P.J. Feeney, D.H. Napper, R.G. Gilbert, The determinants of latex monodispersity in emulsion polymerizations, Journal of Colloid and Interface Science, 118 (1987) 493-505.

[44] E. Frauendorfer, W.D. Hergeth, Industrial Polymerization Monitoring, in: H.U. Moritz, W. Pauer, Polymer Reaction Engineering - 10th International Workshop, VCH Wiley, Weinheim (2011).

[45] W.D. Hergeth, M. Krell, Industrial polymerization monitoring, Analytical and Bioanalytical Chemistry, 384 (2006) 1054-1058.

[46] B.P. Binks, S.O. Lumsdon, Pickering emulsions stabilized by monodisperse latex particles: Effects of particle size, Langmuir, 17 (2001) 4540-4547.

[47] S. Melle, M. Lask, G.G. Fuller, Pickering emulsions with controllable stability, Langmuir, 21 (2005) 2158-2162.

[48] S.U. Pickering, Emulsions, Journal of the Chemical Society, Transactions, 91 (1907) 2001-2021.

[49] H.D. Hwu, Y.D. Lee, Studies of alkali soluble resin as a surfactant in emulsion polymerization, Polymer, 41 (2000) 5695-5705.

[50] M. Buback, L.H. Garciarubio, R.G. Gilbert, D.H. Napper, J. Guillot, A.E. Hamielec, D. Hill, K.F. Odriscoll, O.F. Olaj, J.C. Shen, D. Solomon, G. Moad, M. Stickler, M. Tirrell, M.A. Winnik, Consistent Values of Rate Parameters in Free-Radical Polymerization Systems, Journal of Polymer Science Part C: Polymer Letters, 26 (1988) 293-297.

[51] S.A. Chen, S.T. Lee, Limiting Conversion for Systems of Emulsifier-Free Emulsion Polymerization of Styrene, Macromolecules, 25 (1992) 1530-1533.

[52] J.H. Kim, M. Chainey, M.S. Elaasser, J.W. Vanderhoff, Emulsifier-free Emulsion Copolymerization of Styrene and Sodium Styrene Sulfonate, Journal of Polymer Science Part A: Polymer Chemistry, 30 (1992) 171-183.

[53] W. Muli, M. Zhijun, Z. Dong, Z. Dongyang, Y. Wu, Core-shell latex synthesized by emulsion polymerization using an alkali-soluble resin as sole surfactant, Journal of Applied Polymer Science, 128 (2013) 4224-4230.

[54] S. Caballero, J.C. De la Cal, J.M. Asua, Radical Entry Mechanisms in Alkali-Soluble-Resin-Stabilized Latexes, Macromolecules, 42 (2009) 1913-1919.

[55] M.D. Do Amaral, J.M. Asua, Synthesis of high solid-content latex using alkali-soluble resin as sole surfactant, Macromolecular Rapid Communications, 25 (2004) 1883-1888.

[56] H.Y. Erbil, Vinyl Acetate Emulsion Polymerization and Copolymerization with Acrylic Monomers, CRC Press, Boca Raton (2009).

[57] Website: http://www.wacker.com/ (2014).

[58] K. Masters, Spray-Drying - The Unit Operation Today, Industrial & Engineering Chemistry, 60 (1968) 53-63.

[59] S.J. Lukasiewicz, Spray-Drying Ceramic Powders, Journal of the American Ceramic Society, 72 (1989) 617-624.

[60] D.A. Lee, Comparison of Centrifugal and Nozzle Atomization in Spray Dryers, American Ceramic Society, 53 (1974) 232-233.

[61] K. Masters, M.F. Mohtadi, A Study of Centrifugal Atomisation and Spray Drying, British Chemical Engineering, 12 (1967) 1890-1896.

[62] H. Mollet, A. Grubenmann, Formulierungstechnik: Emulsionen, Supensionen, Fest Formen, Wiley-VCH, Weinheim (2000).

[63] J.A. Duffie, W.R. Marshall, Factors influencing the properties of spray-dried materials, Chemical Engineering Progress, 49 (1953) 480-486.

[64] D.H. Charlesworth, W.R. Marshall, Evaporation from drops containing dissolved solids, AIChE Journal, 6 (1960) 9-23.

[65] H.J. Butt, K. Graf, M. Kappl, Physics and Chemistry of Interfaces, Wiley-VCH, Weinheim (2003).

[66] H. Helmholtz, Über einige Gesetze der Verteilung elektrischer Ströme in körperlichen Leitern, mit Anwendung auf die tierisch-elektrischen Versuche, Annalen der Physik, 165 (1853) 211-233.

[67] O. Stern, Theory of the electrolytic double layer, Zeitschrift für Elektrochemie, 30 (1924) 508-516.

[68] D.C. Grahame, The Electrical Double Layer and the Theory of Electro-capillarity, Chemical Reviews, 41 (1947) 441-501.

[69] J.O. Bockris, M.A. Devanathan, K. Muller, On the Structure of Charged Interfaces, Proceedings of the Royal Society of London. Series A. Mathematical and Physical Sciences, 274 (1963) 55-79.

[70] K.S. Birdi, Handbook of Surface and Colloid Chemistry, CRC Press, Boca Raton (2008).

[71] G. Auernhammer, Surface and Interfacial Forces - From Fundamentals to Applications, Springer, Berlin (2008).

[72] R.J. Hunter, Zeta Potential in Colloid Science: Principles and Applications, Academic Press, London (1988).

[73] C.A. Walker, J.T. Kirby, S.K. Dentel, The Streaming Current Detector: A Quantitative Model, Journal of Colloid and Interface Science, 182 (1996) 71-81.

[74] A.S. Dukhin, P.J. Goetz, Acoustic and electroacoustic spectroscopy, Langmuir, 12 (1996) 4336-4344.

[75] A.S. Dukhin, P.J. Goetz, Acoustic and electroacoustic spectroscopy characterizing concentrated dispersions and emulsions, Advanced Colloid and Interface Science, 92 (2001) 73-132.

[76] A.S. Dukhin, P.J. Goetz, Ultrasound for Characterizing Colloids, Elsevier, Amsterdam (2002).

[77] J. Israelachvili, Intermolecular and Surface Forces, Elsevier, Amsterdam (2011).

[78] H.D. Dörfler, Grenzflächen und Kolloidchemie, Wiley-VCH, Weinheim (1994).

[79] R.H. Ottewill, T. Walker, Influence of non-ionic surface active agents on stability of polystyrene latex dispersions, Kolloid-Zeitschrift und Zeitschrift für Polymere, 227 (1968) 108-116.

[80] R.H. Ottewill, T. Walker, Influence of particle size on stability of polystyrene latices with an adsorbed layer of nonionic surface-active agent, Journal of the Chemical Society - Faraday Transactions I, 70 (1974) 917-926.

[81] P. Hiemenz, R. Rajagopalan, Principles of Colloid and Surface Chemistry, CRC Press, Boca Raton (1997).

[82] J.L. Keddie, A.F. Routh, Fundamentals of Latex Film Formation: Processes and Properties, Springer, Dordrecht (2010).

[83] R.E. Dillon, L.A. Matheson, E.B. Bradford, Sintering of Synthetic Latex Particles, Journal of Colloid Science, 6 (1951) 108-117.

[84] W.A. Henson, D.A. Taber, E.B. Bradford, Mechanism of Film Formation of Latex Paint, Industrial and Engineering Chemistry, 45 (1953) 735-739.

[85] G.L. Brown, Formation of Films from Polymer Dispersions, Journal of Polymer Science, 22 (1956) 423-434.

[86] K. Dragnevski, A. Donald, P. Taylor, M. Murray, S. Davies, E. Bone, Latex Film Formation in the Environmental Scanning Electron Microscope, Macromolecular Symposium, 281 (2009) 119-125.

[87] K.I. Dragnevski, A.F. Routh, M.W. Murray, A.M. Donald, Cracking of Drying Latex Films: An ESEM Experiment, Langmuir, 26 (2010) 7747-7751.

[88] J.L. Keddie, P. Meredith, R.A. Jones, A.M. Donald, Rate-limiting steps in film formation of acrylic latices as elucidated with ellipsometry and environmental scanning electron microscopy, in: T. Provder, M.A. Winnik, M.W. Urban, Film Formation in Waterborne Coatings, American Chemical Society, Washington (1996), 332-348.

[89] J.L. Keddie, P. Meredith, R.A. Jones, A.M. Donald, Kinetics of Film Formation in Acrylic Latices Studied with Multiple-Angle-Of-Incidence Ellipsometry and Environmental SEM, Macromolecules, 28 (1995) 2673-2682.

[90] Y. Ma, H.T. Davis, L.E. Scriven, Microstructure development in drying latex coatings, Progress in Organic Coatings, 52 (2005) 46-62.

[91] E. Gonzalez, C. Tollan, A. Chuyilin, M.J. Barandiaran, M. Paulis, Determination of the Coalescence Temperature of Latexes by Environmental Scanning Electron Microscopy, ACS Applied Materials & Interfaces, 4 (2012) 4276-4282.

[92] Y.J. Park, D.Y. Lee, M.C. Khew, C.C. Ho, J.H. Kim, Effects of Alkali-Soluble Resin on Latex Film Morphology of Poly(n-butyl methacrylate) Studied by Atomic Force Microscopy, Langmuir, 14 (1998) 5419-5424.

[93] D.Y. Lee, H.Y. Choi, Y.J. Park, M.C. Khew, C.C. Ho, J.H. Kim, Kinetics of Film Formation of Poly(n-butyl methacrylate) Latex in the Presence of Poly(styrene/α-methylstyrene/acrylic acid) by Atomic Force Microscopy, Langmuir, 15 (1999) 8252-8258.

[94] C.C. Ho, M.C. Khew, Low Glass Transition Temperature (T_g) Rubber Latex Film Formation Studied by Atomic Force Microscopy, Langmuir, 16 (2000) 2436-2449.

[95] Y. Wang, D. Juhue, M.A. Winnik, O.M. Leung, M.C. Goh, Atomic force microscopy study of latex film formation, Langmuir, 8 (1992) 760-762.

[96] A. Goudy, M.L. Gee, S. Biggs, S. Underwood, Atomic Force Microscopy Study of Polystyrene Latex Film Morphology: Effects of Aging and Annealing, Langmuir, 11 (1995) 4454-4459.

[97] F. Lin, D.J. Meier, A Study of Latex Film Formation by Atomic Force Microscopy. A Comparison of Wet and Dry Conditions, Langmuir, 11 (1995) 2726-2733.

[98] M.A. Linne, A. Klein, G.A. Miller, L.H. Sperling, G.D. Wignall, Film Formation from Latex – Hindered Initial Interdiffusion of Constrained Polystyrene Chains Characterized by Small-Angle Neutron-Scattering, Journal of Macromolecular Science – Physics B, 27 (1988) 217-231.

[99] J. Oberdisse, B. Deme, Structure of latex-silica nanocomposite films: A small-angle neutron scattering study, Macromolecules, 35 (2002) 4397-4405.

[100] M.A. Linne, A. Klein, L.H. Sperling, G.D. Wignall, On the structure and conformation of polymer-chains in latex-particles – small-angle neutron-

scattering characterization of polystyrene latexes of small diameter, Journal of Macromolecular Science-Physics, 27 (1988) 181-216.

[101] S.J. Mears, T. Cosgrove, T. Obey, L. Thompson, I. Howell, Dynamic light scattering and small-angle neutron scattering studies on the poly(ethylene oxide)/sodium dodecyl sulfate/polystyrene latex system, Langmuir, 14 (1998) 4997-5003.

[102] A. Elaissari, Y. Chevalier, F. Ganachaud, T. Delair, C. Pichot, Structure of adsorbed and grafted single-stranded DNA fragments on aminated latex particles: A small-angle neutron scattering study, Langmuir, 16 (2000) 1261-1269.

[103] M.F. Mills, R.G. Gilbert, D.H. Napper, A.R. Rennie, R.H. Ottewill, Small-Angle Neutron-Scattering Studies of Inhomogeneities in Latex-Particles from Emulsion Homopolymerizations, Macromolecules, 26 (1993) 3553-3562.

[104] J.W. Goodwin, R.H. Ottewill, N.M. Harris, J. Tabony, A Study by Small-Angle Neutron-Scattering of the Swelling of Polystyrene Latex-Particles by Monomer, Journal of Colloid and Interface Science, 78 (1980) 253-256.

[105] M.P. Wai, R.A. Gelman, M.G. Fatica, R.H. Hoerl, G.D. Wignall, Small-angle neutron-scattering study on the morphology of seeded emulsion-polymerized latex-particles, Polymer, 28 (1987) 918-922.

[106] Y. Chevalier, Small-angle neutron scattering for studying latex film structure, Trends in Polymer Science, 4 (1996) 197-203.

[107] I.L. Garcia, J.L. Keddie, M. Sferrazza, Probing the early stages of solvent evaporation and relaxation in solvent-cast polymer thin films by spectroscopic ellipsometry, Surface and Interface Analysis, 43 (2011) 1448-1452.

[108] J.L. Keddie, P. Meredith, R.A. Jones, A.M. Donald, Film Formation of Acrylic Latices with Varying Concentrations of Non-Film-Forming Latex Particles, Langmuir, 12 (1996) 3793-3801.

[109] M. Soleimani, S. Khan, D. Mendenhall, W. Lau, M.A. Winnik, Effect of molecular weight distribution on polymer diffusion during film formation of two-

component high-/low-molecular weight latex particles, Polymer, 53 (2012) 2652-2663.

[110] K. Pohl, J. Adams, D. Johannsmann, Correlation between Particle Deformation Kinetics and Polymer Interdiffusion Kinetics in Drying Latex Films, Langmuir, 29 (2013) 11317-11321.

[111] P.A. Steward, J. Hearn, M.C. Wilkinson, An overview of polymer latex film formation and properties, Advances in Colloid and Interface Science, 86 (2000) 195-267.

[112] E.M. Boczar, B.C. Dionne, Z.W. Fu, A.B. Kirk, P.M. Lesko, A.D. Koller, Spectroscopic studies of polymer interdiffusion during film formation, Macromolecules, 26 (1993) 5772-5781.

[113] A.Y. Feng, M.A. Winnik, Direct Non-radiative Energy Transfer across a Sharp Polymer Interface, Chemical Physics Letters, 260 (1996) 296-301.

[114] Y.W. Zhao, Z. Hruska, M.A. Winnik, Molecular aspects of latex film formation. An energy transfer study, Macromolecules, 23 (1990) 4082-4087.

[115] A.M. König, T.G. Weerakkody, J.L. Keddie, D. Johannsmann, Heterogeneous drying of colloidal polymer films: Dependence on added salt, Langmuir, 24 (2008) 7580-7589.

[116] T. Pavlitschek, M. Gretz, J. Plank, Effect of Ca^{2+} Ions on the Film Formation of an Anionic Styrene/n-Butylacrylate Latex Polymer in Cement Pore Solution, Advanced Materials Research, 687 (2013) 322-328.

[117] T. Pavlitschek, Y. Jin, J. Plank, Film Formation of a Non-Ionic Ethylene-Vinyl Acetate Latex Dispersion in Cement Pore Solution, Advanced Materials Research, 687 (2013) 316-321.

[118] Y. Men, Crystallographic deformation in mechanically soft colloidal crystals derived from polymeric latex dispersions, Soft Matter, 8 (2012) 5723-5727.

[119] Z. Li, J. Wang, Y. Song, Self-assembly of latex particles for colloidal crystals, Particuology, 9 (2011) 559-565.

[120] Y. Zhang, J. Wang, Y. Huang, Y. Song, L. Jiang, Fabrication of functional colloidal photonic crystals based on well-designed latex particles, Journal of Materials Chemistry, 21 (2011) 14113-14126.

[121] T. Shinohara, T. Kurokawa, T. Yoshiyama, T. Itoh, I.S. Sogami, N. Ise, Structure of colloidal crystals in sedimenting mixed dispersions of latex and silica particles, Physical Review E, 70 (2004) 0624011-0624014.

[122] T. Ruhl, G.P. Hellmann, Colloidal crystals in latex films: Rubbery opals, Macromolecular Chemistry and Physics, 202 (2001) 3502-3505.

[123] A.H. Cardoso, C.A. Leite, M.E. Zaniquelli, F. Galembeck, Easy polymer latex self-assembly and colloidal crystal formation: the case of poly styrene-co-(2-hydroxyethyl methacrylate), Colloids and Surfaces A: Physicochemical and Engineering Aspects, 144 (1998) 207-217.

[124] E. Yamamoto, M. Kitahara, T. Tsumura, K. Kuroda, Preparation of Size-Controlled Monodisperse Colloidal Mesoporous Silica Nanoparticles and Fabrication of Colloidal Crystals, Chemistry of Materials, 26 (2014) 2927-2933.

[125] Z. Cai, J. Teng, D. Xia, X.S. Zhao, Self-Assembly of Crack-Free Silica Colloidal Crystals on Patterned Silicon Substrates, The Journal of Physical Chemistry C, 115 (2011) 9970-9976.

[126] H.B. Sunkara, J.M. Jethmalani, W.T. Ford, Composite of Colloidal Crystals of Silica in Poly(methyl methacrylate), Chemistry of Materials, 6 (1994) 362-364.

[127] Y. Takeoka, M. Watanabe, Template synthesis and optical properties of chameleonic poly(N-isopropylacrylamide) gels using closest-packed self-assembled colloidal silica crystals, Advanced Materials, 15 (2003) 199-201.

[128] K. Ohno, T. Morinaga, S. Takeno, Y. Tsujii, T. Fukuda, Suspensions of silica particles grafted with concentrated polymer brush: A new family of colloidal crystals, Macromolecules, 39 (2006) 1245-1249.

[129] J.M. Jethmalani, W.T. Ford, G. Beaucage, Crystal structures of monodisperse colloidal silica in poly(methyl acrylate) films, Langmuir, 13 (1997) 3338-3344.

[130] W.A. Winnik, P.J. McDonald, J.L. Keddie, Y. Holl, Drying Modes of Polymer Colloids, in: M.W. Urban, Film Formation in Coatings, Oxford University Press, Oxford (2001).

[131] J.L. Keddie, Y. Holl, P.J. McDonald, W.A. Winnik, Film formation in coatings: Mechanisms, properties and morphology, ACS symposium series, 790 (2001) 2-26.

[132] J.W. Vanderhoff, E.B. Bradford, W.K. Carrington, The transport of water through latex films, Journal of Polymer Science, 41 (1973) 155-174.

[133] D.P. Sheetz, Formation of Films by Drying of Latex, Journal of Applied Polymer Science, 9 (1965) 3759-3773.

[134] S.G. Croll, Drying of latex paint, Journal of Coatings Technology and Research, 58 (1986) 41-49.

[135] S.T. Eckersley, A. Rudin, Drying behavior of acrylic latexes, Progress in Organic Coatings, 23 (1994) 387-402.

[136] M. Okubo, T. Takeya, Y. Tsutsumi, T. Kadooka, T. Matsumoto, Asymmetric porous emulsion film, Journal of Polymer Science: Polymer Chemistry Edition, 19 (1981) 1-8.

[137] A.F. Routh, W.B. Russel, Deformation mechanisms during latex film formation: Experimental evidence, Industrial & Engineering Chemistry Research, 40 (2001) 4302-4308.

[138] J.C. Hwa, Mechanism of film formation from latices - Phenomenon of flocculation, Journal of Polymer Science, 2 (1964) 785-796.

[139] M. Joanicot, K. Wong, J. Maquet, Y. Chevalier, C. Pichot, C. Graillat, P. Lindner, L. Rios, B. Cabane, Ordering of latex particles during film formation, in: M. Zulauf, P. Lindner, P. Terech, Trends in Colloid and Interface Science IV, Steinkopff, Darmstadt (1990).

[140] Y. Chevalier, C. Pichot, C. Graillat, M. Joanicot, K. Wong, J. Maquet, P. Lindner, B. Cabane, Film formation with latex particles, Colloid and Polymer Science, 270 (1992) 806-821.

[141] J.F. M.A. Winnik, Latex Blends: An Approach to Zero VOC Coatings, Journal of Coatings Technology and Research, 68 (1996) 39-50.

[142] M.S. Tirumkudulu, W.B. Russel, Role of capillary stresses in film formation, Langmuir, 20 (2004) 2947-2961.

[143] N.D. Denkov, O.D. Velev, P.A. Kralchevsky, I.B. Ivanov, H. Yoshimura, K. Nagayama, Mechanism of formation of two-dimensional crystals from latex particles on substrate, Langmuir, 8 (1992) 3183-3190.

[144] E. Sutanto, Y. Ma, H.T. Davis, L.E. Scriven, Film formation in coatings: Mechanisms, properties and morphology, ACS symposium series, 790 (2001) 174-192.

[145] F. Parisse, C. Allain, Drying of Colloidal Suspension Droplets: Experimental Study and Profile Renormalization, Langmuir, 13 (1997) 3598-3602.

[146] A.F. Routh, W.B. Russel, Horizontal Drying Fronts During Solvent Evaporation from Latex Films, AIChE Journal, 44 (1998) 2088-2098.

[147] A.F. Routh, J.M. Salamanca, J.L. Keddie, E. Ciampi, D.A. Faux, P.M. Glover, P.J. McDonald, R. Satguru, A. Peters, Lateral Drying in Thick Films of Waterborne Colloidal Particles, Langmuir, 17 (2001) 3202-3207.

[148] G.L. Brown, Formation of films from polymer dispersions, Journal of Polymer Science, 22 (1956) 423–434.

[149] F. Lin, D.J. Meier, A study of latex film formation by atomic force microscopy: A comparison of wet and dry conditions, Langmuir, 11 (1995) 2726-2733.

[150] F. Lin, D.J. Meier, Latex film formation: atomic force microscopy and theoretical results, Progress of Organic Coatings, 29 (1996) 139-146.

[151] F. Dobler, T. Pith, M. Lambla, Y. Holl, Coalescense mechanism of polymer colloids: Coalescence with evaporation of water, Journal of Colloid and Interface Science, 152 (1992) 12-21.

[152] S.T. Eckersley, A. Rudin, Mechanism of film formation from latexes, Journal of Coatings Technology, 62 (1990) 89-100.

[153] J.H. Kim, M. Chainey, J. Hearn, Preparation of polymer latex films by a flash casting technique, Journal of Applied Polymer Science, 30 (1985) 4273-4285.

[154] P.R. Sperry, B.S. Snyder, M.L. O'Dowd, P.M. Lesko, Role of water in particle deformation and compaction in latex film formation, Langmuir, 10 (1994) 2619-2628.

[155] J.W. Vanderhoff, H.L. Tarkowski, M.C. Jenkins, E.B. Bradford, Theoretical consideration of the interfacial forces involved in coalescence of latex particles, Journal of Macromolecular Chemistry, 1 (1966) 361-397.

[156] K. Hahn, G. Ley, H. Schuller, R. Oberthur, On particle coalescence in latex films, Colloid and Polymer Science, 264 (1986) 1082-1096.

[157] D.J. Stokes, Recent advances in electron imaging, image interpretation and applications: environmental scanning electron microscopy, Philosophical Transactions of the Royal Society of London. Series A: Mathematical, Physical and Engineering Sciences, 361 (2003) 2771-2787.

[158] K.I. Dragnevski, A.M. Donald, An environmental scanning electron microscopy examination of the film formation mechanism of novel acrylic latex, Colloids and Surfaces A: Physicochemical and Engineering Aspects, 317 (2008) 551-556.

[159] K.I. Dragnevski, A.M. Donald, Applications of environmental scanning electron microscopy (ESEM) in the study of novel drying latex films, Electron Microscopy and Analysis Group Conference, Bristol (2008).

[160] H. Lutz, Dispersionsanwendungen in der Bauindustrie, in: D. Distler, Wäßrige Polymerdispersionen, Wiley-VCH, Weinheim (1998).

[161] Website: http://www.momentive.com/ (2014).

[162] R. Zurbriggen, Dauerhaftigkeit durch Buttering-Floating: eine materialwissenschaftliche Studie, 6. HeidelbergCement Bauchemie-Tage, Münster (2014).

[163] Website: http://www.gebaeudeenergieberatung-steinhaeuser.de/ (2014).

[164] J. Plank, D. Stephan, C. Hirsch, Bauchemie, in: Winaker, Küchler, Chemische Technik – Prozesse und Produkte, Wiley-VCH, Weinheim (2004).

[165] J.W. Bullard, H.M. Jennings, R.A. Livingston, A. Nonat, G.W. Scherer, J.S. Schweitzer, K.L. Scrivener, J.J. Thomas, Mechanisms of cement hydration, Cement and Concrete Research, 41 (2011) 1208-1223.

[166] H.F.W. Taylor, Cement Chemistry, Academic Press, London (1990).

[167] J. Stark, B. Wicht, Anorganische Bindemittel - Zement - Kalk - Spezielle Bindemittel, Bauhaus-Universität, Weimar (1998).

[168] H. Pöllmann, Calcium Aluminate Cements – Raw Materials, Differences, Hydration and Properties, Reviews in Mineralogy and Geochemistry, 74 (2012) 1-82.

[169] G.S. Smirnov, A.K. Chatterjee, G.I. Zhmoidin, The phase equilibrium diagram of the ternary subsystem CaO-$CaO{\cdot}Al_2O_3$-$11CaO{\cdot}7Al_2O_3{\cdot}CaF_2$, Journal of Materials Science, 8 (1973) 1278-1282.

[170] W. Hörkner, H.K. Müller-Buschbaum, Zur Kristallstruktur von $CaAl_2O_4$, Journal of Inorganic and Nuclear Chemistry, 38 (1976) 983-984.

[171] V.S. Ramachandran, R.F. Feldman, Hydration characteristics of monocalcium aluminate at a low water/solid ratio, Cement and Concrete Research, 3 (1973) 729-750.

[172] D. Sorrentino, F. Sorrentino, M. George, Mechanisms of hydration of calcium aluminate cements, Materials Science of Concrete, 4 (1995) 41-90.

[173] K.L. Scrivener, A. Capmas, Calcium Aluminate Cements, in: Lea's Chemistry of Cement and Concrete, Oxford (2003).

[174] B.F. Cottin, Hydration of calcium silicates and aluminates mixes, 7th International Conference on the Chemistry of Cement, Paris (1980), 113-118.

[175] P. Gu, J.J. Beaudoin, E.G. Quinn, R.E. Myers, Early Strength Development and Hydration of Ordinary Portland Cement/Calcium Aluminate Cement Pastes, Advanced Cement Based Materials, 6 (1997) 53-58.

[176] J. Bensted, High alumina cement - Present state of knowledge, ZKG International, 46 (1993) 560-566.

[177] F. Zhang, Z. Zhou, Z. Lou, Solubility product and stability of ettringite, 10th International Conference on the Chemistry of Cement, Amarkai (1997), 88-93.

[178] F. Götz-Neunhoeffer, R. Zurbriggen, Formation of hydrate spheres in ternary binder systems, ZKG International, 61 (2008) 68-76.

[179] B.R. Currell, R. Grzeskowlak, H.G. Mldgley, J.R. Parsonage, The acceleration and retardation of set high alumina cement by additives, Cement and Concrete Research, 17 (1987) 420-432.

[180] T. Matusinović, D. Čurlin, Lithium salts as set accelerators for high alumina cement, Cement and Concrete Research, 23 (1993) 885-895.

[181] S.A. Rodger, D.D. Double, The chemistry of hydration of high alumina cement in the presence of accelerating and retarding admixtures, Cement and Concrete Research, 14 (1984) 73-82.

[182] F. Götz-Neunhoeffer, The function of Li carbonate and tartaric acid in the hydration of mixtures of calcium aluminate cement (CAC) with calcium sulfate hemihydrate ($CSH_{0.5}$), Cement International, 5 (2007) 90-101.

[183] J. Plank, Z. Dai, H. Keller, F. von Hössle, W. Seidl, Fundamental mechanisms for polycarboxylate intercalation into C_3A hydrate phases and the role of sulfate present in cement, Cement and Concrete Research, 40 (2010) 45-57.

[184] W. Nocun-Wczelik, Z. Konik, A. Stok, Blended systems with calcium aluminate and calcium sulphate expansive additives, Construction and Building Materials, 25 (2011) 939-943.

[185] M.S. Ribeiro, Expansive cement blend for use in shrinkage-compensating mortars, Materials and Structures, 31 (1998) 400-404.

[186] T.A. Bier, F. Estienne, L. Amathieu, Shrinkage and shrinkage compensation in binders containing calcium aluminate cement, International Conference on Calcium Aluminate Cements, Edinburgh (2001), 215-226.

[187] Website: http://ruby.chemie.uni-freiburg.de/ (2014).

[188] Website: http://www.greenmade-development.com/ (2014).

[189] Y. Ohama, Polymer-based admixtures, Cement and Concrete Composites, 20 (1998) 189-212.

[190] Z. Su, K. Sujata, J.M. Bijen, H.M. Jennings, A.L. Fraaij, The evolution of the microstructure in styrene acrylate polymer-modified cement pastes at the early stage of cement hydration, Advanced Cement Based Materials, 3 (1996) 87-93.

[191] A. De Gasparo, M. Herwegh, R. Zurbriggen, K. Scrivener, Quantitative distribution patterns of additives in self-leveling flooring compounds (underlayments) as function of application, formulation and climatic conditions, Cement and Concrete Research, 39 (2009) 313-323.

[192] Y. Tian, X.Y. Jin, N.G. Jin, R. Zhao, Z.J. Li, H.Y. Ma, Research on the microstructure formation of polyacrylate latex modified Cross Mark mortars, Construction and Building Materials, 47 (2013) 1381-1394.

[193] M. Ramli, A.A. Tabassi, K.W. Hoe, Porosity, pore structure and water absorption of polymer-modified mortars: An experimental study under different curing conditions, Composites Part B: Engineering, 55 (2013) 221-233.

[194] A. Muthadhi, S. Kothandaraman, Experimental investigations on polymer-modified concrete subjected to elevated temperatures, Materials and Structures, 47 (2014) 977-986.

[195] G. Barluenga, F. Hernández-Olivares, SBR latex modified mortar rheology and mechanical behaviour, Cement and Concrete Research, 34 (2004) 527-535.

[196] R. Wang, P.M. Wang, Function of styrene-acrylic ester copolymer latex in cement mortar, Materials and Structures, 43 (2010) 443-451.

[197] N. Ukrainczyk, A. Rogina, Styrene–butadiene latex modified calcium aluminate cement mortar, Cement and Concrete Composites, 41 (2013) 16-23.

[198] M. Pei, W. Kim, W. Hyung, A.J. Ango, Y. Soh, Effects of emulsifiers on properties of poly(styrene–butyl acrylate) latex-modified mortars, Cement and Concrete Research, 32 (2002) 837-841.

[199] J. Rottstegge, C.C. Han, W.D. Hergeth, Compatibility investigations on polymer-fiber reinforced cements modified with polymer latexes, Macromolecular Materials and Engineering, 291 (2006) 345-356.

[200] F. Winnefeld, J. Kaufmann, E. Hack, S. Harzer, A. Wetzel, R. Zurbriggen, Moisture induced length changes of tile adhesive mortars and their impact on adhesion strength, Construction and Building Materials, 30 (2012) 426-438.

[201] B.B. Konar, A. Das, P.K. Gupta, M. Saha, Physicochemical Characteristics of Styrene-Butadiene Latex-modified Mortar Composite vis-a-vis Preferential Interactions, Journal of Macromolecular Science: Part A-Pure and Applied Chemistry, 48 (2011) 757-765.

[202] Website: http://www.bauchemie.ch.tum.de/ (2014).

[203] J.V. Brien, K.C. Mahboub, Influence of polymer type on adhesion performance of a blended cement mortar, International Journal of Adhesion and Adhesives, 43 (2013) 7-13.

[204] J. Kaufmann, F. Winnefeld, R. Zurbriggen, Polymer dispersions and their interaction with mortar constituents and ceramic tile surfaces studied by zeta-potential measurements and atomic force microscopy, Cement and Concrete Composites, 34 (2012) 604-611.

[205] F. Merlin, H. Guitouni, H. Mouhoubi, S. Mariot, F. Vallee, H. Van Damme, Adsorption and heterocoagulation of nonionic surfactants and latex particles on cement hydrates, Journal of Colloid and Interface Science, 281 (2005) 1-10.

[206] J. Plank, M. Gretz, Study on the interaction between anionic and cationic latex particles and Portland cement, Colloids and Surfaces A: Physicochemical and Engineering Aspects, 330 (2008) 227–233.

[207] S.Y. Zhong, J.M. Li, K. Ni, D.D. Han, Influences of HPMC on adsorption of styrene-acrylic ester latex particles on cement grains, Construction and Building Materials, 38 (2013) 567-574.

[208] S. Chandra, P. Flodin, Interactions of polymers and organic admixtures on Portland cement hydration, Cement and Concrete Research, 17 (1987) 875-890.

[209] H. Pöllmann, J. Sieksmeier, Dispersion powders in cementitious systems, ZKG International, 9 (2012) 56-61.

[210] D.A. Silva, H.R. Roman, P.J. Gleize, Evidences of chemical interaction between EVA and hydrating Portland cement, Cement and Concrete Research, 32 (2002) 1383-1390.

[211] D.A. Silva, P.J. Monteiro, The influence of polymers on the hydration of Portland cement phases analyzed by soft X-ray transmission microscopy, Cement and Concrete Research, 36 (2006) 1501-1507.

[212] Z. Su, J.M. Bijen, J.A. Larbi, Influence of polymer modification on the hydration of Portland cement, Cement and Concrete Research, 21 (1991) 535-544.

[213] J.A. Larbi, J.M. Bijen, Interaction of polymers with Portland cement during hydration: A study of the chemistry of the pore solution of polymer-modified cement systems, Cement and Concrete Research, 20 (1990) 139-147.

[214] R. Wang, P.M. Wang, Microstructural Aspects of SBR Latex-Modified Cement Paste and Mortar Highlighted by Means of SEM and ESEM, Proceedings of the 6th Asian Symposium on Polymers in Concrete, Shanghai (2009), 289-298.

[215] R. Wang, P.M. Wang, Formation of hydrates of calcium aluminates in cement pastes with different dosages of SBR powder, Construction and Building Materials, 25 (2011) 736-741.

[216] D. Jansen, F. Götz-Neunhoeffer, J. Neubauer, W.D. Hergeth, R. Härzschel, Influence of polyvinyl alcohol on phase development during the hydration of Portland cement, ZKG International, 63 (2010) 100-107.

[217] D. Jansen, F. Götz-Neunhoeffer, J. Neubauer, R. Härzschel, W.D. Hergeth, Effect of polymers on cement hydration: A case study using substituted PDADMA, Cement and Concrete Composites, 35 (2013) 71-77.

[218] D. Jansen, F. Götz-Neunhoeffer, J. Neubauer, W.D. Hergeth, R. Härzschel, In-situ XRD investigations of the influence of PDADMAC on ettringite formation in cement systems, Zeitschrift für Kristallographie, (2009) 359-364.

Paper #1

Role of PVOH and kaolin on colloidal stability of liquid and powder EVA and SB latexes in cement pore solution

S. Baueregger, M. Perello, J. Plank

Colloids and Surfaces A: Physicochemical and Engineering Aspects

434 (2013), 145-153

Colloids and Surfaces A: Physicochem. Eng. Aspects 434 (2013) 145–153

Contents lists available at SciVerse ScienceDirect

Colloids and Surfaces A: Physicochemical and Engineering Aspects

journal homepage: www.elsevier.com/locate/colsurfa

Role of PVOH and kaolin on colloidal stability of liquid and powder EVA and SB latexes in cement pore solution

Stefan Baueregger[a], Margarita Perello[b], Johann Plank[a,*]

[a] Technische Universität München, Lichtenbergstr. 4, 85747 Garching, Germany
[b] Dow Europe GmbH, Bachtobelstr. 3, 8810 Horgen, Switzerland

HIGHLIGHTS

- Colloidal stability of latex dispersions was tested in cement pore solution.
- Carboxylated styrene–butadiene (SB) latex is unstable and coagulates.
- Latex reconstituted from SB powder is more stable than its liquid precursor.
- Reason is shielding effect of polyvinylalcohol/kaolin coating on SB powder surface.
- Nonionic EVA latex (liquid or powder) is stable in cement pore solution.

GRAPHICAL ABSTRACT

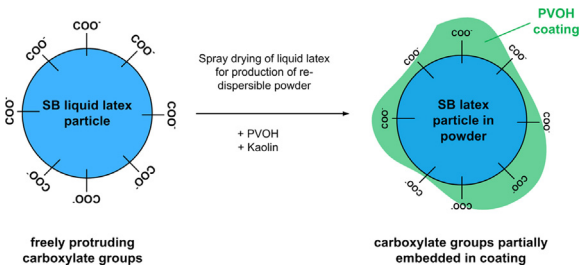

ARTICLE INFO

Article history:
Received 25 January 2013
Received in revised form 7 May 2013
Accepted 9 May 2013
Available online xxx

Keywords:
Polymer dispersion
Colloidal stability
Latex particles
Re-dispersible polymer powder
Cement pore solution

ABSTRACT

The influence of polyvinylalcohol (PVOH) and kaolin on the stability of an ethylene–vinylacetate (EVA) and a carboxylated styrene–butadiene (SB) latex copolymer in synthetic cement pore solution (SCPS) was investigated by photometric turbidity measurements. The dispersions were prepared from liquid EVA/SB latexes or re-dispersible powders (RDPs) obtained by spray drying of the mother liquor with PVOH and kaolin. Colloidal properties of the EVA and SB latex particles were captured by dynamic light scattering (DLS), environmental scanning electron microscopy (ESEM), zeta and streaming potential measurements. The amount of PVOH sorbed onto SB particles was quantified via total organic carbon (TOC) method. It was found that in water, EVA particles generally coagulate and settle with time as a consequence of their nonionic character. In contrast, dispersions of the anionic styrene–butadiene latex show high stability due to repulsion from the pressure of their counter ions clouds. In synthetic cement pore solution, however, the liquid SB latex becomes unstable and shows strong coagulation as a consequence of calcium interaction. Surprisingly, the corresponding SB re-dispersible powder is much more stable in SCPS and exhibits only slight sedimentation. The enhanced stability is attributed to a surface coating of the SB powder particles with a film of PVOH during spray drying. The PVOH coating embeds some of the carboxylate groups located on the surface of the SB powder, as evidenced by a reduced anionic charge density. This way, interaction with calcium is weakened and precipitation via latex–calcium complexation is much reduced. Consequently, addition of PVOH/kaolin during the spray drying of latex polymers not only prevents coalescence and caking of the powder particles, but also enhances their colloidal stability in cementitious systems.

1. Introduction

Latex polymers represent the key components in adhesives, coatings and paints. They provide cohesion, adhesion and flexural strength due to the formation of homogeneous polymer films

* Corresponding author. Tel.: +49 89 289 13151; fax: +49 89 289 13152.
E-mail address: sekretariat@bauchemie.ch.tum.de (J. Plank).

0927-7757/$ – see front matter © 2013 Elsevier B.V. All rights reserved.
http://dx.doi.org/10.1016/j.colsurfa.2013.05.047

which are the result of particle coalescence after dehydration of the dispersion. Furthermore, a major application of latex polymers lies in the production of drymix mortars for construction applications, e.g. of adhesives for external thermal insulation composite systems (ETICS), cementitious tile adhesives (CTAs) or tile grouts. For these applications, re-dispersible latex polymer powders are manufactured from liquid latex dispersions which originate from emulsion polymerization processes. These re-dispersible powders (RDPs) are usually obtained by spray drying of a latex mother liquor under the addition of colloidal stabilizers (e.g. polyalcohols) and anti-caking agents (e.g. clays, calcium carbonate, silica, diatomaceous earth, etc.). In the past, the influence of the colloidal stabilizer polyvinylalcohol (PVOH) and the anti-caking agent kaolin on the performance of latex polymers in cementitious systems which require high latex stability has been the subject of several studies [1–4].

In the literature, many articles can be found which deal with the material properties of polymer-modified cementitious systems [5–11]. Additionally, numerous reports concerning the stability of latex particles in general were published [12–21]. For example, *Kazhuro* and *Koshevar* studied the stability and sedimentation behavior of mixtures prepared from kaolin and synthetic latexes in water [22]. Still, no information on the stability of latex particles in cement pore solution and on the influence of PVOH and kaolin on the electrokinetic surface properties of re-dispersed latex powders is available. However, these properties present key information for a fundamental understanding of the working mechanism of latex polymers in cementitious systems, and for the understanding of potential differences between liquid latexes and re-dispersible powders.

The stability of latex particles in dispersions can be described by the *DLVO* theory which considers the potential between charged surfaces surrounded by a solvent. It explains the combined effect of the van der Waals attraction and the interaction of the electrochemical double layers existing between the particles. Particles surrounded by a polar solvent almost always possess a surface charge e.g. due to dissociation of ions from their surface. This surface charge is balanced by a layer of oppositely charged ions at small distance from the surface. The layer of counterions commonly is referred to as electrochemical double layer and can be divided into a rigid and a diffuse layer of counterions. In dilute solution, the thickness of the diffuse layer of ions is the *Debye* length κ^{-1} which strongly depends on the ionic strength of the solution. The decay of the *Debye* length increases with increasing ionic strength [23,24].

For optimum performance of latex polymers in cementitious systems, sufficient stability is required in cement pore solution which is characterized by high ionic strength owed to increased salt contents (Ca^{2+}, K^{+}, $SO_4{}^{2-}$) and a pH of 12.5. However, in the presence of ions electrostatically stabilized colloidal particle suspensions start to coagulate. As the *Debye* length strongly depends on the ionic strength of the solution, the stability of latex particles in cement pore solution is significantly decreased by the presence of Ca^{2+} ions [25–27].

In this study we investigated the stability of nonionic EVA and anionic SB latex particles dispersed in water and synthetic cement pore solution by means of photometric turbidity measurement over time. Particularly, dispersions prepared from liquid latex and re-dispersible powder were compared to assess whether the electrokinetic properties of latex particles are affected by the spray drying process conducted under addition of PVOH and kaolin. The latexes studied were based on ethylene–vinylacetate and carboxylated styrene–butadiene copolymers. The re-dispersible powders were obtained from the latex mother liquors under addition of PVOH as colloidal stabilizer and kaolin as anti-caking agent. Furthermore, model SB latex powders containing only either PVOH or kaolin were spray dried under the same conditions and tested to evaluate the influence of each individual component on the colloid stability of the latexes. For analysis, diluted dispersions with a polymer content of 0.1 wt.% were prepared and the electrokinetic surface properties of the latex particles were measured via streaming potential and polyelectrolyte titration. Finally, the amount of PVOH sorbed onto the latex particles was quantified via TOC analysis of the unadsorbed portion of PVOH (depletion method). From the data it was hoped to obtain a profound mechanistic understanding of the role of PVOH and kaolin with respect to the colloidal stability of EVA and SB latex in cementitious systems.

2. Materials and methods

2.1. Materials

2.1.1. Chemicals

$CaSO_4{\cdot}2H_2O$, KOH, NaOH, Na_2SO_4, K_2SO_4, $CaCl_2{\cdot}2H_2O$, NaCl, KCl and Titriplex solution (0.1 mol/L) were purchased from Merck, Darmstadt, Germany. Polyvinylalcohol (Mowiol 4–88) was purchased from Kuraray Europe, Frankfurt, Germany. Kaolin (KAMIN HG 90) was obtained from KaMinLLC, Macon, United States.

All chemicals were utilized without further purification. Ultrapure water (resistivity > 18 MΩ cm) was used for all experiments.

2.1.2. Latex dispersions and re-dispersible powders

EVA latex (solid content 52 wt.%), EVA re-dispersible powder, SB latex (solid content 45 wt.%) and SB re-dispersible powder were provided by Dow Olefinverbund GmbH, Schkopau, Germany. The re-dispersible powders were produced by spray drying of EVA or SB latex under addition of polyvinylalcohol as colloidal stabilizer and kaolin as anti-caking agent. The weight ratios between polymer, colloidal stabilizer and anti-caking agent were the same for all samples. Additionally, SB model powders were prepared by spray drying the SB mother liquor with individual PVOH or kaolin at the weight ratios of before. Table 1 presents the composition and properties of the liquid and powder samples tested. Fig. 1 shows their chemical structures.

2.1.3. Synthetic cement pore solution

Time-dependent stability of the latex particles was studied in DI water and synthetic cement pore solution (SCPS) as solvents. SCPS was composed based on the characteristic ion concentrations present in the pore solution of an ordinary Portland cement (CEM I) at a w/c ratio of ~0.5 [28]. The pore solution was prepared by dissolving 1.72 g $CaSO_4{\cdot}2H_2O$, 6.96 g Na_2SO_4, 4.75 g K_2SO_4 and 7.12 g KOH in deionized water. First, the $CaSO_4{\cdot}2H_2O$ was dissolved in 700 mL of water under vigorous stirring. Next, 6.96 g of Na_2SO_4 were solubilized in 150 mL of this $CaSO_4$ solution. Upon complete dissolution of the sodium sulphate, the solution was combined with the remaining $CaSO_4{\cdot}2H_2O$ solution. Next, 4.75 g of K_2SO_4 were added and solved. Afterwards, 7.12 g KOH dissolved in 150 mL of water were introduced into this mixture. Finally, water was added to a volume of 1 L. This method produces a clear, stable solution free of precipitate which incorporates the ion concentrations displayed in Table 2. pH of the SCPS was 12.8.

2.2. Characterization of liquid and powder latexes

All latex dispersions were prepared with the same latex polymer content of 0.1 wt.% and sonicated for 3 min to ensure optimal particle dispersion.

Particle sizes were determined by dynamic light scattering (DLS) utilizing a Zetasizer Nano ZS apparatus (Malvern Instruments, Workestershire, UK). Qualitative electric surface charge of the colloidal particles dispersed in water was measured on the same instrument. Electrophoretic mobility was converted into a value for zeta potential by using the *Smoluchowski* relation.

Table 1
Composition and properties of the liquid latexes and the latex samples reconstituted from the re-dispersible powders.

Component or property	EVA latex	EVA powder	SB latex	SB powder	SB PVOH	SB Kaolin
Polymer content [wt.%]	52	–	45	–	–	–
Colloidal stabilizer	–	PVOH	–	PVOH	PVOH	–
Anti-caking agent	–	Kaolin	–	Kaolin	–	Kaolin
Zeta potential [mV]	−17	−22	−31	−25	−25	−30
pH	5.5	–	9.8	–	–	–
T_g [°C]	20	20	6	6	6	6
MFFT [°C]	3	3	5	5	5	5

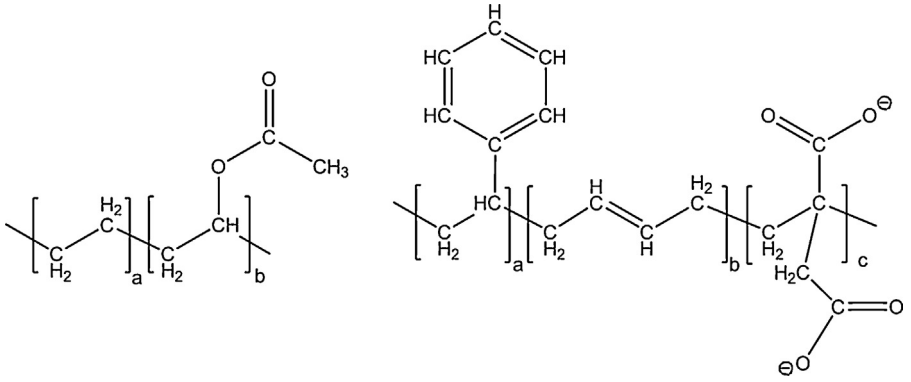

Fig. 1. Chemical structures of ethylene–vinylacetate (left) and of carboxylated styrene–butadiene (right) latex copolymers.

Specific anionic charge densities of the latexes were determined using a particle charge detector PCD 03 pH (Mütek Analytic, Herrsching, Germany). This method allows the experimental determination of the anionic charge of polymers in water or SCPS. 10 mL of 0.1 wt.% latex dispersion were titrated with 0.001 mol/L poly diallyl dimethyl ammonium chloride (polyDADMAC) aqueous solution until the isoelectric point was reached. The PolyDADMAC solution was added continuously from a burette via an automatic feeder system according to a preset titration program controlled by the decrease of the streaming potential [29]. From the consumption of cationic polyelectrolyte required to neutralize the anionic charge of the latex particles, the specific anionic charge density was calculated.

Environmental scanning electron microscopic (ESEM) images of the EVA and SB latex dispersions were captured on a FEI XL 30 FEG microscope (FEI, Eindhoven, Netherlands) equipped with a *Peltier* cooling stage and a gaseous secondary electron detector. The ESEM instrument allows observation of wet samples in their native state. This is essential because under the high vacuum conditions characteristic for conventional SEM, latexes start to form polymer films due to particle coalescence, and differences between samples disappear. SEM images of kaolin particles were taken on the same instrument under high vacuum.

Glass transition temperature (T_g) was measured on a differential scanning calorimeter (DSC) Maia F3 from Netzsch, Selb, Germany. Minimum film formation temperature (MFFT) was determined on a MFFT Bar Thermostair II instrument from Coesfeld Materialtest, Dortmund, Germany.

Table 2
Concentration of ions present in the model cement pore solution used in the study.

Ion	Concentration [g/L]
K^+	7.1
Na^+	2.2
Ca^{2+}	0.4
SO_4^{2-}	8.2
OH^-	1.0

2.3. Photometric turbidity measurements

The stability of latex dispersions in water or SCPS was assessed via turbidity measurements. For this purpose, 15 mL of polymer dispersion in water or SCPS (polymer content 0.1 wt.%) were prepared from EVA latex, EVA powder, SB latex or SB powder. The samples were sonicated for 3 minutes before the test tubes were purged with nitrogen, sealed and stored vertically on a vibration-free table at room temperature. After 0, 1, 2, 3, 6, 10 and 15 days respectively, aliquots of 0.5 mL were taken from the test tubes exactly 1 cm below the surface of the fluid. Afterwards the test tubes were purged with nitrogen and sealed again immediately to prevent carbonation of the dispersions. The samples were transferred into a quartz glass cuvette (diameter 50 mm) and diluted with DI water to a total volume of 10 mL (latex content 0.05 wt.%). The turbidity of the dispersion indicates the latex stability: the higher the turbidity, the more stable is the latex. Turbidity was determined via light absorbance measurement at a wavelength of 550 nm on a Spectroflex 6100 spectral photometer (WTW, Weilheim, Germany). Calibration curves were developed for both EVA and SB latexes by incremental addition of the latex polymers at dosages from 0.01 to 0.05 wt.%. There, absorbance was linearly dependent on the EVA or SB latex concentrations. From all values, absorbance of DI water or SCPS was deducted to eliminate the influence of the solvents. The standard deviation of the values for the absorbance was less than 0.01, thus indicating high accuracy and reliability of the photometric method.

2.4. Mechanistic investigations

2.4.1. Influence of EDTA on latex stability

To assess the influence of Ca^{2+} ions on the stability of the latexes, turbidity tests were performed in SCPS at additions of 0.005–0.01 mol/L EDTA.

2.4.2. Ion specific electrokinetic properties of latex particles

For 10 mL of 0.1 wt.% aqueous latex dispersions adjusted to pH 12.5 with NaOH, streaming potential measurements were

performed using a Mütek PCD 03 pH particle charge detector (BTG, Herrsching, Germany). The surface charges occurring in the presence of calcium, sodium and potassium ions were assessed by adding stepwise 1.5 mL of 100 g/L aqueous $CaCl_2$, NaCl or KCl solutions, respectively.

Additionally, pH and ion specific anionic charge densities of the latex particles were measured by polyelectrolyte titration using the same instrument.

2.4.3. PVOH sorption on SB latex powder

The amount of PVOH sorbed on SB powder was measured using the depletion method. In a typical experiment, 25 mL of the aqueous SB dispersion (polymer content 1.0 wt.%) was sonicated for 3 min, then shaken in a wobbler (VWR International, Darmstadt, Germany) for 2 h at 2400 rpm to dissolve the non-sorbed portion of PVOH from the powder into the aqueous phase. Afterwards, the latex particles were separated by filtration through a 0.1 μm syringe filter. 2.5 mL of the clear filtrate were diluted with 20 mL of DI water. The total organic carbon (TOC) content of the solution was determined via combustion at 890 °C on a High TOC II instrument (Elementar Analysensysteme, Hanau, Germany). From the difference between the TOC content calculated for the known PVOH content which was incorporated in the powder and the TOC content in the filtrate, the amount of PVOH sorbed on the powder particles was calculated. Note that the TOC content in the filtrate was corrected for the carbon content stemming from the emulsifier contained in the latex which is released together with PVOH. This emulsifier content was quantified from the liquid latex dispersed in water and subsequent TOC measurement. Measurements were generally repeated three times and the average was reported as sorbed amount. Achievement of sorption equilibrium was checked by comparing the sorbed amounts after 2 h of mixing with values obtained after 1 day of mixing. In both cases, the same values were found. Additionally, it was confirmed that no interaction between PVOH and the polyethersulfone (PES) filter membrane had occurred, as was evidenced by the same TOC values before and after filtration of a 1.0 wt.% PVOH solution.

3. Results and discussion

3.1. Properties of latex samples

Two different types of latex copolymers were used in this study, namely a nonionic ethylene/vinylacetate copolymer stabilized with PVOH, and an anionic styrene/butadiene copolymer stabilized with itaconic acid. Their chemical structures are displayed in Fig. 1.

The particle size distributions (intensity-based) of both polymers measured via dynamic light scattering are exhibited in Figs. 2 and 3. The EVA polymer particles exhibit a very broad size distribution in the range between 300 and 1750 nm. For the EVA dispersion reconstituted from the powder, the additional minor peak at a particle size of ~200 nm can be attributed to kaolin primary particles. In comparison, the SB liquid latex is monodisperse and exhibits a narrow particle size distribution around 220 nm. The SB dispersion reconstituted from the powder shows particle sizes between 150 and 600 nm.

The particle sizes were confirmed by ESEM microscopy. The images show spherical particles for both EVA and SB type liquid copolymers, with the same particle size distributions as measured before via DLS (Fig. 4). The kaolin particles were found to exhibit the same size (~200 nm) as the SB polymer. However, kaolin particles appear as irregular platelets which form aggregates while SB particles are spherical and therefore easy to differentiate from kaolin.

Specific anionic charge densities were quantified via polyelectrolyte titration employing cationic polyDADMAC as counter electrolyte [30,31]. From the amount of polyDADMAC consumed for complete charge neutralization, the specific anionic charge density was calculated. The results for all latex dispersions at pH 7, 12.5 and in synthetic cement pore solution are displayed in Fig. 5.

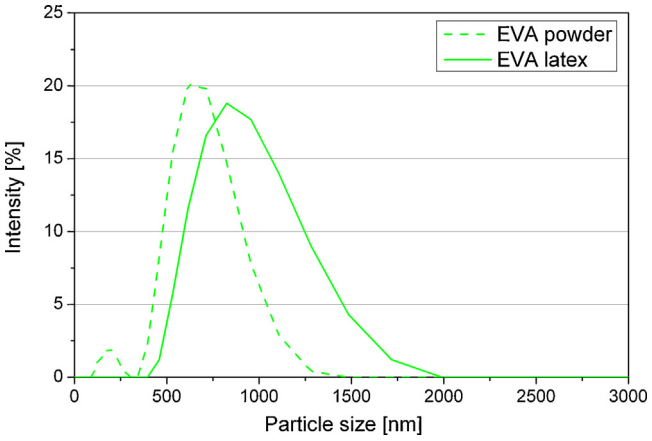

Fig. 2. Particle size distributions of 0.1 wt.% aqueous dispersions prepared from EVA liquid latex or re-dispersible powder, measured by dynamic light scattering.

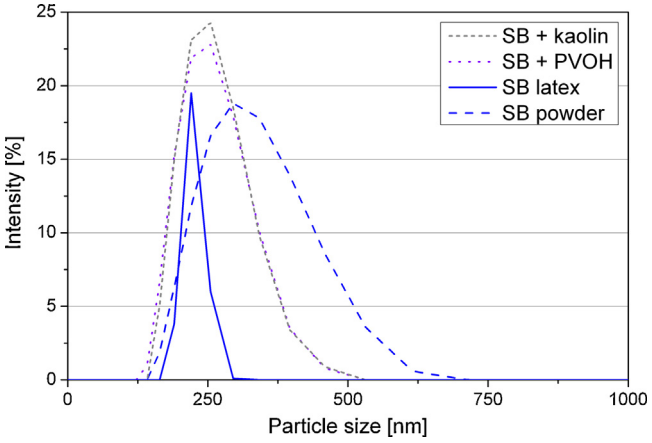

Fig. 3. Particle size distributions of 0.1 wt.% aqueous dispersions prepared from SB liquid latex, SB re-dispersible powder, SB + PVOH powder and SB + kaolin powder, measured by dynamic light scattering.

At pH 7, the surface charge of EVA particles in both liquid and powder dispersion is almost zero. Both monomers ethylene and vinylacetate have no functional groups which can provide a charge. At pH 12.5, a relatively minor charge develops which can be ascribed to deprotonation of hydroxyl groups located on the surface of the latex, originating from PVOH (liquid latex) or PVOH/kaolin (powder). Obviously, kaolin is partly responsible for the higher anionic charge observed for the EVA powder, compared to the liquid EVA latex.

Additional measurements revealed that the specific anionic charge density of individual PVOH is negligible at pH 7 whereas at pH 12.5, it develops a significant negative surface charge (Table 3). However, it has to be considered that the content of PVOH in the

Table 3
Specific anionic charge densities of PVOH at pH 7 and 12.5, measured by polyelectrolyte titration.

Component	Anionic charge density [C/g]	
	pH 7.0	pH 12.5
PVOH	0.6	19.3

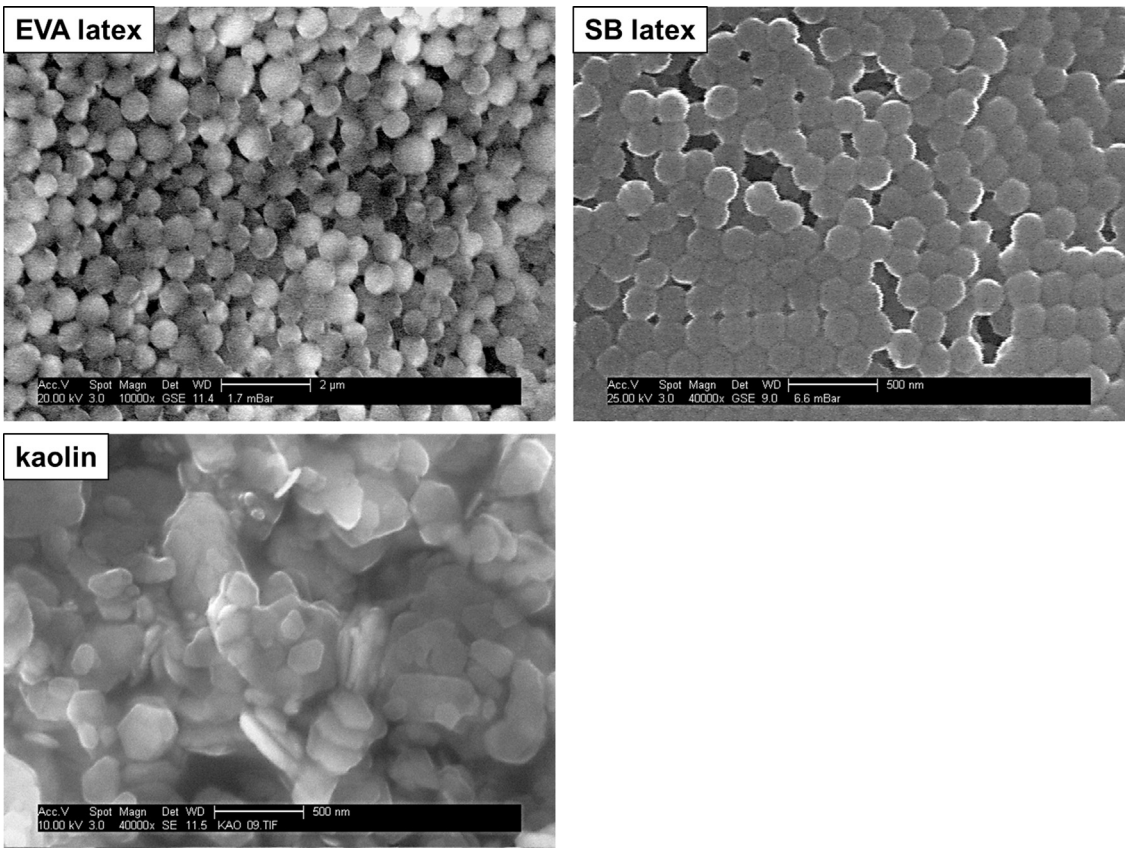

Fig. 4. ESEM micrographs of EVA and SB liquid latex particles dispersed in DI water, and SEM micrograph of kaolin particles.

latex powders is low, and thus its contribution to the overall charge of the latex powder particles is limited.

In synthetic cement pore solution, the EVA particles carry no anionic charge at all. Obviously, the Ca^{2+} ions present in SCPS fully neutralize all negative surface charges developed at high pH values.

The SB polymer generally exhibits a pronounced negative surface charge, owed to the presence of itaconic acid which is copolymerized with SB and provides carboxylate functionalities. The anionic charge of the SB particles is pH-dependent because at higher pH, deprotonation of the carboxylic groups is more complete, thus leading to higher anionic charge density. A comparison between liquid SB latex and latex obtained from re-dispersed powder reveals a lower anionic charge for the powder. This effect can be ascribed to the coating of SB particles with PVOH and/or kaolin during the spray drying process whereby some of the charge-providing carboxylate groups of the SB polymer are embedded in the coating and thus no longer exposed on the surface. The SB model powders which contain only PVOH or kaolin behave similarly, compared to the liquid SB latex. Further experiments revealed that the SB particles show strong interaction with ions from synthetic cement pore solution. For all SB samples, the anionic charge is greatly reduced when tested in SCPS. A plausible explanation for this effect is the adsorption of cations (especially Ca^{2+}) onto the surface of the SB particles holding carboxylate groups.

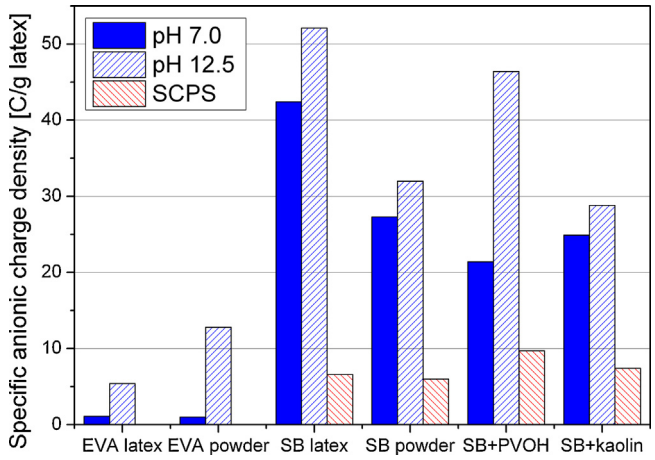

Fig. 5. Specific anionic charge densities of latex particles at pH 7, 12.5 and in synthetic cement pore solution, measured via polyelectrolyte titration using a particle charge detector.

3.2. Latex stability in water and cement

The stability of latex dispersions in water and cement was assessed using the turbidity method. In general, the turbidity of polymer dispersions depends on the polymer concentration, the particle size and the extinction coefficient of the latex which is specific for each type of polymer. Thus, a time-dependent variation in the absorbance of a dispersion indicates that changes in the concentration or particle size of the dispersion have occurred. A variation of the polymer concentration caused by coagulation and ultimately sedimentation clearly indicates instability of a latex dispersion.

At first, calibration curves were developed for both EVA and SB powders to confirm the existence of a linear dependence between polymer concentration and absorbance. Obviously, at a wavelength of 550 nm for both polymers clearly a linear correlation between concentration and absorbance was obtained.

As a next step, the stability of EVA latex (both liquid and powder) dispersed in water or SCPS was studied. The results are displayed in

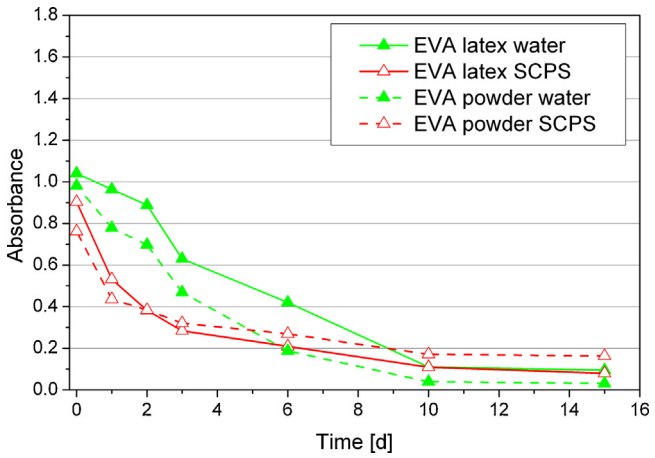

Fig. 6. Stability of EVA dispersions (polymer content 0.05 wt.%) in water or SCPS prepared from liquid EVA latex or powder, measured over a time period of 15 days via photometric turbidity test at a wavelength of 550 nm.

Fig. 6. As a consequence of being essentially nonionic and because of the pronounced polydispersity, the EVA particles are not stable in the aqueous as well as the SCPS fluid system. Generally, stability in the aqueous system was considerably better than in the SCPS which is loaded with electrolytes. It is well known that polydisperse systems exhibit a strong tendency to agglomerate, followed by sedimentation. Here, repulsion between the double layers of the particles is too low and no barrier exists which can prevent this agglomeration process. In the aqueous and SCPS fluid systems, the liquid EVA latex always is slightly more stable than the powder. This effect plausibly is owed to the presence of kaolin which even further increases the polydispersity of the system and precipitates from the dispersion.

The stability of SB dispersions (prepared from liquid latex or powder) in water and synthetic cement pore solution was investigated next. In water, both SB latex and powder exhibit excellent stability over a time period of 15 days (Fig. 7). As was shown in Fig. 5 Fig. 5, there the SB particles are strongly negatively charged, thus repulsion between the double layers prevents coagulation and subsequent sedimentation. Another reason for the superior stability of the SB latex in water is the monodisperse particle size distribution of ~220 nm.

However, in synthetic cement pore solution a completely different behavior of the SB latex was observed. There, a greatly reduced stability was found, particularly for the liquid latex. Apparently, the calcium ions present in SCPS lead to a much reduced anionic charge of the latex, as was shown in Fig. 5. Consequently, the SB latex shows a similar behavior like the nonionic EVA dispersion which is characterized by instability.

Interestingly, the SB powder exhibits a noticeably better stability than the liquid latex. This trend is more pronounced in water than in SCPS. For the powder, much less coagulation and sedimentation was observed. Such result is surprising, because according to Fig. 5 both liquid and powder SB exhibit similar anionic charges in SCPS. Obviously, an additional stabilizing effect arising from the components added in the spray drying of the latex (polyvinylalcohol and/or kaolin) plays a role for this effect.

For comparison, the stability test in SCPS was performed in air, i.e. in the presence of CO_2. There, after ~6 days a part of the coagulated latex sediment became re-dispersed as was evidenced by an increase in turbidity of the supernatant (Fig. 7). Such re-dispersion was observed for all dispersions in SCPS when exposed to air. Apparently, carbonation of the SCPS leads to precipitation of $CaCO_3$ whereby Ca^{2+} ions are removed from the solution. Thus, the ionic strength of the supernatant decreases significantly and the destabilization of the latex particles caused by Ca^{2+} is much reduced.

To elucidate the reason for the different behaviors of liquid SB latex and re-dispersed powder in SCPS, dispersions of liquid SB with added PVOH or kaolin were prepared. This experiment should reveal whether the presence of PVOH or kaolin in the dispersion was responsible for the enhanced stability of the SB powder. Fig. 8 exhibits the result. Obviously, addition of neither PVOH nor kaolin to the liquid SB latex can improve its stability in SCPS. This signifies that a positive effect from PVOH or kaolin only occurs during the spray drying process. There, the individual latex particles are coated with a layer of PVOH to prevent their coalescence into a film, and to avoid compaction and caking during storage of the bagged powder.

To detect which of the two components, PVOH or kaolin, is responsible for the enhanced stability, SB model powders containing only individual PVOH or kaolin were prepared by spray drying with the same contents of PVOH and kaolin as in the actual SB powder. These SB model powders (SB + PVOH/SB + kaolin) were then tested for their stability in water and synthetic cement pore solution. Fig. 9 displays the result. In water, the powder SB + PVOH possesses the same stability as the liquid SB latex while addition of kaolin decreases stability slightly within the first day. This effect can be ascribed to partial sedimentation of kaolin particles. Thus,

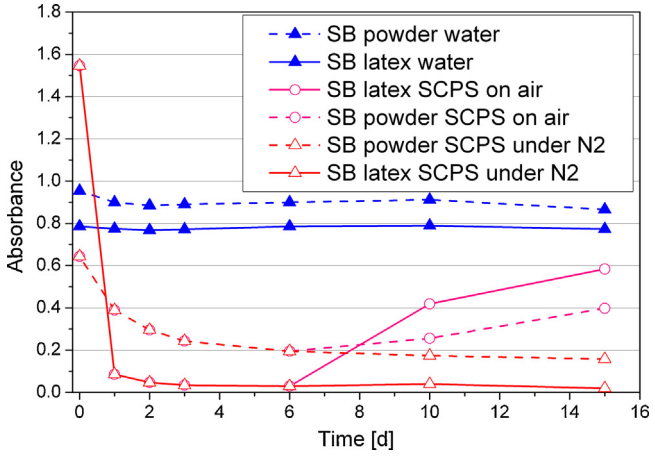

Fig. 7. Stability of SB dispersions (polymer content 0.05 wt.%) in water or SCPS, prepared from liquid SB latex or powder, measured over a time period of 15 days via photometric turbidity test at a wavelength of 550 nm.

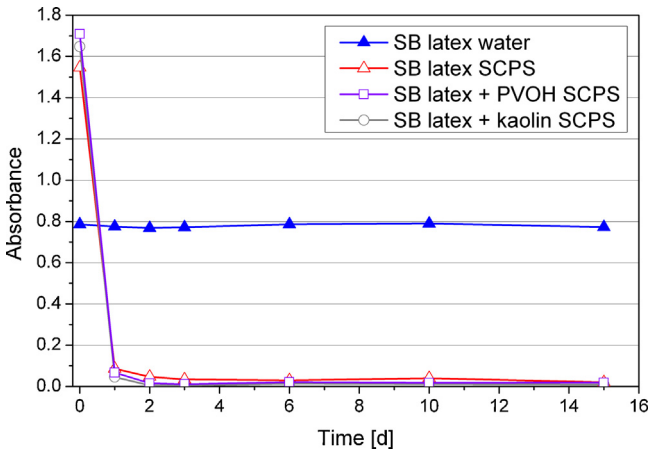

Fig. 8. Stability of SB dispersions (polymer content 0.05 wt.%) in SCPS, prepared from SB liquid latex under addition of individual PVOH or kaolin, measured over a time period of 15 days via photometric turbidity test at a wavelength of 550 nm.

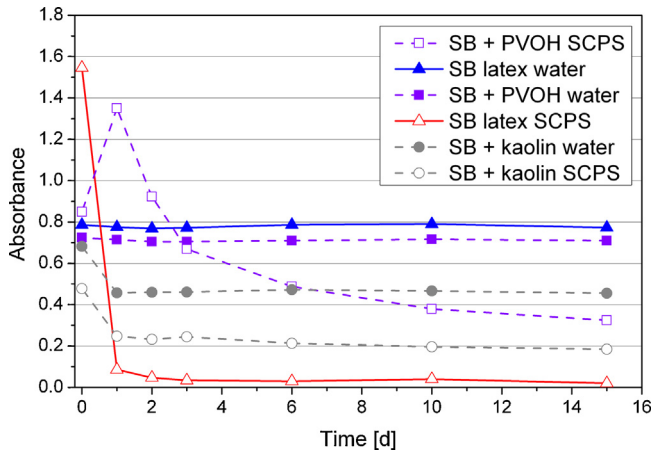

Fig. 9. Stability of SB dispersions (polymer content 0.05 wt.%) in water or SCPS prepared from the spray dried model powders SB + PVOH and SB + kaolin, measured over a time period of 15 days via photometric turbidity test at a wavelength of 550 nm.

the well-known stabilizing effect of PVOH on latex dispersions becomes evident here.

In SCPS, however, addition of PVOH or kaolin generally improves latex stability significantly. The effect is much more pronounced for PVOH than for kaolin. Still, the long-term stability of all SB samples tested in SCPS is less than of those in water.

The results above confirm that the electrokinetic surface properties of the SB latex are much impacted by the spray drying process. There, PVOH is added as colloidal stabilizer and kaolin as anti-caking agent. They decrease the anionic charge of the latex particles (Fig. 5) and thus reduce interaction with divalent Ca^{2+} ions present in SCPS, leading to improved stability in SCPS.

3.3. Mechanistic investigation

3.3.1. Interaction of SB latex with Ca^{2+}

When dispersed in synthetic cement pore solution, immediately after preparation the SB latex starts to coagulate. This collapse of the dispersed system was attributed to the effect of Ca^{2+} ions. To confirm, starting from liquid SB latex dispersions in SCPS were prepared under addition of EDTA at concentrations of 0.005–0.01 mol/L and their stability was measured photometrically. At a high pH of 12.5, EDTA chelates calcium ions selectively in the presence of

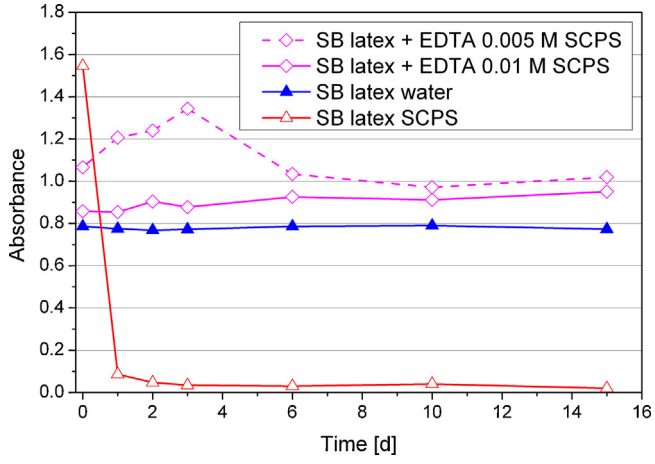

Fig. 10. Stability of SB dispersions (polymer content 0.05 wt.%) in SCPS prepared from liquid SB latex under addition of EDTA, measured over a time period of 15 days via photometric turbidity test at a wavelength of 550 nm.

Table 4
Stability constants of EDTA complexes with Ca^{2+}, Mg^{2+}, Na^{+} and K^{+} ions at pH 12.5.

Ion	log (*K*)
Na^{+}	1.66
K^{+}	0.80
Ca^{2+}	10.69
Mg^{2+}	8.79

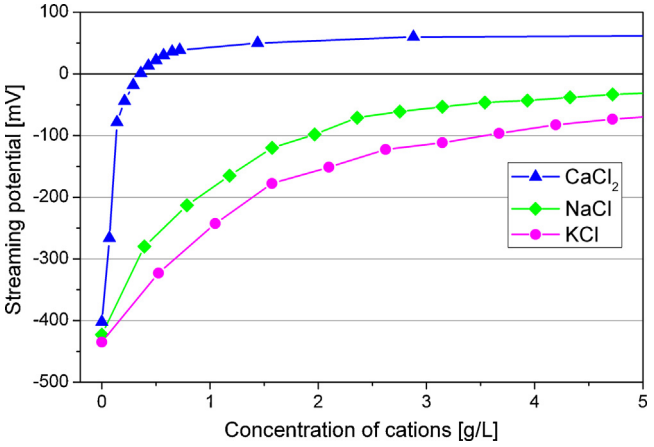

Fig. 11. Streaming potential of liquid SB latex (concentration: 0.1 wt.%) dispersed in sodium hydroxide solution (pH 12.5) at different additions of calcium, sodium and potassium ions, determined via a particle charge detector.

monovalent ions (Na^{+}, K^{+}), as is evidenced by the stability constants displayed in Table 4 [32].

The result is shown in Fig. 10. Obviously, presence of 0.1 mol/L of EDTA in the SCPS system greatly enhances the stability of the anionic SB latex and prevents coagulation. This experiment clearly demonstrates the detrimental effect of calcium ions on the stability of anionic latex dispersions in general.

To confirm the effect of different cations on the stability of the SB latex, the streaming potential of latex dispersions with added $CaCl_2$, NaCl and KCl were determined. Fig. 11 shows that the streaming potential of the latex particles is significantly influenced by those cations. Divalent Ca^{2+} ions reduce the streaming potential much more than the monovalent sodium and potassium ions. Less than 0.5 g/L of Ca^{2+} are required to completely neutralize the anionic

Table 5
Sorbed amounts of polyvinylalcohol on latex polymer powders, measured via total organic carbon method.

Powder	Sorbed PVOH [mg/g latex]
SB powder	50
SB + PVOH	55
EVA powder	52

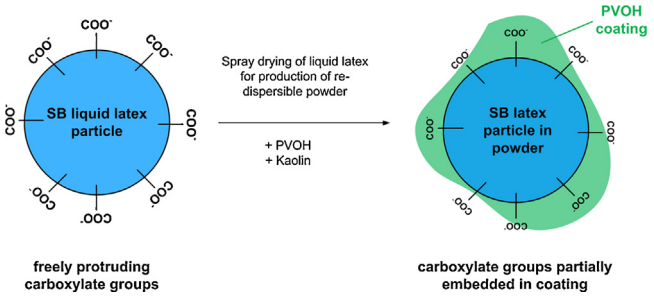

Fig. 12. Formation of a PVOH coating on the surface of carboxylated SB latex particles during spray drying.

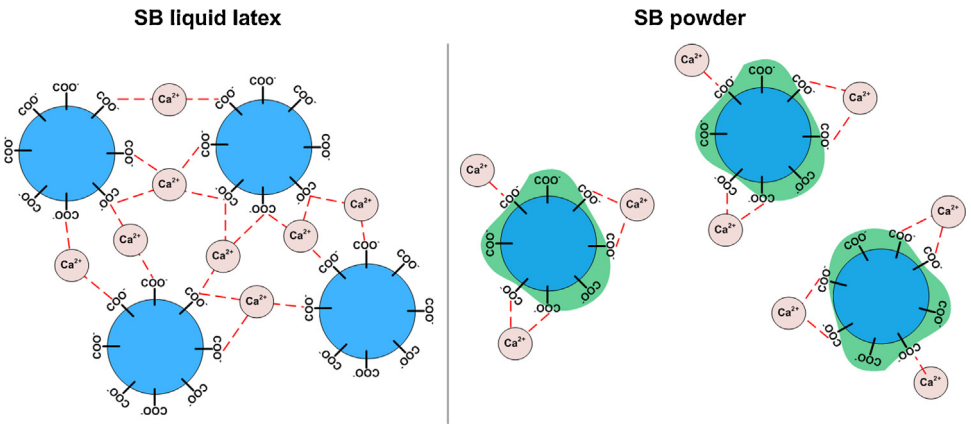

Fig. 13. Schematic illustration of the coagulation and destabilization mechanism for liquid SB latex (left) and of the enhanced colloidal stability of liquid latex reconstituted from SB powder (right) owed to partial embedding of $-COO^-$ functionalities in a PVOH coating.

charge of the SB latex particles. This behavior instigates that in cement pore solution, a dense layer of calcium ions is adsorbed onto the surface of the SB latex particles. In the presence of multivalent ions the Debye length is much less than when using monovalent ions. As a consequence, the potential on the latex particle surface decreases much faster and the thickness of the diffuse counterions cloud is much smaller. Additionally, an overcompensation of the charge of the latex particles can only be achieved by multivalent ions.

3.3.2. Sorption of PVOH on SB latex powder

In synthetic cement pore solution, completely different behaviors were observed for the liquid and the powder SB latexes. The liquid coagulates instantly whereas the SB powder is much more stable (Fig. 7). From the measurements of the anionic charge densities it became evident that the SB powder exhibits a lower anionic charge density, compared to the liquid SB latex (Fig. 5). It was speculated whether this effect can be ascribed to a coating of the SB powder particles with PVOH and/or kaolin. To investigate, the amount of PVOH sorbed by SB and EVA powder was analyzed via the depletion method. After dispersing the SB or EVA powder in water and agitating for 2 h to dissolve the non-sorbed portion of PVOH, the powder particles were separated by filtration and the dissolved amount of PVOH contained in the filtrate was quantified via TOC. From this, the amount of PVOH sorbed onto the latex powder was derived. As is shown in Table 5, ~50 mg PVOH/g latex are sorbed onto the SB or EVA powders during the spray drying process. This amount is independent of the chemical type of latex. The result evidences that the surfaces of both EVA and SB latex powders are coated with sorbed PVOH. However, from this experiment it is not possible to distinguish whether PVOH is physically adsorbed or chemically grafted onto the powder surfaces.

3.3.3. Model describing stability of SB powder in SCPS

Based on the results above, a model for the unexpected stability of the SB powder in SCPS is proposed. The reduced anionic charge density and the sorption of PVOH on SB latex suggest that the carboxylate groups present on the particle surface are partially embedded in a coating formed by PVOH and kaolin (Fig. 12). The shielding effect of PVOH was also described by *Kalaji* et al. using poly (lactic-co-glycolic acid) microspheres [33]. As a result, interaction between the latex and calcium ions is decreased significantly, as is illustrated in Fig. 13. In the liquid SB latex (no PVOH and kaolin present), carboxylate groups can freely protrude into the pore solution and thus chelate with calcium ions. Due to the abundance of $-COO^-$ groups, Ca^{2+} can also coordinate with carboxylate functionalities from different particles. This way, a 3D network of latex–Ca^{2+} complexes forms which results in instantaneous coagulation and sedimentation [34]. Such destabilization is not possible for the latex powder where a significant portion of the $-COO^-$ groups is embedded in a PVOH film and thus cannot offer coordination sites for the interparticle crosslinking mediated by Ca^{2+}. Consequently, such PVOH coated SB powders exhibit a significantly higher stability in cement pore solution. Additionally, a steric stabilization effect of the PVOH coating forming a hairy layer on the surfaces of the latex particles can be assumed, according to findings from another group [35].

4. Conclusion

Our experiments revealed that the electrokinetic surface properties of a carboxylated anionic styrene–butadiene latex are significantly influenced by the addition of PVOH and kaolin in the fabrication of a latex powder from a mother liquor.

Styrene–butadiene dispersions prepared from liquid latex or redispersible polymer powder showed comparable stability in water whereas in cement pore solution, the SB powder is much more stable compared to its liquid form. For an ethylene–vinylacetate copolymer, no differences in stability between the liquid and the powder form were observed in both water and SCPS. This behavior was attributed to the non-ionic character of the EVA dispersion.

By means of streaming potential measurements it was confirmed that calcium ions are responsible for the destabilization of the liquid styrene–butadiene latex. Opposite to this, styrene–butadiene polymer powder is coated with a polyvinylalcohol film whereby the carboxylate groups are partially covered and less sites for interaction with calcium ions are available. Apparently, there only surface adsorption of calcium ions and no crosslinking can occur. The results signify that PVOH and kaolin not only present valuable auxiliaries for the spray drying process. Moreover, they are also significant for the stability of SB latex powder in cementitious systems. Such enhanced stability is of great practical importance in construction applications.

Acknowledgement

The authors would like to thank Dr. Hartmut Kühn and Dr. Jürgen Dombrowski (Dow Olefinverbund GmbH, Schkopau, Germany. for the fabrication of the model latex powders.

References

[1] Y. Ohama, Handbook of Polymer-Modified Concrete and Mortars – Properties and Process Technology, Noyes Publications, New Jersey, 1995.

[2] Y. Ohama, Polymer-based admixtures, Cem. Concr. Compos. 20 (1998) 189–212.
[3] J.W. Kardon, Polymer-modified concrete: review, J. Mater. Civ. Eng. 9 (1997) 85–92.
[4] Y. Chevalier, C. Pichot, C. Graillat, M. Joanicot, K. Wong, J. Maquet, P. Lindner, B. Cabane, Film formation with latex particles, Colloid Polym. Sci. 270 (1992) 806–821.
[5] A.M. Betioli, P.J.P. Gleize, V.M. John, R.G. Pileggi, Effect of EVA on the fresh properties of cement paste, Cem. Concr. Compos. 34 (2012) 255–260.
[6] A.M. Betioli, J. Hoppe, M.A. Cincotto, P.J.P. Gleize, R.G. Pileggi, Chemical interaction between EVA and Portland cement hydration at early-age, Constr. Build. Mater. 23 (2009) 3332–3336.
[7] A. Jenni, M. Herwegh, R. Zurbriggen, T. Aberle, L. Holzer, Quantitative microstructure analysis of polymer-modified mortars, J. Microsc. (Oxford) 212 (2003) 186–196.
[8] A. Jenni, L. Holzer, R. Zurbriggen, M. Herwegh, Influence of polymers on microstructure and adhesive strength of cementitious tile adhesive mortars, Cem. Concr. Res. 35 (2005) 35–50.
[9] A. Jenni, R. Zurbriggen, L. Holzer, M. Herwegh, Changes in microstructures and physical properties of polymer-modified mortars during wet storage, Cem. Concr. Res. 36 (2006) 79–90.
[10] J. Kaufmann, F. Winnefeld, R. Zurbriggen, Polymer dispersions and their interaction with mortar constituents and ceramic tile surfaces studied by zeta-potential measurements and atomic force microscopy, Cem. Concr. Compos. 34 (2012) 604–611.
[11] R. Wang, X.G. Li, P.M. Wang, Influence of polymer on cement hydration in SBR-modified cement pastes, Cem. Concr. Res. 36 (2006) 1744–1751.
[12] X.L. Chu, A.D. Nikolov, D.T. Wasan, Effects of interparticle interactions on stability, aggregation and sedimentation in colloidal suspensions, Chem. Eng. Commun. 150 (1996) 123–142.
[13] O. Vinuesa, M. Rodriguez, H. Alvarez, Colloidal stability of polymer colloids with different interfacial properties: Mechanisms, J. Colloid Interface Sci. 184 (1996) 259–267.
[14] Y. Ishikawa, Y. Katoh, H. Ohshima, Colloidal stability of aqueous polymeric dispersions: Effect of pH and salt concentration, Colloid Surf. B: Biointerfaces 42 (2005) 53–58.
[15] D. Polpanich, P. Tangboriboonrat, A. Elaissari, The effect of acrylic acid amount on the colloidal properties of polystyrene latex, Colloid Polym. Sci. 284 (2005) 183–191.
[16] K. Tauer, T.R. Aslamazova, On the colloidal stability of poly(methyl methacrylate) and polystyrene particles prepared with surface-active initiators, Colloid Surf. A: Physicochem. Eng. Asp. 300 (2007) 260–267267.
[17] V.A. Pripisnova, L.E. Ermakova, E.V. Golikova, A.Y. Menshikova, M.P. Sidorova, Electrochemical properties and stability of emulsifier-free polystyrene latexes in 1:1 electrolyte solutions, Colloid J. 71 (2009) 534–540.
[18] J. Hierrezuelo, A. Vaccaro, M. Borkovec, Stability of negatively charged latex particles in the presence of a strong cationic polyelectrolyte at elevated ionic strengths, J. Colloid Interface Sci. 347 (2010) 202–208.
[19] B.M. Reis, S.P. Armes, S. Fujii, S. Biggs, Characterisation of the dispersion stability of a stimulus responsive core–shell colloidal latex, Colloid Surf. A: Physicochem. Eng. Asp. 353 (2010) 210–215.
[20] Y.B. Pei, X.Y. Zhang, Y.L. Jiang, H. Huang, H.Q. Chen, Redispersibility of acrylate polymer powder and stability of its reconstituted latex, J. Dispersion Sci. Technol. 32 (2011) 1279–1284.
[21] A. Sadeghpour, I. Szilagyi, M. Borkovec, Charging and aggregation of positively charged colloidal latex particles in presence of multivalent polycarboxylate anions, Int. J. Res. Phys. Chem. Chem. Phys. 226 (2012) 597–612.
[22] I.P. Kazhuro, V.D. Koshevar, Sedimentation stability of mixed dispersions of kaolin and synthetic latexes, Russ. J. Appl. Chem. 83 (2010) 1558–1562.
[23] R.J. Hunter, Foundations of Colloid Science, Oxford University Press, New York, 2001.
[24] K. Maruyama, M. Kawaguchi, T. Kato, Heterocoagulation behavior of poly(styrene-co-butadiene) and poly(butyl acrylate) at high particle concentrations, Colloid Surf. A: Physicochem. Eng. Asp. 189 (2001) 211–223.
[25] M. Gretz, J. Plank, An ESEM investigation of latex film formation in cement pore solution, Cem. Concr. Res. 41 (2011) 184–190.
[26] J. Plank, M. Gretz, Study on the interaction between anionic and cationic latex particles and Portland cement, Colloid Surf. A: Physicochem. Eng. Asp. 330 (2008) 227–233.
[27] S. Chandra, P. Flodin, Interactions of polymers and organic admixtures on portland cement hydration, Cem. Concr. Res. 17 (1987) 875–890.
[28] W. Rechenberg, S. Sprung, Composition of the solution in the hydration of cement, Cem. Concr. Res. 13 (1983) 119–126.
[29] J. Plank, B. Sachsenhauser, Experimental determination of the effective anionic charge density of polycarboxylate superplasticizers in cement pore solution, Cem. Concr. Res. 39 (2009) 1–5.
[30] K. Böckenhoff, W. Fischer, Determination of electrokinetic charge with a particle-charge detector, and its relationship to the total charge, J. Anal. Chem. 371 (2001) 670–674.
[31] C.A. Walker, J.T. Kirby, S.K. Dentel, The streaming current detector: a quantitative model, J. Colloid Interface Sci. 182 (1996) 71–81.
[32] D.C. Harris, Quantitative Chemical Analysis, W.H. Freeman, New York, 2011.
[33] N. Kalaji, N. Sheibat-Othman, H. Saadaoui, A. Elaissari, H. Fessi, Colloidal and physicochemical characterization of protein-containing poly(lactide-co-glycolide) (PLGA) microspheres before and after drying, e-Polymers 10 (2009).
[34] S. Boutti, M. Urvoy, I. Dubois-Brugger, Ch Graillat, E. Bourgeat-Lami, R. Spitz, Influence of low fractions of styrene/butyl acrylate polymer latexes on some properties of ordinary portland cement mortars, Macromol. Mat. Eng. 292 (2007) 33–45.
[35] M. Ayoub, N. Ahmed, N. Kalaji, C. Charcosset, A. Magdy, H. Fessi, A. Elaissari, Study of the effect of formulation parameters/variables to control the nanoencapsulation of hydrophilic drug via double emulsion technique, J. Biomed. Nanotechnol. 7 (2011) 255–262.

Paper #2

Influence of anti-caking agent kaolin on film formation of ethylene-vinylacetate and carboxylated styrene-butadiene latex polymers

S. Baueregger, M. Perello, J. Plank

Cement and Concrete Research

58 (2014), 112-120

Cement and Concrete Research 58 (2014) 112–120

Contents lists available at ScienceDirect

Cement and Concrete Research

journal homepage: http://ees.elsevier.com/CEMCON/default.asp

Influence of anti-caking agent kaolin on film formation of ethylene–vinylacetate and carboxylated styrene–butadiene latex polymers

Stefan Baueregger [a], Margarita Perello [b], Johann Plank [a,*]

[a] Technische Universität München, Lichtenbergstr. 4, 85747 Garching, Germany
[b] Dow Europe GmbH, Bachtobelstr. 3, 8810 Horgen, Switzerland

ARTICLE INFO

Article history:
Received 7 February 2013
Accepted 21 January 2014
Available online xxxx

Keywords:
Dispersion (A)
SEM (B)
Polymers (D)
Cement (D)
Latex film formation

ABSTRACT

Colloidal stabilizers (e.g. PVOH) and anti-caking aids (e.g. kaolin) are commonly added during the spray drying of liquid latex dispersions to produce re-dispersible polymer powders for the drymix mortar industry. Here, the influence of kaolin and polyvinylalcohol on polymer film formation of an ethylene–vinylacetate (EVA) and a carboxylated styrene–butadiene (SB) latex dispersion in water and cement pore solution was investigated. Time-dependent ESEM analysis was conducted to analyze the progress of particle coalescence. The results show that both EVA and SB powders form a homogeneous film much faster than their liquid precursors. Surprisingly, this effect was found to result from the presence of kaolin. Consequently, this additive fulfills a dual purpose in re-dispersible powders, it serves as anti-caking agent and also accelerates film formation while polyvinylalcohol retards particle coalescence. The SB latex achieves a coherent polymer film faster than the EVA dispersion, due to its smaller particle size (~200 nm).

1. Introduction

Latex polymers are among the most important admixtures used in cement based building materials. Most latex polymers applied in the construction industry are based on ethylene/vinylacetate, styrene/butadiene or acrylate chemistry. Latex polymers are synthesized as liquid aqueous dispersion via emulsion polymerization. For drymix mortars which are widely used in tile adhesives, tile grouts or external thermal insulation composite systems (ETICS), re-dispersible polymer powders are fabricated by spray drying from a liquid mother latex. During spray drying, protective colloids (e.g. polyalcohols) and anti-caking agents (e.g. clay, silica, calcium carbonate, kaolin, diatomaceous earth etc.) are fed in together with the mother liquor. The addition of latex polymers can improve the properties of fresh and hardened cement. Latex-treated mortars exhibit better cohesion and adhesion and higher flexural strength. The reason behind those improvements is the formation of polymer films within the cementitious matrix as a consequence of latex particle coalescence [1–3].

The impact of anti-caking agents such as kaolin on film formation of re-dispersible polymer powders has not been reported so far. Only few literatures address the interaction between latex particles and mineral substrates such as silica, mica or ceramic tiles [4,5] while a large number of articles focus on the material properties of polymer-modified concrete or mortar [6–11] and composites made from latex polymers and inorganic fillers such as clays [12–15]. Some articles are dealing with film formation in the presence of electrolytes. There, it was shown that in highly ionic systems such as cement pore solution film formation can occur much later, compared to fresh water systems [16–21]. Several reasons have been identified for this effect, the main two being surface coverage of latex particles with adsorbed Ca^{2+} ions from cement, and formation of a salt skin. Both phenomena hinder particle coalescence. These examples suggest that the additives used in the spray drying of latex powders may also strongly impact film formation.

The process of polymer film formation can be divided into four main stages which are illustrated in Scheme 1. Starting from an aqueous latex dispersion (stage I), a dense particle packing (stage II) is the result of dehydration due to evaporation or water consumption during cement hydration. In stage II, particles now are in contact with each other and the interstitial spaces of the dense particle packing are filled with water. After water removal from the interstitial spaces, the latex particles start to deform in order to minimize their interfacial tension. This step only occurs if the temperature is above the so called minimum film forming temperature (MFFT). Now the polymer chains become mobile and particle coalescence into coherent polymer films can occur. The driving force behind the interdiffusion of the polymer chains is minimization of interfacial tension between the latex particles. The result is a molecularly continuous, coherent and homogeneous polymer film [22–24].

* Corresponding author. Tel.: +49 89 289 13151.
E-mail address: sekretariat@bauchemie.ch.tum.de (J. Plank).

0008-8846/$ – see front matter © 2014 Elsevier Ltd. All rights reserved.
http://dx.doi.org/10.1016/j.cemconres.2014.01.017

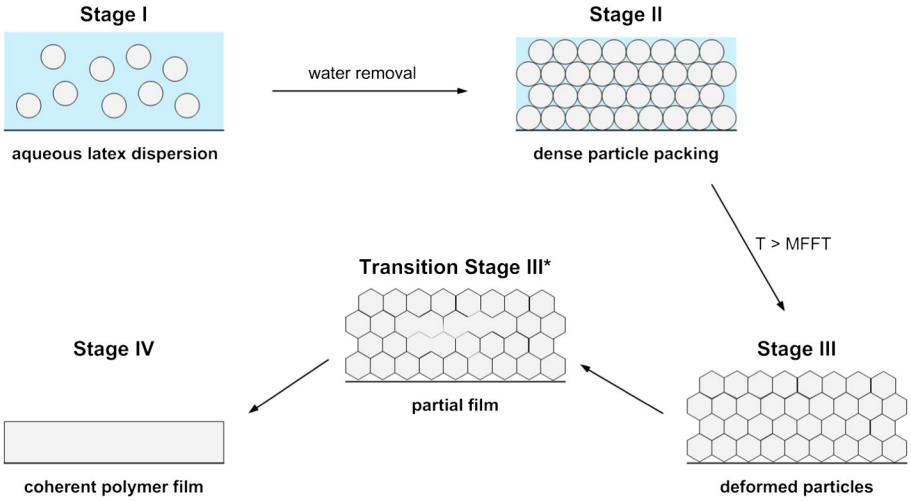

Scheme 1. Schematic illustration of the four main stages occurring during polymer film formation from an aqueous latex dispersion.

Environmental scanning electron microscopy (ESEM) offers the possibility to track the polymer film formation because it allows imaging of wet and insulating samples in their native state such as liquid latex dispersions. In contrast, conventional SEM is not suitable because it requires a high vacuum which will immediately dehydrate the sample and cause premature particle coalescence, compared to actual application conditions. This unique capability of ESEM is owing to the usage of a multiple aperture graduated vacuum system which generates a relatively low vacuum of 1–10 mbar. The atmosphere in the specimen chamber is decreased from ambient conditions to a water vapor pressure of e.g. 7.5 mbar. In combination with cooling of the sample to 3 °C, a saturated water atmosphere can be maintained above the specimen which is thus prevented from dehydration and maintains its original wet state. To achieve this saturated water vapor atmosphere, performance of a specific pump-down sequence is required. The pump-down procedure consists of several evacuation and water vapor addition steps to approach the final water atmosphere in the specimen chamber while ensuring that water is retained in the sample [25–29].

The goal of this study was to investigate whether polymer particle coalescence is hindered or accelerated by the presence of the anti-caking agent kaolin and the protective colloid PVOH. As latex polymers, ethylene–vinylacetate (EVA) and a carboxylated styrene–butadiene (c-SB) latex polymer were used. The kinetics of film formation of the liquid latexes was compared with that of the re-dispersible polymer powders containing kaolin and PVOH. To elucidate the impact of each individual spraying aid, kaolin or PVOH, model powders of c-SB polymer were prepared which contained only either kaolin or PVOH. As fluid systems, deionized (DI) water and synthetic cement pore solution (SCPS) were utilized. The first step in the film forming process, the evaporation of water from the aqueous latex dispersion, was quantified gravimetrically via the weight loss of the dispersions over time. The kinetics of stages II–IV were investigated by time-dependent ESEM monitoring whereby particle coalescence and polymer film formation were recorded. Additionally, the elemental composition of the polymer films formed in the presence of kaolin was determined by means of energy dispersive X-ray (EDX) analysis.

2. Materials and methods

2.1. Materials

EVA liquid latex (solid content 52 wt.%), EVA re-dispersible powder, SB liquid latex (solid content 45 wt.%) and SB re-dispersible powder were provided by Dow Olefinverbund GmbH, Schkopau/Germany. The re-dispersible powders were produced by spray drying of the EVA or SB mother liquors under addition of kaolin as anti-caking agent and polyvinylalcohol as protective colloid. The ratios between polymer, anti-caking agent and colloidal stabilizer were kept constant for all samples. To analyze the effect of individual kaolin or polyvinylalcohol on the film formation of the SB latex, SB model powders were spray dried containing only either kaolin or PVOH. Again, the ratio of SB latex polymer to kaolin or PVOH was kept constant. The composition and properties of the liquid latex dispersions and powders are presented in Table 2.

Kaolin (KAMIN HG 90) was obtained from KaMinLLC, Macon/United States. Polyvinylalcohol (Mowiol 4-88) was purchased from Kuraray Europe, Frankfurt/Germany. $CaSO_4 \cdot 2H_2O$, KOH, Na_2SO_4, and K_2SO_4, were purchased from Merck, Darmstadt/Germany. Poly-diallyl dimethyl ammonium chloride (ZETAG 7568) was obtained from Ciba Specialty Chemicals Ltd, Bradford/UK.

All chemicals were utilized without further purification. Ultrapure water (resistivity >18 MΩ cm) was used for all experiments.

Synthetic cement pore solution (SCPS) was composed based on the characteristic ion concentrations present in the pore solution of an ordinary Portland cement (CEM I) at a w/c ratio of ~0.5 [30]. The pore solution was prepared by dissolving 1.72 g $CaSO_4 \cdot 2H_2O$, 6.96 g Na_2SO_4, 4.75 g K_2SO_4 and 7.12 g KOH in 1 L of deionized water. First, the $CaSO_4 \cdot 2H_2O$ were dissolved in 700 mL of water under vigorous stirring. Next, 6.96 g of Na_2SO_4 were solubilized in 150 mL of this $CaSO_4$ solution. Upon complete dissolution of the sodium sulfate, the solution was combined with the remaining $CaSO_4 \cdot 2H_2O$ solution. Next, 4.75 g of K_2SO_4 were added and solved. Afterwards, 7.12 g KOH dissolved in 150 mL of water were introduced into this mixture. Finally, water was added to a volume of 1 L. This method produces a clear, stable solution free of precipitate which incorporates the ion concentrations displayed in Table 1. The pH of the SCPS was 12.6.

Table 1
Concentration of ions present in the model cement pore solution used in the study.

Ion	Concentration [g/L]
K^+	7.1
Na^+	2.2
Ca^{2+}	0.4
SO_4^{2-}	8.2
OH^-	0.7

Table 2
Composition and properties of the liquid and powder latex samples.

Component or property	EVA latex	EVA powder	SB latex	SB powder	SB PVOH	SB Kaolin
Polymer content [wt.%]	52	–	45	–	–	–
Colloidal stabilizer	–	PVOH	–	PVOH	PVOH	–
Anti-caking agent	–	Kaolin	–	Kaolin	–	Kaolin
Particle size [nm]	350–1750	300–1250	220	150–600	150–500	150–500
Zeta potential [mV]	−17	−22	−31	−25	−25	−30
pH	5.5	–	9.8	–	–	–
T_g [°C]	20	20	6	6	6	6
MFFT [°C]	3	3	5	5	5	5

2.2. Characterization of latexes

All liquid latex dispersions were prepared with the same polymer content of 0.1 wt.%. The re-dispersible powders contain additional amounts of kaolin and/or polyvinylalcohol. Prior to measurements, all samples were treated for 3 min with ultrasound to re-disperse the particles completely.

Particle size was determined via dynamic light scattering (DLS) using a Zetasizer Nano ZS apparatus (Malvern Instruments, Workestershire/UK). Qualitative electric surface charge characterization of the latex particles dispersed in water (polymer content: 0.1 wt.%) was conducted by measuring their electrophoretic mobility on the same instrument. Electrophoretic mobility was converted into a value for zeta potential by using the *Smoluchowski* relation.

The specific anionic charge densities of the latex particles were determined utilizing a particle charge detector PCD 03 pH (Mütek Analytic, Herrsching/Germany). In a typical experiment, 10 mL of 0.1 wt.% latex dispersion were titrated with 0.001 mol/L poly-diallyl dimethyl ammonium chloride (polyDADMAC) aqueous solution until the isoelectric point was reached. The polyDADMAC solution was added continuously from a burette via an automatic feeder system according to a titration program controlled by the decrease of the streaming potential. From the consumption of cationic polyelectrolyte needed to neutralize the anionic charge of the latex particles, the specific anionic charge density of the latex particles was calculated [31]. The pH of the dispersion was adjusted to either 7 or 12.5 using 0.25 mol/L aqueous NaOH or HCl.

Glass transition temperature (T_g) was measured on a differential scanning calorimeter (DSC) Maia F3 from Netzsch, Selb/Germany. Minimum film formation temperature (MFFT) was determined on an MFFT Bar Thermostair II instrument from Coesfeld Materialtest, Dortmund/Germany.

2.3. Preparation of latex dispersions

To track the film forming kinetics, latex dispersions with a polymer content of 5 wt.% were prepared by addition of liquid or powder EVA or SB latexes to deionized water or synthetic cement pore solution. All samples were treated with ultrasound for 3 min before measurements were taken. Note that dispersions prepared from re-dispersible powders contain additional amounts of kaolin or polyvinylalcohol.

2.4. Gravimetric analysis of water evaporation from latex

The weight loss of the polymer dispersions was quantified gravimetrically as follows: 60 μL of aqueous latex dispersion holding a solid content of 5 wt.% polymer were applied on an aluminum container and stored at room temperature. The weight loss of the samples originating from evaporation was measured on a balance at intervals of 10 min.

2.5. ESEM imaging

The kinetics of polymer film formation was studied using time-dependent ESEM imaging following the procedure from *Gretz* and *Plank* [16]. Aqueous dispersions possessing a latex polymer content of 5 wt.% were used. 40 μL of polymer dispersion were deposited on a concave Al disk supplied as sample container for the ESEM instrument by FEI, Eindhoven/Netherlands. The samples were first stored at room temperature to simulate real application conditions. For microstructural analysis and investigation of the progress of latex film formation, samples stored for 1, 2, 3 or 4 h were then transferred into an XL-30 FEG (FEI, Eindhoven/Netherlands) environmental scanning electron microscope equipped with a Peltier cooling stage, a gaseous secondary electron detector and an EDAX X-ray analysis system. The Al disks were placed on the cooling stage in the microscope chamber at a temperature of 3 °C. Cooling of the sample establishes a saturated water vapor atmosphere above the sample surface, and also freezes film formation of the latex sample because temperature is below the MFFT. A gentle pump-down sequence was performed to prevent water evaporation from the sample while reducing the pressure in the specimen chamber. During this process which takes about 3 min, air is progressively replaced by water vapor. Imaging was carried out at accelerating voltages of 10.0 or 25.0 kV (spot size 3) respectively, and at working distances of 8–12 mm. EDX mapping was performed at a spot size of 5 and an accelerating voltage of 20 kV over a scan area of ~1 μm^2.

3. Results and discussion

The aim of this study was to compare the film forming kinetics of the liquid EVA or SB latexes with that of their re-dispersible powders. At first, the liquid and powder samples used were characterized with respect to their colloid-chemical properties. Then the rate of water removal was determined gravimetrically and its impact on polymer film formation was assessed. Finally, particle coalescence was monitored over time by ESEM imaging.

3.1. Colloid-chemical properties of the latex samples

Latex dispersions present colloidal particle suspensions. Therefore, the colloidal properties were analyzed before studying the film formation. The two types of latex polymers used in this study were an ethylene/vinylacetate copolymer stabilized by PVOH, and a styrene/butadiene copolymer stabilized by itaconic acid. Their chemical structures are shown in Fig. 1. The particle size distributions of both polymers measured by dynamic light scattering (DLS) are displayed in Figs. 2 and 3. The EVA latexes (mother liquor and liquid dispersion reconstituted from powder) exhibit a very broad size distribution in the range between 300 and 1750 nm, indicating high polydispersity. The additional peak observed for the powder sample at a particle size around 200 nm can be attributed to kaolin particles (Fig. 2). In comparison, the liquid SB latex exhibits an almost monodisperse particle size at ~220 nm while the latex dispersion obtained from the SB powder shows a broader size distribution ranging between 150 and 600 nm (Fig. 3).

Table 3 shows the results for the anionic charge densities of all samples. As expected, EVA latex particles exhibit no electric surface charge at pH 7. Both monomers ethylene and vinylacetate have no functional groups which can provide a charge under these conditions. At pH 12.5, however, EVA particles develop some negative charge. This

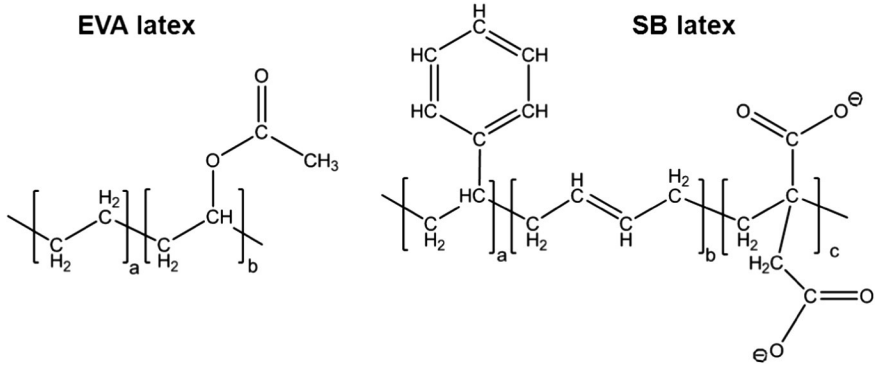

Fig. 1. Chemical structures of ethylene–vinylacetate and of carboxylated styrene–butadiene latex copolymers.

effect is more pronounced for the powder than for the liquid. For the liquid latex, the negative charge is owing to deprotonated hydroxyl groups formed by hydrolysis of vinylacetate. Whereas in the powder, a significant contribution to the charge is provided by the PVOH and – to a lesser extent – by kaolin, as is evidenced by the anionic charges of these individual components.

The SB polymer particles are always negatively charged due to the incorporation of itaconic acid which provides carboxylic groups located on the surface of the SB latex. Similar to the EVA latex, the negative charge of SB latex generally increases with pH, as would be expected from more complete deprotonation. Unlike for EVA, however, the SB powder exhibits a lower anionic charge than the liquid latex. This observation can be explained by a partial coating of the SB particles with PVOH/kaolin during the spray drying process whereby some carboxylate groups of SB are covered by this coating and no longer can contribute to the charge.

3.2. Kinetics of water evaporation from latex

Removal of water is the first step in the polymer film forming process. Here, the kinetics of water evaporation was analyzed gravimetrically as weight loss of the latexes over time and at room temperature (21 °C).

Fig. 4 shows the relative weight losses of the dispersions as a function of time. It becomes obvious that the entire evaporation process can be divided into two sections. At first, the weight loss increases steeply, but then decelerates significantly after ~50 min. This can be explained as follows: at the beginning, water can evaporate unhindered. However, as the water content in the dispersion decreases, the remaining water is retained more effectively by capillary forces and intermolecular interactions. According to Fig. 4, the EVA dispersion generally releases water slightly faster than the SB polymer. This effect is owing to the presence of carboxylic groups on the SB particle surface. The carboxylic groups interact strongly with water due to their pronounced hydrophilic character.

A comparison between the liquid and powder latexes reveals that for both EVA and SB, the powders dehydrate slightly slower than their liquid precursors. This phenomenon can be ascribed to the presence of PVOH and kaolin in the powders. The hydroxyl groups present in PVOH and on the surface of kaolin are hydrophilic and interact with water. As a result, water evaporation from the powders is decelerated.

3.3. Kinetics of particle coalescence

To monitor the course of film formation, at first the entire sample surface was scanned and then representative spots were chosen for imaging. Generally, polymer film formation occurs in those four stages (Scheme 1): water evaporation from dispersion (stage I), dense particle packing (stage II), particle deformation (stage III/III*) and particle coalescence or formation of a homogenous polymer film (stage IV). However, in this study it was found that film formation does not occur in sharply distinguishable steps, but rather a gradual transition occurs whereby different stages (II to IV) coexist. This principle is illustrated in Scheme 2.

3.3.1. Film formation of styrene–butadiene copolymer

At first, film formation of the carboxylated styrene–butadiene latex polymer (T_g = 6 °C/MFFT = 5 °C) was studied. The main goal was a comparison between the liquid and powder latex whereby the latter

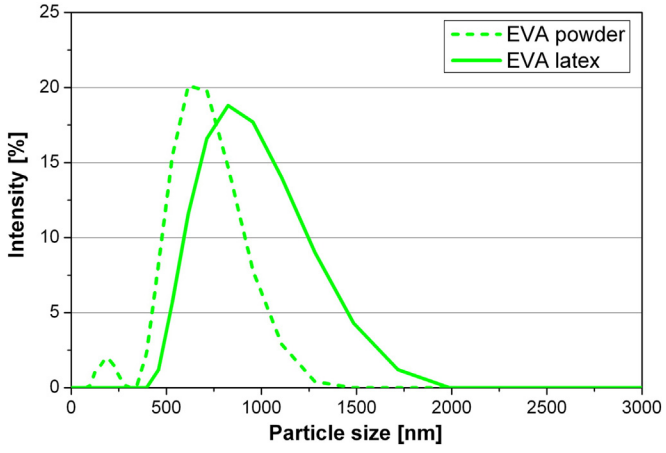

Fig. 2. Particle size distribution (intensity-based) in dispersions of liquid and powder EVA latex, measured by dynamic light scattering.

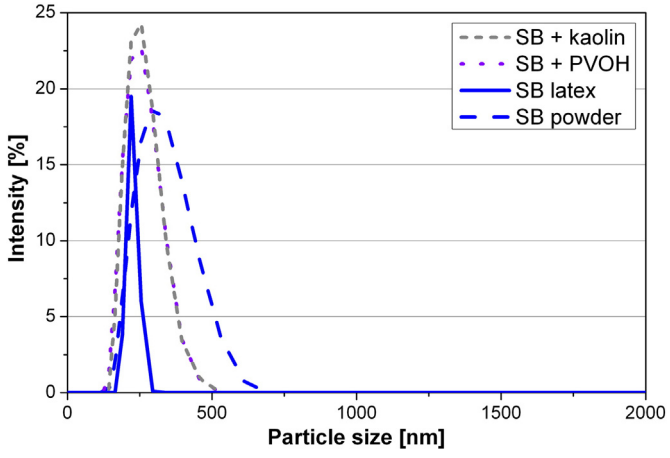

Fig. 3. Particle size distribution (intensity-based) in dispersions of liquid and powder SB latex, of SB + kaolin powder and of SB + PVOH powder, measured by dynamic light scattering.

Table 3
Anionic charge densities of EVA and SB latex samples and of individual kaolin and PVOH at pH 7 and 12.5, measured via polyelectrolyte charge titration.

Polymer or component	Anionic charge density [C/g]	
	pH 7.0	pH 12.5
EVA liquid latex	1.1	5.4
EVA + PVOH/kaolin powder	1.0	12.8
SB liquid latex	42.4	52.1
SB + PVOH/kaolin powder	27.3	32.0
SB + kaolin powder	24.9	28.8
SB + PVOH powder	21.4	46.4
PVOH	0.6	19.3
Kaolin	2.1	5.9

contains additional polyvinylalcohol and kaolin. From these experiments it was hoped to uncover the impact of kaolin and PVOH on the film forming process.

Figs. 5–7 show the results of time-dependent ESEM analysis on the film formation of liquid and powder SB latex in DI water. The first images were taken after 1 h of storage at room temperature. A visual inspection of both dispersions (liquid and powder) revealed that they were both still in a wet state. Consequently, individual latex particles exhibiting the original size of around 220 nm were observed in the ESEM image, which corresponds to stage I of the film forming process (Fig. 5). As mentioned before, it is necessary to remove some water in the ESEM chamber to obtain high quality images. Therefore, some of the particles have already come in contact, but no deformation or coalescence is visible yet.

After 2 h of drying at room temperature, the liquid latex sample mainly shows a dense particle packing or deformed particles including few areas where already a homogeneous film has formed (Fig. 6). Obviously, at this point the SB latex is in a transition between stages III and IV, whereby most parts on the surface still represent stage III. In comparison, most of the SB powder has already formed a homogeneous film and is mostly represented by stage IV. Almost no more individual polymer particles can be seen. Only on some spots bright boundaries are visible on the sample surface which represent residual water, salts, emulsifier and kaolin [16].

After 3 h of storage, a large area of the liquid latex has coalesced and formed a homogeneous film (Fig. 7). However, still some significant parts exhibit a dense particle packing or deformed particles only (stage III), thus indicating incomplete film formation. In contrast to this, the SB powder has completely finished its film formation process. No boundaries, skins or individual particles are visible anymore. The few bright particles embedded into the polymer film represent kaolin particles, as will be shown later.

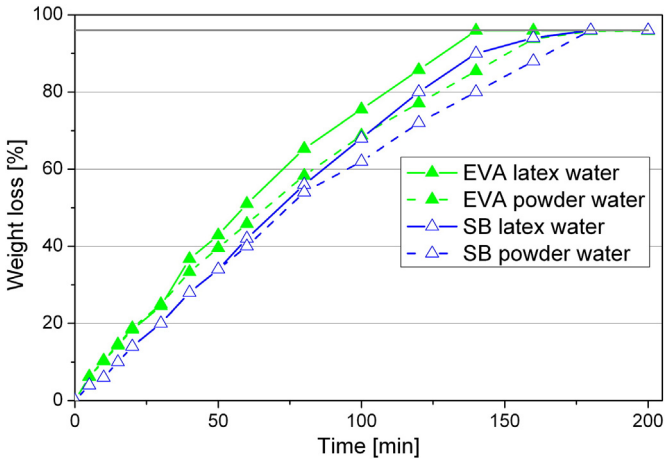

Fig. 4. Time-dependent weight loss of aqueous dispersions prepared from EVA or SB liquid and powder latexes, measured gravimetrically.

To conclude, surprisingly it was found that the SB powder transits much faster into a homogeneous polymer film than its liquid precursor. This observation suggests that one or both components added in the spray drying, kaolin or PVOH, affect the film forming properties of the SB powder.

To uncover the reason behind the accelerated film formation of the SB powder, SB model powders containing only individual kaolin or PVOH were prepared by spray drying. The polymer to kaolin or PVOH ratio, as well as the conditions during spray drying, were identical with those for the SB powder.

After 1 h of storage of the dilute latex samples, no differences between the powder samples SB + kaolin and SB + PVOH were visible. In both cases, individual latex particles were still observed, and no coalescence had occurred. After 2 h of storage, clear differences between the two samples SB + kaolin and SB + PVOH were detected. The sample SB + kaolin had already completely formed a homogeneous film and had reached stage IV of the film forming process, whereas SB + PVOH still exhibited individual copolymer particles which were densely packed (stage II/III) (Fig. 8). The same effect from kaolin was observed in another experiment when kaolin was added to the liquid SB latex. Apparently, PVOH hinders SB particle coalescence (this is the reason why PVOH is used as protective colloid in the spray drying process) while kaolin accelerates polymer film formation. During spray drying, kaolin becomes embedded into the PVOH film present on the surface of the latex powder and obviously stimulates particle coalescence. The detailed mechanism behind this effect remained unclear and requires further investigation.

The results from the water evaporation tests have revealed that liquid and powder SB latex release their water at relatively similar rates. Still, huge differences in the kinetics of film formation were observed, with the powder being much faster than the liquid. This effect was identified as a result from the presence of kaolin in the powder sample. Apparently, kaolin can much accelerate particle coalescence of SB latex.

3.3.2. Film formation of ethylene–vinylacetate copolymer

To investigate whether kaolin selectively influences the film formation of SB polymer only, the same experiment was conducted using an ethylene–vinylacetate copolymer (T_g = 20 °C/MFFT = 3 °C). Fig. 9 displays the results of the time-dependent ESEM study. For the liquid EVA latex it was found that even after 4 h of drying at room temperature, only a dense particle packing or deformed particles (stages II–III) had occurred (Fig. 9). Practically no particle coalescence was observed, thus indicating that the EVA dispersion is even slower in forming polymer films than the SB latex (Fig. 7). Opposite to this, the EVA powder already shows significant portions of homogeneous films on its surface while the remainder consists of densely packed particles (Fig. 9). To confirm again whether the presence of kaolin is the sole reason for the acceleration of film formation, a sample of liquid EVA was added with kaolin at the same dosage which was used in the powder fabrication. The ESEM image displayed in Fig. 9 reveals that also here, the addition of kaolin significantly enhances the film formation. Acceleration is even stronger for the EVA than for the SB powder. Thus, the results suggest that the presence of kaolin generally promotes polymer film formation of latex polymers, but the effect can vary depending on the chemical composition of the latex.

The faster rate of film formation of the SB polymer compared to the EVA latex can be explained by the monodispersity and smaller particle size of the SB latex (Figs. 2 and 3). It is well established that smaller particles coalesce faster due to a higher interfacial tension between particles [1]. As a consequence, the driving force for particle–particle interpenetration is higher for small particles. Another reason is the presence of PVOH in all EVA samples which is added during the emulsion polymerization of EVA dispersions. As was mentioned before, PVOH acts as protective colloid and thus hinders film formation of latex particles.

Scheme 2. Schematic representation of time-dependent gradual film formation, with coexistence of different stages of latex particle coalescence.

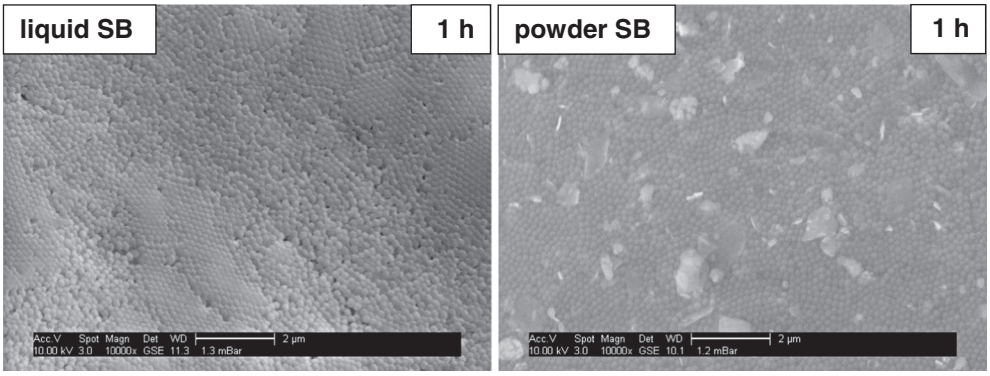

Fig. 5. ESEM micrographs of polymer particles present in aqueous dispersions of liquid and powder SB after 1 h storage at room temperature. Individual, non-coalesced particles are observed.

3.3.3. Film formation in cement pore solution

So far, the processes occurring in DI water have been presented. In actual application systems, however, film formation in cement pore solution is more relevant. To simulate this environment, latex film formation was studied in a synthetic cement pore solution which is loaded with 18.6 g/L of electrolytes, mainly SO_4^{2-}, K^+ and Ca^{2+} ions, and which possess a highly alkaline pH value of ~12.6 (Table 1). Fig. 10 shows the effect of SCPS on the film formation of the SB and EVA liquid and powder latexes, respectively. Obviously, also in SCPS the powder samples form a homogeneous film much faster than their mother liquors. For the liquid EVA or SB latexes, only a dense particle packing was observed after 2 h (SB) or 6 h (EVA) of storage whereas for the powders, coalescence had progressed much more and homogeneous films were visible at those times. These results clearly confirm occurrence of an accelerating effect of kaolin on film formation also in SCPS.

Generally, the ESEM micrographs of latex samples obtained in SCPS were less clear than those from DI water because in SCPS, surfaces were always covered with residual salts. For this reason and better clarity, most of the ESEM images of this study are presented from DI water, although all corresponding images in SCPS were captured as well.

3.3.4. Effect of kaolin on latex film formation

Our results clearly confirm an accelerating effect of kaolin on latex particle coalescence. A potential explanation for this effect is the affinity of latex particles to mineral substrates. For example, *Granier* and *Sartre* [4] revealed that the affinity of latices to mineral surfaces such as silica, mica or calcium carbonate depends on the chemical composition of the substrate. Using atomic force microscopy (AFM) they measured latex adhesion to several substrates and found that strong intermolecular interactions between latex particles and inorganic surfaces can lead to deformation of the latex particles and thus are promoting film formation.

These results were confirmed by an AFM study by *Kaufmann* et al. [5]. These authors showed that the interaction between mineral surfaces (mica, ceramic tiles) and EVA polymers correlates with the glass transition temperature of the latex and the chemistry of the stabilizing system.

Apparently, similar interactions which are owing to kaolin and enhance particle coalescence occur during the film formation of the SB and EVA samples studied here. Acid–base-interactions such as hydrogen bonding between surface hydroxyl groups of kaolin and functional groups of EVA and SB which occur during the drying process of the dispersions can lead to an arrangement of the latices in a dense particle packing. Owing to the high specific surface area of kaolin this effect propagates throughout the matrix and significantly accelerates film formation.

Such enhanced film formation resulting from kaolin can occur especially in application systems which contain a high polymer concentration (e.g. coatings, waterproofing membranes, sealing slurries) because there, individual latex–kaolin composite particles are more likely to get in

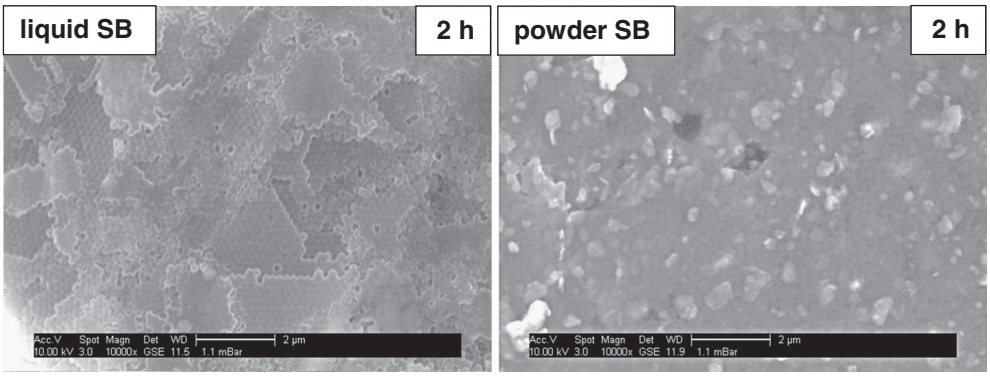

Fig. 6. ESEM micrographs of aqueous dispersions obtained from liquid and powder SB after 2 h storage at room temperature.

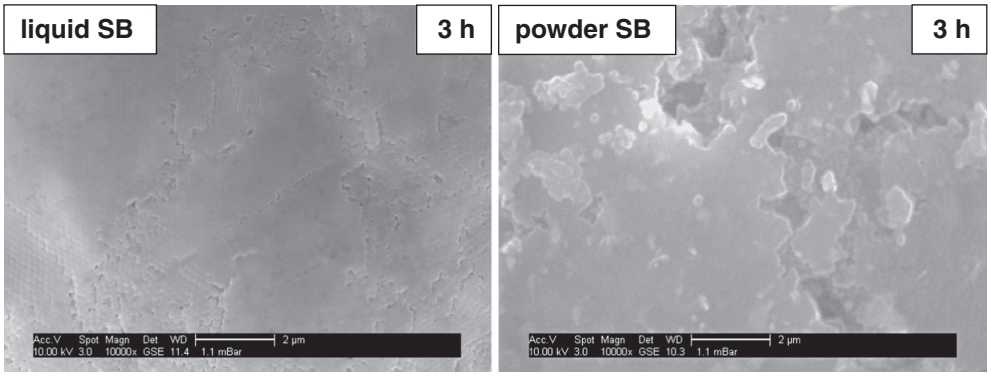

Fig. 7. ESEM micrographs of aqueous dispersions prepared from liquid and powder SB after 3 h storage at room temperature.

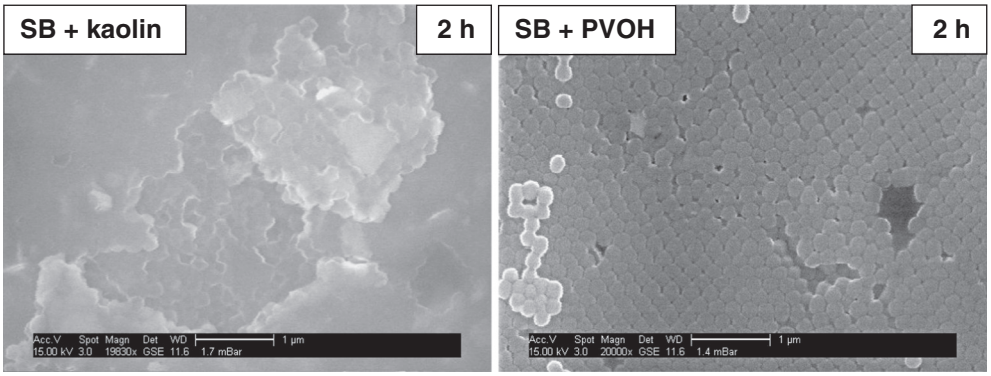

Fig. 8. ESEM micrographs of aqueous dispersions prepared from SB + kaolin and SB + PVOH powders after 2 h storage at room temperature.

contact with each other. While at much lower latex dosages, this effect may play a minor role because of the lower local concentration of the latex particles in the cementitious matrix.

Generally, the film forming ability of latex particles within the mineral matrix is essential for the performance of latex dispersions in application systems such as tile adhesives. The polymer films predominantly

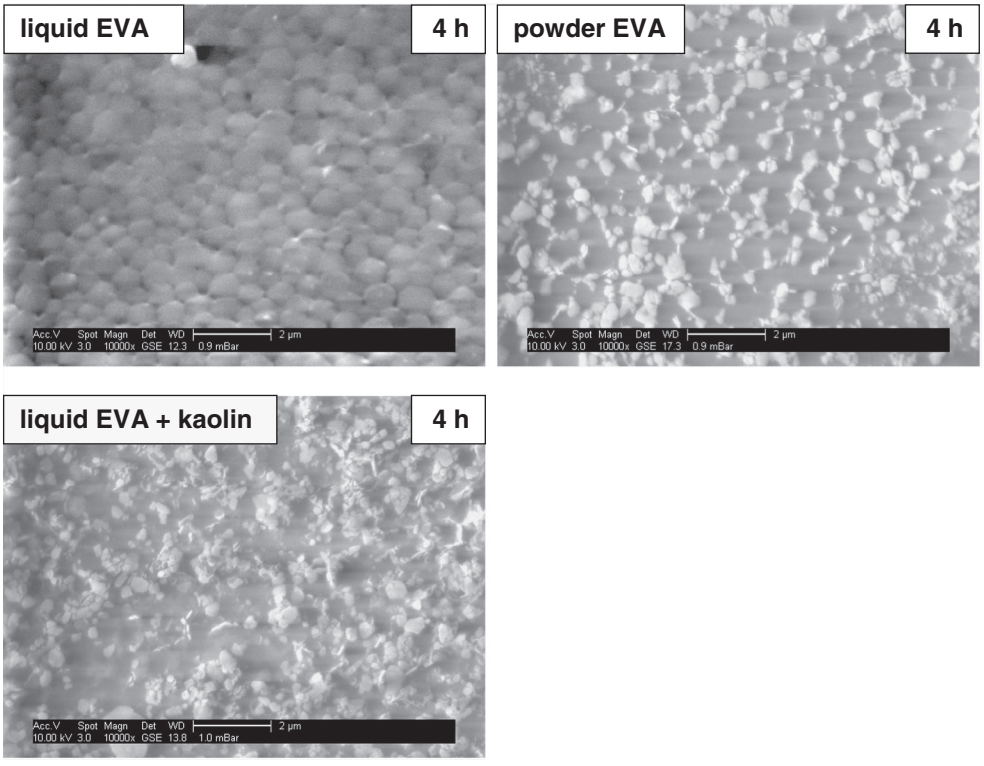

Fig. 9. ESEM micrographs of aqueous dispersions prepared from liquid and powder EVA and from liquid EVA latex blended with kaolin after 4 h storage at room temperature.

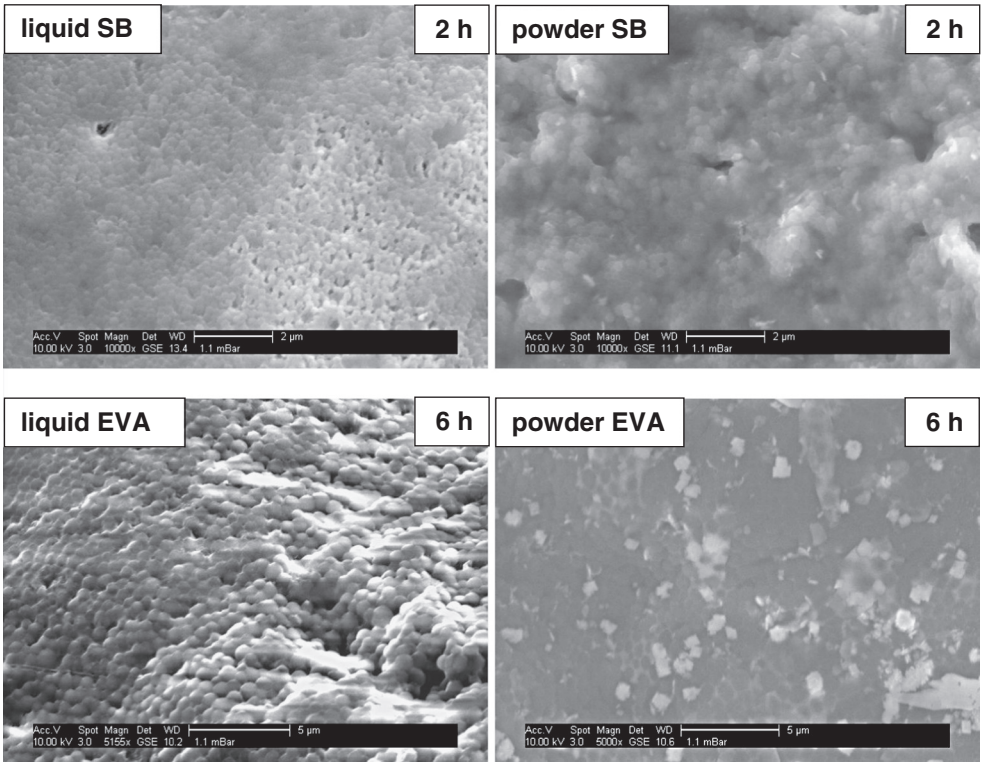

Fig. 10. ESEM micrographs of dispersions prepared from liquid and powder SB or EVA latex in synthetic cement pore solution after 2 h (SB) or 6 h (EVA) storage at room temperature.

form in capillary pores and connect cement hydrates, thus providing a higher bending strength for the hardened mortar.

3.4. EDX analysis of the polymer film

The ESEM images displayed for the SB and EVA powders after completion of the film forming process (Figs. 9 and 10) clearly show the presence of bright particles on the surfaces of their polymer films. The morphology of these particles suggests that they are kaolin particles. To confirm, EDX analysis of an EVA powder film was performed and its elemental composition was determined. Fig. 11 shows the result. The EDX analysis clearly identified elements from the EVA polymer (C and O) as well as from kaolin (O, Al, Si, Na). Similar results were obtained for an SB latex film. This observation suggests that at first kaolin is closely embedded into the PVOH coating present on the surface of the powder particles and is then disparaged from the polymer film.

4. Conclusion

Our results show that in powders made from ethylene–vinylacetate and styrene–butadiene latexes, film formation occurs much faster than in their liquid latex precursors. Kaolin which is added as anti-caking agent during spray drying acts as accelerator for polymer film formation.

The kinetics of polymer film formation for liquid EVA and SB latexes were investigated via gravimetric analysis of water evaporation and time-dependent ESEM imaging (particle coalescence). The main goal was a comparison of the film formation from liquid and powder latex to understand the potential impact of kaolin and polyvinylalcohol. It was found that the rate of water evaporation depends on the hydrophilic character of the latex polymer. Therefore, powders containing PVOH and kaolin which both contain hydrophilic hydroxyl groups exhibit slower water evaporation compared to their liquid latexes. ESEM analysis revealed that surprisingly polymer film formation occurs much faster from the

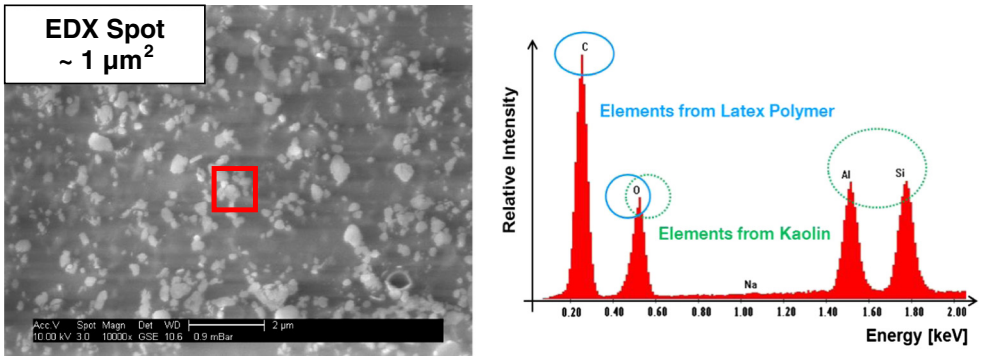

Fig. 11. Elemental composition (right) of a section from the surface of a polymer film obtained from EVA powder, measured by EDX analysis. The ESEM micrograph (left) shows the spot which was chosen for the elemental mapping.

powders than from the liquids. This effect was attributed to the presence of kaolin in the powders which much accelerates film formation. Obviously, the strong effect of kaolin overrides the effect of deceleration on film formation originating from PVOH.

In spite of all the experiments above, the mechanism behind the acceleration of film formation by kaolin could not be clarified completely. Apparently, a specific interaction between the latex particles and kaolin which enhances deformation of the latices and thus promotes film formation is responsible for this effect. Future studies should focus on this type of interaction which is highly relevant for the application of latex polymers in construction.

Acknowledgment

The authors would like to thank Dr. Hartmut Kühn and Dr. Jürgen Dombrowski (Dow Olefinverbund GmbH, Schkopau/Germany) for the preparation of the model latex powders.

References

[1] Y. Ohama, Handbook of Polymer-Modified Concrete and Mortars — Properties and Process Technology, Noyes Publications, New Jersey, 1995.
[2] Y. Ohama, Polymer-based admixtures, Cem. Concr. Compos. 20 (1998) 189–212.
[3] J.W. Kardon, Polymer-modified concrete: review, J. Mater. Civ. Eng. 9 (1997) 85–92.
[4] V. Granier, A. Sartre, Ordering and adhesion of latex particles on model inorganic surfaces, Langmuir 11 (1995) 2179–2186.
[5] J. Kaufmann, F. Winnefeld, R. Zurbriggen, Polymer dispersions and their interaction with mortar constituents and ceramic tile surfaces studied by zeta-potential measurements and atomic force microscopy, Cem. Concr. Compos. 34 (2012) 604–611.
[6] A.M. Betioli, P.J.P. Gleize, V.M. John, R.G. Pileggi, Effect of EVA on the fresh properties of cement paste, Cem. Concr. Compos. 34 (2012) 255–260.
[7] B.B. Konar, A. Das, P.K. Gupta, M. Saha, Physicochemical characteristics of styrene–butadiene latex-modified mortar composite vis-a-vis preferential interactions, J. Macromol. Sci. Part A — Pure Appl. Chem. 48 (2011) 757–765.
[8] A.M. Betioli, J. Hoppe, M.A. Cincotto, P.J.P. Gleize, R.G. Pileggi, Chemical interaction between EVA and Portland cement hydration at early-age, Constr. Build. Mater. 23 (2009) 3332–3336.
[9] J. Plank, M. Gretz, Study on the interaction between anionic and cationic latex particles and Portland cement, Colloid Surf. A — Physicochem. Eng. Asp. 330 (2008) 227–233.
[10] A. Jenni, R. Zurbriggen, L. Holzer, M. Herwegh, Changes in microstructures and physical properties of polymer-modified mortars during wet storage, Cem. Concr. Res. 36 (2006) 79–90.
[11] A. Jenni, M. Herwegh, R. Zurbriggen, T. Aberle, L. Holzer, Quantitative microstructure analysis of polymer-modified mortars, J. Microsc. — Oxf. 212 (2003) 186–196.
[12] O. Yilmaz, A hybrid polyacrylate/OMMT nanocomposite latex: synthesis, characterization and its application as a coating binder, Prog. Org. Coat. 77 (2014) 110–117.
[13] S. Chuayjuljit, C. Worawas, Nanocomposites of EVA/polystyrene nanoparticles/montmorillonite, J. Compos. Mater. 45 (2011) 631–638.
[14] M.J. Patel, V.R. Gundabala, A.F. Routh, Modeling film formation of polymer–clay nanocomposite particles, Langmuir 26 (2010) 3962–3971.
[15] Ş. Uğur, A. Alemdar, Ö. Pekcan, The effect of clay particles on film formation from polystyrene latex, Polym. Compos. 27 (2006) 299–308.
[16] M. Gretz, J. Plank, An ESEM investigation of latex film formation in cement pore solution, Cem. Concr. Res. 41 (2011) 184–190.
[17] T. Pavlitschek, M. Gretz, J. Plank, Effect of Ca^{2+} ions on the film formation of an anionic styrene/n-butylacrylate latex polymer in cement pore solution, 14th International Congress on Polymers in Concrete (ICPIC), Tongji University Shanghai, 2013.
[18] A. Jenni, L. Holzer, R. Zurbriggen, M. Herwegh, Influence of polymers on microstructure and adhesive strength of cementitious tile adhesive mortars, Cem. Concr. Res. 35 (2005) 35–50.
[19] S. Chandra, P. Flodin, Interactions of polymers and organic admixtures on portland cement hydration, Cem. Concr. Res. 17 (1987) 875–890.
[20] A.M. Koenig, T.G. Weerakkody, J.L. Keddie, D. Johannsmann, Heterogeneous drying of colloidal polymer films: dependence on added salt, Langmuir 24 (2008) 7580–7589.
[21] S. Erkselius, L. Wadsö, O. Karlsson, Drying rate variations of latex dispersions due to salt induced skin formation, J. Colloid Interface Sci. 317 (2007) 83–95.
[22] J.L. Keddie, Film formation of latex, Mater. Sci. Eng. R — Rep. 21 (1997) 101–170.
[23] Y. Chevalier, C. Pichot, C. Graillat, M. Joanicot, K. Wong, J. Maquet, P. Lindner, B. Cabane, Film formation with latex particles, Colloid Polym. Sci. 270 (1992) 806–821.
[24] J.L. Keddie, P. Meredith, R.A.L. Jones, A.M. Donald, Film formation of acrylic latices with varying concentrations of non-film-forming latex particles, Langmuir 12 (1996) 3793–3801.
[25] K. Dragnevski, A. Donald, P. Taylor, M. Murray, S. Davies, E. Bone, Latex film formation in the environmental scanning electron microscope, Macromol. Symp. 281 (2009) 119–125.
[26] K.I. Dragnevski, A.M. Donald, Applications of environmental scanning electron microscopy (ESEM) in the study of novel drying latex films, in: R.T. Baker, G. Mobus, P.D. Brown (Eds.), Emag: Electron Microscopy and Analysis Group Conference 2007, Iop Publishing Ltd, Bristol, 2008.
[27] K.I. Dragnevski, A.M. Donald, An environmental scanning electron microscopy examination of the film formation mechanism of novel acrylic latex, Colloid Surf. A — Physicochem. Eng. Asp. 317 (2008) 551–556.
[28] D.J. Stokes, Recent advances in electron imaging, image interpretation and applications: environmental scanning electron microscopy, Phil. Trans. Roy. Soc. London Series A: Math., Phys. Eng. Sci. 361 (2003) 2771–2787.
[29] A.M. Donald, C. He, C.P. Royall, M. Sferrazza, N.A. Stelmashenko, B.L. Thiel, Applications of environmental scanning electron microscopy to colloidal aggregation and film formation, Colloid Surf. A — Physicochem. Eng. Asp. 174 (2000) 37–53.
[30] W. Rechenberg, S. Sprung, Composition of the solution in the hydration of cement, Cem. Concr. Res. 13 (1983) 119–126.
[31] J. Plank, B. Sachsenhauser, Experimental determination of the effective anionic charge density of polycarboxylate superplasticizers in cement pore solution, Cem. Concr. Res. 39 (2009) 1–5.

Paper #3

On the role of colloidal crystal-like domains in the film forming process of a carboxylated styrene-butadiene latex copolymer

S. Baueregger, M. Perello, J. Plank

Progress in Organic Coatings

77 (2014), 685-690

Progress in Organic Coatings 77 (2014) 685–690

Contents lists available at ScienceDirect

Progress in Organic Coatings

journal homepage: www.elsevier.com/locate/porgcoat

On the role of colloidal crystal-like domains in the film forming process of a carboxylated styrene-butadiene latex copolymer

Stefan Baueregger[a], Margarita Perello[b], Johann Plank[a,*]

[a] Technische Universität München, Lichtenbergstr. 4, Garching 85747, Germany
[b] Dow Europe GmbH, Bachtobelstr. 3, Horgen 8810, Switzerland

ARTICLE INFO

Article history:
Received 5 July 2013
Received in revised form 6 December 2013
Accepted 10 December 2013
Available online 10 January 2014

Keywords:
ESEM
Latex polymer
Colloidal crystal
Particle packing
Film formation

ABSTRACT

Environmental scanning electron microscopy (ESEM) was employed to study the mechanism of film formation of a carboxylated styrene-butadiene latex copolymer with a glass transition temperature (T_g) of 6 °C. ESEM allows the investigation of wet samples in their native state which is required to study the drying process of latex dispersions. The film forming process was tracked by time-dependent ESEM monitoring of the latex particle morphology and by observing the different stages occurring during the drying process. The focus of our study was an analysis of the three-dimensional (3D) arrangement of the latex particles and a comparison of their appearance on the surface and in the center of the coalesced film. It was found that in the course of film formation, the latex particles arrange in domains which are similar to colloidal crystals. Such domains occur at the stage of dense particle packing. Particle coalescence appears to begin first in these domains before a continuous and homogeneous film is formed which then spreads across the entire substrate. The results suggest that for our carboxylated styrene-butadiene copolymer the current model known for the film forming mechanism which includes four main steps should be complemented by two additional ones, namely the arrangement of particles in crystal-like domains and the beginning of coalescence within these domains. This specific behavior only occurs for monodisperse latices.

1. Introduction

Latex polymer dispersions are well known as important ingredients in paints, coatings and adhesives which have a wide field of applications, especially in construction. Key property of latex polymers is their ability to form flexible and homogeneous polymer films after dehydration. Thus, latex polymers present organic binders which provide good adhesion and cohesion due to the formation of a three-dimensional organic polymer matrix [1,2].

The process occurring during the transition of an aqueous latex dispersion to a dry polymer film is known as polymer film formation and has been the subject of numerous papers. Based on the current state of the art, the film forming process can be divided into four main stages which are illustrated in Scheme 1. In stage I (the native state of a latex dispersion), polymer particles are randomly dispersed in water. When water is removed due to evaporation, dehydration or consumption by a chemical reaction, a dense particle packing (stage II) is achieved whereby the particles contact each other and the interstitial spaces between them are still filled with water. Upon wet or dry sintering or capillary deformation, the latex particles start to deform in order to minimize their surface free energy. There, the interfacial tension between polymer and solvent (wet sintering), polymer and air (dry sintering), or solvent and air (capillary deformation) is reduced whereby an ordered array of hexagonally deformed particles (stage III) results. In the final step, particle coalescence occurs and a continuous and homogeneous polymer film is achieved. The driving force behind the interdiffusion of the polymer chains (coalescence) is the minimization of the interfacial tension between the latex particles and the increasing entropy of the polymer chains. To achieve particle coalescence, a temperature above the T_g is required where the polymer chains start to become flexible and then can intertwine [3–10].

Some authors discuss the existence of an intermediate stage II* between stages II and III which is characterized by a randomly packed array of deformed particles surrounded by interspaces filled with water [4]. Furthermore, following this particle deformation some latex polymers possessing a hydrophilic surface were suggested to form polyhedral cells separated by hydrophilic layers (transition stage III*) [3].

In 2009, *Dragnevski* et al. investigated the film forming process of acrylic latex particles stabilized with polysaccharide derivates [11]. Based on investigation of the film surface they found that instead of deformed particles or coalescence, well-ordered arrays occur whereby their microstructure consists of individual particles

* Corresponding author. Tel.: +49 89 289 13151; fax: +49 89 289 13152.
E-mail address: sekretariat@bauchemie.ch.tum.de (J. Plank).

0300-9440/$ – see front matter © 2013 Elsevier B.V. All rights reserved.
http://dx.doi.org/10.1016/j.porgcoat.2013.12.006

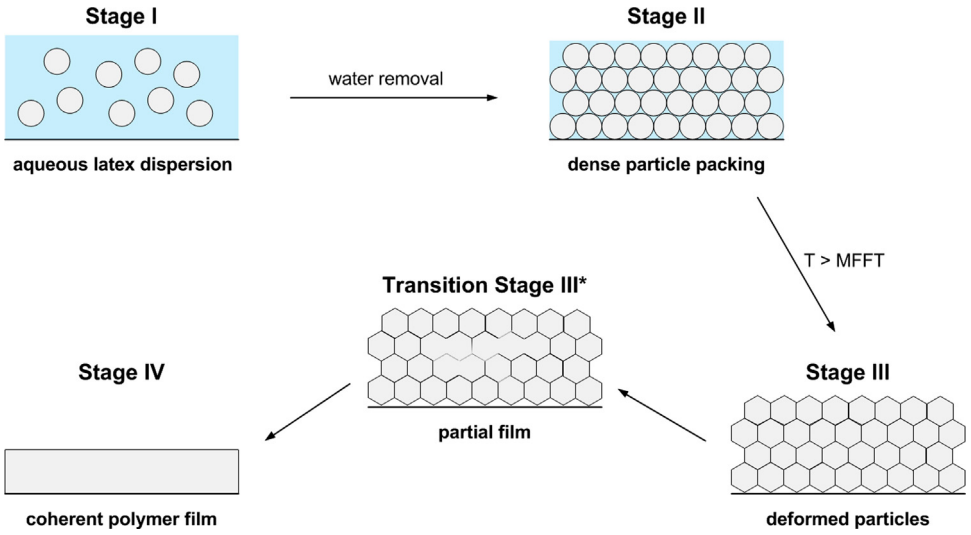

Scheme 1. Schematic illustration of the four main stages occurring during polymer film formation from an aqueous latex dispersion.

and clusters. Recently, *Dragnevski* et al. also studied the drying behavior of a non-film forming poly(methyl methacrylate) based latex system [12]. There, upon drying they observed not only the common hexagonal or square close particle packing, but also a random arrangement of the latex particles in a crystal-like structure. Using cryo-SEM, *Scriven* et al. described the arrangement of latex in layers of ordered, close-packed particles [13,14].

These results indicate that the process of film formation is not yet entirely understood and that under specific conditions, the current model of the film forming mechanism is not conclusive. Especially the potential effect of crystal-like particle assemblies on the coalescence behavior of a film-forming latex would be highly interesting.

ESEM technique offers the possibility of investigating the latex polymer film forming process because it allows high quality imaging of samples under water vapor. Compared to conventional scanning electron microscopy (SEM) which requires high vacuum for imaging, ESEM is suitable to analyze wet and non-conductive samples in their native state under a low vacuum. The ability to analyze wet specimens is required in this case as film formation starts from an aqueous dispersion. With ESEM technique, observation of samples under water vapor is possible due to a multiple aperture graduated vacuum system. During imaging, the atmosphere in the specimen chamber is decreased from ambient conditions to a water vapor pressure of around 7.5 mbar, while gun and column stay under high vacuum. In combination with cooling of the sample holder to 3 °C, a saturated water atmosphere is maintained on the surface of the sample. This way, the specimen is prevented from dehydration and it remains in its original wet state. To establish a saturated water vapor atmosphere, a specific pump-down sequence is necessary. The pump-down procedure consists of several evacuation and water vapor addition steps until the final water atmosphere in the specimen chamber is achieved, thus ensuring that water is retained in the sample [15–21].

In our study, the film forming mechanism of a carboxylated styrene-butadiene (c-SB) polymer latex was investigated by means of ESEM imaging. In order to study the different stages occurring during the dehydration of the latex dispersion, the aqueous c-SB dispersion was deposited on an aluminum container (sample holder) and stored under ambient conditions. Images of the samples were captured at different points of time to monitor the time-dependent progress of film formation and to evaluate the different stages occurring during the drying process. Focus of our investigation was an analysis of the surface and the core of the latex sample. From this it was sought to clarify whether the particle morphology visible on the surface of the latex sample is also representative for the core material. Additionally, it was attempted to identify the various microstructural arrangements of the latex particles occurring during film formation.

2. Experimental

The aqueous carboxylated styrene-butadiene latex possessing a solid content of 45 wt.% and a pH of 9.8, and the corresponding c-SB re-dispersible powder were provided by Dow Olefinverbund GmbH, Schkopau/Germany. The re-dispersible powder (RDP) was produced by spray drying of the liquid latex dispersion under addition of kaolin as anti-caking agent. All materials were utilized without further purification. Ultrapure water (resistivity > 18 MΩ cm) was used for all experiments.

Particle size distribution of the latex polymer was determined by dynamic light scattering (DLS) with a Zetasizer Nano ZS (Malvern Instruments, Workester-shire/UK). To assess their electric surface charge, electrophoretic mobility of the colloidal latex particles dispersed in water (polymer content: 0.1 wt.%) was measured on the same instrument. Electrophoretic mobility was converted into a value for zeta potential by using the *Smoluchowski* relation. Glass transition temperature (T_g) was measured on a differential scanning calorimeter (DSC) Maia F3 from Netzsch, Selb/Germany. Minimum film forming temperature (MFFT) was determined on an MFFT Bar Thermostair II instrument from Coesfeld Materialtest, Dortmund/Germany.

For the analysis of the polymer film forming process, latex dispersions with a latex polymer content of 5 wt.% were prepared by addition of SB latex or powder to deionized water. Afterwards, the samples were sonicated for 3 min in order to redisperse the latex particles completely. 40 μL of the sonicated dispersion was deposited on a concave Al disk supplied by FEI, Eindhoven/Netherlands as sample container for the ESEM instrument. The samples were stored outside of the ESEM instrument at room temperature to simulate application conditions. For the microstructural analysis and investigation of the latex film forming process, after different drying periods individual samples were transferred into the XL-30 FEG (FEI, Eindhoven/Netherlands) ESEM instrument equipped with a *Peltier* cooling stage and a gaseous secondary electron detector. The Al disks were placed on the cooling stage of the microscope chamber possessing a temperature of 3 °C. Cooling of the sample ensures a saturated water vapor atmosphere

Table 1
Pump-down sequence for ESEM imaging of the latex polymer samples.

Step	Water vapor pressure, p [mbar]
1	Atm. → 8.5
2	8.5 → 12.5
3	12.5 → 8.5
4	8.5 → 7.5

above the surface of the sample while at the same time film formation in the ESEM chamber is prevented as the sample temperature is maintained below MFFT. Generally, ESEM monitoring was performed following a test protocol established by *Gretz* et al. [20]. A gentle pump-down sequence (Table 1) was performed to prevent water evaporation or dehydration of the sample while reducing the pressure in the specimen chamber. During this process which takes about 3 min, air is progressively replaced by water vapor. The decrease of water vapor to a pressure of 7.5 mbar in combination with a cooling of the sample to 3 °C allows to establish a saturated water atmosphere on the sample surface (dew point of water at 3 °C: 7.5 mbar). Imaging was carried out at accelerating voltages of 10.0–25.0 kV, a spot size of 3 and at working distances of 8–12 mm.

3. Results and discussion

3.1. Properties of the latex

The c-SB latex polymer was obtained via emulsion polymerization of the monomers styrene, butadiene and itaconic acid. The latter was incorporated into the polymer structure as internal stabilizer as it provides an anionic charge on the particle surface. Colloidal size and electrokinetic properties much determine the behavior of colloidal particle suspensions such as latex dispersions. Therefore, these properties were analyzed before the film formation was studied.

First, dynamic light scattering (DLS) was conducted to analyze the particle size distribution of the aqueous c-SB latex. The results confirmed an almost monodisperse size distribution with an average diameter of ~220 nm (Fig. 1). The surface charge was determined via zeta potential measurement. According to this method, the c-SB latex particles possess a zeta potential of −30 mV. This clearly shows their negative charge in aqueous dispersion which is owed to the presence of carboxylate groups on the particle surface stemming from itaconic acid. Due to the hydrophilicity of the carboxylate groups, the interfacial tension between the polymer particles and the solvent water is minimized during

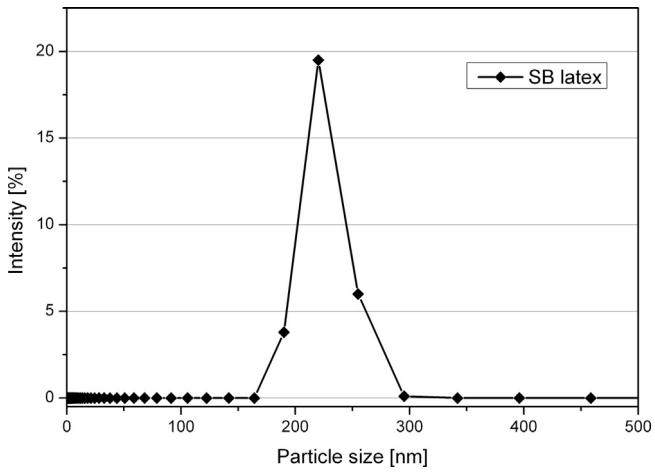

Fig. 1. Particle size distribution (intensity-based) of the carboxylated styrene-butadiene latex dispersion, measured by dynamic light scattering.

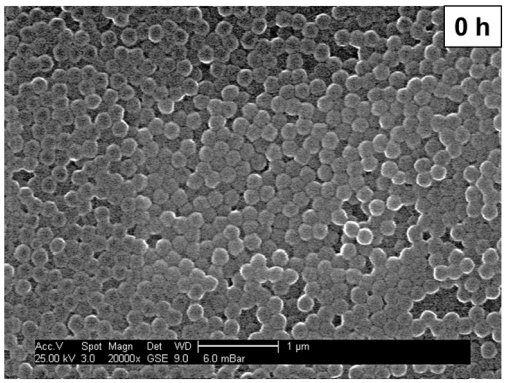

Fig. 2. ESEM micrograph of the liquid carboxylated styrene-butadiene (c-SB) latex particles dispersed in DI water (solid content 5 wt.%).

the polymerization process. Generally, the two key parameters for the film formation of latex polymers are the glass transition temperature (T_g) and the minimum film forming temperature (MFFT). The latter is measured on the so-called *Kofler* bench while T_g is captured by differential scanning calorimetry (DSC). T_g represents the temperature where the polymer chains become flexible enough to achieve interpenetration or interdiffusion at the stage of particle coalescence. For the c-SB polymer studied here, T_g and MFFT were found to be similar at a temperature of 5–6 °C. Thus, for this latex film formation at room temperature is possible which allows to study its behavior under actual application conditions.

3.2. Polymer film formation

To study the mechanism of film formation, latex dispersions with a polymer content of 5 wt.% prepared from liquid latex or RDP were placed in the Al containers and stored at room temperature, thus simulating application conditions. After certain time intervals, samples were transferred into the ESEM instrument, rapidly cooled to 3 °C and imaging was performed to observe the different stages occurring during the drying process. For 3D microstructural analysis, the dried polymer films were sliced at a 60° angle to the film with a sharp scalpel and the cut surface was looked at. Here, the thickness of the sliced polymer films was ~10 μm. The progress in film formation was monitored by observing the sample surface and also representative sections present in the core of the sample.

Figs. 2–6 show the results of time-dependent ESEM monitoring performed with the diluted liquid c-SB latex dispersion (concentration: 5 wt.%). Immediately after preparation, only individually dispersed particles are visible (Fig. 2). The ESEM micrograph confirms the particle size distribution measured before by DLS. A nearly monodisperse system with an average particle diameter of around 220 nm is observed. To obtain these images, a slight decrease of the water vapor pressure from 7.5 to 6.0 mbar in the ESEM chamber is necessary. As a result, water is removed partially from the sample surface, whereby some particles already attain contact with each other, but no packing, deformation or coalescence had occurred yet. This partial removal of water is necessary to break up the water film existing on the specimen surface and to make the particles visible under the electron beam.

1 h after deposition of the dispersion on the Al container and storage at room temperature, visual inspection still showed a rather wet sample. Under the ESEM instrument, distinct and randomly distributed particles still can be observed, as is shown in Fig. 3a. They correspond to the transition step between stages I and II of the film forming process as presented in Scheme 1. Interestingly, some latex particles have assembled in domains with a certain array. Owed to evaporation of the main amount of solvent, the

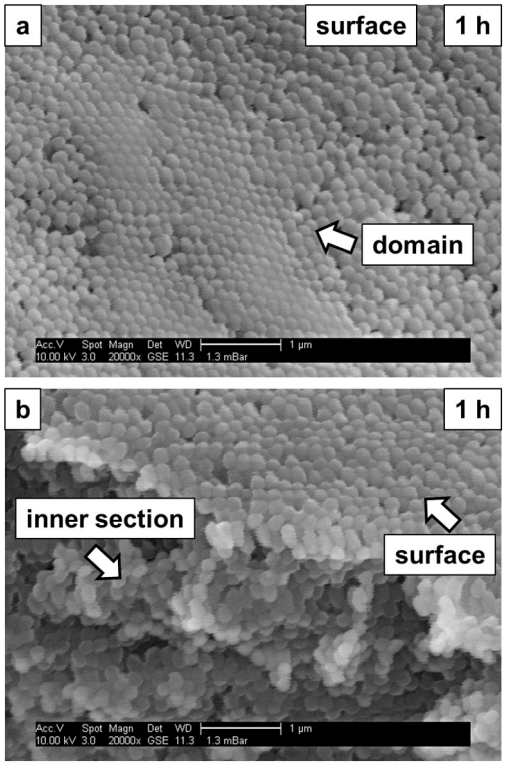

Fig. 3. ESEM micrographs of the carboxylated styrene-butadiene latex dispersion (solid content 5 wt.%) stored for 1 h at room temperature before imaging was performed.

sample was viscous enough to allow vertical slicing and analysis of the particle assembly array. The inner sections revealed a similar microstructure, compared to that formed on the sample surface (Fig. 3b).

After 2 h at room temperature, the latex sample visually appears as a transparent and completely dry film. However, the ESEM micrographs (Fig. 4a–c) only show a dense particle packing or deformed particles, while only few sections of the surface have already formed a homogeneous film. This clearly evidences that an optically transparent film not necessarily constitutes a homogeneous film at the microscopic scale.

Furthermore, within the array of hexagonally deformed particles exhibiting a honeycomb structure, defects can be observed (Fig. 4a). They are surrounded by bright haloes and result from separation of emulsifier and electrolytes at the surface of the latex. Generally, the packing of the c-SB latex observed here is very dense due to the nearly monodisperse particle size distribution.

Interestingly, some particles were found to have arranged in domains where particles are well-ordered, similar to that in colloidal crystals (Fig. 4b). Within these domains, particle interpenetration seems to be more advanced and coalescence of the particles is likely to first begin in these domains whereby layers of polymer films are formed (Fig. 4c).

This observation was confirmed by further analysis of the 3D microstructure of the sample (Fig. 5a and b). There, regular arrangements of particles in domains distributed across the entire polymer matrix can be seen. Comparable microstructures were found on the surface and in the inner part of the polymer matrix. The domains formed by the latex particles clearly exhibit the arrays characteristic for colloidal crystals.

Under continued dehydration of the dispersion, increased particle coalescence occurs until a coherent and homogeneous film is formed (Fig. 6a and b). Apparently, the particle arrangement in colloidal crystal-like domains affects the progress of film formation

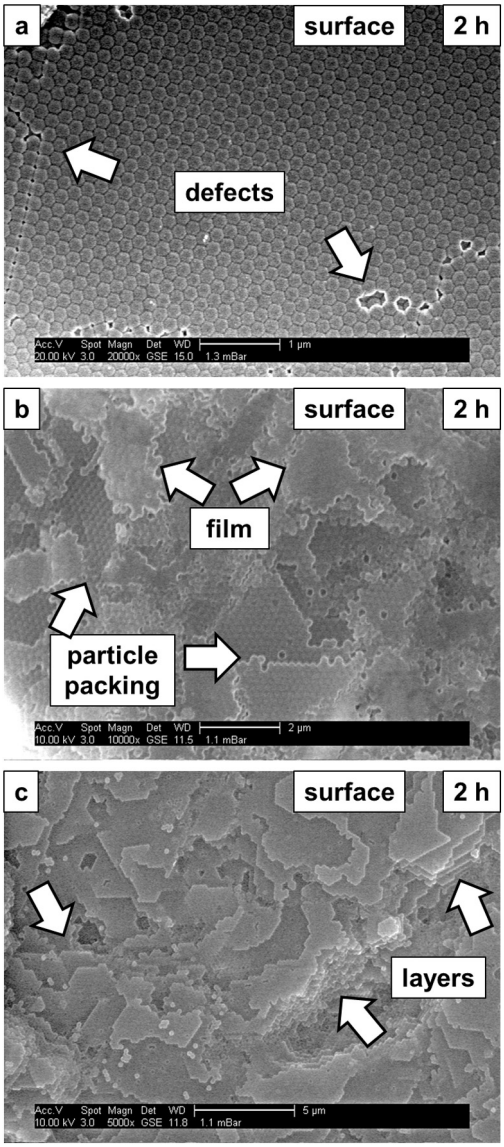

Fig. 4. ESEM micrographs of the carboxylated styrene-butadiene latex dispersion (solid content 5 wt.%) stored for 2 h at room temperature before imaging of the surface was performed.

(particle coalescence). Particle interdiffusion likely first begins in these domains and spreads from there until a homogeneous film is formed across the entire matrix. This film which is shown in Fig. 6b presents the final stage and results from interdiffusion and coalescence of the domains.

The occurrence of domains of crystal-like arrays of latex particles was also confirmed for the powder c-SB latex. Fig. 7a shows the inner section of a sample (c = 5 wt.%) which was stored for 1.5 h at room temperature and then analyzed. Again, the sample exhibits domains in which latex particles have assembled in a crystal-like array, similar to those displayed in Fig. 5. After 2 h of storage, an almost homogeneous polymer film can be observed, with some intermittent solid inorganic particles originating from the spray drying process (Fig. 7b).

The results from above suggest that for our c-SB latex, the current model for the film forming process as shown in Scheme 1 needs to be complemented by two more intermediate steps: first, the arrangement of particles in domains resulting in a colloidal crystal-like structure, similar to that which have been reported for other latexes before [12,13], and second, the observation that particle

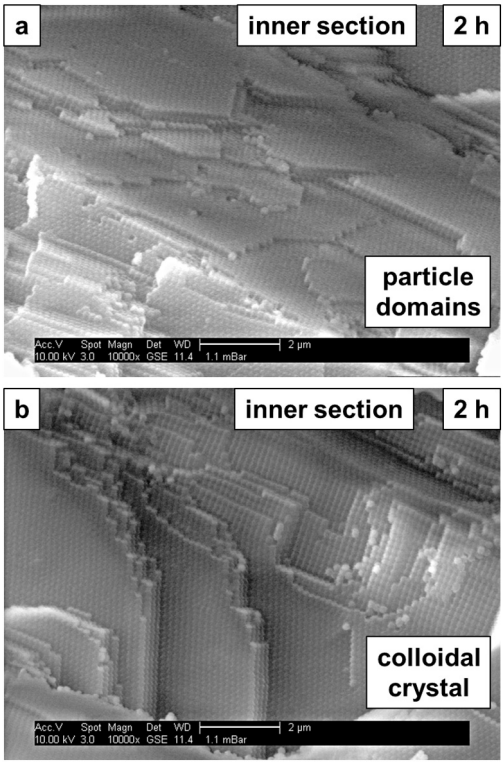

Fig. 5. ESEM micrographs of the carboxylated styrene-butadiene latex dispersion (solid content 5 wt.%) stored for 2 h at room temperature before imaging of the inner section was performed.

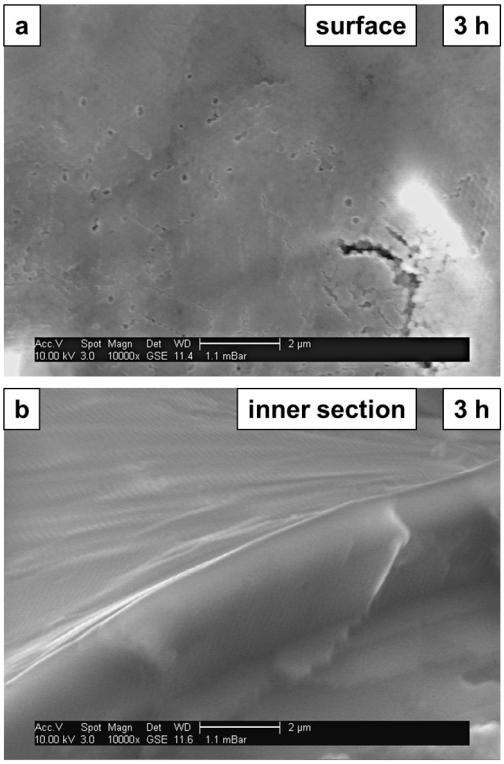

Fig. 6. ESEM micrographs of the carboxylated styrene-butadiene latex dispersion (solid content 5 wt.%) stored for 3 h at room temperature before imaging of the sample surface (a) and the inner section (b) was performed.

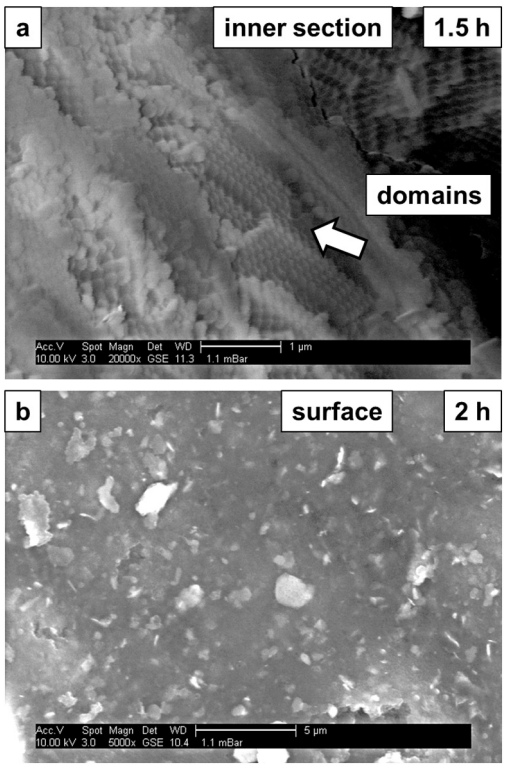

Fig. 7. ESEM micrographs of a carboxylated styrene-butadiene powder analyzed after (a) 1.5 h and (b) 2 h of storage at room temperature.

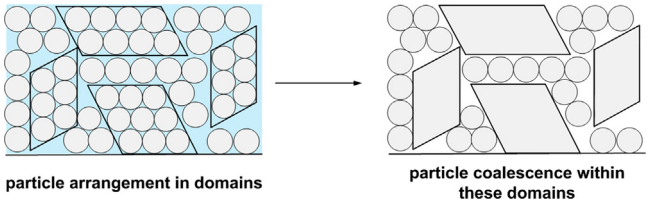

Scheme 2. Schematic illustration of additional steps occurring during the dehydration of a carboxylated styrene-butadiene latex dispersion. At the stage of dense particle packing, the polymer particles arrange in domains with arrays characteristic for colloidal crystals; this is followed by particle coalescence within these domains.

coalescence first begins in these domains and then spreads across the entire assembled latex particles. These two steps are illustrated in Scheme 2.

The effect that particle coalescence first begins in these domains is ascribed to the high packing density there. Within these domains, particles arrange in a hexagonal (hcp) or cubic close packing (ccp). Due to the high packing density in the hcp or ccp, interaction of the latex particles is more pronounced there, leading to enhanced particle interpenetration compared to the surrounding particles which are packed randomly.

4. Conclusion

The film forming mechanism of a carboxylated styrene-butadiene latex was studied via time-dependent monitoring of the dehydration process of the latex dispersion using environmental scanning electron microscopic (ESEM) imaging. The results suggest that for the anionic SB latex, the film forming process involves more than the four known stages which include particles dispersed in the solvent (stage I), dense particle packing while interstitial spaces still are filled with water (stage II), particle deformation (stage III) and coalescence into a coherent polymer film (stage IV). For the c-SB

latex sample it was found that at the stage of dense particle packing, a colloidal crystal-like assembly of polymer particles in domains occurs. Particle coalescence and film formation appears to begin first in these domains and to spread then until a homogeneous and coherent polymer film is formed. Furthermore, a 3D analysis of the polymer microstructure during film formation revealed that the processes observed on the surface are also representative for those occurring inside the latex sample. Our results suggest that the process of film formation from latex polymers can be more complicated than described by the current four stage model. The formation of colloidal crystals occurs only for monodisperse latices. Complementary experiments revealed that polydisperse latices do not form such colloidal crystals.

Another finding from the study was that for the powder c-SB latex, film formation occurs faster than for the liquid latex (2 h vs. 3 h) which is surprising. The reason behind this effect remained unclear and will be the subject of another study.

References

[1] Y. Ohama, Polymer-based admixtures, Cem. Concr. Compos. 20 (1998) 189–212.
[2] J.W. Kardon, Polymer-modified concrete: review, J. Mater. Civ. Eng. 9 (1997) 85–92.
[3] Y. Chevalier, C. Pichot, C. Graillat, M. Joanicot, K. Wong, J. Maquet, P. Lindner, B. Cabane, Film formation with latex particles, Colloid Polym. Sci. 270 (1992) 806–821.
[4] J.L. Keddie, P. Meredith, R.A.L. Jones, A.M. Donald, Kinetics of film formation in acrylic latices studied with multiple-angle-of-incidence ellipsometry and environmental SEM, Macromolecules 28 (1995) 2673–2682.
[5] J.L. Keddie, P. Meredith, R.A.L. Jones, A.M. Donald, Rate-limiting steps in film formation of acrylic latices as elucidated with ellipsometry and environmental scanning electron microscopy, in: T. Provder, M.A. Winnik, M.W. Urban (Eds.), Film Formation in Waterborne Coatings, Washington, J. Am. Chem. Soc., 1996, pp. 332–348.
[6] J.L. Keddie, P. Meredith, R.A.L. Jones, A.M. Donald, Film Formation of Latices, Springer, Dordrecht, 1998.
[7] P.A. Steward, J. Hearn, M.C. Wilkinson, An overview of polymer latex film formation and properties, Adv. Colloid Interface Sci. 86 (2000) 195–267.
[8] M. Visschers, J. Laven, R. van der Linde, Film formation from latex dispersions, J. Coat. Technol. Res. 73 (2001) 49–55.
[9] D. Distler, G. Kanig, Feinstruktur von Polymeren aus wäßriger Dispersion, Colloid Polym. Sci. 256 (1978) 1052–1060.
[10] W.A. Henson, D.A. Taber, E.B. Bradford, Mechanism of film formation of latex paint, Ind. Eng. Chem. 45 (1953) 735–739.
[11] K. Dragnevski, A. Donald, P. Taylor, M. Murray, S. Davies, E. Bone, Latex film formation in the environmental scanning electron microscope, Macromol. Symp. 281 (2009) 119–125.
[12] O. Islam, K.I. Dragnevski, C.R. Siviour, On some aspects of latex drying – ESEM observations, Prog. Org. Coat. 75 (2012) 444–448.
[13] E. Sutano, Y. Ma, H.T. Davis, L.E. Scriven, Cryogenic scanning electron microscopy of early stages of film formation in drying latex coatings, ACS Symp. Ser. 790 (2001) 174–192.
[14] Y. Ma, H.T. Davis, L.E. Scriven, Microstructure development in drying latex coatings, Prog. Org. Coat. 52 (2005) 46–62.
[15] K.I. Dragnevski, A.F. Routh, M.W. Murray, A.M. Donald, Cracking of drying latex films: an ESEM experiment, Langmuir 26 (2010) 7747–7751.
[16] K.I. Dragnevski, A.M. Donald, S.M. Clarke, A. Maltby, Novel applications of ESEM and EDX for the study of molecularly thin amide monolayers on polymer films, Colloid Surf. A – Physicochem. Eng. Asp. 337 (2009) 47–51.
[17] K.I. Dragnevski, A.M. Donald, An environmental scanning electron microscopy examination of the film formation mechanism of novel acrylic latex, Colloid Surf. A – Physicochem. Eng. Asp. 317 (2008) 551–556.
[18] K.I. Dragnevski, A.M. Donald, Applications of environmental scanning electron microscopy (ESEM), in the study of novel drying latex films, in: R.T. Baker, G. Mobus, P.D. Brown (Eds.), Emag: Electron Microscopy and Analysis Group Conference 2007, IOP Publishing Ltd., Bristol, 2008.
[19] E. Gonzalez, C. Tollan, A. Chuyilin, M.J. Barandiaran, M. Paulis, Determination of the coalescence temperature of latexes by environmental scanning electron microscopy, Appl. Mater. Interfaces 4 (2012) 4276–4282.
[20] M. Gretz, J. Plank, An ESEM investigation of latex film formation in cement pore solution, Cem. Concr. Res. 41 (2011) 184–190.
[21] D.J. Stokes, Recent advances in electron imaging, image interpretation and applications: environmental scanning electron microscopy, Philos. Trans. R. Soc. Lond. Ser. A: Math. Phys. Eng. Sci. 361 (2003) 2771–2787.

Paper #4

Influence of Carboxylated Styrene-Butadiene Latex Copolymer on Portland Cement Hydration

S. Baueregger, M. Perello, J. Plank

Cement and Concrete Composites

(submitted on September 3, 2014, under review)

Influence of Carboxylated Styrene-Butadiene Latex Copolymer on Portland Cement Hydration

Stefan Baueregger [a], Margarita Perello [b], Johann Plank [a1]

[a] Technische Universität München, Lichtenbergstr. 4, 85747 Garching / Germany

[b] Dow Europe GmbH, Bachtobelstr. 3, 8810 Horgen / Switzerland

[1] Tel.: +49 89 289 13151
Fax: +49 89 289 13152.
E-mail: sekretariat@bauchemie.ch.tum.de

KEYWORDS

cement hydration

styrene-butadiene latex

adsorption

zeta potential

calorimetry

ABSTRACT

The influence of carboxylated styrene-butadiene (SB) latex on the hydration of ordinary Portland cement was investigated by means of isothermal heat flow calorimetry, in-situ X-ray diffraction, electroacoustic zeta potential measurement and ion analysis of the cement pore solution. In particular, to assess the influence of the spraying aids polyvinylalcohol (colloidal stabilizer) and kaolin (anti-caking agent) on cement hydration, the impact of the liquid SB latex was compared with that of its re-dispersible powder. It was found that anionic SB generally retards both the aluminate and silicate reactions. This effect can be ascribed to adsorption of SB particles onto positively charged clinker or hydrate phases and the chelation of calcium ions present in cement pore solution by the carboxylate groups of the SB sample. SB powder exhibits a lower anionic charge density due to PVOH coating, thus interacts less strongly with cement and retards slightly less, compared to liquid SB latex.

1. Introduction

The hydration of ordinary Portland cement (OPC) represents a complex process which derives from the reactions of the two main cement constituents, the silicate and the aluminate phases. Owed to its complexity, it still is the subject of scientific papers which contribute to an increased understanding of this process [1]. The silicate and especially the aluminate reaction may significantly be impacted by the presence of admixtures such as superplasticizers, retarders, accelerators etc., as was reported in numerous previous studies [2, 3].

Latex polymers represent key components in many drymix mortar formulations, e.g. in repair mortars, tile adhesives and grouts, in waterproofing membranes or self-leveling underlayments (SLUs) [4]. They provide cohesion of the fresh mortar and good adhesion on various substrates. Additionally, latex polymers increase the flexural strength of hardened mortar due to the formation of elastic polymer films within the inorganic mortar matrix [5].

For drymix mortar applications, the latex mother liquors are transformed into powders. There, the liquid latex is spray dried under addition of spraying aids (a colloidal stabilizer and an anti-caking agent) which prevent coalescence of the latex particles during the drying process and provide a non-compacting powder [6]. Typically, partially hydrolyzed, water-soluble polyvinylalcohol is used as protective colloid while inorganic compounds such as clays (e.g. kaolin), diatomaceous earth, microsized silica or calcium carbonate serve as anti-caking agent. In a previous study we have reported about the effects of the spraying aids PVOH and kaolin on the

colloidal properties of carboxylated SB and ethylene-vinylacetate latexes [7]. They increase the colloidal stability of the re-dispersed latex powder and promote film formation of the latex powder. In the present study, the influence of latex mother liquor and of the re-dispersible latex powder on cement hydration was investigated.

In the literature, many articles on the interaction between polymers and mineral phases in general can be found. For example, *Jansen et al.* [8, 9] examined the impact of polyvinylalcohol and of poly diallyl dimethyl ammonium chloride (PDADMAC) on the formation of cement hydrates using quantitative X-ray diffraction. *Plank* and *Gretz* [10] confirmed the adsorption of anionic and cationic latex particles onto cement via zeta potential and adsorption measurements. *Su et al.* [11] reported that styrene-acrylate or vinylpropionate-vinylidenechloride latex dispersions retard the setting and hydration of cement. *Larbi* and *Bijen* [12] investigated the influence of the same polymers on the composition of cement pore solution and showed that Ca^{2+} ions are chelated by the polymers. *Betioli et al.* [13] and *Silva et al.* [14] examined the interaction between ethylene-vinylacetate copolymers and Portland cement via thermogravimetric analysis. They presented that upon EVA hydrolysis in alkaline cement pore solution, calcium acetate is formed and as a result the calcium hydroxide content in the fresh and hardened cement paste decreases. *R. Wang et al.* [15-19] investigated the effect of liquid styrene-butadiene rubber (SBR) latex and powder on ettringite and portlandite formation via X-ray diffraction, and of C-S-H formation via environmental scanning electron microscopy. They found that both liquid SBR latex and powder promote ettringite formation, whereas C-S-H and portlandite crystallization are reduced. However, in these works no information on the

specific composition (e.g. charge character or spraying aids) of the latex polymers was given.

Despite of these many literatures, no work exists which reflects the different colloidal properties of liquid latexes and their re-dispersible powders, the consequences for their presumably different interaction with cement and their overall influence on cement hydration. However, the colloidal properties of latex particles such as surface charge or particle size are most critical for their interaction with mineral phases or ions in cement pore solution. The chemical composition of the polymer appears to be less relevant here, because the electrokinetic surface properties represent the main driving force behind such physical interactions.

Therefore, in this work we focused on the surface properties of carboxylated styrene-butadiene latex and powder and the impact of the spraying aids polyvinylalcohol and kaolin on the hydration of OPC. Their influence was tracked via isothermal heat flow calorimetry. Time-dependent evolution of the main hydration phases ettringite and portlandite was monitored via in-situ X-ray diffraction. Complementary, the SO_4^{2-} and Ca^{2+} ion concentrations present in cement pore solution were quantified via ion chromatography (SO_4^{2-}) or atomic absorption spectroscopy (Ca^{2+}). Electroacoustic zeta potential measurements of cement slurries were performed in order to investigate adsorption of the latex particles on cement. From these experiments it was hoped to obtain a thorough understanding of the colloidal properties of liquid SB latex and powder, on their interaction with specific cement hydrates and a mechanistic view of the processes involved in these interactions.

2. Materials and Methods

2.1 Materials

The cement used in this study was an ordinary Portland cement CEM I 52.5 N from HeidelbergCement, Geseke plant, Germany which is commonly used as base cement in drymix mortar formulations. Its phase composition as determined by quantitative X-ray diffraction (Bruker AXS D8 Advance, Karlsruhe, Germany) using *Rietveld* refinement (software Topas 4.0) is shown in **Table 1**.

Average particle size (d_{50} value) of the cement sample measured via laser granulometry (Cilas 1064, Cilas Company, Marseille, France) was found at 11.8 µm. Specific density of the cement was 3.2 kg/L as obtained by Helium pycnometry (Ultrapycnometer 1000, Quantachrome Instruments, Boynton Beach, USA).

Table 1 Phase composition of the CEM I 52.5 N sample, as was determined via Q-XRD using *Rietveld* refinement.

Phase	**Content [wt.%]**
C_3S	57.91
C_2S	23.47
C_3A, cubic	4.38
C_3A, orthorhombic	3.58
C_4AF, orthorhombic	2.49
CaO (free lime)	0.28
MgO (periklas)	0.14
$CaSO_4$	2.08

$CaSO_4 \cdot 0.5\ H_2O$	0.38
$CaSO_4 \cdot 2\ H_2O$	0.66
Calcite	3.33
Quartz	0.82
Arcanite	0.48

Liquid (solid content 45 wt.%) and powder SB latex samples were provided by Dow Olefinverbund GmbH, Schkopau, Germany. The SB re-dispersible powder was produced by spray drying of an SB mother liquor under addition of polyvinylalcohol (~ 10 wt.%) as colloidal stabilizer and kaolin (~ 12 wt.%) as anti-caking agent. Polyvinylalcohol (Mowiol 4 – 88) was purchased from Kuraray Europe, Frankfurt/Germany and kaolin (KAMIN HG 90) was obtained from KaMinLLC, Macon, United States.

Table 2 summarizes the main properties of the liquid and powder SB latex samples. Particle size, zeta potential, anionic charge density, glass transition temperature (T_g) and minimum film forming temperature (MFFT) of the liquid and powder SB samples were determined as described in a previous paper [7].

Table 2 Properties of the liquid and powder SB latex samples used in this study.

Sample	**Polymer content [wt.%]**	**d [nm]**	**Zeta potential [mV]**	**T_g [°C]**	**MFFT [°C]**	**Colloidal stabilizer**	**Anti-caking agent**
Liquid SB	45	220	- 31	+ 6	+ 6	-	-
Powder SB	78	150-600	- 25	+ 6	+ 6	PVOH	kaolin

2.2 Preparation of polymer-modified cement pastes

Hydration of CEM I 52.5 N was monitored in the presence and absence of SB polymer, PVOH and kaolin using isothermal heat flow calorimetry, in-situ X-ray diffraction, electroacoustic zeta potential and analysis of the chemical composition of the cement pore solution.

For all experiments, cement pastes were prepared at a constant water-to-cement (w/c) ratio of 0.5 using the following procedure: first, the liquid SB latex or SB powder or kaolin were added to deionized mixing water and sonicated for three minutes. This way, the latex powder or kaolin are fully dispersed into their primary particles. Second, cement powder was added to the SB or kaolin dispersion and shaken on a vortex shaker (Reax, VWR International, Darmstadt, Germany) for one minute. In additional experiments with PVOH, this polymer was completely dissolved under stirring in the mixing water before it was mixed with cement as described above.

SB polymer dosages (stated by weight of cement) were chosen at 5, 10 or 20 %bwoc respectively. Thus, cement pastes modified with powder SB contained additional PVOH and kaolin and less polymer compared to the liquid SB. For the investigation on the impact of spraying aids, the respective amounts of PVOH or kaolin contained in the SB powder were applied.

2.3 Isothermal heat flow calorimetry

Hydration of CEM I 52.5 N in the presence and absence of SB polymer was tracked via heat flow calorimetry using a TAM Air isothermal heat conduction calorimeter from Thermometric, Järfälla, Sweden.

In a typical experiment, 4 g of cement were mixed at a w/c ratio of 0.5 in a 10 mL tubular glass ampoule with water holding the SB latex either in liquid or powder form. The glass ampoules were sealed with a metal lid, shaken for 1 minute on a vortex mixer to homogenize the paste and transferred into the instrument. Heat flow curves were recorded for 72 h at 20 °C.

2.4 In-situ X-ray diffraction

In-situ XRD was conducted to study the time-dependent evolution of the hydration products ettringite and portlandite. 4 g cement paste were prepared following the procedure described in paragraph 2.2, filled into a metal XRD sample container and covered with a Kapton® polyimide foil in order to prevent carbonation or water evaporation from the surface of the cement paste. Immediately after preparation, measurement was started on a Bruker AXS D8 Advance instrument equipped with Bragg-Brentano geometry. Complete scans were taken during the first 48 hours at intervals of 30 minutes. Measurements were taken in the range between 8 and 44° 2θ, at a step size of 0.034° and a time per step of 144 s. The X-ray beam was generated from a Cu Kα X-ray source.

2.5 Electroacoustic zeta potential

Adsorption of colloidal SB particles on cement was studied via electrophoretic zeta potential measurement on a DT 1200 instrument (Dispersion Technology, Bedford Hills, USA).

According to *Dukhin* and *Goetz* [20], the value for the zeta potential of suspended cement particles can be calculated from the colloidal vibration current (CVI). The total vibration current (TVI) which is measured by the instrument is the sum of the colloidal (CVI) and the ionic (IVI) vibration current. Thus, for calculation of the CVI, the IVI which represents the ionic background must be known. IVI was determined from cement pore solution whereby pore solution was separated from the cement paste (w/c 0.5) via centrifugation for 10 min at 8500 rpm.

For the measurement, 450 g of cement paste (w/c 0.5) were prepared, filled into the sample container of the zeta potential instrument and stirred at 250 rpm during the experiment. Aqueous SB dispersions obtained from either liquid or powder SB latex with a solid content of 45 wt.% were titrated to the cement paste, and the zeta potential was measured. From this experiment, dosage-dependent zeta potential evolution was captured. Additionally, time-dependent zeta potentials of neat and SB latex-modified cement slurries were taken over an interval of 60 min.

2.6 Analysis of cement pore solution

Concentrations of SO_4^{2-} and Ca^{2+} ions present in the cement pore solution of SB-modified cement pastes were quantified via ion chromatography (SO_4^{2-}) or atomic absorption spectroscopy (Ca^{2+}) and compared with those of the neat cement sample.

In analysis, 20 g of cement were mixed at a w/c ratio of 0.5 with the SB dispersions (polymer dosage: 5 wt.-%) in a 50 mL centrifuge tube for 1 minute on a vortex tumbler. The cement samples were stored at room temperature for 0, 20, 40, 60, 80, 100, 120, 140, 160, 180, 210, 240 and 270 minutes and then centrifuged for 10 minutes at 8500 rpm (Biofuge Primo R, Heraeus Instruments, Hanau, Germany). Next, the supernatant solution/dispersion was filtered off using a 0.1 µm syringe filter in order to separate residual solids (mainly latex particles).

For quantification of the Ca^{2+} concentration, 1 g of the clear filtrate was immediately adjusted to a neutral pH by adding 1 g of hydrochloric acid (concentration 0.8 wt.%) to prevent carbonation, and then was further diluted with 18 g of DI water. The Ca^{2+} content was obtained via atomic absorption spectroscopy (Perkin Elmer 1100, Waltham, USA).

For quantification of the SO_4^{2-} concentration, an aliquot of 0.8 mL from the AAS samples was diluted in a plastic vial with DI water to a total volume of 4 mL, sealed with a cap and analyzed via ion chromatography (ICS-2000 apparatus, Dionex, Idstein, Germany).

3. Results and discussion

3.1 Colloidal properties of liquid and powder SB latex

In this study, an anionic styrene-butadiene copolymer which is electrostatically stabilized via incorporation of itaconic acid was used. The chemical structure of the carboxylated styrene-butadiene copolymer is displayed in **Figure 1**.

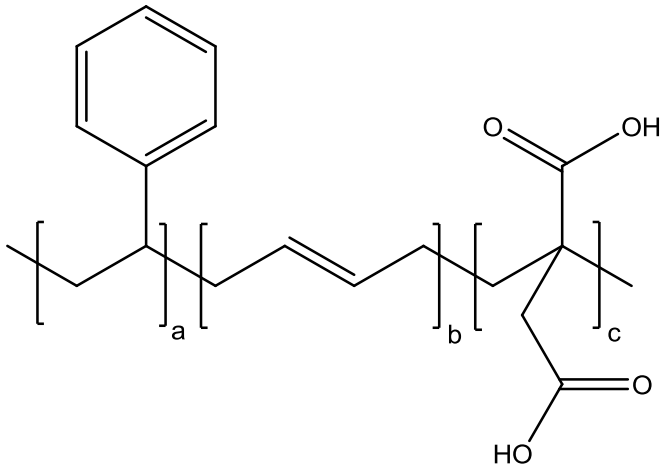

Figure 1 Chemical structure of the carboxylated styrene-butadiene copolymer sample. The molar ratio of a:b was 18:55.

The powder SB sample was fabricated via spray drying of the latex mother liquor under addition of polyvinylalcohol as colloidal stabilizer and kaolin as anti-caking agent. In the spray drying process, individual latex particles are coated with a layer of PVOH and arrange into powder particles under dense packing. The surface of such powder particles is partially covered with platelets of kaolin, as is shown in **Figure 2**. When this powder is re-dispersed in water, then the powder particles become disintegrated and reconstitute to a liquid latex similar to that of the mother liquor.

Dynamic light scattering measurements revealed a monodisperse particle size distribution for the liquid latex of around 220 nm.

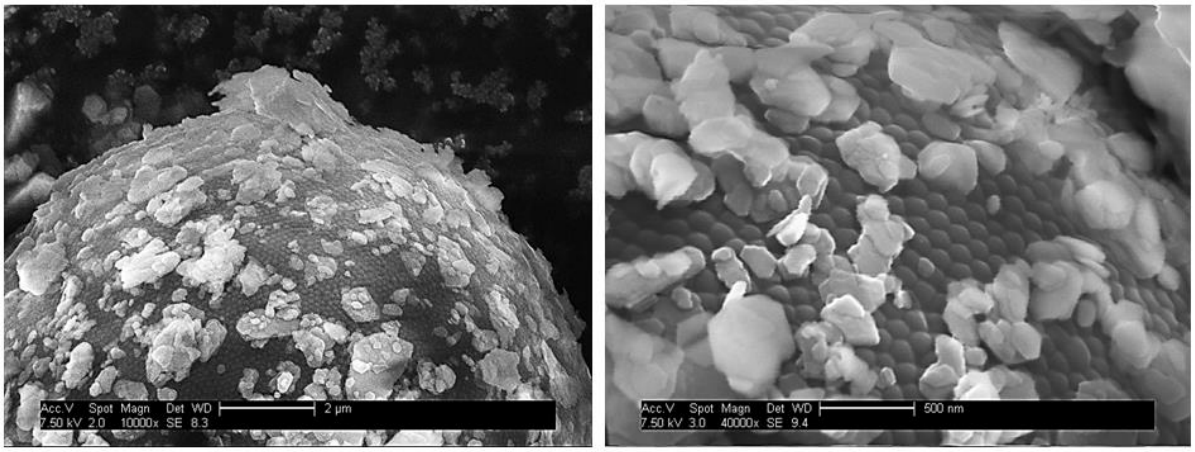

Figure 2 SEM images of a SB powder particle showing a dense packing of individual latex particles on its surface. The surface of the SB particle is partially covered with irregularly shaped platelets of the anti-caking agent kaolin.

Quantitative charge titration of the liquid and powder SB latex with cationic polyDADMAC revealed a pronounced anionic character for the SB particles, as shown in **Table 3**. Due to the incorporation of itaconic acid into the SB copolymer, an anionic surface charge which originates from carboxylate groups develops on surfaces of the latex particles. Moreover, the anionic charge density of the SB particles is pH-dependent. The higher the pH, the more complete is the deprotonation of the carboxylic groups. A comparison between the surface charge of the SB mother liquor and of liquid latex reconstituted from the re-dispersed SB powder reveals a lower anionic charge density for the SB powder. As we presented in another study [7], upon spray drying SB particles are coated with a thin layer of PVOH whereby some carboxylate groups become partially embedded in the coating. As a

consequence, these carboxylate groups are no longer exposed on the surface and thus cannot contribute to the anionic charge.

Table 3 Specific anionic charge amounts of liquid and powder SB latex at pH 7 and 12.5, respectively, measured by polyelectrolyte titration.

Sample	**Anionic charge density [C/g]**	
	pH = 7.0	**pH = 12.5**
Liquid SB	- 42	- 52
Powder SB	- 27	- 32

3.1 Isothermal heat flow calorimetry

Hydration of ordinary Portland cement in the presence and absence of liquid and powder SB latex was monitored via time-dependent heat flow calorimetry. The dosages of SB polymer (5, 10 and 20 %bwoc) were chosen such as to represent actual application conditions. For example, samples containing 5 %bwoc SB polymer are characteristic for tile adhesives, while cement modified with 20 %bwoc SB polymer corresponds more to a waterproofing membrane.

As is evident from **Figure 3** and **Figure 4** the addition of liquid or powder SB latex results in a significant retardation of cement hydration. Especially the dormant period is prolonged in the presence of SB polymer, while the acceleration and deceleration periods maintain their characteristic time span. For example, at 10 % SB latex addition the maximum of the heat release of OPC is shifted from 9.5 h to 20 h. The retarding effect of both, liquid and powder SB latex, is almost linearly dependent on SB dosage. Addition of 1 %bwoc of SB latex causes a delay of the dormant period of

~ 40 min. Generally, the retarding effects of liquid and powder SB latex are comparable. This result indicates that the SB polymer, and not the spraying aids, is responsible for the retardation.

Additionally, the neat cement paste exhibits a characteristic ‘sulfate depletion’ peak which is caused by late ettringite formation or conversion of ettringite to monosulfate [1]. In the presence of SB polymer, this ‘sulfate depletion’ peak has disappeared completely for the liquid latex, and appears very weak for the powder SB. Thus, such a late ettringite formation or conversion is much suppressed when SB polymer is present.

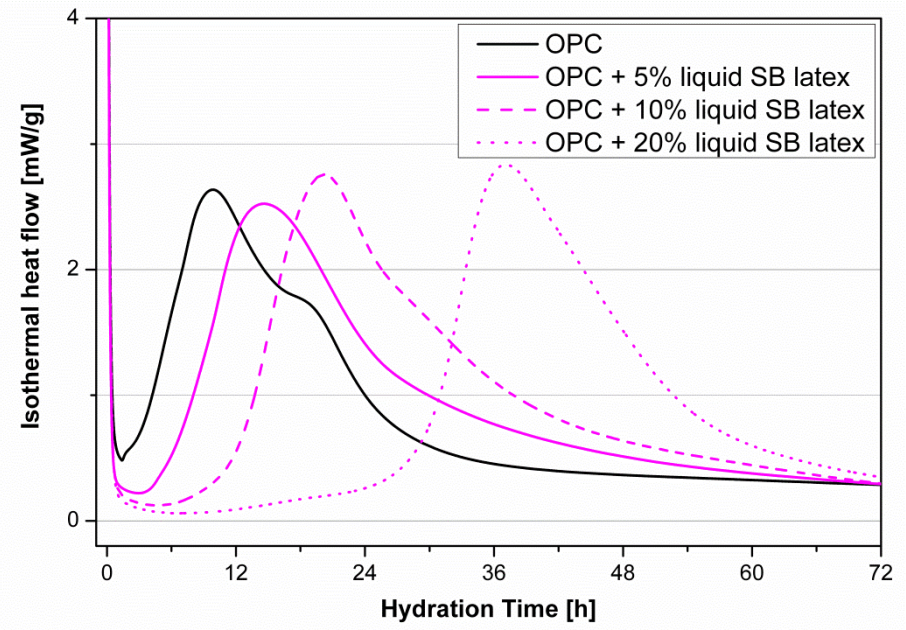

Figure 3 Time-dependent heat flow of OPC pastes recorded in the presence and absence of liquid SB latex (dosages: 5, 10 and 20 %bwoc.).

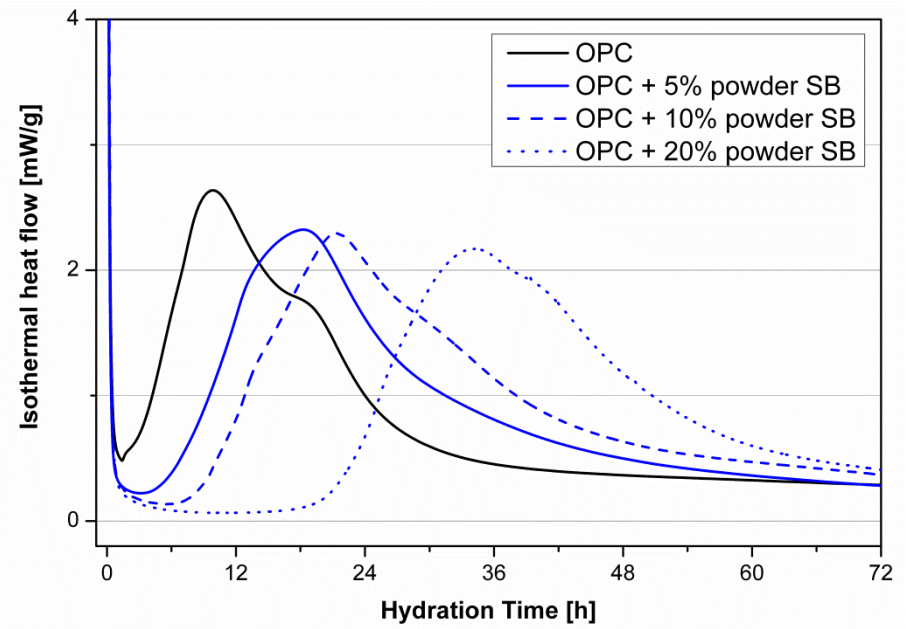

Figure 4 Time-dependent heat flow of OPC pastes recorded in the presence and absence of SB powder (dosages: 5, 10 and 20 %bwoc.).

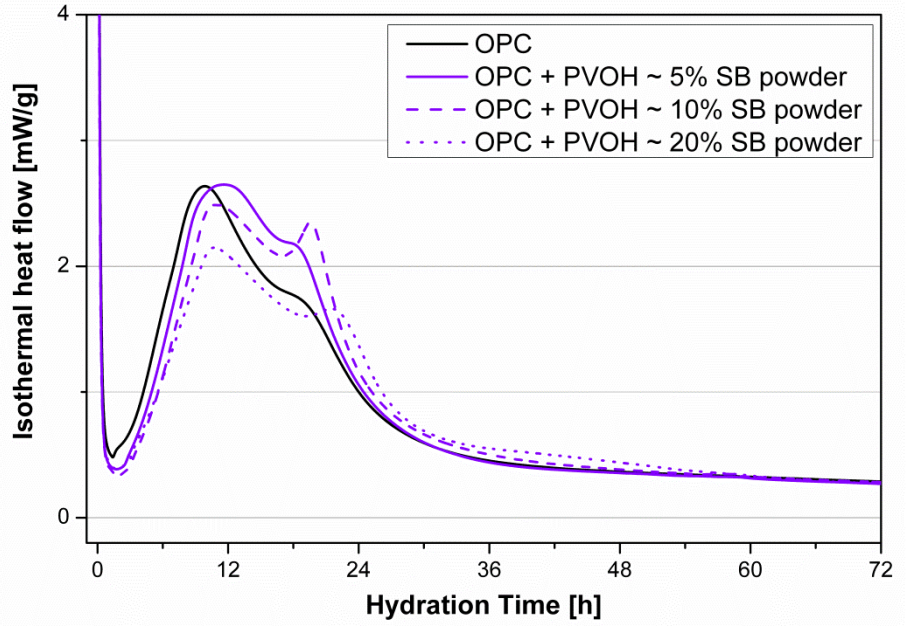

Figure 5 Time-dependent heat flow of OPC pastes recorded in the presence and absence of PVOH (dosage same as contained in 5, 10 and 20 %bwoc additions of powder SB).

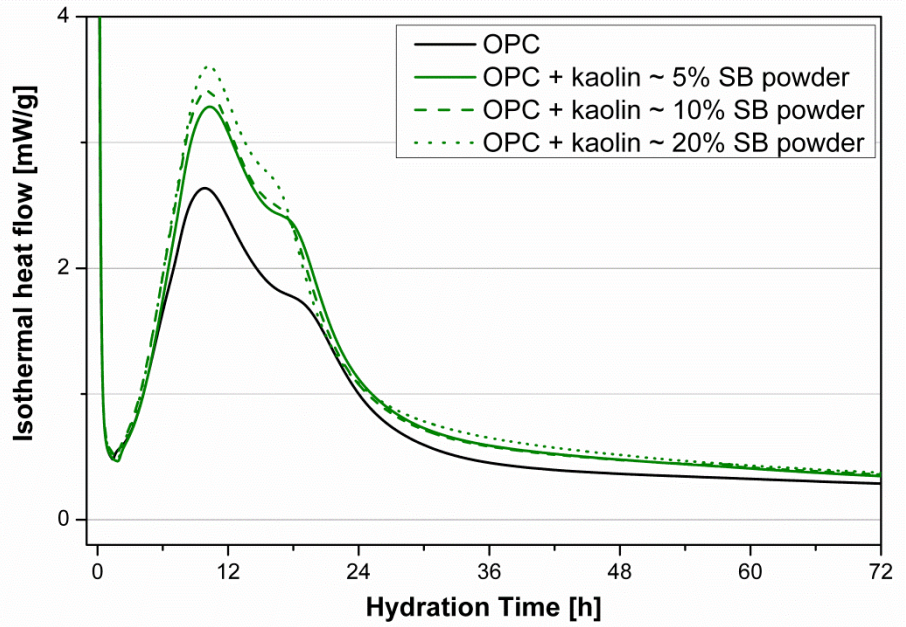

Figure 6 Time-dependent heat flow of OPC pastes recorded in the presence and absence of kaolin (dosage same as contained in 5, 10 and 20 %bwoc additions of powder SB).

Figure 5 and **Figure 6** display the heat flow curves of OPC slurries modified with the individual spraying aids PVOH and kaolin. The dosages of the spraying aids were chosen such as to correspond with those introduced at additions of 5, 10 and 20 %bwoc of SB powder. In the following, this is indicated by the term ' ~ x % SB powder'.

Generally, both spraying aids PVOH or kaolin show a minor effect on heat evolution of OPC, compared to that observed from the SB polymer (**Figure 3** and **Figure 4**). PVOH slightly decreased the maximum heat development of cement. The effect increases with increasing PVOH dosage. The second maximum of heat release (the 'sulfate depletion' peak) becomes more pronounced, compared to neat OPC. *Jansen* et al. [8] presented similar results for PVOH-modified OPC pastes. By using quantitative XRD, these authors confirmed that this effect is owed to late ettringite

formation. Kaolin does not shift the acceleration and deceleration periods, but increases the overall heat development, thus suggesting an accelerating effect on cement hydration.

3.2 In-situ X-ray diffraction

The calorimetric measurements confirmed that the main heat evolution from OPC modified with SB polymer occurs in the first 48 h of hydration. Therefore, complementary to the heat flow calorimetric experiments the evolution of the main crystalline reaction products of OPC, ettringite and portlandite, was measured within the first 48 h in intervals of 30 min using in-situ XRD.

Figure 7 summarizes the time-dependent evolution of ettringite within the first 48 h of hydration in the presence and absence of SB latex, SB powder, PVOH and kaolin. For the neat cement paste, ettringite crystallization starts immediately after mixing with water and reaches its maximum during the first 10 h. In the presence of SB latex, ettringite formation is almost completely suppressed. Obviously, SB latex strongly interferes with the aluminate reaction by interacting with C_3A or initially formed ettringite nuclei. In comparison, SB powder exhibits a less pronounced impact on ettringite formation. The influence depends on the dosage of SB powder and increases with higher SB additions. The results suggest that the spraying aids PVOH and kaolin reduce the strong suppressing effect of pure SB latex on ettringite formation.

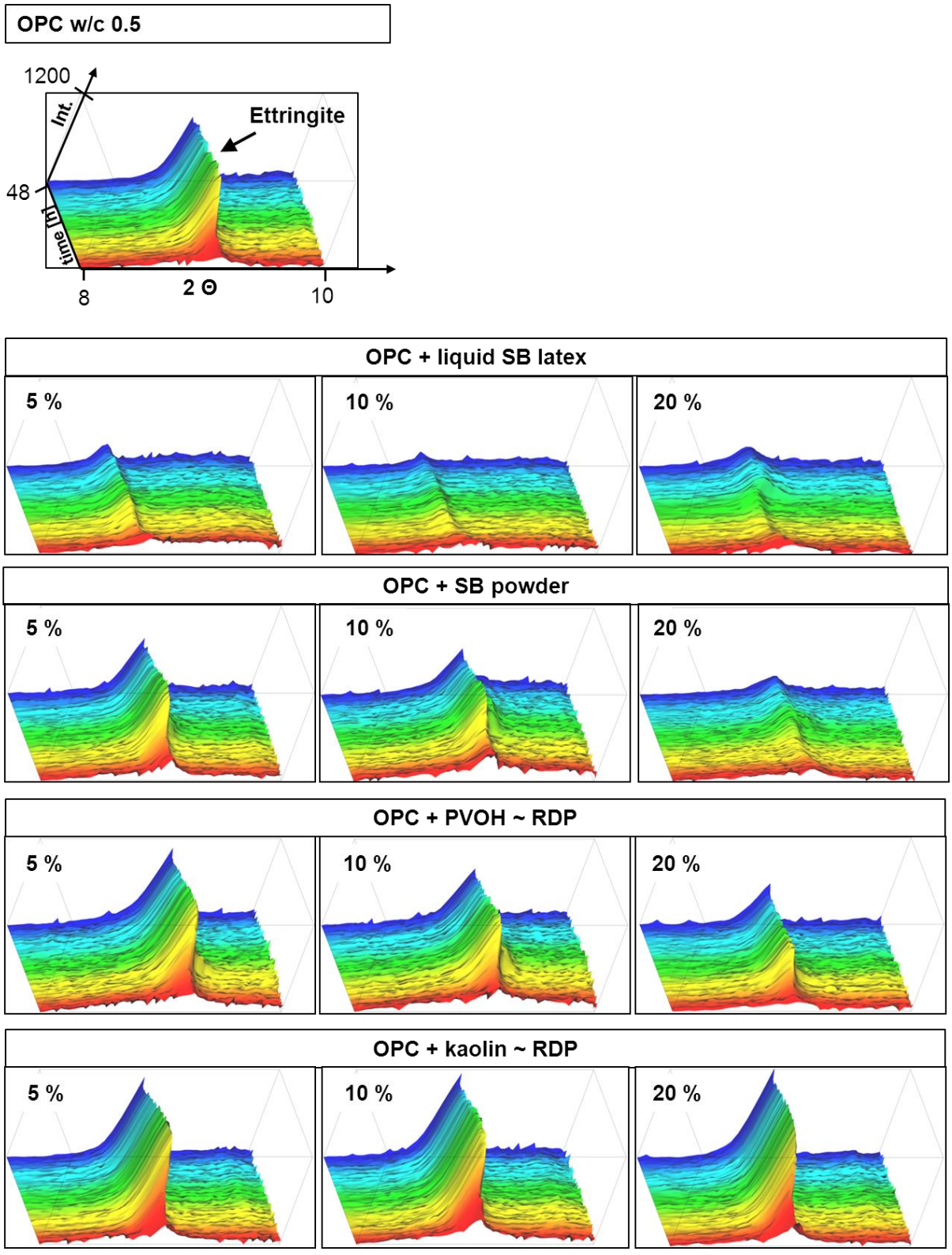

Figure 7 Time-dependent evolution of ettringite during OPC hydration in the absence and presence of liquid or powder SB latex, PVOH and kaolin. The scaling of all XRD patterns is similar (2Θ range: 8-10; time frame: 48 h; intensity: 1200 counts).

Individual PVOH and kaolin show no significant effect on ettringite formation. Only at very high PVOH dosages, ettringite formation is reduced. This result indicates that the influence of SB powder on the aluminate reaction is mainly caused by the anionic SB latex particles. The spraying aids PVOH and kaolin change the colloidal properties of the SB particles by reducing their anionic charge, compared to that of the primary latex particles present in the mother liquor.

The main reaction product of the silicate phases C_2S and C_3S are C-S-H phases whereby portlandite ($Ca(OH)_2$) is formed as well. Since C-S-H phases are X-ray amorphous, portlandite was used to track the silicate reaction.

Figure 8 summarizes the time-dependent evolution of portlandite within the first 48 h of hydration in the presence and absence of SB latex, SB powder, PVOH and kaolin. In the neat cement paste, portlandite crystallization starts ~ 4 h after mixing with water. In the presence of SB latex and powder, portlandite formation is significantly retarded to start at around 8 h at 5 %bwoc, 12 h at 10 %bwoc and 22 h for 20 %bwoc. Thus, SB latex and powder not only impact the aluminate reaction, they also strongly retard the hydration of the silicates. A plausible explanation is that the SB particles chelate ions present in cement pore solution and thus retard the crystallization of hydrate phases.

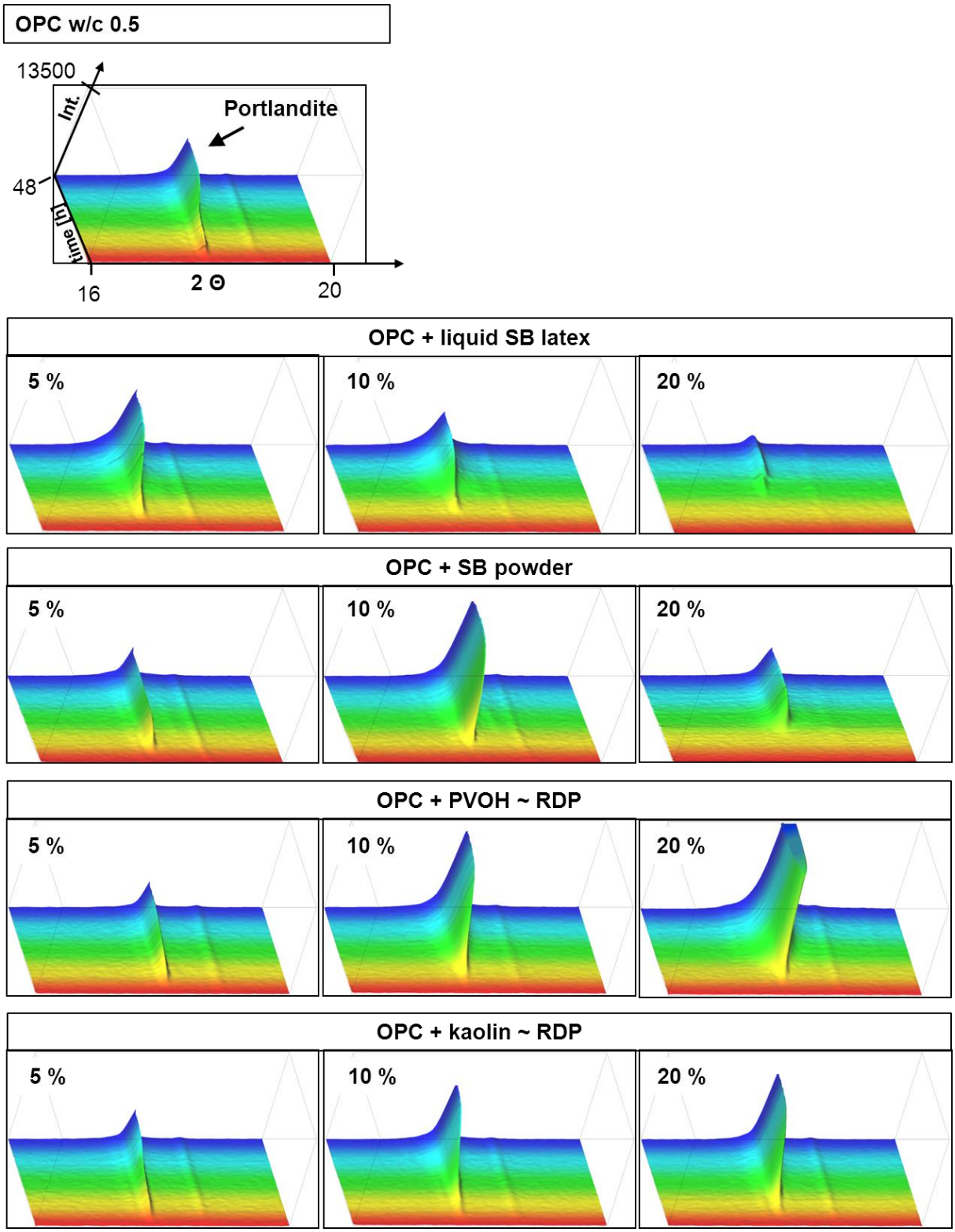

Figure 8 Time-dependent evolution of portlandite during OPC hydration in the absence and presence of liquid or powder SB latex, PVOH and kaolin. The scaling of all XRD patterns is similar (2Θ range: 16-20; time frame: 48 h; intensity: 13500 counts).

Next, the influence of the spraying aids PVOH and kaolin was studied. In the presence of PVOH, portlandite crystallization is slightly retarded to begin at 8 h for the 20 % ~ RDP system. Additionally, the signal intensity increases significantly with PVOH dosage. The reason for this effect is the hydrolysis of PVOH in the cement paste whereby hydroxide ions are consumed and thus the pH of the cement slurry decreases. For example, the pH value of the neat cement slurry decreased from 13.5 to 13.0 at 20 % PVOH ~ SB powder. Resulting from the lower pH, solubility of the silicate phases C_2S and C_3S increases and thus more Ca^{2+} ions can precipitate as $Ca(OH)_2$. **Table 4** shows the pH values of cement slurries measured 10 min after mixing with water by using a pH electrode.

Table 4 pH values of cement slurries measured in the presence and absence of SB latex, SB powder or PVOH.

Sample	**pH**
OPC	13.5
OPC + 5 % SB latex	13.5
OPC + 10 % SB latex	13.5
OPC + 20 % SB latex	13.5
OPC + 5 % SB powder	13.4
OPC + 10 % SB powder	13.2
OPC + 20 % SB powder	13.0
OPC + PVOH ~ 20% RDP	13.0

Interestingly, kaolin appears to accelerate the silicate reaction, as is evidenced by a more intense peak for portlandite, especially after ~ 24 hours (**Figure 8**). This confirms the calorimetric investigation displayed **Figure 6**. A similar trend was observed for the SB powder at 10 % addition when compared with the liquid latex.

Surprisingly, this effect decreased at 20 % addition, which needs further investigation.

3.3 Zeta potential

Cement particles dispersed in water develop a heterogeneous surface charge due to the formation of different hydrate phases. Silicate hydrates (e.g. C-S-H and portlandite) exhibit a negative surface charge whereas aluminate hydrates (e.g. ettringite) possess positively charged surfaces. As a result, cement suspensions provide adsorption sites for positively as well as negatively charged polymers. The overall surface charge of cement can be measured electroacoustically via zeta potential which presents from the positively and negatively charged surfaces. Adsorption of latex polymers onto the charged sites of cement results in a change of the zeta potential value.

The zeta potential of the neat cement slurry and of slurries containing SB latex, SB powder, PVOH or kaolin was measured in order to investigate their potential adsorption. **Figure 9** shows the evolution of zeta potential of the neat cement paste and in the presence of SB latex or powder at varying dosages (5, 10 and 20 %bwoc) within the first hour after mixing with water. For all samples, the value for the zeta potential was found almost constant during the first hour of hydration. Only a minor increase in zeta potential occurred, e.g. for the neat cement paste from – 5.4 to – 3.8 mV. Thus, changes in zeta potential values can be ascribed to interactions between the cement particles. Pastes modified with SB polymer follow a similar trend over time. Additionally, in the presence of anionic SB zeta potentials are significantly deceased, for both SB latex and powder, as is shown in **Figure 10**. This result

indicates that negatively charged SB particles adsorb onto positively charged areas of the cement particle. The adsorbed amount strongly depends on the polymer dosage and the charge density of the SB particles. With increasing polymer dosage, the value for the zeta potential is continuously decreased until a constant value (saturation dosage) is reached.

SB powder decreases the zeta potential of cement pastes less than SB latex (**Figure 10**). This effect is explained by the lower anionic charge density of SB powder due to coating with PVOH, as illustrated in **Figure 11**. During spray drying, the SB particles become partially covered with a layer of PVOH whereby some carboxylate groups of the latex particle surface are embedded into this PVOH coating and no longer can contribute to the anionic charge (see **Table 3**). As a consequence, adsorption of SB powder particles onto cement becomes less.

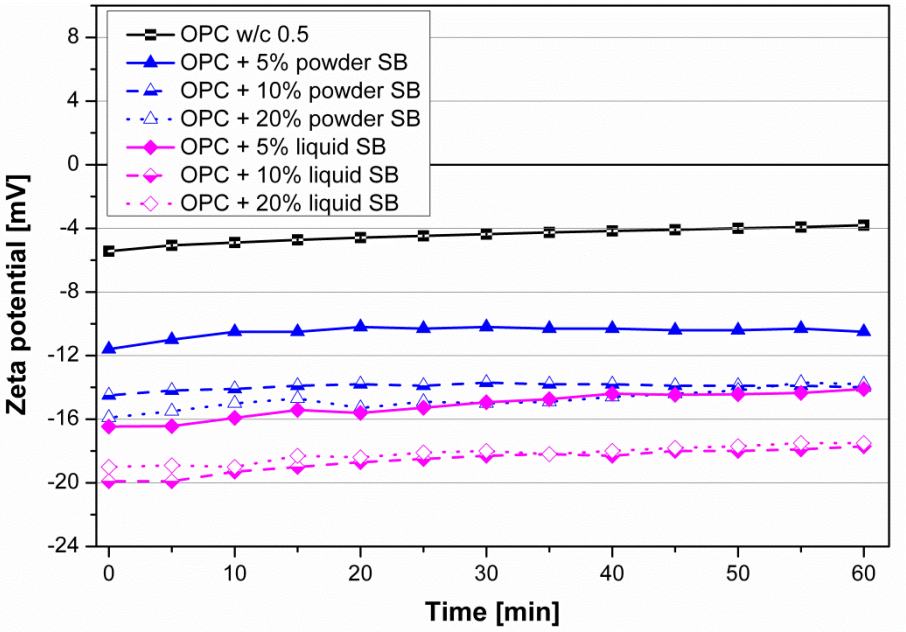

Figure 9 Time-dependent zeta potential of cement pastes (w/c 0.5) in the presence and absence of liquid and powder SB latex (dosages: 5, 10 and 20 %bwoc).

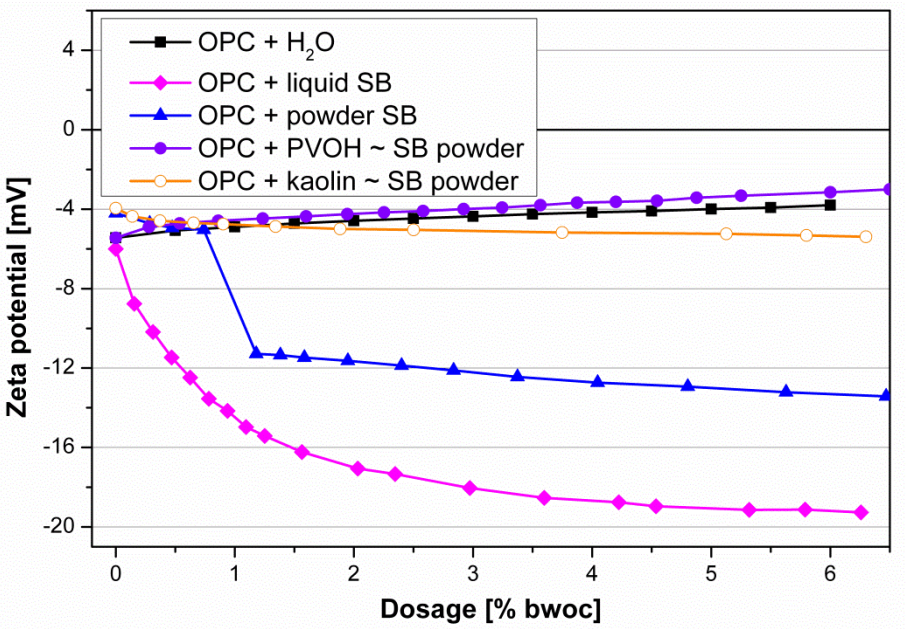

Figure 10 Zeta potential of cement pastes (w/c 0.5) as a function of increasing SB latex, SB powder, PVOH and kaolin dosages.

These observations can be linked with the analysis of the phase development during cement hydration as obtained via in-situ XRD (**Figure 7** and **Figure 8**). As was shown there, in the presence of SB latex ettringite formation is almost completely suppressed, even at the lowest dosage of 5 %bwoc. The zeta potential measurements suggest that SB latex reaches saturation adsorption at a dosage of around 5 %bwoc (**Figure 10**). This indicates that the SB particles adsorb onto positively charged ettringite crystals and hinder their further growth. The adsorbed SB layer represents a barrier for water molecules or ions from the cement pore solution, thus continued crystal growth is prevented.

SB powder suppresses ettringite formation not so completely like liquid SB latex. Apparently, SB powder does not adsorb in such high amount as liquid latex, due to

its lower anionic charge. Consequently, SB powder particles do not impact ettringite formation as strong as SB latex particles.

Individual PVOH and kaolin show no significant impact on zeta potential of cement slurries. This indicates that both compounds do not adsorb onto cement. Again, the results can be linked with the phase development observed before as shown in **Figure 7**.

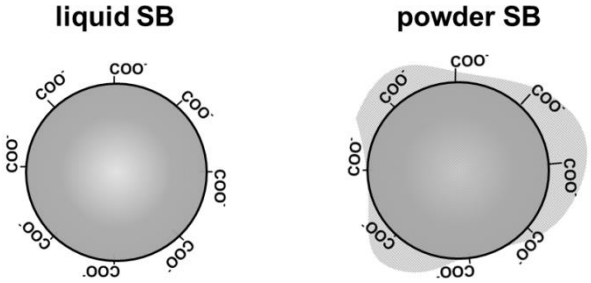

Figure 11 Illustration of the anionic charge density of SB latex and powder particles. SB powder particles are partially covered with a layer of PVOH during the spray drying, leading to a reduced anionic charge density.

3.4 Analysis of cement pore solution

The crystallization of cement hydrate phases results from oversaturation of the cement pore solution with ions like SO_4^{2-} or Ca^{2+}. Thus, analysis of the ion concentrations present in cement pore solution can provide important information on the influence of the polymers on cement hydration or their interaction with specific ions.

Figure 12 exhibits the sulfate concentration of the cement pore solution in the presence and absence of 5 %bwoc SB latex, SB powder, PVOH and kaolin within the first 270 min after mixing with water. In the presence of SB latex and powder, the equilibrium concentration for sulfate is higher compared to that in neat cement. This effect is more pronounced for liquid SB. A potential explanation is the suppression of ettringite formation, as is shown in **Figure 7**. When ettringite crystallization is decelerated, then no sulfate ions are consumed and the sulfate concentration in the pore solution increases.

Figure 13 demonstrates that the SB polymer chelates Ca^{2+} ions via its carboxylate groups and thus reduces the content of free Ca^{2+} ions in the pore solution. As a result, crystallization of portlandite is retarded, as was evidenced before via in-situ XRD (**Figure 8**). Additionally, the Ca^{2+} concentration is strongly influenced by the colloidal stabilizer PVOH. In alkaline cement pore solution, partially hydrolyzed PVOH undergoes hydrolysis whereby hydroxide ions are consumed and thus the pH of the pore solution decreases. As a consequence, solubility of the silicate phases C_2S and C_3S is enhanced and the calcium concentration of the cement pore solution increases. Therefore, portlandite formation is increased in samples containing PVOH such as SB powder or individual PVOH.

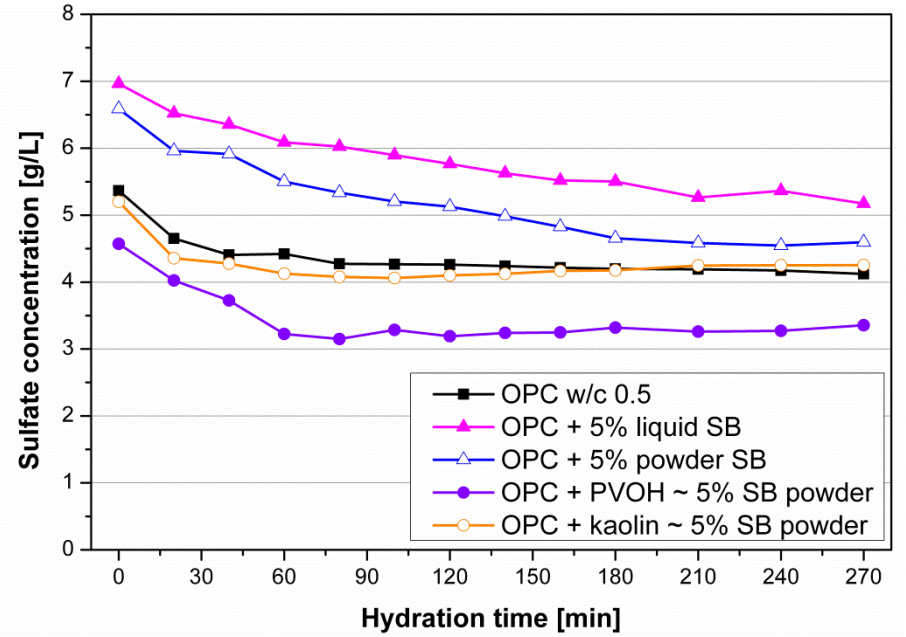

Figure 12 Sulfate concentration in the pore solution of OPC hydration in the presence and absence of SB latex, SB powder, PVOH and kaolin, measured during the first 270 min of hydration.

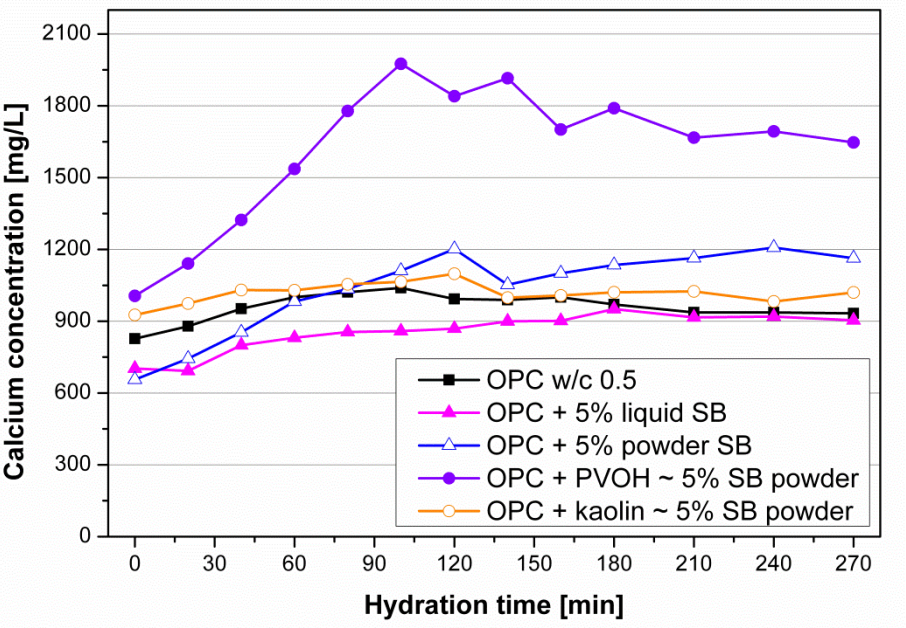

Figure 13 Concentration of calcium ions in the pore solution of OPC hydrating in the presence and absence of SB latex, SB powder, PVOH and kaolin, measured during the first 270 min of hydration.

4. Conclusion

The experiments suggest that the colloidal properties of anionic styrene-butadiene latex particles, and in particular their surface properties, determine their interaction with mineral surfaces (clinker or hydrate phases) or ions present in cement pore solution. As a consequence, SB powder exhibits a different influence on cement hydration, compared to its liquid precursor. This effect is owed to the spraying aids PVOH and kaolin which are present in SB powder. Upon spray drying, the SB powder particles are coated with a layer of PVOH whereby the anionic surface charge of the SB powder particles is reduced, compared to liquid precursor. This way, carboxyl groups present on SB powder particles are partially embedded into this PVOH coating and therefore show less interaction with cement, hydrate phases or ions.

As evidenced from heat flow calorimetry and in-situ XRD, anionic SB particles strongly retard or suppress the silicate and aluminate reaction in the hydration of ordinary Portland cement. Zeta potential measurements confirmed that the mechanism for suppressed ettringite formation is based on adsorption of the anionic SB particles onto the positively charged surfaces of hydrating cement. Additionally, the carboxylate groups of the SB particles chelate calcium ions present in cement pore solution. This way, the silicate reaction and precipitation of portlandite are retarded. All effects are more pronounced for the liquid SB latex from which the re-dispersible powder was produced. The reason for this behavior can be ascribed to the higher anionic charge density of liquid SB which results in stronger electrostatic interactions with mineral phases.

Contrary to *R. Wang et al.* [15-19] we found that ettringite formation is suppressed in the presence of anionic SB copolymer. This indicates that the exact composition of the liquid or powder latex samples should to be known when their interaction with cement is investigated. Otherwise it can be difficult to distinguish whether the effects of the copolymer on cement hydration are caused by the colloidal properties of the latex or the spraying aids.

Generally, our results demonstrate that during the fabrication of latex powders from liquid latex dispersions via spray drying the colloidal properties of the latex particles can change. As a consequence, the influence of liquid and powder latex samples on cement hydration can be different, depending on the colloidal properties of the polymer particles. Still, different behaviors can be expected for different latex copolymers. For example, nonionic ethylene-vinylacetate dispersions can be expected to exhibit a minor difference between the liquid and the powder product. More research is needed to acquire a more comprehensive understanding of the colloidal properties of the different kinds of latex copolymers.

References

[1] Bullard JW, Jennings HM, Livingston RA, Nonat A, Scherer GW, Schweitzer JS. Mechanisms of cement hydration. Cement and Concrete Research. 2011;41(12):1208-23.

[2] Chandra S, Flodin P. Interactions of polymers and organic admixtures on portland cement hydration. Cement and Concrete Research. 1987;17(6):875-90.

[3] Ramachandran VS. Concrete Admixtures Handbook: Properties, Science, and Technology: Noyes Publications; 1995.

[4] Bayer R., Lutz H. Dry mortars. Ullmann's encyclopedia of industrial chemistry. 2009;541-579.

[5] Kardon JW. Polymer-Modified Concrete: Review. Journal of Materials in Civil Engineering. 1997;9(2):85-92.

[6] Ohama Y. Polymer-based admixtures. Cement and Concrete Composites. 1998;20(2–3):189-212.

[7] Baueregger S, Perello M, Plank J. Role of PVOH and kaolin on colloidal stability of liquid and powder EVA and SB latexes in cement pore solution. Colloids and Surfaces A: Physicochemical and Engineering Aspects. 2013;434(0):145-53.

[8] Jansen D, Götz-Neunhoeffer F, Neubauer J, Hergeth WD, Härzschel R. Influence of polyvinyl alcohol on phase development during the hydration of Portland cement. ZKG International. 2010;63(7-8):100-7.

[9] Jansen D, Goetz-Neunhoeffer F, Neubauer J, Haerzschel R, Hergeth WD. Effect of polymers on cement hydration: A case study using substituted PDADMA. Cement and Concrete Composites. 2013;35(1):71-7.

[10] Plank J, Gretz M. Study on the interaction between anionic and cationic latex particles and Portland cement. Colloids and Surfaces A: Physicochemical and Engineering Aspects. 2008;330(2-3):227-33.

[11] Su Z, Bijen JM, Larbi JA. Influence of polymer modification on the hydration of portland cement. Cement and Concrete Research. 1991;21(4):535-44.

[12] Larbi JA, Bijen JM. Interaction of polymers with portland cement during hydration: A study of the chemistry of the pore solution of polymer-modified cement systems. Cement and Concrete Research. 1990;20(1):139-47.

[13] Betioli AM, Hoppe J, Cincotto MA, Gleize PJP, Pileggi RG. Chemical interaction between EVA and Portland cement hydration at early-age. Construction and Building Materials. 2009;23(11):3332-6.

[14] Silva DA, Roman HR, Gleize PJP. Evidences of chemical interaction between EVA and hydrating Portland cement. Cement and Concrete Research. 2002;32(9):1383-90.

[15] Wang R, Wang PM. Action of redispersible vinyl acetate and versatate copolymer powder in cement mortar. Construction and Building Materials. 2011;25(11):4210-4.

[16] Wang R, Wang PM. Effect of styrene-butadiene rubber latex/powder on cement hydrates. Journal of the Chinese Ceramic Society. 2008;36(7):912-19, 92619, 926.

[17] Wang R, Wang PM. Formation of hydrates of calcium aluminates in cement pastes with different dosages of SBR powder. Construction and Building Materials. 2011;25(2):736-41.

[18] Wang R, Li XG, Wang PM. Influence of polymer on cement hydration in SBR-modified cement pastes. Cement and Concrete Research. 2006;36(9):1744-51.

[19] Wang R, Yao LJ, Wang PM. Mechanism analysis and effect of styrene-acrylate copolymer powder on cement hydrates. Construction and Building Materials. 2013;41:538-44.

[20] Dukhin AS, Goetz PJ. Ultrasound for Characterizing Colloids. Studies in Interface Science. Elsevier. 2002.

Paper #5

Impact of Carboxylated Styrene-Butadiene Copolymer on the Hydration Kinetics of OPC and OPC/CAC/AH: The Effect of Ca^{2+} Sequestration from Pore Solution

S. Baueregger, M. Perello, J. Plank

Cement and Concrete Research

(submitted on September 12, 2014, under review)

Impact of Carboxylated Styrene-Butadiene Copolymer on the Hydration Kinetics of OPC and OPC/CAC/AH: The Effect of Ca^{2+} Sequestration from Pore Solution

Stefan Baueregger [a], Margarita Perello [b], Johann Plank [a1]

[a] Technische Universität München, Lichtenbergstr. 4, 85747 Garching / Germany

[b] Dow Europe GmbH, Bachtobelstr. 3, 8810 Horgen / Switzerland

[1] Tel.: +49 89 289 13151
Fax: +49 89 289 13152.
E-mail: sekretariat@bauchemie.ch.tum.de

KEYWORDS

Cement (D)

Hydration (A)

Dispersion (A)

Calorimetry (A)

Latex

ABSTRACT

It was found that carboxylated styrene-butadiene latex copolymer retards OPC and accelerates a ternary binder system based on OPC/CAC/anhydrite. The reason behind both effects is sequestration of Ca^{2+} ions from the pore solution. In the case of OPC, the depletion of Ca^{2+} hinders the formation of cement hydrates and thus retards hydration of OPC, whereas for the ternary binder system the depletion of Ca^{2+} shifts the solubility equilibrium of $CaSO_4$ in favor of sulfate. As a result, dissolution of anhydrite is accelerated and ettringite formation is enhanced. The consequence of these processes is earlier strength development which is highly desirable in drymix mortar applications. The results explain why anionic SB latex performs particularly well in ternary binder systems.

1. Introduction

Drymix mortars represent multicomponent systems which contain mineral binders (e.g. Portland cements or calcium sulfates), organic binders (e.g. latex polymers), aggregates (e.g. silica sand, limestone powder or lightweight fillers) and additives (e.g. cellulose ethers, superplasticizers, defoamers, retarders or accelerators etc.) [1].

The mineral binder controls the setting and strength development of the mortars. Some formulations such as repair mortars or self-leveling underlayments (SLUs) require fast setting and strength development. For this reason, ordinary Portland cement (OPC) is supplemented there with calcium alumina cement (CAC). The main clinker phase present in CAC is monocalcium aluminate (CA) which is highly reactive when getting in contact with water. Less reactive constituents of CAC include CA_2 and $C_{12}A_7$ [2, 3]. The much accelerated hydration of OPC/CAC mixtures are owed to enhancement of early ettringite formation, as described by *Beaudoin* et al. [4, 5] and *Scrivener* et al. [6].

Shrinkage-compensated mortars contain calcium sulfate binders (hemihydrate or anhydrite) in addition to OPC and CAC. *Hansen* et al. [7] found that the kind of the sulfate influences the products which are formed during the hydration of CAC. When anhydrite is used, large quantities of ettringite are formed in the hydration reaction. As ettringite incorporates 48.9 wt.-% of water into its crystal structure, it consumes large amounts of water which explains the fast setting of the mortars due to chemical

desiccation. The massive uptake of water and the growth of ettringite needles lead to expansion and this way shrinkage is compensated.

In such ternary binder systems (TBS) additives such as e.g. lithium carbonate (Li_2CO_3) and *Seignette* salt (K/Na-tartrate) are used to control hydration kinetics in order to achieve a sufficiently long workability period and at the same time provide high early strength [8-10]. *Goetz-Neuenhoeffer* developed a model for the working mechanism of Li_2CO_3 and tartaric acid in CAC/hemihydrate mixtures [11]. Li_2CO_3 selectively accelerates the hydration of CA by increasing its dissolution rate and forming a lithium aluminum layered double hydroxide (LDH) compound. In the absence of Li^+ ions a non-crystalline layer of aluminum hydroxo hydrate $[Al(OH)_x(H_2O)_y]$ is formed due to the low solubility of Al^{3+} under these slightly alkaline conditions. This aluminum hydroxo hydrate wraps the CA phases, thus acting as a diffusion barrier and preventing its further dissolution. In the presence of Li_2CO_3, Al^{3+} is converted into lithium aluminum hydroxide hydrate LDH (LA_2H_{10}) which presents a precursor for ettringite formation. This way Li^+ ions act as a catalyst for the ettringite crystallization.

The retarding effect of *Seignette* salt which is specific for Portland cement can be ascribed to the complexation of Ca^{2+} ions from cement pore solution and the formation of a calcium tartrate precipitate which covers the surfaces of the clinker and thus limits the access of water via diffusion [12, 13].

Latex polymers represent key components in most drymix mortars. They improve the cohesion and adhesion of the fresh mortar on solid substrates and increase the

flexural strength of the hardened mortar [14]. Most common are copolymers made from ethylene/vinylacetate, styrene/butadiene or styrene/acrylates [15]. In literature, several works on the influence of latex polymers on OPC hydration exist [16-21]. Nonetheless, no work dealing with the influence of latex polymers on the hydration of the ternary binder system OPC/CAC/anhydrite has been published. Owed to the widespread use of such TBS in drymix mortar formulations it is highly relevant to study the interaction between the mineral and polymer binders.

Here, we present a comparative study on the influence of carboxylated styrene-butadiene copolymer on the hydration of ordinary Portland cement OPC and a ternary binder system consisting of OPC, CAC and anhydrite. The impact of the carboxylated SB copolymer on the hydration of OPC and TBS was tracked via isothermal heat flow calorimetry. In-situ X-ray diffraction was conducted to monitor the time-dependent evolution of cement hydrate phases. The chemical composition of the cement pore solutions (SO_4^{2-} and Ca^{2+} ion concentrations) were quantified via ion chromatography (SO_4^{2-}) or atomic absorption spectroscopy (Ca^{2+}).

2. Materials and methods

2.1 Materials

The ordinary Portland cement used in this study was a CEM I 52.5 N sample from HeidelbergCement, Geseke plant, Germany which is common in drymix mortar formulations. Its phase composition was determined by quantitative X-ray diffraction

(Bruker AXS D8 Advance, Bruker, Karlsruhe, Germany) using *Rietveld* refinement (software Topas 4) and was found as follows (wt.%): C_3S (57.91), C_2S (23.47), C_3A (cubic: 4.38, orthorhombic: 3.58), C_4AF (2.49), anhydrite (2.08), hemihydrate (0.38), gypsum (0.66), calcite (3.33), free lime (0.28), periklas (0.14), quartz (0.82) and arcanite (0.48). The average particle size (d_{50} value) of the cement was measured via laser granulometry (Cilas 1064, Cilas Company, Marseille, France) and was found at 11.8 µm. Specific density of the cement was 3.2 kg/L as measured by Helium pycnometry (Ultrapycnometer 1000, Quantachrome Instruments, Boynton Beach, USA).

Calcium aluminum cement with approximately 70 wt.% Al_2O_3 (Ternal®White) was purchased from Kerneos S.A, Neuilly Sur Seine, France. The principal phases contained in CAC are CA and CA_2 as evidenced via XRD. As secondary phases $C_{12}A_7$, C_3A and A_α were present in minor amounts.

Anhydrite II was obtained from Fluorchemie Stulln GmbH, Stulln, Germany. Grinded Li_2CO_3 with a particle size of less than 40 µm was purchased from Chemetall GmbH, Langelsheim, Germany. Rochelle salt (K/Na tartrate) was obtained from Jungbunzlauer GmbH, Ladenburg, Germany.

The binder system was prepared by dry-blending OPC, CAC, anhydrite, Li_2CO_3 and tartrate using an overhead shaker (Reax 20, Heidolph Instruments GmbH & Co. KG, Schwabach, Germany) to achieve a homogeneous mix. Shaking time was two hours. **Table 1** presents the composition of the ternary binder system used in this study.

Table 1 Components of the ternary binder system.

Component	Content [wt.%]
OPC	83.08
CAC	10.72
Anhydrite	5.36
Li_2CO_3	0.27
K/Na tartrate	0.53

Styrene-butadiene latex (solid content 45 wt.%) was provided by Dow Olefinverbund GmbH, Schkopau, Germany. The average particle size of the SB latex was determined by dynamic light scattering (DLS) utilizing a Zetasizer Nano ZS apparatus (Malvern Instruments, Workestershire, UK) and found at 220 nm (monodisperse particle size distribution). Zeta potential of the SB particles was measured in aqueous dispersion on the same instrument. Here, the electrophoretic mobility was converted into a value for the zeta potential using the *Smoluchowski* relation. The SB particles exhibit a negative zeta potential of – 31 mV. Glass transition temperature (T_g) as well as minimum film forming temperature (MFFT) were found at 6 °C. Glass transition temperature was measured on a differential scanning calorimeter (Maia F3, Netzsch, Selb, Germany) while MFFT was determined on a *Kofler* bench (MFFT Bar Thermostair II, Coesfeld Materialtest, Dortmund, Germany). **Figure 1** shows the chemical structure of the carboxylated styrene-butadiene latex used in this study.

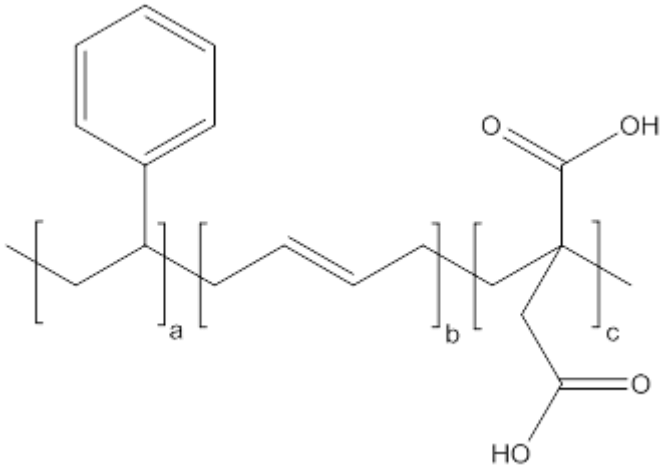

Figure 1 Chemical structure of the carboxylated styrene-butadiene copolymer.

In all experiments, cement pastes were prepared at a constant water to binder (w/b) ratio of 0.5. There, OPC or TBS powder was added to the mixing water or liquid SB dispersion and mixed on a vortex tumbler for one minute. SB dosages were 5, 10 or 20 % by weight of binder (bwob).

2.2 Isothermal heat flow calorimetry

The hydration reaction of OPC and TBS in the presence and absence of anionic SB latex was tracked via heat flow calorimetry using a TAM Air isothermal heat conduction calorimeter from Thermometric, Järfälla, Sweden. In a typical experiment, 4 g of OPC or TBS were mixed in a 10 mL tubular glass ampoule with the SB dispersion at a w/b ratio of 0.5. The glass ampoules were then sealed with a metal lid, shaken for 1 minute on a vortex tumbler to homogenize the paste and transferred into the instrument. Heat flow curves were recorded at 20 °C until heat release ceased.

2.3 In-situ X-ray diffraction

The time-dependent dissolution of the clinker phases or anhydrite and the formation of hydrate phases were monitored via in-situ XRD. Prior to measurement, 20 g of OPC or TBS were mixed in a 50 mL centrifuge tube with the SB dispersion at a w/b ratio of 0.5. The metal XRD sample container was filled with around 5 g of binder slurry and covered with a Kapton® polyimide foil in order to prevent carbonation and desiccation of the fresh paste. Immediately after preparation, measurement was started on a Bruker AXS D8 Advance (Bruker, Karlsruhe, Germany) equipped with a Bragg-Brentano geometry. During the first 16 hours complete scans were taken in intervals of 30 min. Measurements were taken in a range between 8 and 44° 2θ at a step size of 0.034° and a time per step of 144 s. The X-ray beam was generated from a Cu Kα X-ray source.

2.4 Analysis of cement pore solution

Ion chromatography (IC) and atomic absorption spectroscopy (AAS) were applied to quantify the concentrations of SO_4^{2-} (IC) and Ca^{2+} (AAS) ions respectively in pore solutions of SB-modified binder pastes. Binder slurries were prepared in a 50 mL centrifuge tube by adding 20 g of OPC or TBS to the SB dispersion at a w/b ratio of 0.5. The pastes were then shaken for 1 min on a vortex tumbler for homogenization and stored at room temperature for 0, 20, 40, 60 and 90 min. Next, the binder pastes were centrifuged for 10 min at 8,500 rpm (Biofuge Primo R, Heraeus Instruments, Hanau, Germany). The supernatant solution/dispersion was filtered over a 0.1 µm syringe filter in order to separate residual solids (mainly latex particles). 1 g of the

clear filtrate was adjusted to a neutral pH with 1 g of 0.8 wt.% hydrochloric acid and further diluted with 18 g of DI water. The Ca^{2+} concentration of the samples was analyzed via atomic absorption spectroscopy (Perkin Elmer 1100, Waltham, USA). For quantification of the SO_4^{2-} content, in a plastic vial, 0.8 mL from the AAS samples were further diluted with DI water to a total volume of 4 mL, sealed with a cap and measured via ion chromatography (ICS-2000 apparatus, Dionex, Idstein, Germany).

3. Results and discussion

3.1 Colloidal properties of the carboxylated styrene-butadiene copolymer

The aqueous dispersion of the carboxylated styrene-butadiene latex polymer exhibited a monodisperse particle size distribution of ~ 220 nm. For its preparation, the monomers styrene and butadiene were copolymerized with itaconic acid in an emulsion polymerization process. As a result, an anionic surface charge develops on the surface of the latex particles originating from the carboxylate groups. The specific anionic charge density of the SB particles depends on the pH value. In the alkaline cement pore solution the carboxylic groups are completely deprotonated and the maximum surface charge develops. Quantitative charge titration with a cationic polymer found a specific anionic charge density of - 42 C/g at pH 7, compared to - 52 C/g at pH 12.5 [22].

The carboxylate groups situated on the surface of the latex particles strongly interact with cations, as was presented in a previous paper [23]. Especially divalent cations

such as e.g Ca^{2+} are chelated by the carboxylate groups. This way, the SB particles significantly impact the ion composition of the cement pore solution.

3.2 Isothermal heat flow calorimetry

The reactivities of OPC and TBS in the presence and absence of the liquid SB latex (dosages: 5, 10 and 20 % bwob) were tracked via isothermal heat flow calorimetry.

The anionic SB copolymer significantly retards the hydration of ordinary Portland cement, as is shown in **Figure 2**. Depending on the dosage of the SB polymer, the maximum of the heat evolution is shifted from 9.5 to 40 hours owed to a prolonged dormant period. Complementary in-situ XRD measurements revealed that the silicate reaction and the portlandite formation are retarded, as was evidenced in the heat flow curves. Opposite to this, ettringite formation is almost completely suppressed in the presence of SB polymer. These effects can be ascribed to complexation of Ca^{2+} ions present in the cement pore solution and adsorption of the anionic SB particles onto positively charged clinker or hydrate phases.

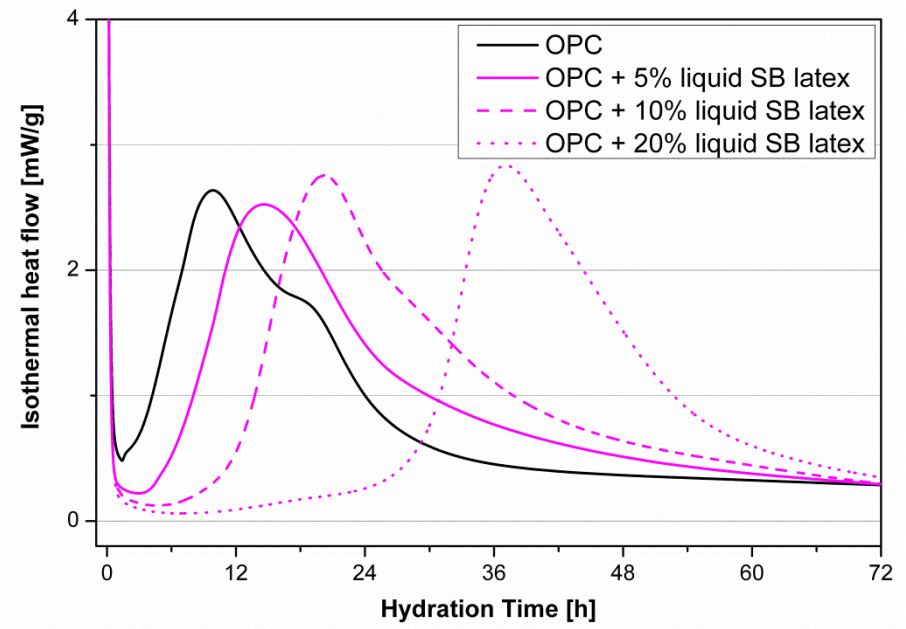

Figure 2 Time-dependent heat flow of OPC pastes recorded in the presence and absence of liquid SB latex (dosages: 5, 10 and 20 % bwoc.).

The ternary binder system shows a completely different hydration pathway which can be divided into an early aluminate reaction and a late silicate reaction, as displayed in **Figure 3**. From the calcium aluminum cement monocalcium aluminate (CA) dissolves very quickly and reacts with sulfate stemming from anhydrite, thus forming large quantities of ettringite. The silicate reaction of the OPC contained in the TBS occurs later compared to neat OPC.

In the presence of the SB polymer, both the ettringite formation and the silicate reaction are accelerated in the TBS. The first maximum of heat release is accelerated from 8 hours (neat TBS) to 2 hours at a latex dosage of 20 % bwob while the second heat maximum is shifted from 5.5 to 3.5 days. The higher the SB dosage, the more pronounced is this effect.

The calorimetric data clearly demonstrate that the effect of the anionic SB latex on the hydration of OPC and TBS differs completely. Depending on the mineral binder, anionic SB latex can either significantly accelerate (TBS) or retard (OPC) the hydration reaction.

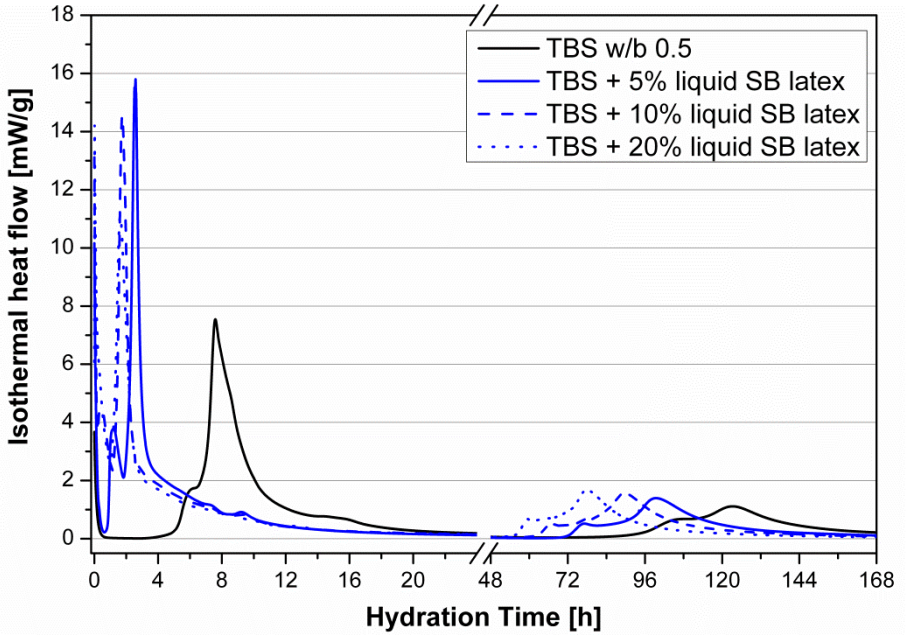

Figure 3 Time-dependent heat flow of TBS pastes recorded in the presence and absence of liquid SB latex (dosages: 5, 10 and 20 % bwob).

Exactly the same accelerating effect was found when instead of liquid SB latex a highly soluble sulfate salt like K_2SO_4 or Na_2SO_4 was added to the ternary binder system (see **Figure 4**). This result indicates that the effect of the SB polymer on the hydration of the TBS originates from its impact on the sulfate concentration in the pore solution.

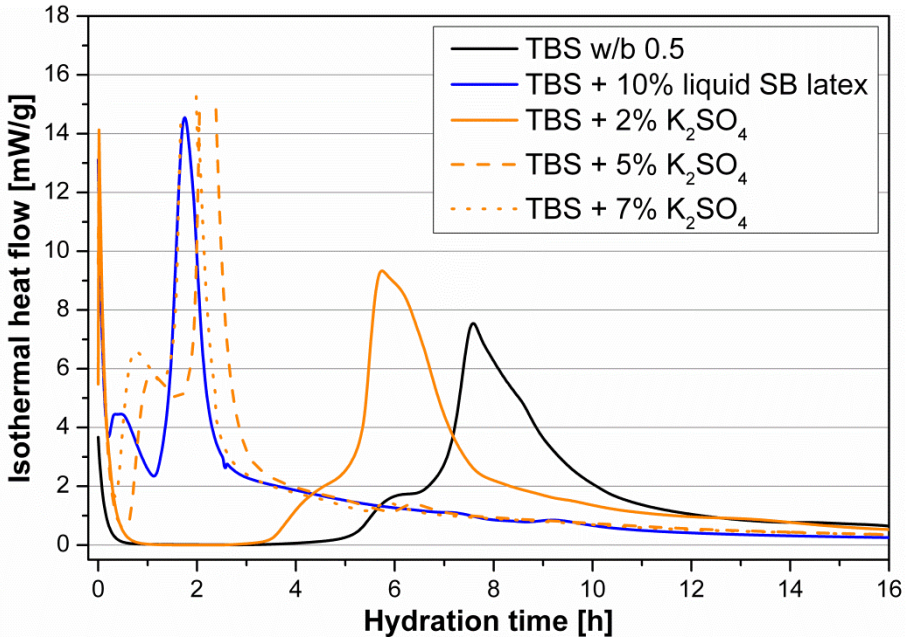

Figure 4 Time-dependent heat flow of TBS pastes recorded in the presence and absence of 10 % liquid SB latex or 2 - 7 % bwob K_2SO_4.

3.3 In-situ X-ray diffraction

The time-dependent dissolution of mineral phases or formation of hydration products from the ternary binder system was monitored over the first 16 h of hydration via in-situ XRD measurements.

Figure 5 displays the time-dependent XRD pattern (8 - 26 2Θ) for the hydration of the ternary binder system in the presence and absence of 10 % bwob of liquid SB latex. The signals appearing at 9.1, 15.8, 18.9 and 22.9 2Θ can be assigned to ettringite (E) whereas the peak at 25.5 2Θ represents anhydrite (AH). Obviously, the crystallization of ettringite starts within the first 5 h of hydration and correlates well with the dissolution of anhydrite, as evidenced by the weakening of the signal.

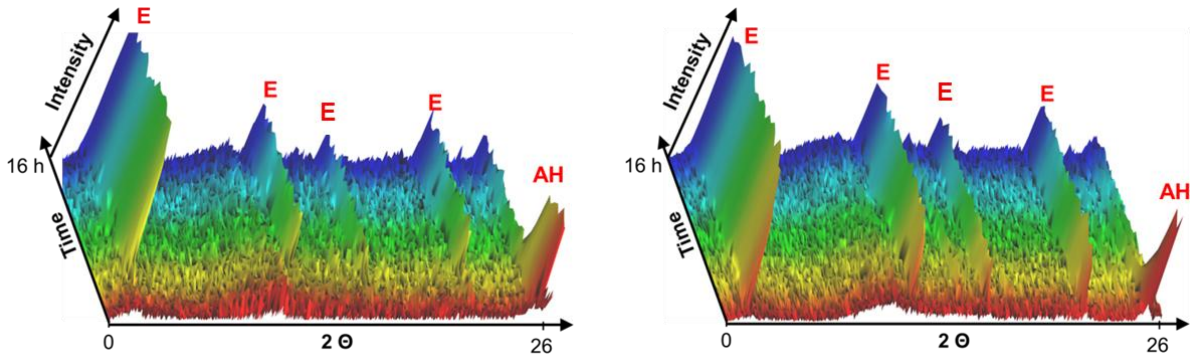

Figure 5 In-situ XRD pattern (8-26 2Θ, 0-16 h) of the hydrating OPC/CAC/anhydrite binder system in the absence (left) and presence (right) of 20 % bwob of liquid SB.

For a more precise evaluation of the data the ettringite formation and anhydrite dissolution were tracked within the first hours of hydration. Corresponding **Figure 6** and **Figure 7** show the formation of ettringite and the dissolution of anhydrite respectively during the first 2.5 h of hydration. Liquid SB dosages were 5, 10 and 20 % bwob. For this evaluation, the ettringite signal from 8-10 2Θ and the anhydrite signal from 24-26 2Θ were plotted.

The results confirm the significant acceleration of the early aluminate reaction of the TBS by anionic SB polymer. In the presence of liquid SB, both ettringite crystallization and anhydrite dissolution are shifted from 5 to 1.5 h at the highest SB dosage (20 % bwob). The higher the dosage of the SB polymer, the more pronounced is this effect. The XRD results confirm the calorimetric data where the first maximum of heat evolution was shown to shift to earlier times. Furthermore, the XRD data confirm that the massive early heat evolution observed in the calorimetry can be ascribed to the formation of ettringite which involves a strong exothermic reaction of the aluminate.

Exactly the same trend can be observed for the anhydrite dissolution. This result indicates that the formation of ettringite starts when anhydrite dissolution begins. Obviously, SB latex fosters the dissolution of anhydrite, e.g. via chelation of Ca^{2+} ions from the pore solution. As a consequence, the sulfate concentration in the pore solution increases and ettringite crystallization can start.

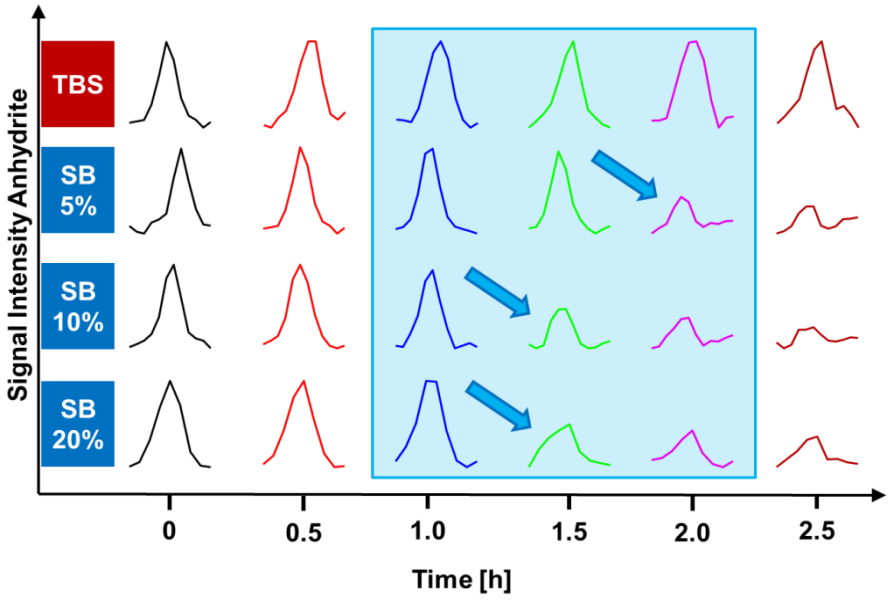

Figure 6 Time-dependent evolution of the anhydrite signal (24 - 26 2Θ) of the hydrating ternary binder system (w/b 0.5) in the presence and absence of 5, 10 and 20 % bwob of liquid SB, measured via in-situ XRD.

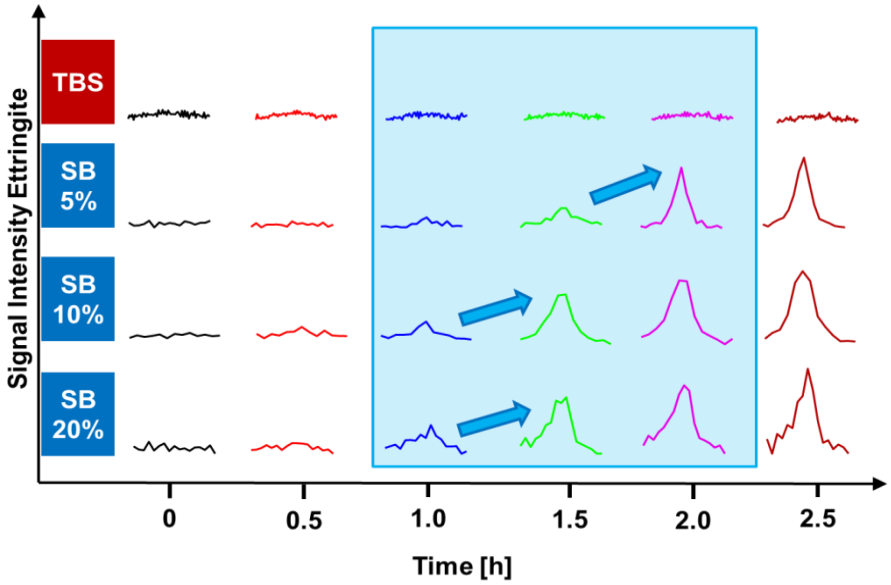

Figure 7 Time-dependent evolution of the ettringite signal (8 - 10 2Θ) of the hydrating ternary binder system (w/b 0.5) in the presence and absence of 5, 10 and 20 % bwob of liquid SB, measured via in-situ XRD.

3.4 Pore solution analysis

The time-dependent concentrations of the SO_4^{2-} and Ca^{2+} ions present in the TBS pore solutions were quantified via ion chromatography (SO_4^{2-}) and atomic absorption spectroscopy (Ca^{2+}).

Figure 8 presents the concentration of the sulfate ions in the pore solution of the ternary binder system within the first 90 min of hydration. In the presence of 10 % bwob of SB latex, the equilibrium concentration of sulfate in solution is increased from ~ 9 mg/L (neat TBS) to 12 - 14 mg/L. This result confirms that the dissolution of anhydrite is significantly accelerated in the TBS paste containing 10 % bwob of SB polymer. Furthermore, this explains the similar effects on the TBS

by SB polymer or a highly soluble sulfate (e.g. K_2SO_4 or Na_2SO_4), as was shown in **Figure 4**.

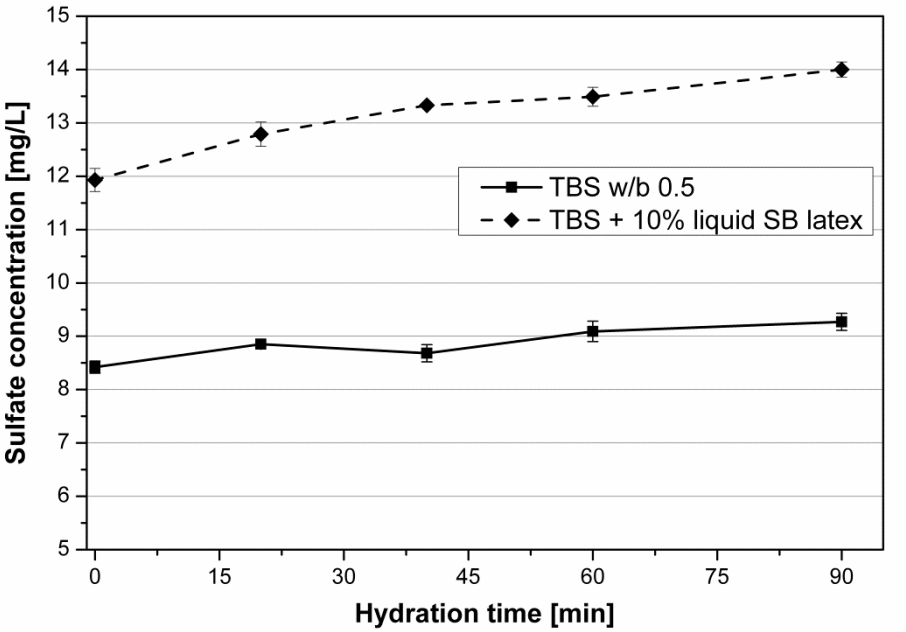

Figure 8 Concentration of sulfate ions present in the pore solution of the ternary binder system hydrating in the presence and absence of 10 % bwob of SB latex, measured during the first 90 min of hydration.

The evolution of the calcium ion concentration present in the pore solution of the ternary binder system within the first 90 min of hydration is displayed in **Figure 9**. For the neat TBS paste, the calcium ion concentration is slightly decreased from 660 to 570 mg/L within this time period. In the presence of 10 % bwob of SB latex, however, the Ca^{2+} concentration drops immediately from the beginning of hydration and becomes zero at a hydration time of 60 min.

Obviously, the anionic SB particles sequester Ca^{2+} ions from the pore solution via their carboxylate groups and thus reduce the Ca^{2+} concentration. This way, the

solution equilibrium for $CaSO_4$ is shifted and the dissolution of sulfate from anhydrite is enhanced. Additionally, the depletion of Ca^{2+} in the pore solution can be ascribed to the early ettringite formation which starts at the same time (see **Figure 7**).

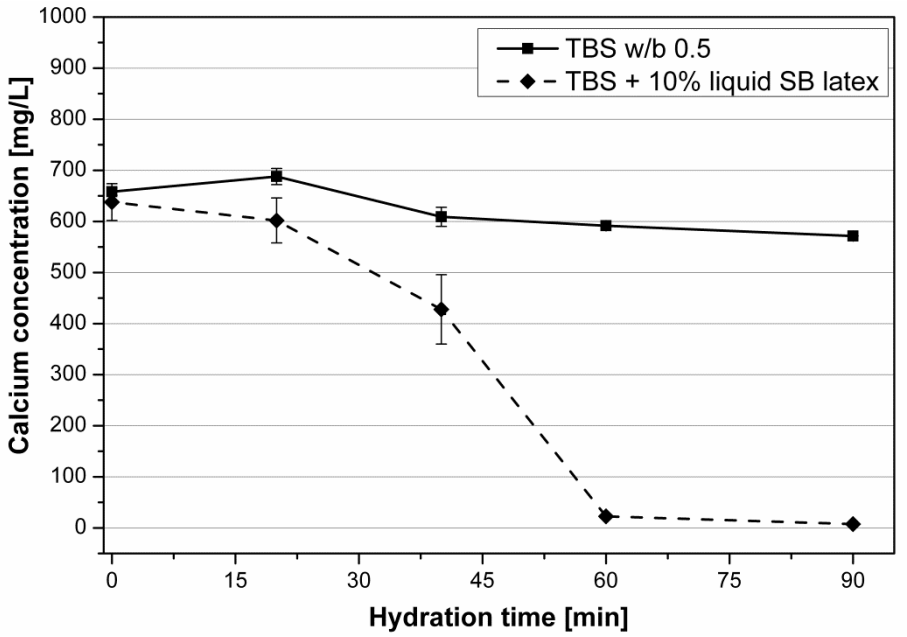

Figure 9 Calcium concentration present in the pore solution of the ternary binder system hydrating in the presence and absence of 10 % bwob SB latex, measured during the first 90 min of hydration.

In order to confirm whether the anionic SB latex indeed initiates the dissolution of anhydrite, time-dependent SO_4^{2-} and Ca^{2+} concentrations of aqueous anhydrite suspensions at pH of 12.5 were measured. The pH of the aqueous suspensions adjusted with sodium hydroxide simulates the alkaline conditions occurring in the pore solution of the ternary binder system. For this purpose, anhydrite was suspended in DI water at the same concentration as contained in the ternary binder system at a water-to-binder ratio of 0.5 and stirred at 750 rpm to prevent phase

separation. The amount of SB latex was that contained in a TBS paste at a dosage of 10 % bwob latex.

Figure 10 presents the molar concentrations of Ca^{2+} and SO_4^{2-} obtained from the aqueous anhydrite suspensions in the presence and absence of SB latex. For the neat anhydrite suspension the concentrations of Ca^{2+} and SO_4^{2-} increase over time. Their molar concentration is exactly the same since the molar ratio of Ca^{2+} and SO_4^{2-} is 1:1 in anhydrite. However, when anionic SB polymer is present in the anhydrite suspension, the Ca^{2+} concentration declines whereas the concentration of SO_4^{2-} increases significantly. This result clearly demonstrates that anhydrite dissolution is promoted in the presence of anionic SB latex. As illustrated in **Figure 11**, the anionic SB particles consume Ca^{2+} and remove them from the pore solution. Therefore, in systems containing SB latex the molar concentrations of Ca^{2+} and SO_4^{2-} differ from that in a neat anhydrite suspension.

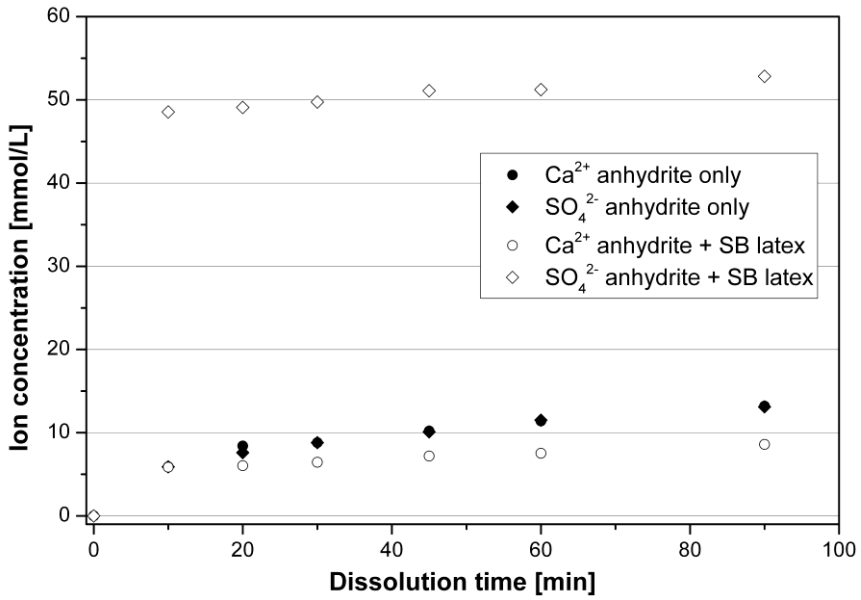

Figure 10 Time-dependent concentrations of Ca^{2+} and SO_4^{2-} of aqueous anhydrite suspensions in the presence and absence of SB latex.

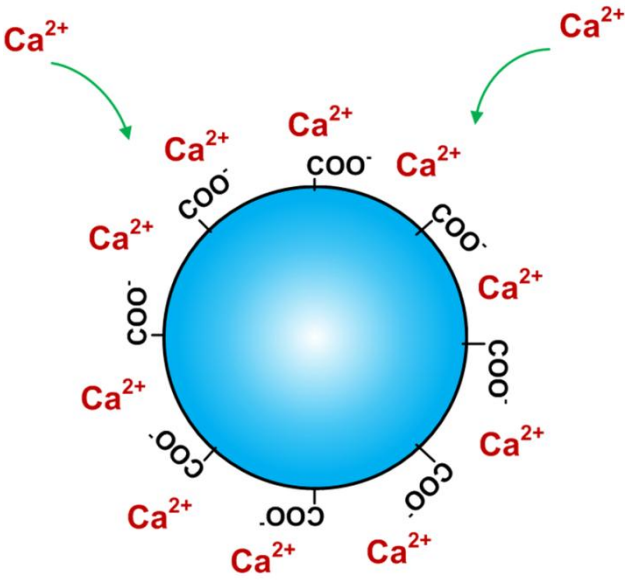

Figure 11 Schematic illustration of the sequestration of Ca^{2+} ions by carboxylate groups located on the latex particle surface of anionic SB particles.

4. Conclusion

Latex polymers represent key components in drymix mortars which often contain a combination of different inorganic binders (e.g. Portland cement, calcium aluminum cement, hemihydrate or anhydrite) in order to control the set and shrinkage behavior of the mortar. Ternary binder systems composed of Portland cement, calcium aluminum cement and anhydrite are used for applications such as self-leveling underlayments (SLUs) or repair mortars which require a fast setting and low shrinkage.

Our study demonstrates that the influence of latex polymers on the hydration of ternary binder systems is completely different, compared to that of ordinary Portland cement. For the anionic SB latex sample here significant retardation of OPC

hydration was found, characterized by a strong delay of the silicate reaction and an almost complete suppression of ettringite formation. Both effects were found to be owed to adsorption of the negatively charged latex particles onto positively charged surfaces of cement and the sequestration of cations from the cement pore solution.

Conversely, anionic SB latex significantly accelerates ettringite formation (aluminate reaction) in the ternary binder system OPC/CAC/anhydrite. Our experiments propose that the anionic latex particles foster the dissolution of sulfate from anhydrite and thus accelerate the crystallization of ettringite. The mechanism behind this effect is a shift in the solution equilibrium for $CaSO_4$ triggered by the sequestration of Ca^{2+} ions from the pore solution by the carboxylate groups present in the latex particles resulting in a a depletion of Ca^{2+} from solution. As a consequence, anhydrite dissolution is accelerated to compensate the depletion of Ca^{2+} ions and the sulfate concentration increases significantly, thus promoting early ettringite formation.

Our results suggest that tailor-made latex polymers not only can improve the well-known properties of fresh or hardened mortar such as adhesion, cohesion or flexural strength. Moreover, they also can positively impact the setting behavior of multicomponent mineral binder systems. Especially charged latex polymers (either negatively or positively) can interact with oppositely charged ions or mineral phases, thus providing unique effects.

References

[1] R. Bayer, H. Lutz, Dry mortars, Ullmann's encyclopedia of industrial chemistry, (2009) 541-579.

[2] H. Pöllmann, Calcium Aluminate Cements – Raw Materials, Differences, Hydration and Properties, Reviews in Mineralogy and Geochemistry, 74 (2012) 1-82.

[3] K.L. Scrivener, A. Campas, Calcium Aluminate Cement, Lea's Chemistry of Cement and Concrete, 13 (1998) 709-778.

[4] P. Gu, J.J. Beaudoin, E.G. Quinn, R.E. Myers, Early Strength Development and Hydration of Ordinary Portland Cement/Calcium Aluminate Cement Pastes, Advanced Cement Based Materials, 6 (1997) 53-58.

[5] P. Gu, Y. Fu, J.J. Beaudoin, A study of the hydration and setting behaviour of OPC-HAC pastes, Cement and Concrete Research, 24 (1994) 682-694.

[6] L. Amathieu, T. Bier, K.L. Scrivener, Mechanisms of set acceleration of Portland cement through CAC addition, Proceedings of the International Conference on Calcium Aluminate Cements, (2001) 303-317.

[7] C.E. Evju, C. Solberg, S. Hansen, Crystal structures of cementitious compounds - Part 2: Calcium aluminates and calcium alumino ferrites, ZKG International, 55 (2002) 80-84.

[8] S.A. Rodger, D.D. Double, The chemistry of hydration of high alumina cement in the presence of accelerating and retarding admixtures, Cement and Concrete Research, 14 (1984) 73-82.

[9] B.R. Currell, R. Grzeskowlak, H.G. Mldgley, J.R. Parsonage, The acceleration and retardation of set high alumina cement by additives, Cement and Concrete Research, 17 (1987) 420-432.

[10] T. Matusinović, D. Čurlin, Lithium salts as set accelerators for high alumina cement, Cement and Concrete Research, 23 (1993) 885-895.

[11] F. Goetz-Neunhoeffer, The function of Li carbonate and tartaric acid in the hydration of mixtures of calcium aluminate cement (CAC) with calicum sulfate hemihydrate ($CSH_{0.5}$), Cement International, 5 (2007) 90-101.

[12] J.-R. Hill, J. Plank, Retardation of setting of plaster of paris by organic acids: Understanding the mechanism through molecular modeling, Journal of Computational Chemistry, 25 (2004) 1438-1448.

[13] M. Bishop, A.R. Barron, Cement hydration inhibition with sucrose, tartaric acid, and lignosulfonate: Analytical and spectroscopic study, Industrial and Engineering Chemical Research, 45 (2006) 7042-7049.

[14] Y. Ohama, Handbook of Polymer-Modified Concrete and Mortars - Properties and Process Technology, Noyes Publications, New Jersey, 1995.

[15] A. Jenni, L. Holzer, R. Zurbriggen, M. Herwegh, Influence of polymers on microstructure and adhesive strength of cementitious tile adhesive mortars, Cement and Concrete Research, 35 (2005) 35-50.

[16] S. Chandra, P. Flodin, Interactions of polymers and organic admixtures on portland cement hydration, Cement and Concrete Research, 17 (1987) 875-890.

[17] A.M. Betioli, J. Hoppe, M.A. Cincotto, P.J.P. Gleize, R.G. Pileggi, Chemical interaction between EVA and Portland cement hydration at early-age, Construction and Building Materials, 23 (2009) 3332-3336.

[18] J. Plank, M. Gretz, Study on the interaction between anionic and cationic latex particles and Portland cement, Colloids and Surfaces A: Physicochemical and Engineering Aspects, 330 (2008) 227-233.

[19] R. Wang, X.G. Li, P.M. Wang, Influence of polymer on cement hydration in SBR-modified cement pastes, Cement and Concrete Research, 36 (2006) 1744-1751.

[20] D.A. Silva, H.R. Roman, P.J.P. Gleize, Evidences of chemical interaction between EVA and hydrating Portland cement, Cement and Concrete Research, 32 (2002) 1383-1390.

[21] Z. Su, J.M. Bijen, J.A. Larbi, Influence of polymer modification on the hydration of portland cement, Cement and Concrete Research, 21 (1991) 535-544.

[22] S. Baueregger, M. Perello, J. Plank, Influence of anti-caking agent kaolin on film formation of ethylene–vinylacetate and carboxylated styrene–butadiene latex polymers, Cement and Concrete Research, 58 (2014) 112-120.

[23] S. Baueregger, M. Perello, J. Plank, Role of PVOH and kaolin on colloidal stability of liquid and powder EVA and SB latexes in cement pore solution, Colloids and Surfaces A: Physicochemical and Engineering Aspects, 434 (2013) 145-153.

Paper #6

Use of a Nano Clay for Early Strength Enhancement of Portland Cement

S. Baueregger, L. Lei, M. Perello, J. Plank

Proceedings of the 5th International Symposium on Nanotechnology in Construction (NICOM 5)

(submitted on August 14, 2014, accepted)

Use of a Nano Clay for Early Strength Enhancement of Portland Cement

Stefan Baueregger[*], Lei Lei[*], Margarita Perello[+] and Johann Plank[*]

[*] Technische Universität München, Chair for Construction Chemistry, Lichtenbergstraße 4, 85747 Garching, Germany, sekretariat@bauchemie.ch.tum.de

[+] Dow Europe GmbH, Bachtobelstraße 3, 8810 Horgen, Switzerland, mperello1@dow.com

Abstract

In this study it is reported that additions of kaolin, a natural and abundant clay mineral, can significantly increase the early strength of Portland cements. Its effectiveness greatly depends on the particle size which ideally should be less than 500 nm. For example, 5 % by weight of cement of nano-sized kaolin (d ~ 200 nm) increased the 16 hrs compressive and tensile strengths of a CEM I 42.5 R sample by 50 % and 60 % respectively. Strength enhancement occurs predominantly in slower reacting cements (CEM I 32.5, 42.5). Analysis via heat flow calorimetry and X-ray diffraction revealed that the nano clay in particular activates the hydration of the silicate phases C_3S and C_2S. Furthermore, rheological measurements evidenced an only minor effect on mortar viscosity. The results suggest that nano-sized kaolin represents an inexpensive additive which can boost the early strength of Portland cement without negatively affecting workability and other properties.

1 Introduction

Nanoparticles (e.g. nano silica) are known to increase the strength and durability of concrete or mortar. Capillary pores present in the cementitious matrix are filled with these nano particles resulting in an optimized packing density of the microstructure. Thus, strength of the hardened cement is enhanced and permeability is decreased by this filling effect. A typical application of micro and nano silica is ultra-high performance concrete (UHPC) where the interstitial spaces between cement and aggregates are filled completely with graded solids [1-5].

Furthermore, also nano C-S-H crystals (X-Seed®, BASF) prepared through templating with PCE superplasticizers were found to accelerate the silicate reaction of cement significantly and therefore enhance the early strength. The main advantage of this product compared to conventional accelerators is that the final strength is not negatively impacted which is the major drawback of e.g. calcium salts such as $CaCl_2$, $Ca(NO_3)_2$ or $Ca(HCOO)_2$. When dispersed in the cement pore solution these nano C-S-H particles initiate the crystallization of C-S-H by acting as seeding crystals. Owed to this homogeneous nucleation, the activation energy

for C-S-H crystallization from cement is reduced, leading to accelerated formation of hydrate phases and early setting [6, 7].

Clay minerals which represent aluminosilicates are known to decrease the workability of concrete or mortar severely. Especially harmful is montmorillonite which can chemically sorb conventional polycarboxylate superplasticizers in its interlayer region [8]. Additionally, clay minerals decrease the final strength of concrete. Their layered structure and high surface area allow the incorporation and sorption of large quantities of water molecules, leading to a swelling of the clay particles. This way, workability is decreased by the significant water consumption and the microstructure is negatively impacted due to the presence of hydrated clay particles.

Upon calcination, the crystalline structure present in most clays is decomposed. Calcined clay minerals (e.g. metakaolinite) are amorphous pozzolanic materials which are known to boost the final strength of cement. These partially or non-crystalline aluminosilicates convert with calcium hydroxide in a pozzolanic reaction to C-S-H phases which contribute to the final strength. Supplementary cementitious materials (SCMs) such as fly ash or blast furnace slag which contain non-crystalline silica show a similar behavior. In composite cements (CEM II and III), these pozzolanic active SCMs are used to partially substitute cement clinker. Unfortunately, these materials possess a low reactivity only and therefore do not increase the early strength of cement [9-12].

Here, we present the possibility to enhance the early strength of Portland cement by adding crystalline nano-sized kaolin clay.

2 Materials and methods

For investigation of the material properties of Portland cement in the presence of nano clays, two types of kaolin, namely K1 (KaMin HG90, KaMin LLC, Macon, US) and K2 (Chinafill 800, Amberger Kaolinwerke, Hirschau, Germany) were used. Their main difference is the particle size distribution, as is shown in **Fig. 1a**. Accordingly, the specific surface area and the anionic surface charge of K1 is higher compared to K2, due to the smaller particle size of K1. **Table 1** summarizes these results.

The XRD pattern (**Fig. 1b**) of the kaolin powder samples revealed crystallinity for both K1 and K2. Sample K2 contains minor amounts of illite clay and quarz impurities. SEM analysis of the clay samples (**Fig. 2**) revealed the characteristic platelet shape of the kaolin particles.

The cement used in this study was a CEM I 52.5 N (d_{50} = 11.8 µm, HeidelbergCement, Geseke plant, Germany). For comparison, cement samples CEM I 42.5 R (d_{50} = 18.1 µm) and CEM I 52.5 R (d_{50} = 4.5 µm, Schwenk, Allmendingen plant, Germany) were used.

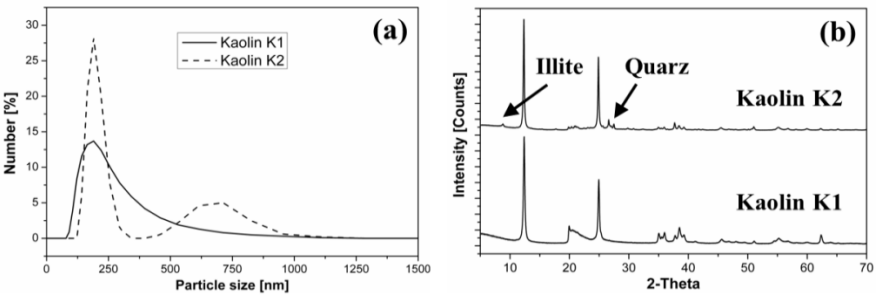

Fig. 1. (a) Particle size distribution, measured via dynamic light scattering (DLS), and (b) powder XRD pattern of the kaolinite samples K1 and K2.

Compressive and tensile strength tests were carried out after 12, 16, 24 h and 28 d. Mortar specimens (nine prisms for each system, size: 160*40*40 mm) were prepared and tested according to DIN EN 196-1 at a w/c ratio of 0.5 for each system. The kaolin was added in two ways: (a) dry-blended together with cement and sand before addition of water and (b) dispersed in the mixing water via sonication.

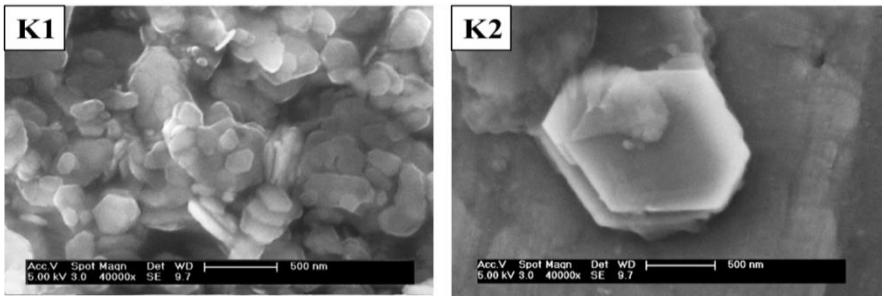

Fig. 2. Scanning electron mircoscope (SEM) images of dry kaolin samples K1 (left) and K2 (right).

For further characterization, hydration of OPC pastes in the presence and absence of kaolin was monitored via isothermal heat flow calorimetry at 20 °C and through in-situ XRD measurements. Ion contents present in cement pore solutions were analyzed via atomic absorption spectroscopy (AAS).

Table 1. pH-dependent anionic charge density and specific surface area (BET) of the kaolinite samples K1 and K2.

Sample	Anionic charge amount [C/g]			Specific surface area, BET [m^2/g]
	pH 7	pH 12.5	SCPS	
Kaolin K1	- 2.1	- 5.9	- 3.1	21
Kaolin K2	- 1.0	- 2.5	- 1.6	10

3 Results and discussion

3.1 Compressive and tensile strength

The 16 h compressive and tensile strength of mortars prepared from CEM I 52.5 N with the addition of kaolin samples K1 and K2 at dosages of 1, 2 and 5 % bwoc are presented in **Fig. 3**. It was found that both, the 16 h compressive and tensile strength, were significantly increased when kaolin was present in the mortar.

The effect of strength enhancement depends on the dosage of the kaolin clay – the higher the dosage, the more pronounced is this effect. Additionally, this effect depends on the mode of kaolin addition, whether it is dry-blended together with cement and sand before mixing with water, or whether the clay is dispersed in the mixing water via sonication. The strongest enhancement of early strength can be achieved when kaolin is dispersed in the mixing water. For example, mortars prepared with 5 % of kaolin dispersed in the mixing water revealed a boost of compressive and tensile strength of around 30 % with CEM I 52.5 N.

Upon sonication, the kaolin agglomerates are decomposed and individual kaolin platelets are present in the mixing water. This confirms that the effect of kaolin on strength development much depends on the particle size of the clay mineral.

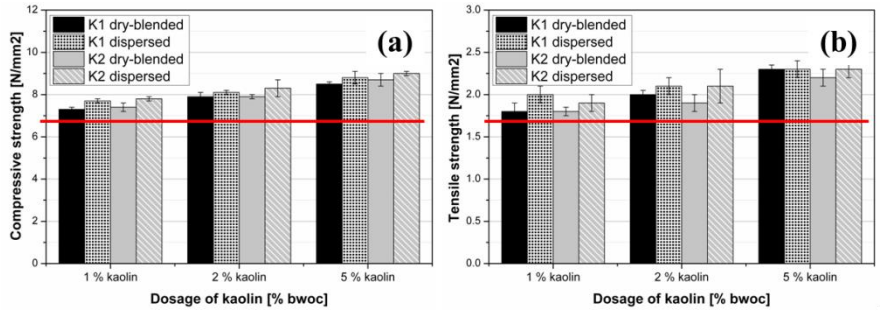

Fig. 3. Compressive (left) and tensile (right) strength after 16 h of mortar specimens prepared from CEM I 52.5 N containing 1, 2 or 5 % bwoc of kaolin sample K1 or K2. The red line represents the strength of the reference mortar without kaolin.

Table 2 presents the time-dependent results for the compressive and tensile strength of mortars prepared from CEM I 52.5 N and sample K2. Remarkably, by this kaolin strength is only enhanced at a curing time of 16 hours. Another interesting effect is that the final strength (28 days) is not negatively influenced by nano kaolin.

Table 2. Compressive and tensile strength of CEM I 52.5 N after 12, 16, 24 h and 28 d in the presence and absence of 2 % bwoc kaolinite K2 (dispersed).

	Compressive / tensile strength [N/mm^2]			
	12 h	16 h	24 h	28 d
CEM I 52.5 N	3.0 / 0.9	7.1 / 1.7	14.2 / 3.5	73.1 / 8.3
CEM I 52.5 N + 2 % K2	3.0 / 0.9	8.3 / 2.1	14.6 / 3.5	73.4 / 8.3

For comparison, the effect of kaolin sample K2 on the 16 h early strength of CEM I 42.5 R and CEM I 52.5 R was tested. As is shown in **Table 3**, 5 % of K2 increase the compressive strength of CEM I 42.5 R by around 50 % and the tensile strength up to 60 %. For this slowly reacting cement a much stronger effect on the 16 h early strength is observed compared to previous CEM I 52.5 N (**Table 2**).

In contrast, no enhancing effect of kaolin on the strength of the much faster reacting CEM I 52.5 R can be seen. This result indicates that nano kaolin especially boosts the early strength of cements which exhibit a low reactivity. Here, the ion concentration in pore solution is lower compared to fast reacting cements, thus initiation of crystallization affects the overall hydration rate more.

Table 3. 16 h compressive and tensile strengths of CEM I 42.5 R and CEM I 52.5 R in the presence and absence of 2 % bwoc of kaolin sample K2 (dispersed).

System	Compressive strength [N/mm^2]	Tensile strength [N/mm^2]
CEM I 42.5 R	4.5	1.2
CEM I 42.5 R + 1 % K 2	5.1	1.4
CEM I 42.5 R + 2 % K 2	5.9	1.6
CEM I 42.5 R + 5 % K 2	6.6	1.9
CEM I 52.5 R	26.2	5.5
CEM I 52.5 R + 2 % K 2	26.1	6.0
CEM I 52.5 R + 5 % K 2	26.7	5.7

3.2 Heat calorimetry

Fig. 4 shows the isothermal heat flow curves of cement pastes prepared from CEM I 52.5 N in the presence and absence of 1, 2 and 5 % bwoc of kaolin sample K1 which was dispersed in the mixing water via sonication. The result clearly demonstrates that the overall heat of hydration increases with increasing dosage of the kaolin clay whereas the time of the maximum heat flow is not affected. In the presence of kaolin, the slope in the cumulative heat of hydration curve particularly increases between 12 and 20 hours. During this time period, cement hydration is promoted by kaolin K1. A similar trend was found for kaolin K2. These observations explain the results for the compressive and tensile strengths which in the presence of kaolin are especially increased around 16 h.

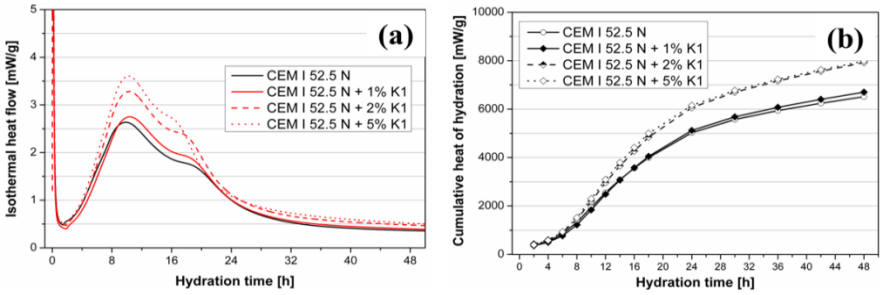

Fig. 4. (a) Isothermal heat flow and (b) cumulative heat of hydration of cement pastes (CEM I 52.5 N) modified with 1, 2 or 5 % bwoc of kaolin sample K1.

3.3 In-situ X-ray diffraction

Complementary to the calorimetric tests, the formation of crystalline hydrate phases during cement hydration was monitored for the first 48 h via in-situ XRD. **Fig. 5** presents the time-dependent evolution of the hydrate phases portlandite and ettringite. In the kaolin modified cement pastes, especially portlandite formation is significantly enhanced and ettringite formation is slightly increased. Thus, the XRD results confirm an enhanced silicate reaction which is responsible for strength development. Again, this effect is linked to the dosage of kaolin clay. The higher the dosage, the more pronounced is this effect. These results explain the increased heat flow observed for cement pastes containing kaolin, as presented above (**Fig. 4**).

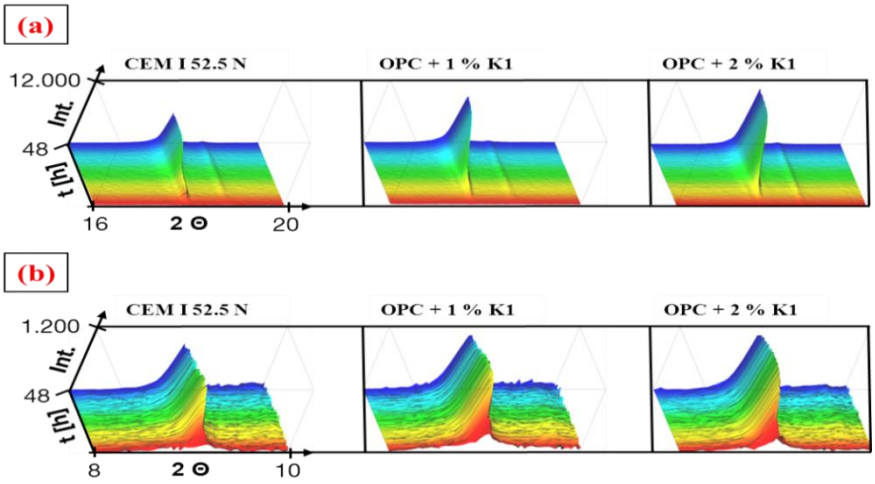

Fig. 5. Time-dependent evolution of (a) portlandite and (b) ettringite in cement pastes (CEM I 52.5 N) modified with 1 or 2 % bwoc of kaolin K1, measured via in-situ XRD.

3.4 Analysis of cement pore solution

Analysis of the cement pore solution demonstrates that the concentration of Al^{3+} is increased in the presence of kaolin K1 and K2, whereas the concentrations of Ca^{2+}, K^+ and SO_4^{2-} are not influenced. Obviously, aluminum is leached from the kaolin clay into the alkaline cement pore solution and forms tetra hydroxo aluminate $[Al(OH)_4]^-$. This result explains the acceleration of the aluminate reaction in the presence of kaolin.

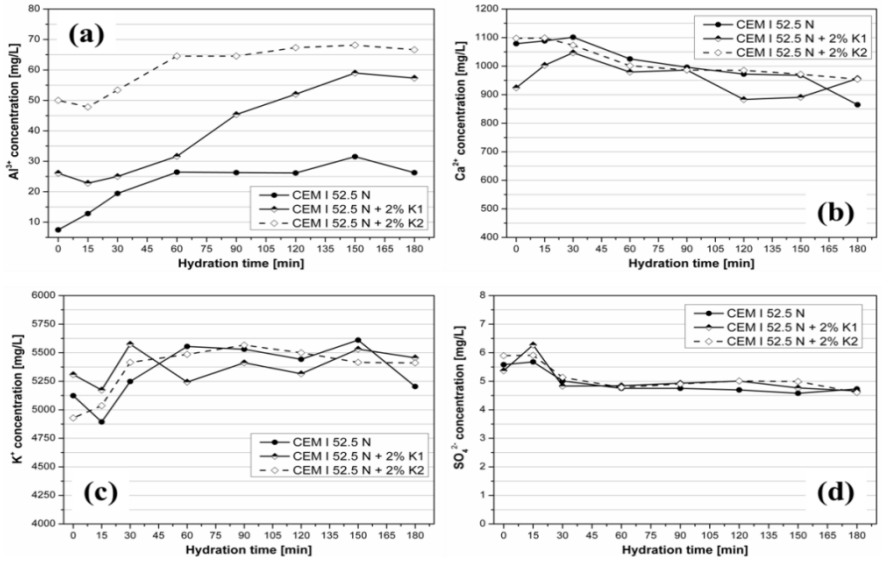

Fig. 6. Time-dependent concentrations of (a) Al^{3+}, (b) Ca^{2+}, (c) K^+ and (d) SO_4^{2-} in cement pore solutions of CEM I 52.5 N in the presence and absence of 2 % bwoc of kaolin samples K1 and K2.

4 Conclusion

Our study demonstrates that nano kaolin clay can boost the early 10-24 h compressive and tensile strength of Portland cement without negatively impacting the final strength after 28 d. This effect is not caused by an optimized particle packing of the cementitious matrix (filler effect). Instead, such nano-sized kaolin clay increases the reactivity of the silicate and aluminate phases, as was evidenced via calorimetric and in-situ XRD measurements.

It was found that this effect is linked to the particle size and the mode of addition of the nano clay to mortar (dry-blended into cement or dispersed in the mix-

ing water). A potential explanation for its performance is a seeding effect. Owed to heterogeneous nucleation, the activation energy for the crystallization of cement hydrates is reduced and thus early strength development is promoted. Additionally, aluminum is dissolved from kaolin into the cement pore solution, as was evidenced via AAS. This way, the crystallization of the aluminate hydrates is initiated.

References

1. Shaikh F., Supit S., Sarker P. (2014) A study on the effect of nano silica on compressive strength of high volume fly ash mortars and concretes. Mater. Des. 60:433-442.
2. Biricik H., Sarier N. (2014) Comparative study of the characteristics of nano silica-, silica fume- and fly ash-incorporated cement mortars. Mat. Res. 17:570-582.
3. Oltulu M., Sahin R. (2014) Pore structure analysis of hardened cement mortars containing silica fume and different nano-powders. Con. Build. Mat. 53:658-664.
4. Haruehansapong S., Pulngern T., Chucheepsakul S. (2014) Effect of the particle size of nanosilica on the compressive,strength and the optimum replacement content of cement mortar containing nano-SiO_2. Con. Build. Mat. 50:471-477.
5. Abd El Aleem S., Heikal M., Morsi WM. (2014) Hydration characteristic, thermal expansion and microstructure of cement containing nano-silica. Con. Build. Mat. 59:151-160.
6. Bräu M., Ma-Hock L., Hesse C., Nicoleau L., Strauss V., Treumann S., Wiench K., Landsiedel R. Wohlleben W. (2012) Nanostructured calcium silicate hydrate seeds accelerate concrete hardening: a combined assessment of benefits and risks. Arch. Toxicol. 86:1077-1087.
7. Thomas J., Jennings H., Chen J. (2009) Influence of Nucleation Seeding on the Hydration Mechanisms of Tricalcium Silicate and Cement. J. Phys. Chem. 113:4327-4334.
8. Lei L., Plank J. (2014) A Study on the Impact of Different Clay Minerals on the Dispersing Force of Conventional and Modified Vinyl Ether Based Polycarboxylate Superplasticizers. Cem. Concr. Res. 60:1-10.
9. Rashad AM. (2014) A comprehensive overview about the effect of nano-SiO_2 on some properties of traditional cementitious materials and alkali-activated fly ash. Con. Build. Mat. 52:437-464.
10. Quercia G., Spiesz P., Husken G., Brouwers H. (2014) SCC modification by use of amorphous nano-silica. Cem. Concr. Compos. 45:69-81.
11. Morsy M., Al-Salloum Y., Almusallam T., Abbas H. (2014) Effect of nano-metakaolin addition on the hydration characteristics of fly ash blended cement mortar. J. Therm. Anal. Calorim. 116:845-852.
12. Frias M., Martinez-Ramirez S. (2009) Use of micro-Raman spectroscopy to study reaction kinetics in blended white cement pastes containing metakaolin. J. Raman Spectrosc. 40:2063-2068.

Contributions which are not part of this thesis

Paper #7-9

Paper #7

A kinetic and mechanistic investigation on the film formation of a carboxylated styrene-butadiene latex

S. Baueregger, M. Perello, J. Plank

GDCh Monographie

46 (2013), 57-60

A Kinetic and Mechanistic Investigation on the Film Formation of a Carboxylated Styrene-Butadiene Latex

S. Baueregger[1], M. Perello[2], J. Plank[1]
[1] Technische Universität München, Chair for Construction Chemicals, Garching, Germany
[2] Dow Europe GmbH, Horgen, Switzerland

Introduction

Latex dispersions are well known as important ingredients in paints, coatings and adhesives. A key property of latex polymers is their ability to form flexible and homogeneous polymer films after dehydration. Thus, latex polymers improve the properties of fresh and hardened cement such as cohesion, adhesion or flexural strength. Liquid latex dispersions are produced via emulsion polymerization. For the application in drymix mortars, these latex dispersions are spray dried under addition of colloidal stabilizers (e.g. polyalcohols) and anti-caking agents (e.g. clays) to obtain a free-flowing powder /1/.
The film forming process of latex polymers can be divided into four main stages: first, polymer particles are randomly dispersed in water. After removal of water, a dense particle packing is achieved. Upon wet or dry sintering or capillary deformation, the latex particles start to deform in order to minimize their surface free energy. In the final step, particle coalescence occurs and a homogeneous polymer film is achieved /2/.
Environmental scanning electron microscopy (ESEM) allows to study wet samples in their native state and is therefore an appropriate method for monitoring of the drying process of latex dispersions /3/.
In our study the kinetics of the film formation and the stages occurring during dehydration of a carboxylated styrene-butadiene latex were investigated using ESEM imaging.

Materials

The polymer used in this study was a carboxylated styrene-butadiene latex with a monodisperse particle size distribution around 220 nm. Due to the incorporation of itaconic acid into the SB copolymer, the surface of the latex particles was negatively charged owed to

carboxylate groups. The corresponding re-dispersible powder (RDP) was obtained by spray drying of the mother liquor under addition of PVOH as colloidal stabilizer and kaolin as anti-caking agent. **Table 1** summarizes the properties of the latex samples used in this study.

Table 1: Composition and properties of the liquid latexes and the latex samples reconstituted from the re-dispersible powder.

Property or component	SB latex	SB powder
Particle size [nm]	220	150 - 600
Zeta potential [mV]	- 31	- 25
T_g [°C]	6	6
Colloidal stabilizer	-	PVOH
Anti-caking agent	-	Kaolin

Results and discussion

First, the rate of the polymer film formation was investigated via time-dependent ESEM imaging. The objective was a comparison of the kinetics of film formation for the mother liquor and its corresponding re-dispersible powder. The aim was to evaluate the potential influence of the auxiliary additives PVOH and kaolin on the rate of film formation.
Aqueous latex dispersions with a polymer content of 5 wt.-% prepared from the mother liquor or RDP were deposited on the ESEM sample holder and stored at room temperature. After defined time intervals the samples were transferred into the ESEM instrument and imaging was carried out following a test protocol established by Gretz *et al.* /4/. Cooling of the sample to a temperature below the MFFT in combination with a gentle pump-down sequence ensured that in the ESEM chamber no premature film formation could occur.

The results show that film formation of the latex reconstituted from the powder occurs faster, compared to its liquid precursor. **Fig. 1** compares the progress of the film forming process for the SB liquid and powder latex after a drying time of 3 h. The liquid latex sample still exhibits individual particles which are densely packed whereas the latex prepared from the RDP already shows a homogeneous polymer film.
Basically, the process of film formation can be divided into two steps, the evaporation of water and the subsequent latex particle coalescence. Measurements of the weight loss of the dispersions over time confirmed that the accelerated film formation of the RDP is not caused by a faster evaporation rate. Consequently, acceleration of the film formation of RDP is owed to the second step of the process, the

particle coalescence. From spray dried model powders containing only PVOH or kaolin it was found that the anti-caking agent kaolin is responsible for the acceleration of the film formation whereas PVOH retards the film formation. Upon spray drying, PVOH coats the latex particles and thus prevents particle coalescence because the PVOH layer acts as a barrier between the latex cores /5/. Kaolin overrides the retarding effect of PVOH on film formation by enhancing particle interpenetration. Exactly the same behaviour was found for a non-ionic ethylene-vinylacetate copolymer. This allows to generalize the positive effect of kaolin on film formation.

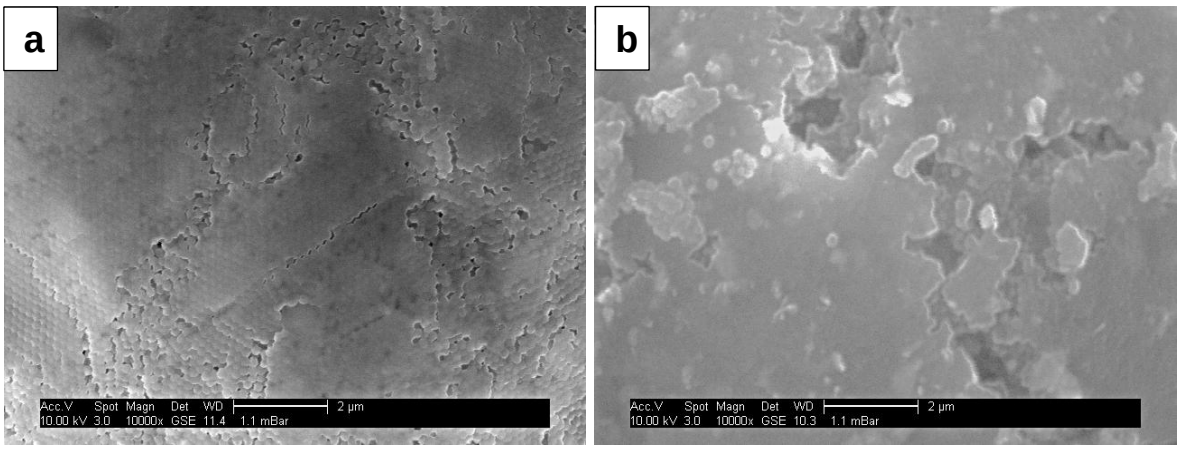

Fig. 1: ESEM micrographs of the SB film prepared from the liquid latex (a) and latex reconstituted from powder (b) after 3 h of storage at room temperature.

As a next step, the film forming mechanism of the SB latex polymer was investigated. By using ESEM imaging, the different stages occurring during the dehydration of the aqueous SB dispersion were analyzed. The SB dispersion was deposited on an aluminum container and stored under ambient conditions. Images of the samples were captured at different points of time to monitor the time-dependent progress of film formation and to evaluate the different stages occurring during the drying process. Here, the aim was to analyze the surface and the core of the latex samples to find out whether the progress of particle coalescence was different on the surface and in the inner sphere of a latex particle. For analysis of the inner section, the samples were sliced with a scalpel and the cut surface was looked at.
There, it was found that the latex particles had arranged in well-ordered domains, similar to that of colloidal crystals. The monodisperse particles self-assemble in a hexagonal or cubic close packing. Within these domains, particle interpenetration is more advanced due to the high packing density there (**Fig. 2**). Regular arrays of particles in domains distributed across the entire polymer matrix are observed.

When dehydration of the dispersion continues, particle coalescence proceeds until a coherent and homogeneous film is formed. The results allow to conclude that particle coalescence first begins in these domains whereby layers of polymer films are formed.

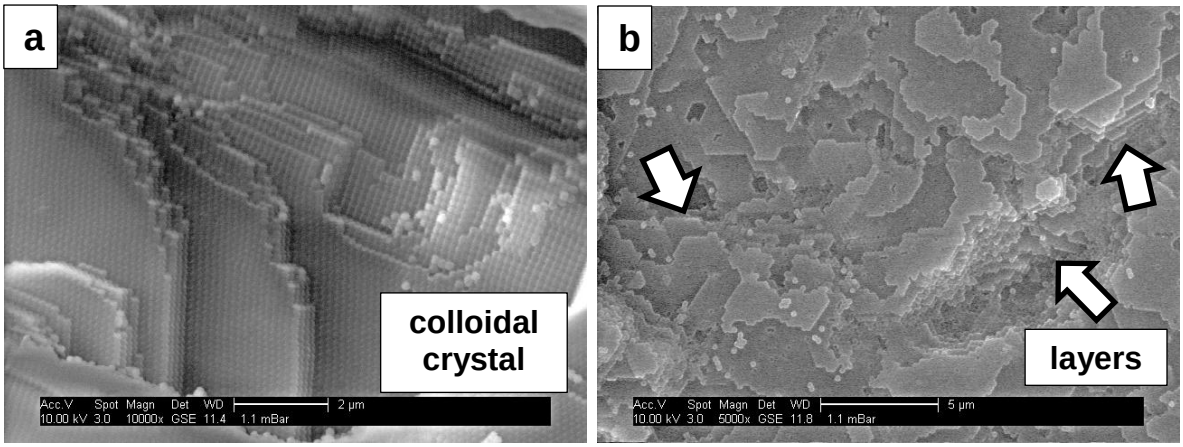

Fig. 2: ESEM micrographs of SB latex (a) at the stage of dense particle packing showing the arrangement of particles in domains and (b) beginning film formation within these domains showing layers which later spread across the entire matrix.

Conclusion

Our experiments reveal that PVOH and kaolin do not only represent auxiliaries for the spray drying of latex dispersions. Instead, they significantly impact key properties of latexes such as the rate of film formation and their colloidal stability. Upon drying, monodisperse latexes self-assemble as colloidal crystals and form well-ordered arrays. Apparently, film formation does not occur randomly. Instead, particle coalescence starts within such domains before it spreads across the entire matrix.
Our results confirm that the overall behaviour of latexes much depends on their colloidal properties such as particle size or surface charge.

Bibliographical references

/1/ Y. Ohama: “Handbook of Polymer-Modified Concrete and Mortars - Properties and Process Technology”, Noyes Publications (1995).
/2/ J.L. Keddie: “Film formation of latex” Mater. Sci. Eng. R-Rep., (1997) 21, 101-170.
/3/ O. Islam, K.I. Dragnevski, C.R. Siviour: “On some aspects of latex drying - ESEM observations”, Prog. Org. Coat., (2012) 75 , 444-448.
/4/ M. Gretz, J. Plank: “An ESEM investigation of latex film formation in cement pore solution”, Cem. Concr. Res., (2011) 41, 184-190.
/5/ S. Baueregger, M. Perello, J. Plank: “Role of PVOH and Kaolin on Colloidal Stability of Liquid and Powder EVA and SB Latexes in Cement Pore Solution”, Colloid Surf. A: Physicochem. Eng. Asp., (2013) 434, 145-153.

Paper #8

Einfluss von Latexpolymeren auf die Hydratation von Portlandzement sowie des ternären Bindemittelsystems OPC / CAC / Anhydrit

S. Baueregger, M. Perello, J. Plank

GDCh Monographie

47 (2014), 248-251

Einfluss von Latexpolymeren auf die Hydratation von Portlandzement sowie des ternären Bindemittelsystems OPC / CAC / Anhydrit

S. Baueregger[1], M. Perello[2], J. Plank[1]
[1] Technische Universität München, Chair for Construction Chemicals, Garching, Germany
[2] Dow Europe GmbH, Horgen, Switzerland

Einleitung

Latexpolymere sind wesentliche Bestandteile vieler Trockenmörtelformulierungen. Sie verbessern die Kohäsion und Adhäsion des frischen Mörtels auf Oberflächen sowie die Flexibilität des Zementsteingefüges. Für die Verwendung in Trockenmörteln werden Dispersionspulver ausgehend von wässrigen Latexdispersionen mittels Sprühtrocknung unter Zugabe von Sprühhilfen hergestellt. /1/

Zur Beschleunigung der Festigkeitsentwicklung enthalten bestimmte Trockenmörtelformulierungen wie z.B. Reparaturmörtel oder Selbstverlaufsmassen neben Portlandzement auch Calciumaluminatzement. Einige Applikationen erfordern zudem ein geringes Schwindverhalten, weshalb ternäre Bindemittelsysteme bestehend aus OPC, CAC und Anhydrit zum Einsatz kommen. /2, 3/

In dieser Studie wurde der Einfluss von nichtionischen Ethylen-Vinylacetat und anionischen Styrol-Butadien Dispersionen bzw. Dispersionspulvern auf die Hydratation von Portlandzement sowie des ternären Bindemittelsystems OPC / CAC / Anhydrit untersucht.

Materialien und Methoden

Für die Untersuchungen wurden nichtionische Ethylen-Vinylacetat (EVA) sowie anionische Styrol-Butadien (SB) Copolymere verwendet. Beide Polymere wurden als Dispersion und Dispersionspulver (RDP) eingesetzt, um den Einfluss der Sprühhilfen Polyvinylalkohol (PVOH) und Kaolin ermitteln zu können. Die anionische Ladung des Styrol-

Butadien Copolymers wurde durch Einbau von Itaconsäure in das SB Polymer generiert. **Tabelle 1** zeigt die Eigenschaften der Polymere.

Tabelle 1: Chemische Eigenschaften der EVA und SB Copolymere /4/.

Eigenschaft	SB latex	EVA latex
Partikelgröße [nm]	220	300 - 1500
Zeta potential [mV]	- 31	- 17
T_g / MFFT [°C]	+ 6 / + 6	+ 20 / + 3

Als Bindemittel wurde ein Portlandzement CEM I 52.5 N (Milke® classic, HeidelbergCement) verwendet. Das ternäre Bindemittelsystem wurde aus folgenden Komponenten formuliert: OPC CEM I 52.5 N (83.08 %), CAC (Ternal® White, Kerneos) mit 70 % Al_2O_3-Gehalt (10.72 %), Anhydrit II (5.36 %), Li_2CO_3 (0.27 %) und K/Na-Tartrat (0.53 %).
Die Hydratation der Bindemittel wurde bei einem Wasser zu Bindemittel (w/b) Wert von 0.5 und Polymerdosierungen von 5, 10 und 20 %-bwob (by weight of binder) mittels Wärmekalorimetrie, in-situ XRD und Zeta-Potential untersucht.

Ergebnisse und Diskussion

Mittels isothermer Wärmekalorimetrie wurde die Hydratationswärmeentwicklung von OPC und des TBS (w/b 0.5) in Gegenwart und Abwesenheit von EVA und SB Polymer gemessen (**Abbildung 1**).

In reinem OPC wirkt das anionische SB Polymer stark verzögernd. In-situ XRD Messungen zeigten eine nahezu vollständige Unterdrückung der Ettringitbildung sowie eine signifikante Verzögerung der Portlanditkristallisation, welche zeitlich mit der Wärmeentwicklung korreliert. Zeta Potential-Messungen sowie die Analyse der Zementporenlösung bestätigten, dass die Ursachen für diese Effekte die Adsorption /5/ der anionischen SB Partikel auf positiv geladenen Klinker- bzw. Zementhydratphasen sowie die Komplexierung von Ca^{2+}-Ionen sind.

Diese Effekte sind bei Verwendung des SB Pulvers im Vergleich zur SB Dispersion schwächer ausgeprägt, was auf die geringere anionische Ladungsdichte der SB Pulverpartikel als Folge ihres PVOH Coatings zurückzuführen ist /6/. Folglich ergeben sich geringere physikalische Wechselwirkungen mit Ionen und mineralischen Oberflächen.

Im ternären Bindemittelsystem wirkt das anionische SB Polymer hingegen beschleunigend auf die Hydratation. In-situ XRD Messungen zeigten, dass die Auflösung von Anhydrit beschleunigt und somit eine frühe Ettringitbildung stark begünstigt wird. Eine mögliche Erklärung ist die Verschiebung des Löslichkeitsgleichgewichts aufgrund einer Ca^{2+}-Komplexierung durch anionische SB Partikel.

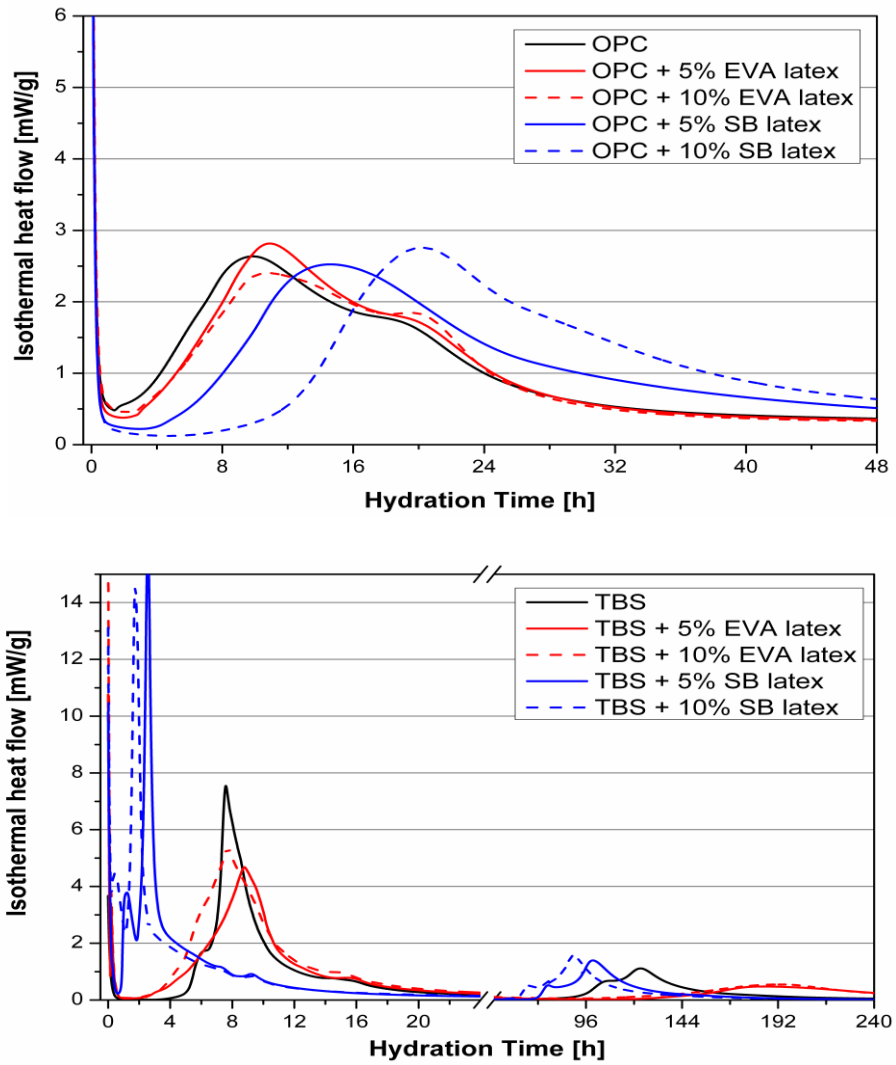

Abbildung 1: Hydratationswärmeentwicklung von OPC (oben) und des TBS (unten) in Gegenwart und Abwesenheit von EVA und SB Latexdispersion.

Der Einfluss nichtionischer EVA Polymere auf die Hydratation von OPC ist aufgrund fehlender physikalischer Wechselwirkungen gering und wird hauptsächlich durch die Anwesenheit des Schutzkolloids PVOH gesteuert. PVOH, welches als Vinylacetat-Vinylalkohol-Copolymer vorliegt, hydrolysiert in der alkalischen Zementporen-lösung, senkt somit deren pH Wert und führt zu einer verstärkten Auflösung der Silikatphasen. Dieses Verhalten ist beim EVA Pulver aufgrund des höheren PVOH Gehalts im Vergleich zur EVA Dispersion deutlich stärker ausgeprägt.

Im ternären Bindemittelsystem führt das EVA Polymer zu keiner Beeinflussung der frühen Ettringitbildung, jedoch zu einer starken Verzögerung der späten Silikatreaktion.

Zusammenfassung und Ausblick

Die Interaktion von Latexpartikeln mit anorganischen Bindemitteln wird durch die kolloidchemischen Eigenschaften der Latexpartikel bestimmt. Die bei der Sprühtrocknung wässriger Dispersionen zugegebenen Schutzkolloide und Antibackmittel können die kolloidchemischen Eigenschaften der Latexpartikel beeinflussen. Folglich können sich Dispersionspulver und ihre wässrigen Ausgangsdispersionen bezüglich des Einflusses auf die Zementhydratation unterscheiden.

Insbesondere bei anionischen SB Polymeren ist der Unterschied zwischen Pulver und Dispersion bezüglich der Zementhydratation auf veränderte kolloidchemische Eigenschaften zurückzuführen. Anionische Polymere können mit ihren ladungstragenden funktionellen Gruppen physikalisch mit Klinker- bzw. Zementhydratphasen sowie Ionen aus der Zementporenlösung wechselwirken. Diese Wechselwirkungen sind stark von der anionischen Ladungsdichte abhängig.

Nichtionische Polymere zeigen vergleichsweise geringe physikalische Wechselwirkungen mit mineralischen Oberflächen. Folglich wird der unterschiedliche Einfluss von Pulver und Dispersion auf die Zementhydratation nicht durch die Latexpartikel an sich, sondern durch die Anwesenheit von Sprühhilfen verursacht.

Referenzen

/1/ Y. Ohama: “Polymer-based admixtures”, Cem. Concr. Compos., (1998) 20, 189-212.

/2/ A. Jenni, L. Holzer, R. Zurbriggen, M. Herwegh: „Influence of polymers on microstructure and adhesive strength of cementitious tile adhesive mortars”, Cem. Concr. Res., (2005) 35, 35-50.

/3/ R. Bayer, H. Lutz, “Dry mortars”, Ullmann's encyclopedia of industrial chemistry, (2009), 579-541.

/4/ S. Baueregger, M. Perello, J. Plank: „Influence of anti-caking agent kaolin on film formation of ethylene–vinylacetate and carboxylated styrene–butadiene latex polymers”, Cem. Concr. Res., (2014) 58, 112-120.

/5/ M. Gretz, J. Plank: “Study on the interaction between anionic and cationic latex particles and Portland cement”, Colloid Surf. A: Physicochem. Eng. Asp., 330 (2008) 227–233.

/6/ S. Baueregger, M. Perello, J. Plank: “Role of PVOH and Kaolin on Colloidal Stability of Liquid and Powder EVA and SB Latexes in Cement Pore Solution”, Colloid Surf. A: Physicochem. Eng. Asp., (2013) 434, 145-153.

Paper #9

Optimization of Admixtures for Calcium Sulfate Based Building Products

S. Baueregger, J. Plank

Alit Inform

(2014), in print

Optimization of Admixtures for Calcium Sulfate Based Building Products

Stefan Baueregger*, Johann Plank [*1]

[*] Technische Universität München, Lichtenbergstr. 4, 85747 Garching / Germany

[1] Tel.: +49 89 289 13150
Fax: +49 89 289 13152.
E-mail: sekretariat@bauchemie.ch.tum.de

KEYWORDS

Gypsum; polycarboxylate; polyphosphate; methyl cellulose; admixture

ABSTRACT

In this article, new results on the performance, application and working mechanism of polycarboxylate superplasticizers, polyphosphate retarders and methyl cellulose water retention agents in $CaSO_4$ systems are presented.

At first, the effectiveness of polycarboxylate (PCE) superplasticizers possessing different chemical compositions was investigated in anhydrite-based floor screeds. It was found that PCEs possessing high anionic charge density disperse anhydrite significantly better than those with low anionic charge. The reason behind the difference is competitive adsorption between the PCE molecules and sulfate ions. The latter hinder and reduce adsorption of PCE polymers possessing low anionic charge.

Next, the retarding effect of linear sodium polyphosphates exhibiting different chain lengths on α-calcium sulfate hemi hydrate was investigated. The results confirmed that polyphosphates present highly effective retarders which work at low dosages and constitute a viable alternative to commonly used tartaric or citric acid. Polyphosphates exhibiting short chain lengths (e.g. $n_{PO3} = 4$) work best.

In the third part, performance of the water retention agent methyl hydroxypropyl cellulose (MHPC) in gypsum plaster was studied. It was found that the high sulfate concentrations present in gypsum pore solution can affect the water retention capacity of MHPC significantly by hindering the formation of large hydrocolloidal MHPC associates which are responsible for the water retention effect. This result explains why higher dosages of MHPC are required to achieve comparable water retention than in cement based systems.

1. Introduction

Gypsum-based building materials offer some important advantages over cementitious ones. First, the industrial fabrication of gypsum binders is considerably more eco friendly, because it requires only about one quarter of the energy needed to produce cement. Furthermore, large quantities of gypsum or anhydrite are available as by-products from industrial processes including flue-gas desulfurization, and the manufacture of titanium dioxide, phosphoric acid and fluoro hydrogen (HF). In addition, gypsum is fully recyclable, unlike cement. Moreover, gypsum exhibits some material properties such as e.g. fire resistance and low shrinkage which are superior over those from cement. Typical applications for gypsum binders include floor screeds, wallboards and interior wall plasters which provide a healthy indoor climate due to their high water sorption/desorption capacity. In all those applications, chemical admixtures are applied to improve the properties of the formulations.

Superplasticizers are used to provide high fluidity to anhydrite floor screeds and to the gypsum slurry prepared in wallboard production. In anhydrite floor screeds, melamine-formaldehyde-sulfite-based superplasticizers are commonly applied. Their disadvantage is the emission of formaldehyde which is especially critical in indoor applications. In addition, their water reduction capacity is limited. In contrast to this, polycarboxylate-based superplasticizers were found to exhibit higher effectiveness resulting in lower dosage, and they do not release toxic fumes. However, applicators have reported numerous cases of disappointing results with PCE products, meaning that specific PCE polymers which work exceptionally well in cement perform only poor in anhydrite, or they fail completely. The reason behind this incompatibility is

investigated in this study, and specific PCE structures which work well in anhydrite floor screeds are identified.

Next to superplasticizers, retarders play an important role in gypsum formulations. Commonly applied retarders for calcium sulfate based systems include α-hydroxy carboxylic acids such as e.g. tartaric or citric acid, pyrrol-formaldehyde-sulfite polycondensates, polysuccinimide and poly aspartic acid [1-3]. Here, a novel type of retarder based on polyphosphates is evaluated with respect to its performance in α-calcium sulfate hemi hydrate paste. More specifically, the impact of the chain length of various sodium polyphosphates on their retardation effectiveness is probed and the molecules exhibiting the best performance are identified.

In gypsum-based wall renders and plasters, water retention agents are required to prevent an uncontrolled water loss to porous substrates such as brick, lime-sandstone or aerated concrete. There, cellulose ethers (CEs) are applied as effective water retention agents. In plaster formulations, methyl hydroxypropyl cellulose (MHPC) is preferred over methyl hydroxyethyl cellulose (MHEC), because it introduces air voids into the binder which increase the yield and improve the insulating properties of the plaster. In previous work it has been shown that the high water retention capacity of cellulose ethers is owed to high water sorption ability of the CE molecules and to the formation of large CE associates which effectively plug the pores at the transition zone plaster/substrate and thus retain the water in the slurry [4, 5]. However, applicators generally observe that in gypsum-based plasters, higher CE dosages are required to achieve water retention values comparably to those in cement. Here, the reason behind this effect is investigated.

2. Materials and Methods

2.1 Study on anhydrite floor screed

2.1.1 Materials

Anhydrite floor screeds generally consist of four main components: anhydrite binder, sand and fillers, cement and/or potassium sulfate as activator, and a superplasticizer. As examples, recipes for three different types of anhydrite floor screeds are presented in **Table 1**. In our study, a floor screed was formulated from flue-gas desulfurization (FGD) anhydrite as binder.

Table 1: Sample formulations for anhydrite floor screeds

Component	**Binder**		
	Natural anhydrite	**FGD anhydrite**	**Synthetic (fluoro) anhydrite**
Anhydrite	550 g	350 g	350 g
Norm sand (0-2 mm)	429 g	535 g	645 g
Quartz powder	-	100 g	-
CEM I 42.5 R	16.5 g	10.5 g	-
K_2SO_4	2.75 g	2.5 g	3.5 g
Superplasticizer (MFS)	1.4 g	2 g	1.2 g
Methyl cellulose	-	0.3 g	0.07 g

The PCE superplasticizers used in this part were synthesized via free radical aqueous copolymerization from the monomers methacrylic acid and ω-methoxy polyethylene glycol methacrylate ester macromonomer with $K_2S_2O_8$ as initiator and 2-mercapto ethanol as chain transfer agent [6]. The molar ratio between methacrylic acid and MPEG-methacrylate ester was varied between 1.5:1, 3:1 or 6:1.

Additionally, the side chain length of the macromonomers varied between 9 or 45 ethylene oxide units. **Figures 1** and **2** display the chemical structure of the synthesized PCE molecules and their molecular architectures.

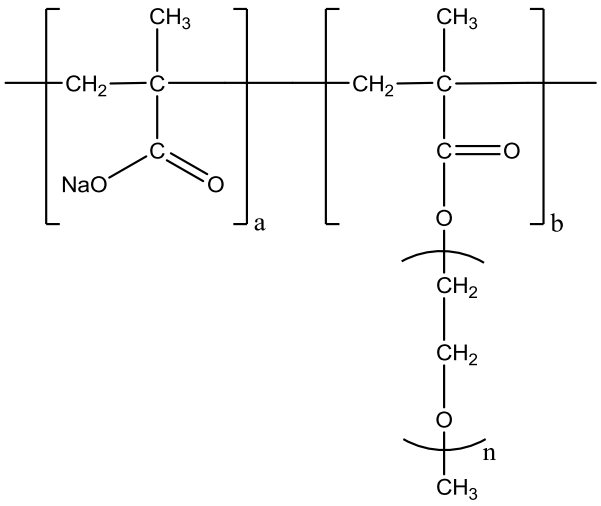

Figure 1: Chemical composition of the synthesized methacrylate ester-based PCE polymers

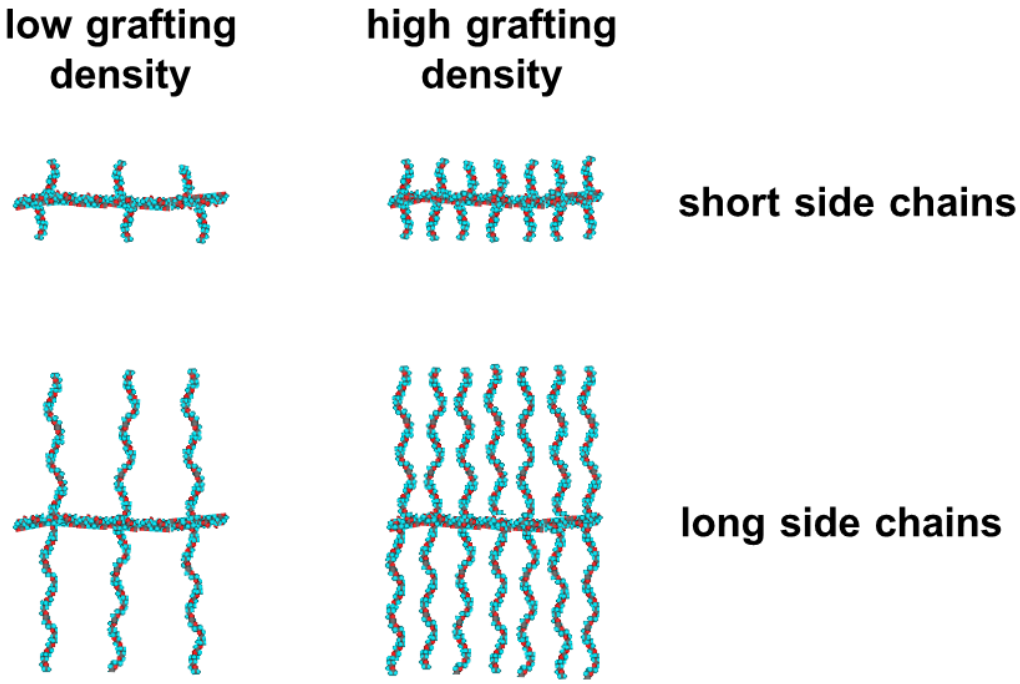

Figure 2: Molecular architectures of the synthesized PCE polymers exhibiting different side chain lengths and grafting densities

2.1.2 Mini-slump testing

For determination of the paste flow, a ‘mini slump’ test according to DIN EN 1015 was utilized and carried out as follows: First, an anhydrite floor screed was prepared from FGD anhydrite by dry blending the components shown in **Table 1**. The blend was then mixed with water for 1 min and filled into a Vicat cone on a glass plate. After the Vicat ring was lifted, the spread of the binder paste was measured. The spread value of the paste without superplasticizer was 18 cm (reference value).

2.1.3 PCE adsorption on anhydrite

The amount of PCE adsorbed on anhydrite was determined using the depletion method, i.e. the non-adsorbed portion of polymer remaining in solution at equilibrium condition was quantified via the total organic carbon (TOC) method of the solution. In a typical experiment, 20 g of anhydrite were agitated for 2 min with water, filled into a 50 mL centrifuge tube, shaken for 2 min at 2400 rpm in a wobbler (VWR International, Darmstadt, Germany) and then centrifuged for 10 min at 8500 rpm. The supernatant was carefully retrieved using a syringe and then diluted with DI water. The TOC content of the solution was determined on a High TOC II instrument (Elementar Analysesysteme, Hanau, Germany) by combustion at 890 °C. From the difference between the TOC content of the polymer reference sample and the TOC content of the supernatant, the adsorbed amount of superplasticizer was calculated.

2.2 Study on polyphosphate retarders

2.2.1 Materials

Sodium polyphosphate samples (supplied by Chemische Fabrik Budenheim KG, Budenheim, Germany) exhibiting three different chain lengths (n_{PO3} = 4, 6 and 12) were tested to assess the influence of the chain length on the retarding effect. **Figure 3** displays the general chemical structure of the linear sodium polyphosphates.

α-Calcium sulfate hemi hydrate binder (purity 97%) was received from Knauf Gips KG (Iphofen, Germany). It was produced from FGD gypsum. The average particle size (d_{50} value) of the α-$CaSO_4 \cdot 0.5\ H_2O$ was found at 36 µm.

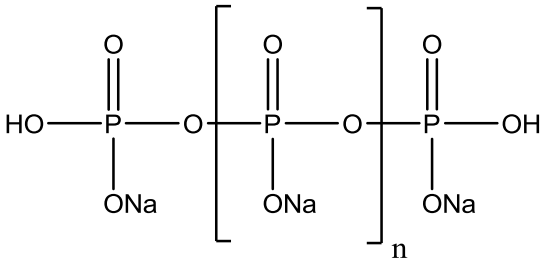

Figure 3: Chemical structure of the linear sodium polyphosphates tested in the study

2.2. Heat flow calorimetry

Hydration of α-calcium sulfate hemi hydrate in the presence and absence of the sodium polyphosphate retarders was tracked via heat flow calorimetry using a TAM Air isothermal heat conduction calorimeter. In a typical experiment, 4 g of hemi hydrate binder were filled into 10 mL tubular glass ampoules and mixed with 1.3 mL of DI water or polyphosphate solution (w/b ratio = 0.33). The samples were shaken for 1 min in a vortex tumbler and then transferred to the instrument. The heat flow curve was recorded at 20 °C for a time period of 20 hours.

2.2.3 Degree of hydration of α-$CaSO_4 \cdot 0.5\ H_2O$

The retarding effect of sodium polyphosphates was quantified by measuring the time-dependent degree of hydration of α-$CaSO_4 \cdot 0.5\ H_2O$. As degree of hydration, the amount of gypsum present relative to the amount of nonhydrated binder was taken. The amount of gypsum formed during the hydration was quantified gravimetrically [7]. The binder slurries were prepared according to the procedure for mini-slump testing as described in 2.1.2. After specific time intervals, small portions (~ 5 g) of the binder slurry were poured into an excess of isopropanol to stop hydration. Then the solid was separated via vacuum filtration, washed twice using isopropanol and dried for several hours at 60 °C. The dry solid was then calcined in an oven for 12 h at 700 °C. During the calcination process, hemihydrate or gypsum release their crystal water and are converted to anhydrite. Form the weight loss, the amount of gypsum present in the mixture was determined and the degree of hydration was calculated.

2.3 Study on cellulose ethers

2.3.1 Materials

The cement used for this study was a CEM I 52.5 N (HeidelbergCement AG, Leimen, Germany). As gypsum plaster, a fully formulated industrial blend containing all components (β-hemihydrate, hydrated lime, fine sand, lightweight aggregate and tartaric acid) except the CE was obtained from Hasit Trockenmörtel GmbH, Freising, Germany. The cellulose ether was a commercial sample of methyl hydroxypropyl cellulose obtained from SE Tylose GmbH & Co KG, Wiesbaden, Germany with a degree of substitution (DS / Methyl) of 1.6 and a molar degree of substitution (MS / HP) of 0.2. Its chemical structure is illustrated in **Figure 4**.

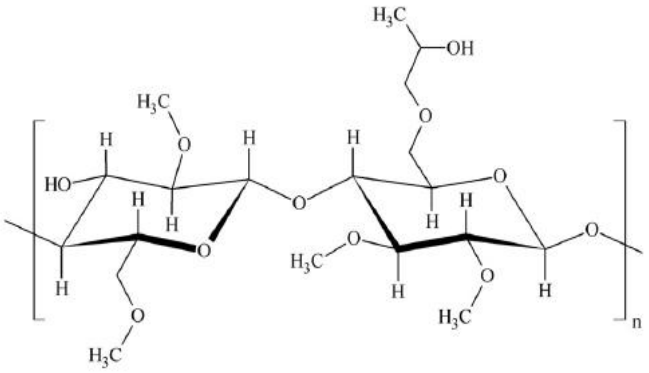

Figure 4: Approximated chemical structure of the methyl hydroxypropyl cellulose (MHPC) sample

2.3.2 Preparation of binder pastes

700 g of the plaster were dry-blended with the respective amount of HMPC and homogenized. Within 15 s, this mixture was added to the mixing water placed in the cup of a blade type laboratory (‘Waring’) blender and stirred for 35 s at ‘low’ speed (4500 rpm).

2.3.3 Water retention capacity

The water retention capacity of the plasters was quantified using the filter paper method according to EN 495-2 as illustrated in Figure 5. In a typical experiment, the render was filled into a Vicat cone which was placed on a stack of 15 half-folded filter papers covered on top by a tissue. After 7.5 min suction time, the Vicat cone containing the slurry and the tissue was removed. Then the weight of the stack of filter paper was measured. From the amount of water sorbed by the filter paper the water retention value was calculated as follows:

$$\text{water retention capacity } (\%) = \left(1 - \frac{w}{w_0}\right) \times 100$$

whereby w represents the amount of water sorbed by the filter paper, and w_0 constitutes the amount of mixing water added.

Figure 5: Illustration of the filter paper test used for quantification of the water retention of a plaster.

3. Results and Discussion

3.1 Effectiveness of PCEs in anhydrite floor screed

In this part, the effectiveness of PCE superplasticizers in anhydrite floor screeds under variation of the type of activator was investigated. At room temperature, anhydrite exhibits a low water solubility of 2.7 g/L which is only slightly less than that of gypsum (2.0 g/L). As a consequence, anhydrite needs to be activated by potassium sulfate or cement. They provide potassium and/or sulfate ions which accelerate the crystallization of gypsum by shifting the solubility equilibrium of $CaSO_4$. In addition, potassium sulfate leads to the formation of the double salt syngenite ($K_2SO_4 \cdot CaSO_4 \cdot H_2O$) which acts as a nucleus for the crystallization of gypsum.

Here, the influence of the activator system (cement vs. potassium sulfate) on the performance of the synthesized PCE polymers was assessed via mini-slump testing. As presented in **Table 2**, the effectiveness of the PCE superplasticizers strongly depends on the type of activator. When potassium sulfate is added, the PCE dosage required to achieve a spread flow of 26 cm is much higher than in the presence of cement. These results indicate that PCE superplasticizers generally are sensitive to potassium sulfate. Furthermore, the decrease of the performance depends on the specific chemical composition of the PCE superplasticizer. PCEs possessing low anionic charge density (PCE 1 in **Table 2**) exhibit a much more pronounced sensitivity (decrease in performance) than PCEs exhibiting high anionic charge (PCE 2).

Table 2: Influence of the kind of activator (K_2SO_4 or cement) on the effectiveness of PCE superplasticizers in anhydrite floor screed

Polycarboxylate sample	**PCE dosage for spread flow of 26 cm (wt.% bwoa)**	
	3.3 % CEM I 42.5 R	1.2 % K_2SO_4
PCE 1* (low charge density)	0.15	> 1.0
PCE 2** (high charge density)	0.05	0.09

* molar ratio acid : ester = 1.5:1; side chain length n_{EO} = 45

** molar ratio acid : ester = 6:1; side chain length n_{EO} = 45

It is generally accepted that the dispersing power of superplasticizers correlates with their amount adsorbed onto binder particles. Therefore, adsorption of the PCE samples onto anhydrite as a function of activator dosage was measured via TOC method. The results are shown in **Figure 6**.

Evidently, the dosage of K_2SO_4 greatly influences the adsorption of the PCEs. At increased K_2SO_4 additions, the adsorbed amount of PCE generally decreases. The negative effect is most pronounced for PCEs possessing low anionic charge. For example, at K_2SO_4 dosages above 1.2 % bwob, polymer PCE 1 possessing a low anionic charge no longer can adsorb. This finding demonstrates the strong impact of sulfate on the dispersing ability of PCEs possessing low anionic charge. Whereas, when polymer PCE 2 exhibiting a high anionic charge is present, the adsorbed amount decreases much less (by ~ 30% only). Therefore, even in the presence of high activator concentrations a sufficient dispersing effect is maintained for this polymer as is shown in **Table 2**.

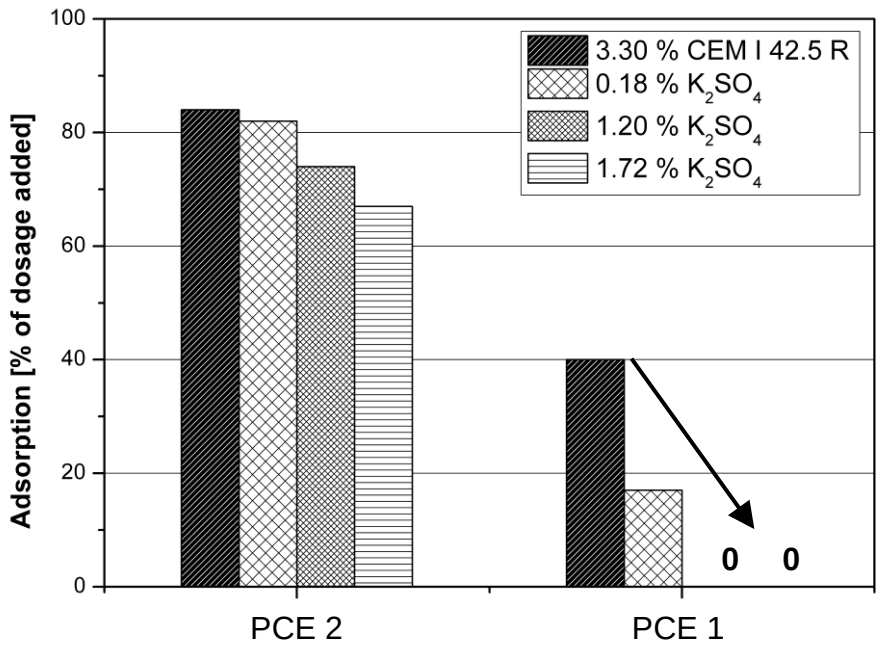

Figure 6: Adsorption of polymer samples PCE 1 and 2 on anhydrite at varying K_2SO_4 dosages and in the presence of cement

The results reveal a strong impact of the sulfate concentration on the effectiveness of PCE superplasticizers. Sulfate ions possess a high anionic charge density and therefore exhibit a high affinity for the positively charged surfaces of anhydrite. As a

consequence, the PCE polymers have to compete with sulfate ions for adsorption sites on the binder surface. The higher the anionic charge of a PCE molecule, the higher is its tendency to adsorb. Therefore, PCE molecules exhibiting high anionic charge density can successfully resist desorption from the anhydrite surface by sulfate ions and thus achieve high dispersing effectiveness.

Second, the effect of the side chain length of the PCE products on their dispersing ability was assessed by measuring the dosages required for a 26 cm slump flow and the respective adsorbed amounts. **Table 3** summarizes the results.

From the experiments it becomes evident that PCE polymers possessing longer side chains (here: 45 EO units) present more powerful dispersants compared to their short-side chain counterparts, provided that they exhibit high anionic charge. While for PCE polymers with low anionic charge, shorter side chains appear to be more favorable. Apparently, the anionic charge amount per gram of polymer is driving their adsorption behavior and thus their resistance to desorption by sulfate.

Table 3: Dosages required for 26 cm slump flow and amounts of different PCE polymers adsorbed on FGD anhydrite, activated by cement or K_2SO_4

PCE sample	**Activator for FGD anhydrite**			
	CEM I 42.5 R (w/a = 0.43)		**K_2SO_4 (w/a = 0.41)**	
	PCE dosage [%]	**Adsorbed amount [% of dos. added]**	**PCE dosage [%]**	**Adsorbed amount [% of dos. added]**
9 PC 1.5	0.30	21	0.85	16
9 PC 3	0.24	67	0.30	43
9 PC 6	0.20	94	0.20	81
45 PC 1.5	1.00 (24 cm)	2	1.00 (19 cm)	1
45 PC 3	0.15	18	0.25	19
45 PC 6	0.13	45	0.12	47

3.2 Retarding effectiveness of sodium polyphosphates

Calcium sulfate hemihydrate presents a highly reactive binder which in almost all applications needs to be retarded in order to achieve a sufficient workability period. Linear polyphosphates constitute a versatile, inexpensive chemical which is produced industrially in large quantities e.g. for detergents [8]. Here, the retardation effectiveness of three linear polyphosphates with varying chain length (n_{PO3} = 4, 6 and 12) was tested.

The reaction of α-$CaSO_4 \cdot 0.5\ H_2O$ with water is exothermic and therefore can be monitored via time-dependent heat calorimetry. As displayed in **Figure 7**, a neat hemihydrate slurry produces a strong peak of heat release already few minutes after mixing with water. Such highly reactive binder looses its workability within a few minutes only and therefore is impractical in actual applications such as plastering or placing floor screeds. It is therefore highly remarkable that when linear polyphosphates are added to hemihydrate, the maximum of heat evolution is shifted to no less than 10 to 14 hours, depending on the dosage and chain length of the polyphosphate sample. The shorter the side chain length of the polyphosphate, the more pronounced is their retarding effect. These results demonstrate the exceptional efficiency of linear polyphosphates with respect to the retardation of hemihydrate hydration. Second, it becomes evident that polyphosphates possessing short chain lengths (n_{PO3} = 4) present more powerful retarders than those exhibiting longer chains (n_{PO3} = 12).

Furthermore, the time-dependent paste flow in the absence and presence of the three polyphosphates was recorded (dosage: 0.025 % bwoc; **Figure 8**). It was found that in the absence of a polyphosphate the paste flow dropped rapidly within 15 min,

thus indicating an extremely short workability period. While in the presence of polyphosphates, flowability is maintained for at least 45 to 75 min, depending on the chain length. Again, polyphosphates made of shorter chains extend the workability period more, as was observed in heat calorimetry before (see **Figure 7**).

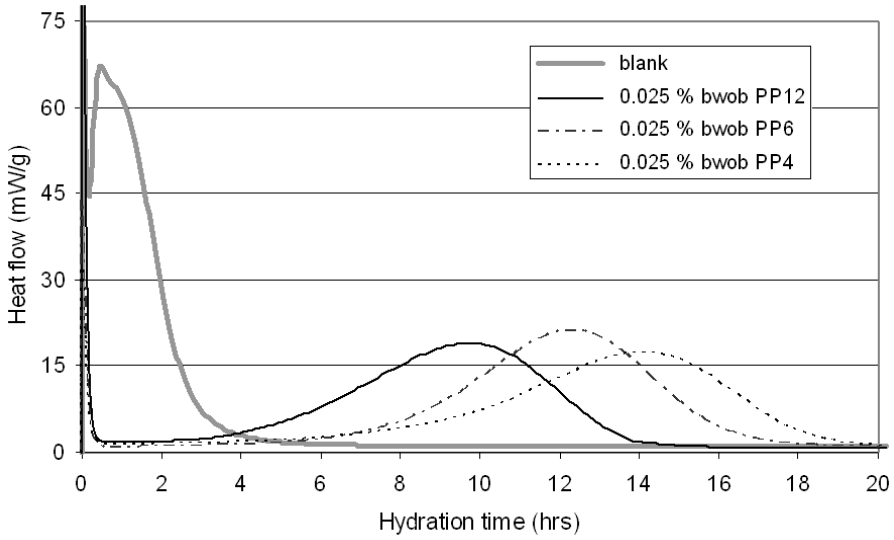

Figure 7: Time-dependent heat flow of α-$CaSO_4 \cdot 0.5\ H_2O$ / water suspensions, measured in the absence and presence of different polyphosphate samples

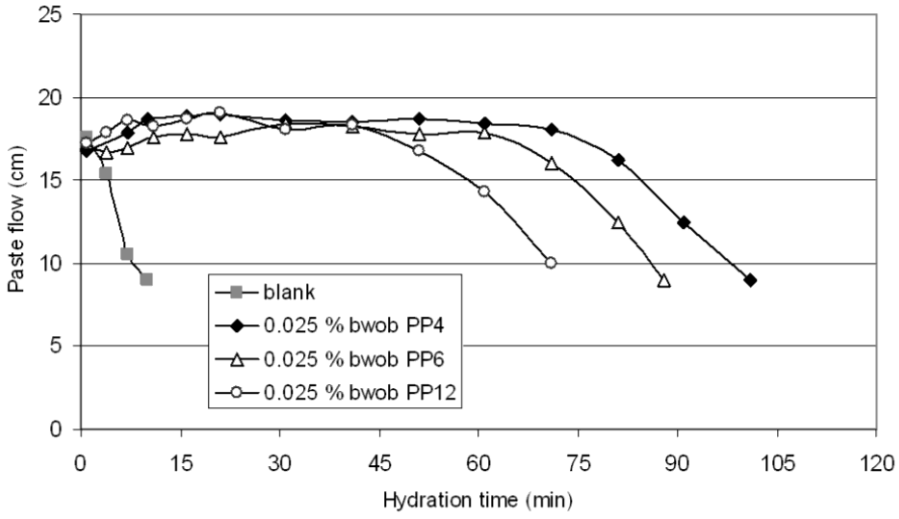

Figure 8: Time-dependent paste flow (workability) of α-$CaSO_4 \cdot 0.5\ H_2O$ pastes, measured in the absence and presence of sodium polyphosphates

To quantify the retarding effectiveness of the polyphosphates, the time-dependent degree of hydration of hemihydrate was monitored. Generally, the hydration of hemihydrate comprises three main steps: First, hemihydrate dissolves in water. Next, the pore solution becomes supersaturated with calcium sulfate from which in a third step gypsum is precipitated. This process can be tracked via measuring the percentage of hemihydrate which has already converted to gypsum.

Figure 9 confirms that in the absence of polyphosphates, hydration occurs rather fast. After 15 min, more than 50 % of the hemihydrate have converted into gypsum. While in the presence of polyphosphates, an induction period of 30 to 60 min is observed before hydration even begins. After this period, hydration proceeds at a rate similar to that of the neat hemihydrate. These results demonstrate that polyphosphates greatly delay the initial set of the hemihydrate, while the final set (represented by nearly complete hydration) remains mostly unchanged.

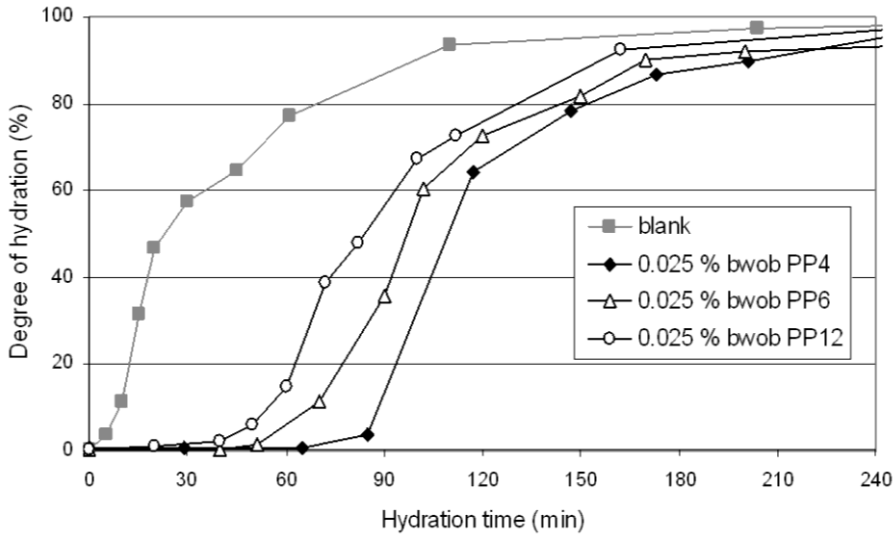

Figure 9: Time-dependent degree of hydration of α-$CaSO_4 \cdot 0.5\ H_2O$ pastes, measured in the absence and presence of sodium polyphosphates

3.3 Study on cellulose ethers

Gypsum plasters present a porous system which can sorb or desorb significant quantities of water and thus control the indoor climate. Typically, plasters are machine-sprayed under pressure on porous substrates which can dehydrate the plaster due to a capillary suction effect. To prevent such dehydration, cellulose ethers are applied as water retention agents.

Here, we compared the water retention capacity of a methyl hydroxypropyl cellulose sample in cement and in an industrial gypsum plaster. **Figure 10** shows its effectiveness depending on dosage. In the cement-based system, even at the very low MHPC dosage of 0.1 % bwoc high water retention (~ 98 %) is achieved. In comparison, the dosage required to achieve the same water retention in the gypsum plaster is double (0.2 %). These results clearly demonstrate that MHPC is more effective in cement-based than in gypsum-based plasters, a fact which is well-known by applicators. We speculated that the elevated sulfate concentration present in the gypsum pore solution might be responsible for the differences between cement and gypsum. To investigate, cement slurries containing additional amounts of sodium sulfate were prepared and the water retention achieved by MHPC was assessed. **Figure 11** shows the results. Indeed, at increased sulfate concentrations a decrease in the water retention capacity of MHPC was found.

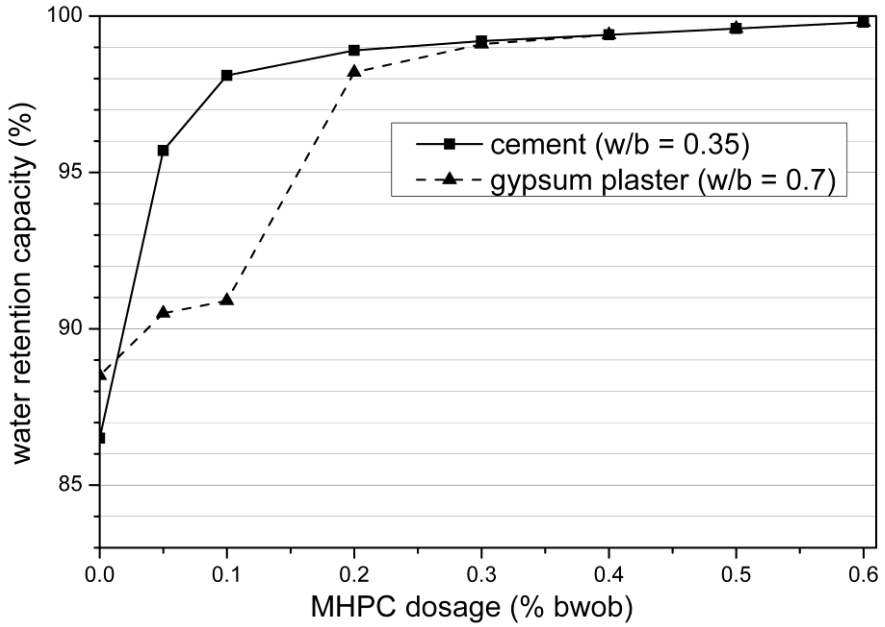

Figure 10: Dosage-dependent water retention capacity of MHPC, measured in cement and gypsum plaster

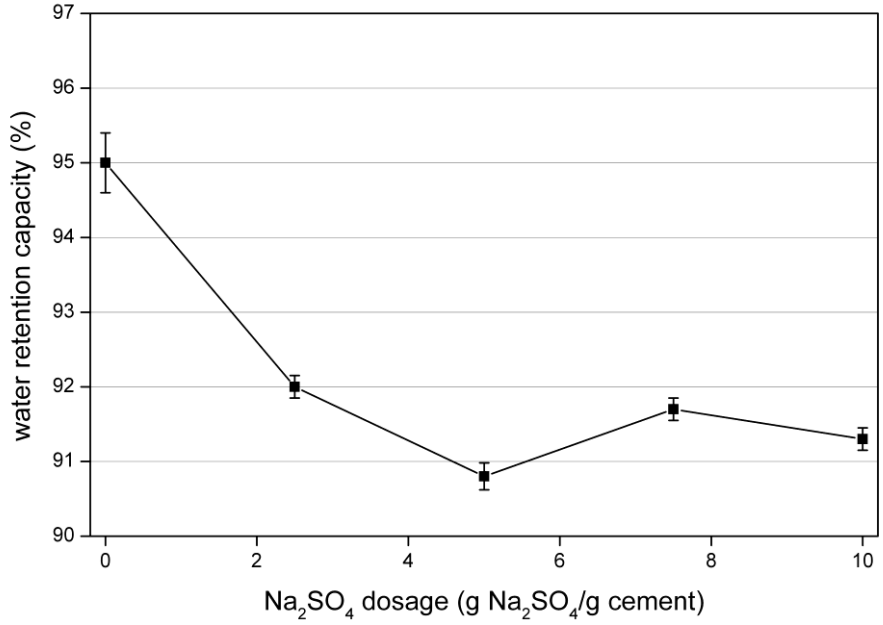

Figure 11: Water retention capacity of MHPC in cement, depending on Na_2SO_4 addition

Next, the reason for the negative impact of sulfate ions on the performance of MHPC was analyzed. Generally, the working mechanism of cellulose ethers is based on their strong water sorption capacity and their ability to form large polymeric associates which plug the pores of the binder paste [4, 5]. Formation of such associates occurs when a specific (so-called ‘overlapping’) concentration is exceeded. Beyond this concentration, the viscosity of the binder paste increases significantly.

Figure 12 displays the dynamic viscosities of cement and gypsum plaster pore solutions holding different MHPC concentrations. It clearly shows that from a certain MHPC dosage (the ‘overlapping concentration’), the dynamic viscosities of the pore solution rise significantly. The ‘overlapping concentration’ is much lower in cement pore solution, compared to that in the gypsum pore solution (~ 4 vs. 6 g/L). This result explains the better water retention performance of MHPC in cement because here, the formation of hydrocolloidal associates which are responsible for the effectiveness is not hindered by sulfate and thus occurs at much lower MHPC dosages.

Furthermore, the hydrodynamic size of the MHPC associates depending on the sulfate concentration was measured via dynamic light scattering technique. **Figure 13** reveals that the size of the associates decreases with increasing sulfate concentration in solution. At high sulfate concentration, formation of the associates is entirely prevented, thus making MHPC less effective as water-retention agent.

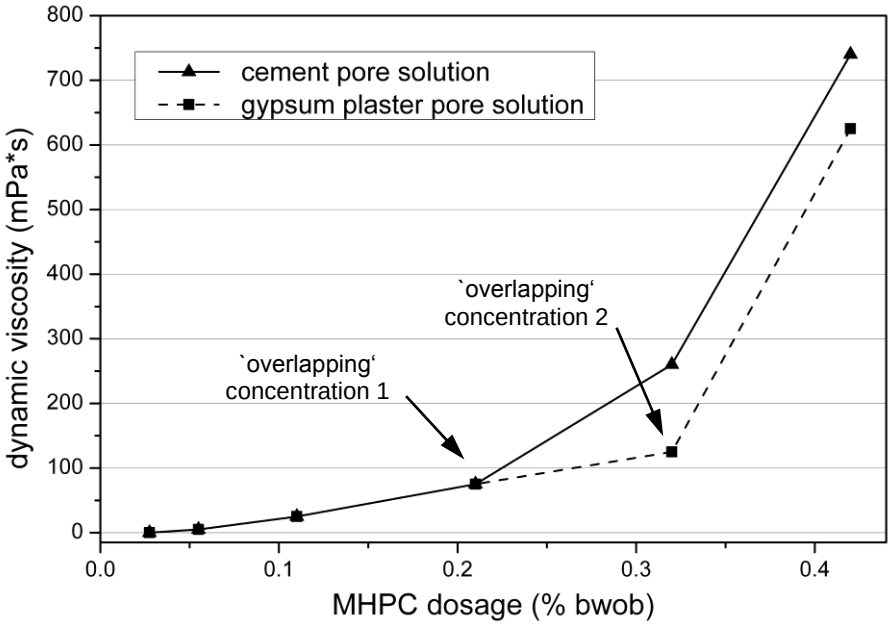

Figure 12: Dynamic viscosity of the cement or gypsum pore solutions, measured as a function of MHPC dosage

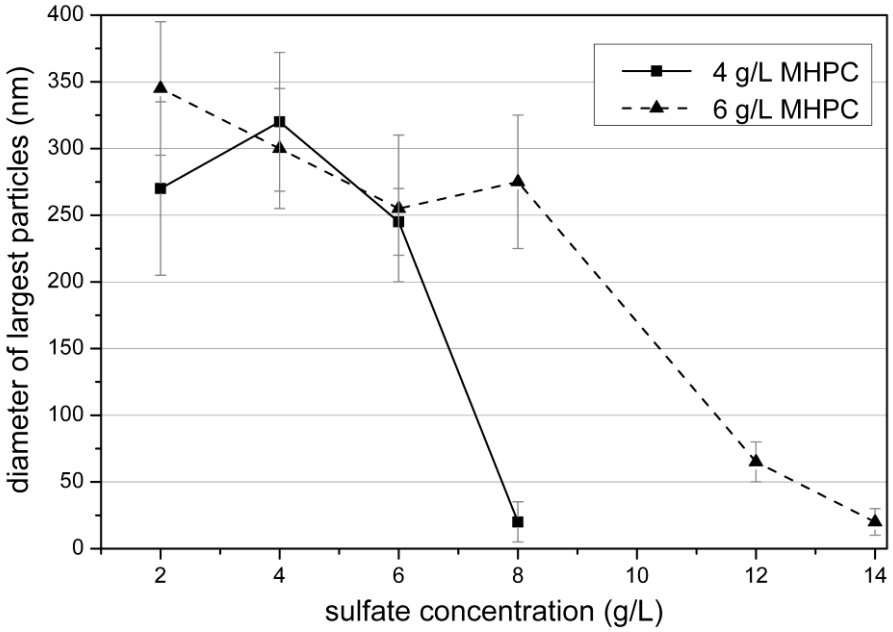

Figure 13: Average particle size of MHPC associates in dependence of the sulfate concentration in solution

4. Conclusion

Our studies demonstrate that the performance of admixtures used in gypsum-based building materials differs from that in cement and can be greatly optimized.

In the first part it is presented that PCE superplasticizers exhibit a high sensitivity against sulfate ions. Both, the PCE superplasticizer as well as the sulfate ions compete for adsorption sites present on the surface of the $CaSO_4$ binder. However, PCEs possessing low anionic charge are unable to compete with sulfate ions in the adsorption process and therefore show poor performance. Whereas PCEs of high anionic charge exhibit a high enough affinity to the binder surface and therefore can provide good dispersing effect even in $CaSO_4$ systems. These results demonstrate that in order to achieve optimum results, specific PCE molecules need to be selected for the application in gypsum, and that experience from cementitious systems may not apply.

In the second part it is shown that common gypsum retarders such as tartaric or citric acid can be replaced by linear polyphosphates which are even more cost-effective than those. The retarding effectiveness of polyphosphates depends on their chain length, whereby short-chain polyphosphates perform better than long-chain polyphosphates. Again, this example demonstrates that for optimum results, the specific chemical composition of the admixture (here the chain length) needs to be tailored to the application.

In the third part, the impact of elevated concentrations sulfate ions present in the pore solutions of gypsum binders on cellulose ether (MHPC) was investigated. The

experiments revealed that increased sulfate concentrations hinder the formation of large hydrocolloidal MHPC associates which are responsible for the water retention effect. Thus, higher dosages of MHPC have to be applied to overcome this negative effect of the sulfate anions and to achieve the ‘overlapping concentration’ at which those associates form. The results explain why in gypsum based systems higher MHPC dosages are required compared to those commonly used in cement.

References

[1] M. Singh, M. Garg, “Retarding action of various chemicals on setting and hardening characteristics of gypsum plaster at different pH”, Cement and Concrete Research, 27 (1997) 947-950.

[2] J. Hill, J. Plank, “Retardation of setting of plaster of Paris by organic acids: understanding the mechanism through molecular modeling”, Journal of Computational Chemistry, 25 (2004) 1438-1448.

[3] A. Ersen, A. Smith, T. Chotard, “Effect of malic and citric acid on the crystallisation of gypsum investigated by coupled acoustic emission and electrical conductivity techniques”, Journal of Materials Science, 41 (2006) 7210-7217.

[4] D. Bülichen, J. Kainz, J. Plank, “Working mechanism of methyl hydroxyethyl cellulose (MHEC) as water retention agent”, Cement and Concrete Research, 42 (2012) 953-959.

[5] D. Bülichen, J. Plank, “Water retention capacity and working mechanism of methyl hydroxypropyl cellulose (MHPC) in gypsum plaster - Which impact has sulfate?”, Cement and Concrete Research, 46 (2013) 66-72.

[6] J. Plank, K. Pöllmann, N. Zouaoui, P.R. Andres, C. Schäfer, “Synthesis and performance of methacrylic ester based polycarboxylate superplasticizers possessing hydroxy terminated poly(ethylene glycol) side chains”, Cement and Concrete Research, 38 (2008) 1210-1216.

[7] V. Nilles, J. Plank, “Study of the retarding mechanism of linear sodium polyphosphates on α-calcium sulfate hemihydrate”, Cement and Concrete Research, 42 (2012) 736-744.

[8] K.G. Cooper, L.G. Hanlon, G.M. Smart, R.E. Talbot, “25 years of experience in the development and application of scale inhibitors”, Desalination, 31 (1979) 243-255.